BUREAU INTERNATIONAL DES POIDS ET MESURES

BIPM – SUPPLEMENTARY INFORMATION FOR THE ITS-90 – 1997

SUPPLEMENTARY INFORMATION FOR

THE INTERNATIONAL TEMPERATURE SCALE OF 1990

1997

Pavillon de Breteuil, F-92312 Sèvres

Organisation intergouvernementale de la Convention du Mètre

SUPPLEMENTARY INFORMATION FOR

THE INTERNATIONAL TEMPERATURE SCALE OF 1990

1997 reprinting of the 1990 first edition

ISBN 92-822-2111-3

SUPPLEMENTARY INFORMATION FOR

THE INTERNATIONAL TEMPERATURE SCALE OF 1990

1997 reprinting of the 1990 first edition

When this monograph, prepared by Working Group 1 of the Comité Consultatif de Thermométrie (CCT), was published in 1990, it was expected that a revised and updated edition would follow in five to seven years. This intended revision is still a few years away.

In this reprinting of the first edition, the CCT has added only the revised values for ($t_{90} - t_{68}$) from 630 °C to 1064 °C (*Metrologia*, 1994, **31**, 149-153). These appear here as a new Appendix 2.

T.J. Quinn

Director, BIPM
President, CCT

July 1997

FOREWORD

This document replaces the earlier document of 1983 "Supplementary Information for the IPTS-68 and the EPT-76". It differs from the earlier one not only in being related to another, and radically different, temperature scale, but in having taken account of a number of advances in thermometry that have been developed in the intervening seven years. Such advances may be expected to continue, and to take account of these new editions of this document will be generated at suitable intervals ; at present these intervals are envisaged as being in the range of five to ten years.

As was the case for the companion document, "Techniques for Approximating the ITS-90" and for the ITS-90 itself, this document has been prepared by the members of the Comité Consultatif de Thermométrie (CCT). Members of the Working Group of the CCT who assembled the material, and who are listed below, would like to record their very great appreciation of the continual assistance they have received from their colleagues on the Committee. As is usually the case in such matters there have been many sources of information, but the selection has been by the Working Group who are responsible for any infelicities or errors of omission or commission that remain.

H. PRESTON-THOMAS
President of the CCT

T.J. QUINN
Director of the BIPM

December 1990

WORKING GROUP 1 : H. PRESTON-THOMAS, National Research Council of Canada
P. BLOEMBERGEN, Van Swinden Laboratorium, Holland
T.J. QUINN, Bureau International des Poids et Mesures

SUPPLEMENTARY INFORMATION FOR THE ITS-90

CHAPTER HEADINGS

CONTENTS

CONTENTS (Cont'd)

CONTENTS (Cont'd)

CONTENTS (Cont'd)

CAPTIONS TO TABLES AND FIGURES

TABLES :

FIGURES :

1. INTRODUCTION

1.1 Scope

From 1927 to 1975, the various international temperature scales have incorporated a moderate amount of supplementary information concerning their practical realization. However, limitations of space prevented this supplementary information's being exhaustive, while the lengthy periods, ranging from seven to twenty-one years, between scale editions allowed much of it to become outdated. The low temperature scale of 1976 (EPT-76)[1.1] provided no such information ; this information was instead given, in a more extensive and comprehensive form, and for both the EPT-76 and the IPTS-68, in a separate document. The first edition of such a document, "Supplementary Information for the IPTS-68 and the EPT-76" was published in 1983. This present, second, edition of the "Supplementary Information" has been prepared for ITS-90 by Working Group 1 of the CCT and approved by the CCT (the English version of the ITS-90 is reproduced here as Appendix 1).

This document describes methods by which the ITS-90 can be realised successfully. However, it should not be taken as laying down how it *must* be done. The description of any particular apparatus is more for illustration than prescription, and considerable variations can often be effective. Likewise, quoted numerical data and dimensions are mostly for guidance only. Methods of realizing the Scale will continue to evolve, and this will be reflected in periodic revisions of this text.

1.2 Historical Background

The ITS-90 [CIPM 1989, Preston-Thomas (1990)] has evolved from a series of earlier international temperature scales. These were formulated so as to allow measurements of temperature to be made precisely and reproducibly and with temperatures measured on these scales being as close an approximation as possible to the corresponding thermodynamic temperatures. A full description of these scales together with a historical review can be found in, for example, Quinn (1990) ; a brief description,

---

1.1 The extended form of this and other abbreviations is given in Appendix 2.

particularly including the changes introduced between scales and between editions, is as follows:

1.2.1 Normal Hydrogen Scale

The normal hydrogen scale was adopted by the CIPM at its sixth session [CIPM (1887)] and was subsequently approved by the first Conférence Générale des Poids et Mesures [CGPM (1889)]. This temperature scale had been developed by Chappuis in the laboratories of the Bureau International des Poids et Mesures (BIPM) ; it was based on gas thermometer measurements using the ice and steam points of 0 °C and 100 °C as fixed points, and was transferred to mercury-in-glass thermometers for distribution to other laboratories. At that time the temperature range of this scale was from −25 to +100 degrees centigrade,[1.2] a range that was gradually extended in subsequent years. In 1913, the fifth Conférence Générale approved the use of gases other than hydrogen, and expressed its readiness to substitute thermodynamic temperatures in place of the Normal Hydrogen Scale as soon as that became practicable.

1.2.2 ITS-27

The seventh Conférence Générale adopted provisionally, pending the acquisition of better thermodynamic data, the International Temperature Scale of 1927 [CGPM (1927)]. The ITS-27 was based upon a number of reproducible temperatures, or fixed points, to which numerical values were assigned, and three standard instruments, each of the instruments being calibrated at one or more of the fixed points ; the calibrations gave the constants for the formulae that defined temperatures in the various temperature ranges. A platinum resistance thermometer was used for the lowest, a platinum 10% rhodium-platinum (Pt-10% Rh-Pt)[1.3] thermocouple

1.2 The Conférence Générale of 1889 also endorsed the name centigrade. In 1948, the ninth Conférence Générale requested the CIPM to select one name from the three suggestions of centigrade, centesimal and celsius: acting on the CIPM's advice, that Conference then adopted the name Celsius.

1.3 Percentages are by weight.

for the middle, and an optical pyrometer for the highest temperature range[1.4].

The fixed points for the platinum resistance thermometer range were the melting point of ice (0,000 °C) and the boiling points of oxygen, water and sulphur then defined as being −182,97 °C, 100,000 °C, and 444,60 °C respectively. The resistance-temperature interpolating formulae were the Callendar equation (a quadratic) between 0 °C and 660 °C and the Callendar-van Dusen equation (a quadratic plus a quartic term) between −190 °C and 0 °C. The permitted range of the constants of these formulae imposed some degree of quality control in the thermometer construction.

The fixed points for the Pt-10% Rh-Pt thermocouple range were the melting points (more precisely, the temperature of equilibrium between the solid and the liquid phases of the material at normal atmospheric pressure) of silver and gold, then defined as being 960,5 °C and 1063 °C respectively, while a third calibration (but not fixed) point was the freezing point of antimony (≈ 630,5 °C) *as measured* by a calibrated standard platinum resistance thermometer. The emf-temperature interpolating formula was a quadratic that defined temperatures between 660 °C and 1063 °C ; here too, the permitted ranges of the constants imposed a degree of quality control, this time on the composition of the thermocouple wires.

It will be appreciated that both the lower and upper limits of the temperature range assigned to the platinum resistance thermometer were significant extensions beyond the associated calibration temperatures of approximately 90 K and 444 °C. One awkward result of the upper extension was the non-existence of an official freezing temperature for aluminium! This freezing temperature was extremely close to the assigned changeover point of 660 °C ; however, it proved to be a little above the assigned upper limit of the platinum resistance thermometer, yet a little below the, supposedly identical, lower limit assigned to the platinum rhodium-platinum thermocouple. At the other end of the resistance thermometer range it was found that for temperatures significantly below the lowest calibration temperature, departures from thermodynamic temperatures were unacceptably high.

1.4 The foregoing description is also applicable to the two immediate successors of the International Temperature Scale of 1927 (ITS-27), the International Temperature Scale of 1948 (ITS-48) and the International Practical Temperature Scale of 1968 (IPTS-68).

The fixed point for the optical pyrometer was the melting point of gold, which was used in conjunction with the (approximate) Wien radiation law ($L_\lambda(T) = \pi^{-1}c_1\lambda^{-5}\exp[-c_2/\lambda T]$) relating spectral concentration of radiance to temperature. The value assigned to the constant c_2 was $1{,}432.10^{-2}$ m•K (c_1 disappears in the comparison between the unknown and the calibration temperatures). Wavelength restrictions were the use of "visible" monochromatic radiation with $\lambda T \leq 3 \times 10^{-3}$ m•K. The various errors arising from the use of the Wien law and from the values assigned to the gold point and to c_2 were not in general significant for, or even detectable by, the users of that period.

1.2.3.1 ITS-48

The ninth Conférence Générale adopted the International Temperature Scale of 1948 [CGPM (1948)]. Changes from the ITS-27 were: the lower limit of the platinum resistance thermometer range was changed to the defined oxygen boiling point, and the junction of this range and the thermocouple range became the measured antimony freezing point ; the silver freezing point was defined as being 960,8 °C ; the gold melting became the gold freezing point ; the Wien law was replaced by the Planck radiation law ; the value assigned to the second radiation constant became $1{,}438 \times 10^{-2}$ m•K ; the permitted ranges for the constants in the interpolating formulae for the platinum resistance thermometers and thermocouples were modified ; the limitation on λT for optical pyrometry was removed.

1.2.3.2 IPTS-48

The eleventh Conférence Générale adopted the International Practical Temperature Scale of 1948, amended edition of 1960 [CGPM (1960)]. The modifications to the ITS-48 were : the triple point of water, which in 1954 had become the sole point defining the unit of thermodynamic temperature, the kelvin, replaced the melting point of ice as the calibration point in this region ; the freezing point of zinc, defined as being 419,505 °C, became a preferred alternative to the sulphur boiling point as a calibration point ; the permitted ranges of the constants of the

interpolation formulae for the platinum resistance thermometers and the thermocouples were further modified ; the restriction to "visible" radiation for optical pyrometry was removed.

Inasmuch as the numerical values of temperature on the ITS-48 were the same as on the IPTS-48, the latter was not a revision of the scale of 1948 but merely a revision of its text.

1.2.4.1 IPTS-68

In 1968 the Comité International des Poids et Mesures promulgated the International Practical Temperature Scale of 1968, having been invited to do so by the thirteenth Conférence Générale of 1967-68 [CGPM (1967-68)]. The IPTS-68 incorporated very extensive changes from the IPTS-48. These included numerical changes, intended to bring it more nearly in accord with thermodynamic temperatures, that were sufficiently large to be apparent to many users. Other changes were as follows: the lower limit of the scale was extended down to 13,81 K ; at even lower temperatures (0,5 K to 5,2 K) the use of a 1958 ^{4}He vapour pressure scale [Brickwedde *et al.* (1960)] and a 1962 ^{3}He vapour pressure scale [Sydoriak *et al.* (1964)] were recommended ; six new fixed points were introduced - the triple point of equilibrium hydrogen (13,81 K), an intermediate equilibrium-hydrogen vapour-pressure point (17,042 K), the boiling point of equilibrium hydrogen (20,28 K), the boiling point of neon (27,102 K), the triple point of oxygen (54,361 K), and the freezing point of tin (231,9681 °C) which became a permitted alternative to the boiling point of water ; the boiling point of sulphur was deleted ; the values assigned to four fixed points were changed - the boiling point of oxygen (90,188 K), the freezing point of zinc (419,58 °C), the freezing point of silver (961,93 °C), and the freezing point of gold (1064,43 °C) ; the interpolating formulae for the resistance thermometer range became very much more complex ; the value assigned to c_2 became $1{,}4388 \times 10^{-2}$ m•K ; the permitted ranges of the constants for the interpolation formulae for the platinum resistance thermometers and thermocouples were again modified.

1.2.4.2 IPTS-68(75)

The International Practical Temperature Scale of 1968, amended edition of 1975 [CGPM (1975), Preston-Thomas (1976)], was adopted by the fifteenth Conférence Générale in 1975. As was the case for the IPTS-48 vis-à-vis the ITS-48, the IPTS-68(75) introduced no numerical changes in any measured temperature T_{68}. Most of the extensive textual changes in the Scale were intended only to clarify and simplify its use. More substantive changes were: the condensation point of oxygen replaced, with no change in numerical value, the boiling point of oxygen ; the triple point of argon (83,798 K) was introduced as a permitted alternative to the condensation point of oxygen ; the recommendation to use the helium vapour pressure scales was withdrawn.

1.2.5 EPT-76

The 1976 Provisional 0,5 K to 30 K Temperature Scale, EPT-76 [BIPM (1979)], was adopted in order to provide an agreed basis for thermometry in that temperature range. It was intended in particular to provide a smooth interpolation in place of the erratic interpolation which had been found in the IPTS-68 below 27 K ; to correct the errors in the 1958 ^{4}He and 1962 ^{3}He vapour pressure scales ; and also to bridge the gap between 5,2 K and 13,81 K in which there had not previously been an international scale. In contrast with the IPTS-68, and to ensure its rapid adoption, several methods of realizing the EPT-76 were approved. These included using a thermodynamic interpolation instrument and one or more of eleven listed reference points (that included five superconducting transitions) ; taking differences from the IPTS-68 above 13,81 K ; taking differences from helium vapour pressure scales below 5 K ; taking differences from certain well-established laboratory scales. To the extent that these methods lacked internal consistency it was admitted that slight differences between realizations might be introduced. However the advantages to be gained by adopting the EPT-76 as a working scale until such time as the IPTS-68 was revised and extended were considered to outweigh the disadvantages [Durieux *et al.* (1979) and *see* also Pfeiffer and Kaeser (1982)].

1.2.6 ITS-90

The International Temperature Scale of 1990 was adopted by the CIPM in 1989 [CIPM (1989)] in accordance with the request embodied in Resolution 7 of the 18th CGPM (1987) and came into effect on 1st of January 1990. The full text of the ITS-90 is given here in Appendix 1 ; the following excerpt (the introduction to Section 3 of the text of the ITS-90) constitutes a brief description:

> Between 0,65 K and 5,0 K T_{90} is defined in terms of the vapour-pressure temperature relations of ^{3}He and ^{4}He.
>
> Between 3,0 K and the triple point of neon (24,556 1 K) T_{90} is defined by means of a helium gas thermometer calibrated at three experimentally realizable temperatures having assigned numerical values (defining fixed points) and using specified interpolation procedures.
>
> Between the triple point of equilibrium hydrogen (13,803 3 K) and the freezing point of silver (961,78 °C) T_{90} is defined by means of platinum resistance thermometers calibrated at specified sets of defining fixed points and using specified interpolation procedures.
>
> Above the freezing point of silver (961,78 °C) T_{90} is defined in terms of a defining fixed point and the Planck radiation law.

The ITS-90 differs from the IPTS-68 in a number of important respects:

- it extends to lower temperatures, 0,65 K instead of ≈ 13,8 K, and hence also replaces the EPT-76 from 0,65 K to 30 K,
- it is in closer agreement with thermodynamic temperatures,
- it has improved continuity and precision,
- it has a number of overlapping ranges and sub-ranges, and in certain ranges it has alternative but substantially-equivalent definitions,
- new versions of the helium vapour-pressure scales are not merely recommended but are an integral part of the Scale,
- it includes a gas thermometer, calibrated at three fixed points, as one of the defining instruments,
- the upper limit of the platinum resistance thermometer as defining instrument has been raised from 630 °C to the silver point (≈ 962 °C),
- the Pt-10%Rh-Pt thermocouple is no longer a defining instrument of the Scale, and thus the slope discontinuity which existed in IPTS-68 at 630 °C,

the junction between the platinum resistance thermometer and thermocouple ranges, has been removed,

- the range based upon the Planck radiation law begins at the silver point instead of at the gold point, and any one of the silver, gold or copper points may be selected as the reference point for this part of the Scale.

The design of the ITS-90 is shown schematically in Figure 1.1 and the list of defining fixed points is given in Table 1.1.

One of the guiding principles in setting up the ITS-90 was that it should allow the user as much choice in its realization as was compatible with an accurate and reproducible scale. For this reason the scale includes many sub-ranges ; within all except one of these T_{90} is defined independently of calibration points outside the range[1.5]. Thus, if a platinum resistance thermometer is to be calibrated over the whole of the low temperature range from ≈ 13,8 K to 273,16 K, all of the eight calibration points in that range must be used ; if, however, a calibration only in the range from the argon point (≈ 84 K) to the triple point of water is required, then only the three calibration points in this range are needed, ≈ 84 K, ≈ 234 K (Hg triple point) and 273,16 K. Similarly, in the range above 0 °C, a thermometer may be calibrated from 0 °C to 30 °C using just the triple point of water and melting point of gallium. This last range offers the simplest possible way of achieving the highest accuracy thermometry in the room temperature range ; it allows the user to avoid the trouble and expense of setting up calibration points at temperatures outside the range of interest, and in addition it allows the thermometer itself to be maintained under the best possible conditions by not requiring it to be heated significantly above the temperature of normal use. The price that is paid for this useful flexibility in the Scale is the presence of a certain level of sub-range inconsistency and increased non-uniqueness compared with a scale having no overlapping ranges or sub-ranges ; this is discussed in Section 1.3.2, and some current quantitative results are shown in Figures 1.5 and 1.6.

The estimated uncertainties of the thermodynamic temperatures of most of the defining fixed points of the ITS-90 are given in Table 1.2 together with the very much smaller uncertainties estimated to be

---

1.5 The exception is the platinum-resistance-thermometer range extending upwards from the triple point of neon(≈ 24,5 K) which calls for a calibration at the triple-point of hydrogen (≈ 13,8 K).

currently attainable under the best experimental conditions, in their realization on the ITS-90 itself.

1.3 Numerical

1.3.1 Differences Between Scales

Differences between various international scales are shown graphically in Figures 1.2, 1.3 and 1.4 and are tabulated in Tables 1.3, 1.4 and 1.5. Equations providing an analytic realization of the differences $T_{90} - T_{68}$ and $t_{90} - t_{68}$ are given in Table 1.6.

The helium vapour-pressure equations for the ITS-90 are those originally derived for the EPT-76, thus in the range below 4,2 K (omitted from Table 1.5) the differences $T_{90} - T_{76}$ can be considered to be zero. In the range from 4,2 K to 24,5561 K the differences $T_{90} - T_{76}$ are best given by the relation which was originally adopted for the difference $T_{\mathrm{NPL-75}} - T_{76}$ at the time the EPT-76 was derived, namely

$$T_{90} - T_{76} = -5{,}6 \times 10^{-6} \, (T_{76})^2 \, . \qquad (1.1)$$

The accuracy of the differences $t_{90} - t_{68}$ between 630,6 °C and 1064,18 °C is limited by the accuracy (reproducibility) of the IPTS-68 in this region ($1\,\sigma \approx 0{,}1$ K) ; these differences should therefore be considered as conventional ones. Because of the slope discontinuity which existed in IPTS-68 at t_{68} = 630,74 °C, care must be taken to avoid spurious effects from data converted from IPTS-68 to ITS-90 in this range.

Above 1064,18 °C $T_{90} - T_{68}$ is given by equation 1.5 of Table 1.6. The differences given by this equation are wavelength dependent. The values given in Table 1.5 are those for the domain in which the Wien equation is a close approximation to the Planck equation and for which equation 1.5 reduces to a quadratic in temperature. For the temperature range shown in the table this domain covers practically all of the visible region of the spectrum and thus the values given apply with negligible error at wavelengths near 0,65 µm (see Footnote 1.12 to Table 1.5) . At a wavelength of 1 µm and at temperatures above 3000 °C, however, the values calculated from equation (1.5) of Table 1.6 will differ from those in the table by upward of about 20 mK.

The differences $t_{48} - t_{27}$ are smaller than the imprecision of the great majority of temperature measurements carried out between those dates ; thus the 1948 change of temperature scale required little or no

retroactive numerical adjustments when comparing pre-1948 with post-1948 experimental work. In contrast, the differences $t_{68} - t_{48}$, $T_{76} - T_{68}$ and $T_{90} - T_{68}$ are substantially larger than the imprecision quoted in the scientific literature of those periods, and numerical corrections are often necessary for comparisons of work before and after these transition dates.

The conversion of IPTS-68 platinum resistance thermometer calibrations to ITS-90 is not straightforward. There are no simple analytical relations between the coefficients of ITS-90 and those (e.g. α and δ) of the IPTS-68. Conversion of IPTS calibrations to ITS-90 therefore consists of calculating the resistance ratios $W(T_{68}) = R(T_{68})/R(0\ °C)$ at the IPTS-68 values of the required ITS-90 fixed points, converting the ratios to $W(T_{90}) = R(T_{90})/R(0{,}01\ °C)$, by multiplying by 0,9999601 and applying the appropriate formula and temperature values as specified in the ITS-90.

For the triple points of neon and mercury, the melting point of gallium and the freezing point of indium, which were not defining fixed points of the IPTS-68, the values of T_{68} should be taken as 24,5616 K, 234,3082 K, 302,9219 K and 429,7850 K respectively [Rusby *et al.* (1990)]. Note that where the IPTS-68 calibration used the condensation point of oxygen, rather than the triple point of argon, the T_{68} value most appropriately assigned to the argon point may differ slightly from the value (83,798 K) specified in the IPTS-68. The freezing point of aluminium lay beyond the range of the platinum resistance thermometer in the IPTS-68, but on extrapolating the IPTS-68 equations its value was found to be 933,607 K [Bedford et al. (1984)] although this could be in error by 5 mK or more.

1.3.2 Non-Uniqueness and Sub-Range Inconsistency of the ITS-90

The non-uniqueness of ITS-90 must be considered in each of its ranges. There is presumptively non-uniqueness in those parts of the Scale in which there exists more than one definition, more than one interpolating instrument, or when different individual examples of one of the designated interpolating instruments are not identical. Thus, the only range in which there is, in principle, no non-uniqueness is between 0,65 K and 1,25 K. However, except for the platinum resistance thermometer

range, the non-uniqueness is considered to be below the normal measurement uncertainty.

The non-uniqueness of the ITS-90 found experimentally for a group of eleven thermometers in the range below 0 °C covered by the platinum resistance thermometer is illustrated in Figure 1.5. This non-uniqueness, that shows itself at temperatures between the fixed points, results, apart from the contribution of experimental error, from those intrinsic differences between the properties of individual interpolating thermometers that are not offset by the calibration procedures. Non-uniquenesses existed for earlier scales, but those in the ITS-90 are to some extent exacerbated as the result of the existence of overlapping ranges and sub-ranges. However, they are significantly smaller than those in IPTS-68 [Mangum *et al.* (1990)].

In addition to a non-uniqueness there exists also a sub-range inconsistency of the ITS-90 ; examples are shown in Figure 1.6. Sub-range inconsistency arises from the possibility of using a single thermometer to realize certain temperatures in more than one way. The scale has been designed so that for high quality platinum resistance thermometers the magnitude of the sub-range inconsistency substantially never exceeds 0,5 mK within their range of normal use.

1.3.3 The Propagation of Calibration Errors in the Platinum Resistance Thermometer Range of the ITS-90

The effects of 1 mK errors at the calibration points in the platinum resistance thermometer ranges and sub-ranges of the ITS-90 are shown in Figure 1.7.[1.6]. For a discussion on the propagation of errors in the platinum resistance thermometer ranges of ITS-90 *see* De Groot *et al.* (1991).

1.6 For the effects of errors in the range of the interpolating gas thermometer *see* Section 5 and in that of the radiation thermometer *see* Section 6.

TABLE 1.1

The defining fixed points of the ITS-90.

Number	Temperature		Sub-stance[1.7]	State[1.8]	$W_r(T_{90})$
	T_{90}/K	t_{90}/°C			
1	3 to 5	−270,15 to −268,15	He	vp	
2	13,8033	−259,3467	e-H_2	tp	0,001 190 07
3	≈ 17	≈ −256,15	e-H_2 (or He)	vp (or gp)	(0,002 296 46)[1.9]
4	≈ 20,3	≈ −252,85	e-H_2 (or He)	vp (or gp)	(0,004 235 36)[1.9]
5	24,5561	−248,5939	Ne	tp	0,008 449 74
6	54,3584	−218,7916	O_2	tp	0,091 718 04
7	83,8058	−189,3442	Ar	tp	0,215 859 75
8	234,3156	−38,8344	Hg	tp	0,844 142 11
9	273,16	0,01	H_2O	tp	1,000 000 00
10	302,9146	29,7646	Ga	mp	1,118 138 89
11	429,7485	156,5985	In	fp	1,609 801 85
12	505,078	231,928	Sn	fp	1,892 797 68
13	692,677	419,527	Zn	fp	2,568 917 30
14	933,473	660,323	Al	fp	3,376 008 60
15	1234,93	961,78	Ag	fp	4,286 420 53
16	1337,33	1064,18	Au	fp	
17	1357,77	1084,62	Cu	fp	

1.7 All substances except helium (both ^{3}He and ^{4}He are used) are of natural isotopic composition, e-H_2 is hydrogen at the equilibrium concentration of the ortho- and para-molecular forms.

1.8 For complete definitions and advice on the realization of these various states, *see* Section 2. The symbols have the following meaning: vp: vapour pressure point ; tp: triple point (temperature at which the solid, liquid and vapour phases are in equilibrium) ; gp: gas thermometer point ; mp, fp: melting point, freezing point (temperature, at a pressure of 101 325 Pa, at which the solid and liquid phases are in equilibrium)

1.9 The values corresponding to fixed points numbers 3 and 4 are calculated for T_{90} = 17,035 K and T_{90} = 20,27 K respectively (*see* Section 2.3.4).

TABLE 1.2

Estimates of the (1 σ) uncertainty in the values of thermodynamic temperature ΔT_1, and in the current (1990) best practical realizations ΔT_2 of the defining fixed points of the ITS-90 .

Fixed points	T_{90}/K	ΔT_1/mK	ΔT_2/mK
^{4}He vp[(a)]	4,2221	0,3	0,1
H_2 tp	13,8033	0,5	0,1
H_2 vp	≈ 17	0,5	0,2
H_2 vp	≈ 20,3	0,5	0,2
Ne tp	24,5561	0,5	0,2
O_2 tp	54,3584	1	0,1
Ar tp	83,8058	1,5	0,1
Hg tp	234,3156	1,5	0,05
H_2O tp	273,16	0	0,02
	t_{90}/°C		
Ga mp	29,7646	1	0,05
In fp	156,5985	3	0,1
Sn fp	231,928	5	0,1
Zn fp	419,527	13	0,1
Al fp	660,323	25	0,3
Ag fp	961,78	40	1[(b)], 10[(c)]
Au fp	1 064,18	50	10[(c)]
Cu fp	1 084,62	60	15[(c)]

(a) ^{4}He vp: boiling point at a pressure of 101 325 Pa of ^{4}He (not a defining fixed point of the ITS-90)

(b) for platinum resistance thermometry

(c) for radiation thermometry

TABLE 1.3

Approximate differences $(t_{48} - t_{27})$, in kelvins, between the values of temperature given by ITS-48 or IPTS-48[1.10] and ITS-27

t_{48}/°C	0	10	20	30	40	50	60	70	80	90	100
	$(t_{48} - t_{27})$/K										
600				0,00	0,04	0,08	0,12	0,15	0,18	0,21	0,24
700	0,24	0,27	0,29	0,31	0,33	0,35	0,37	0,38	0,40	0,41	0,41
800	0,41	0,42	0,43	0,43	0,43	0,43	0,43	0,42	0,41	0,41	0,40
900	0,40	0,38	0,37	0,36	0,34	0,32	0,30	0,28	0,26	0,23	0,20
1000	0,20	0,18	0,15	0,11	0,08	0,05	0,01				

t_{48}/°C	0	100	200	300	400	500	600	700	800	900	1000
	$(t_{48} - t_{27})$/K										
1000		−0,15	−0,60	−1,11	−1,68	−2,32	−3,01	−3,77	−4,59	−5,48	−6,43
2000	−6,43	−7,44	−8,52	−9,67	−10,88	−12,17	−13,54	−14,98	−16,50	−18,11	−19,81
3000	−19,81	−21,61	−23,51	−25,51	−27,62	−29,86	−32,22	−34,72	−37,35	−40,14	−43,09

1.10 Note that there are no numerical differences between ITS-48 and IPTS-48.

TABLE 1.4

Approximate differences ($t_{68} - t_{48}$), in kelvins, between the values of temperature given by the IPTS-68 and the IPTS-48

t_{68} °C	0	−10	−20	−30	−40	−50	−60	−70	−80	−90	−100
−100	0,022	0,013	0,003	−0,006	−0,013	−0,013	−0,005	0,007	0,012		
0	0,000	0,006	0,012	0,018	0,024	0,029	0,032	0,034	0,033	0,029	0,022

t_{68} °C	0	10	20	30	40	50	60	70	80	90	100
0	0,000	−0,004	−0,007	−0,009	−0,010	−0,010	−0,010	−0,008	−0,006	−0,003	0,000
100	0,000	0,004	0,007	0,012	0,016	0,020	0,025	0,029	0,034	0,038	0,043
200	0,043	0,047	0,051	0,054	0,058	0,061	0,064	0,067	0,069	0,071	0,073
300	0,073	0,074	0,075	0,076	0,077	0,077	0,077	0,077	0,077	0,076	0,076
400	0,076	0,075	0,075	0,075	0,074	0,074	0,074	0,075	0,076	0,077	0,079
500	0,079	0,082	0,085	0,089	0,094	0,100	0,108	0,116	0,126	0,137	0,150
600	0,150	0,165	0,182	0,200	0,23	0,25	0,28	0,31	0,34	0,36	0,39
700	0,39	0,42	0,45	0,47	0,50	0,53	0,56	0,58	0,61	0,64	0,67
800	0,67	0,70	0,72	0,75	0,78	0,81	0,84	0,87	0,89	0,92	0,95
900	0,95	0,98	1,01	1,04	1,07	1,10	1,12	1,15	1,18	1,21	1,24
1000	1,24	1,27	1,30	1,33	1,36	1,39	1,42	1,44			

t_{68} °C	0	100	200	300	400	500	600	700	800	900	1000
1000		1,5	1,7	1,8	2,0	2,2	2,4	2,6	2,8	3,0	3,2
2000	3,2	3,5	3,7	4,0	4,2	4,5	4,8	5,0	5,3	5,6	5,9
3000	5,9	6,2	6,5	6,9	7,2	7,5	7,9	8,2	8,6	9,0	9,3

TABLE 1.5

Differences between ITS-90 and EPT-76, and between ITS-90 and IPTS-68 for specified values of T_{90} and t_{90}. *See* Section 1.3.1. for a note on the differences above 1064 °C.

$(T_{90} - T_{76})$/mK

T_{90}/K	0	1	2	3	4	5	6	7	8	9
0						−0,1	−0,2	−0,3	−0,4	−0,5
10	−0,6	−0,7	−0,8	−1,0	−1,1	−1,3	−1,4	−1,6	−1,8	−2,0
20	−2,2	−2,5	−2,7	−3,0	−3,2	−3,5	−3,8	−4,1		

$(T_{90} - T_{68})$/K

T_{90}/K	0	1	2	3	4	5	6	7	8	9
10					−0,006	−0,003	−0,004	−0,006	−0,008	−0,009
20	−0,009	−0,008	−0,007	−0,007	−0,006	−0,005	−0,004	−0,004	−0,005	−0,006
30	−0,006	−0,007	−0,008	−0,008	−0,008	−0,007	−0,007	−0,007	−0,006	−0,006
40	−0,006	−0,006	−0,006	−0,006	−0,006	−0,007	−0,007	−0,007	−0,006	−0,006
50	−0,006	−0,005	−0,005	−0,004	−0,003	−0,002	−0,001	0,000	0,001	0,002
60	0,003	0,003	0,004	0,004	0,005	0,005	0,006	0,006	0,007	0,007
70	0,007	0,007	0,007	0,007	0,007	0,008	0,008	0,008	0,008	0,008
80	0,008	0,008	0,008	0,008	0,008	0,008	0,008	0,008	0,008	0,008
90	0,008	0,008	0,008	0,008	0,008	0,008	0,008	0,009	0,009	0,009
T_{90}/K	0	10	20	30	40	50	60	70	80	90
100	0,009	0,011	0,013	0,014	0,014	0,014	0,014	0,013	0,012	0,012
200	0,011	0,010	0,009	0,008	0,007	0,005	0,003	0,001		

$(t_{90} - t_{68})$/°C

t_{90}/°C	0	−10	−20	−30	−40	−50	−60	−70	−80	−90
−100	0,013	0,013	0,014	0,014	0,014	0,013	0,012	0,010	0,008	0,008
0	0,000	0,002	0,004	0,006	0,008	0,009	0,010	0,011	0,012	0,012
t_{90}/°C	0	10	20	30	40	50	60	70	80	90
0	0,000	−0,002	−0,005	−0,007	−0,010	−0,013	−0,016	−0,018	−0,021	−0,024
100	−0,026	−0,028	−0,030	−0,032	−0,034	−0,036	−0,037	−0,038	−0,039	−0,039
200	−0,040	−0,040	−0,040	−0,040	−0,040	−0,040	−0,040	−0,039	−0,039	−0,039
300	−0,039	−0,039	−0,039	−0,040	−0,040	−0,041	−0,042	−0,043	−0,045	−0,046
400	−0,048	−0,051	−0,053	−0,056	−0,059	−0,062	−0,065	−0,068	−0,072	−0,075
500	−0,079	−0,083	−0,087	−0,090	−0,094	−0,098	−0,101	−0,105	−0,108	−0,112
600	−0,115	−0,118	−0,122	−0,125[1.11]	−0,08	−0,03	0,02	0,06	0,11	0,16
700	0,20	0,24	0,28	0,31	0,33	0,35	0,36	0,36	0,36	0,35
800	0,34	0,32	0,29	0,25	0,22	0,18	0,14	0,10	0,06	0,03
900	−0,01	−0,03	−0,06	−0,08	−0,10	−0,12	−0,14	−0,16	−0,17	−0,18
1000	−0,19	−0,20	−0,21	−0,22	−0,23	−0,24	−0,25	−0,25	−0,26	−0,26
t_{90}/°C	0	100	200	300	400	500	600	700	800	900
1000		−0,26	−0,30	−0,35	−0,39	−0,44	−0,49	−0,54	−0,60	−0,66
2000	−0,72	−0,79	−0,85	−0,93	−1,00	−1,07	−1,15	−1,24	−1,32	−1,41
3000[1.12]	−1,50	−1,59	−1,69	−1,78	−1,89	−1,99	−2,10	−2,21	−2,32	−2,43

1.11 A discontinuity in the first derivative of $(t_{90} - t_{68})$ occurs at a temperature of t_{90} = 630,6 °C, at which $(t_{90} - t_{68})$ = −0,125 °C.

1.12 The differences $t_{90} - t_{68}$ between 3000 °C and 3900 °C calculated for a wavelength of 0,65 µm are: −1,50, −1,59, −1,68, −1,78, −1,88, −1,99, −2,09, −2,20, −2,31, −2,42 °C (*see* Section 1.3.1).

TABLE 1.6

Equations giving the differences $T_{90} - T_{68}$ and $t_{90} - t_{68}$ shown in Table 1.5

The polynomial representations of the differences between 13,8 K and 1064,18 °C are due to R.L. Rusby (1990).

- From 13,8 K to 83,8 K (accuracy approximately ± 1 mK)

$$(T_{90} - T_{68})/\mathrm{K} = a_0 + \sum_{i=1}^{12} a_i \left((T_{90} - 40\ \mathrm{K})/40\ \mathrm{K}\right)^i \qquad (1.2)$$

- From 83,8 K to +630,6 °C (accuracy approximately ± 1,5 mK up to 0 °C, and ± 1 mK above 0 °C)

$$(t_{90} - t_{68})/°\mathrm{C} = \sum_{i=1}^{8} b_i \left(t_{90}/630\ °\mathrm{C}\right)^i \qquad (1.3)$$

- From 630,6 °C to 1064,18 °C (accuracy approximately ± 10 mK)

$$(t_{90} - t_{68})/°\mathrm{C} = c_0 + \sum_{i=1}^{7} c_i \left((t_{90} - 900\ °\mathrm{C})/300\ °\mathrm{C}\right)^i \qquad (1.4)$$

- Above 1064,18 °C (see Section 1.3.1 for range of applicability)

$$T_{90} - T_{68} = \Delta T(\mathrm{Au}) \cdot \left(\frac{T_{90}}{T(\mathrm{Au})}\right)^2 \cdot \frac{L_\lambda(T(\mathrm{Au}))}{L_\lambda(T_{90})} \cdot \frac{\exp\left[c_2/\lambda(T(\mathrm{Au}))\right]}{\exp\left[c_2/\lambda T_{90}\right]} \qquad (1.5)$$

where $L_\lambda(T_{90})$ and $L_\lambda(T(\mathrm{Au}))$ are given in equation (6.1), $T(\mathrm{Au})$ = 1337,33 K and $\Delta T(\mathrm{Au})$ = −0,25 K.

The coefficients a_i, b_i and c_i of equations (1.2), (1.3) and (1.4) are

i	a_i	b_i	c_i
0	−0,005903	0	−0,00317
1	0,008174	−0,148759	−0,97737
2	−0,061924	−0,267408	1,25590
3	−0,193388	1,080760	2,03295
4	1,490793	1,269056	−5,91887
5	1,252347	−4,089591	−3,23561
6	−9,835868	−1,871251	7,23364
7	1,411912	7,438081	5,04151
8	25,277595	−3,536296	0
9	−19,183815	0	0
10	−18,437089	0	0
11	27,000895	0	0
12	−8,716324	0	0

Figure 1.1. Schematic representation of the ranges, sub-ranges and interpolation instruments of ITS-90. The temperatures shown are approximate only.
Section 1.2.6

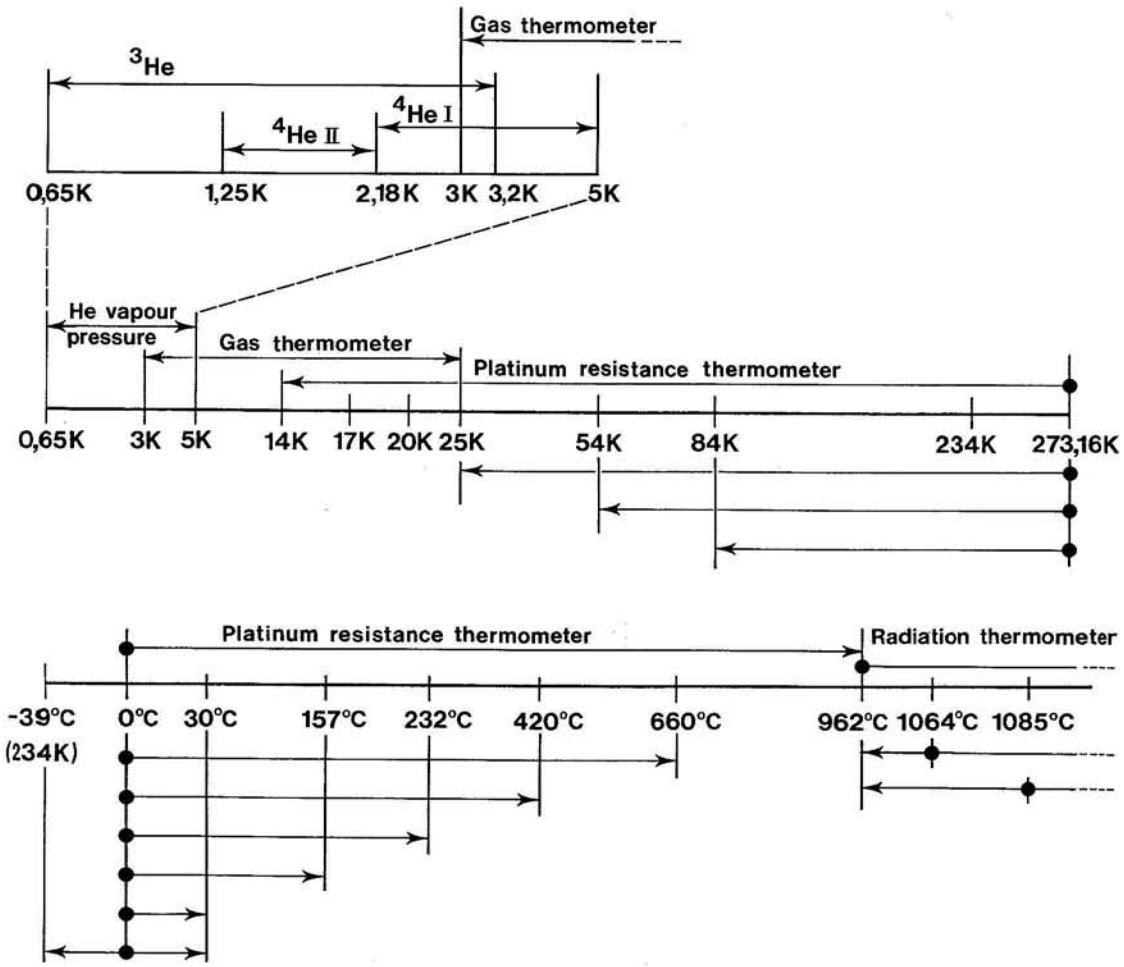

Figure 1.2 The differences $t_{48} - t_{27}$ as a function of t_{48} [after Hall (1955)].
Section 1.3.1.

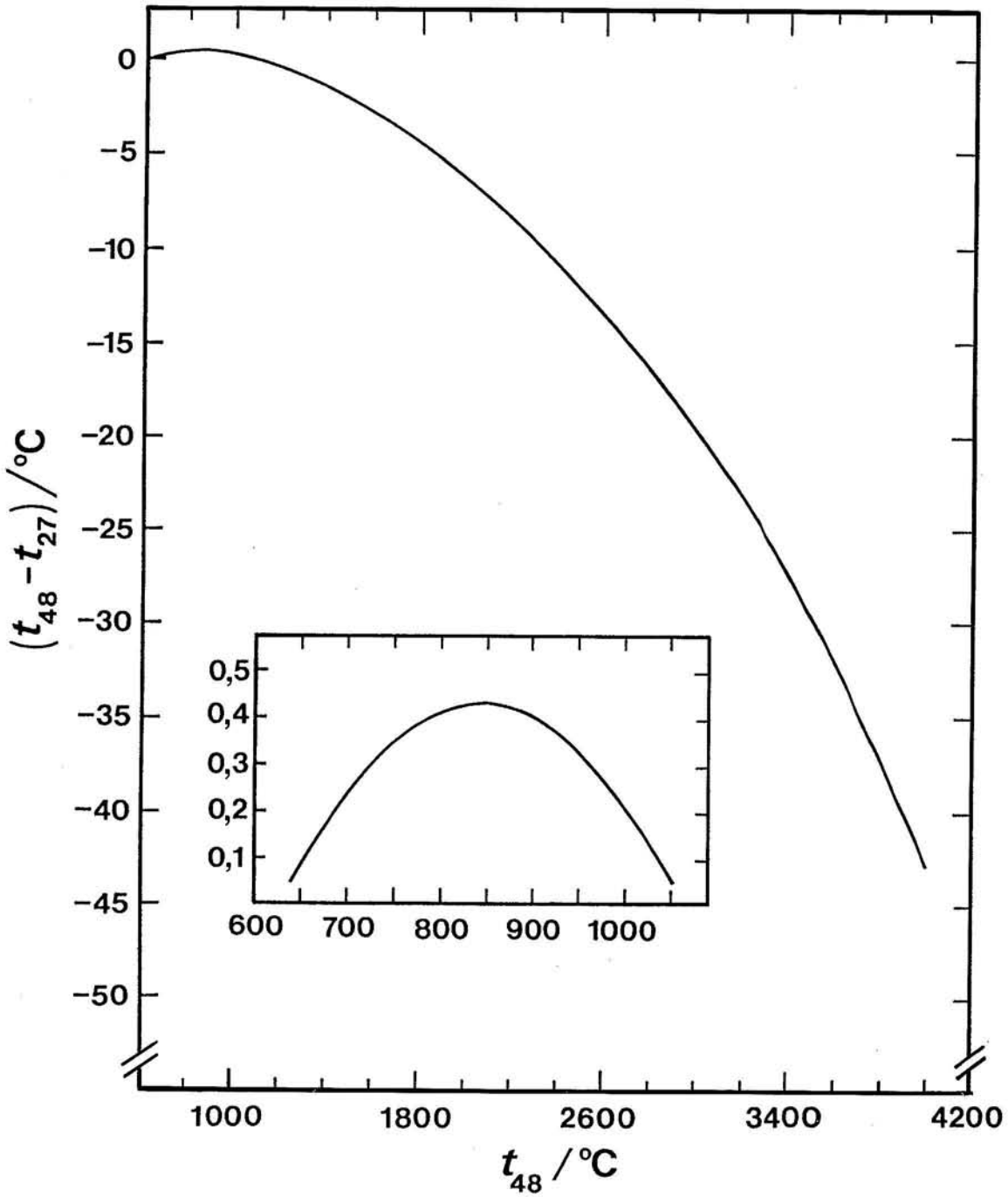

Figure 1.3 The differences $t_{68} - t_{48}$ as a function of t_{68} [Bedford *et al.* (1970]).
Section 1.3.1.

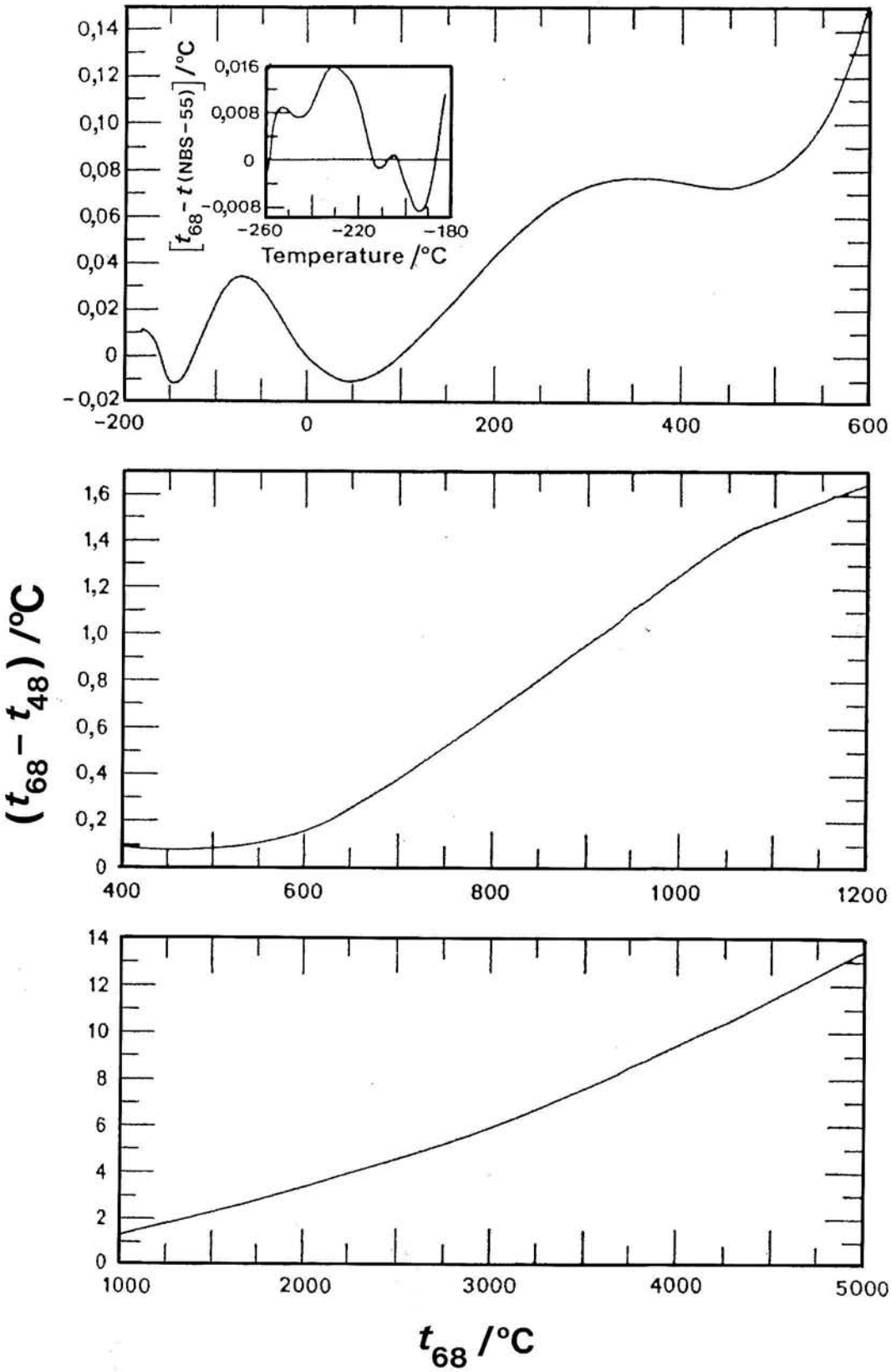

Figure 1.4. The differences $t_{90} - t_{68}$ as a function of t_{90}.
Section 1.3.1.

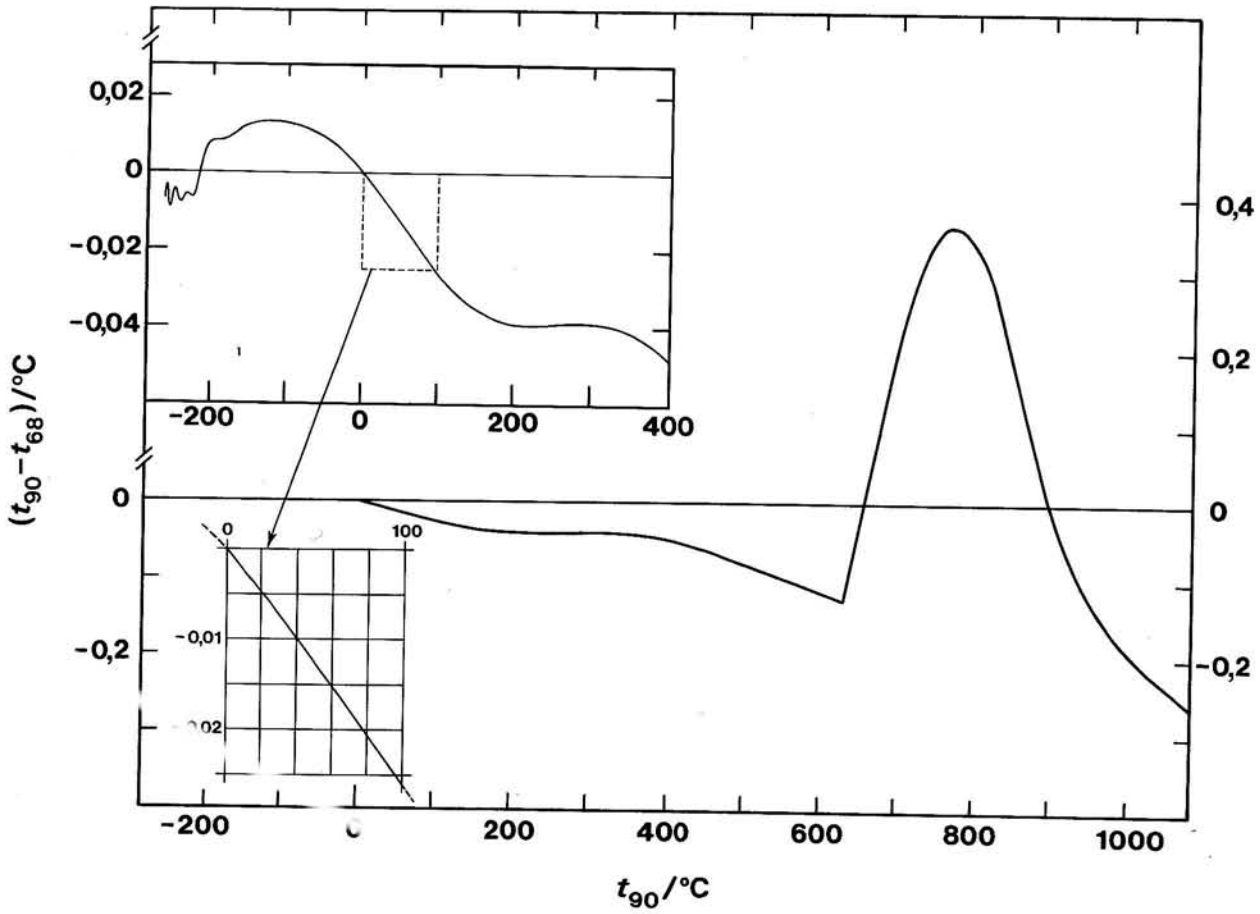

Figure 1.5 The non-uniqueness ΔT of the ITS-90 in the range 13,8 K to 273,16 K for a set of eleven platinum resistance thermometers.
Differences ΔT between individual thermometers and a reference thermometer are given for the range and for the sub-ranges shown of temperature T_{90}. (Figure prepared by R.C. Kemp)
Sections 1.2.6, 1.3.2.

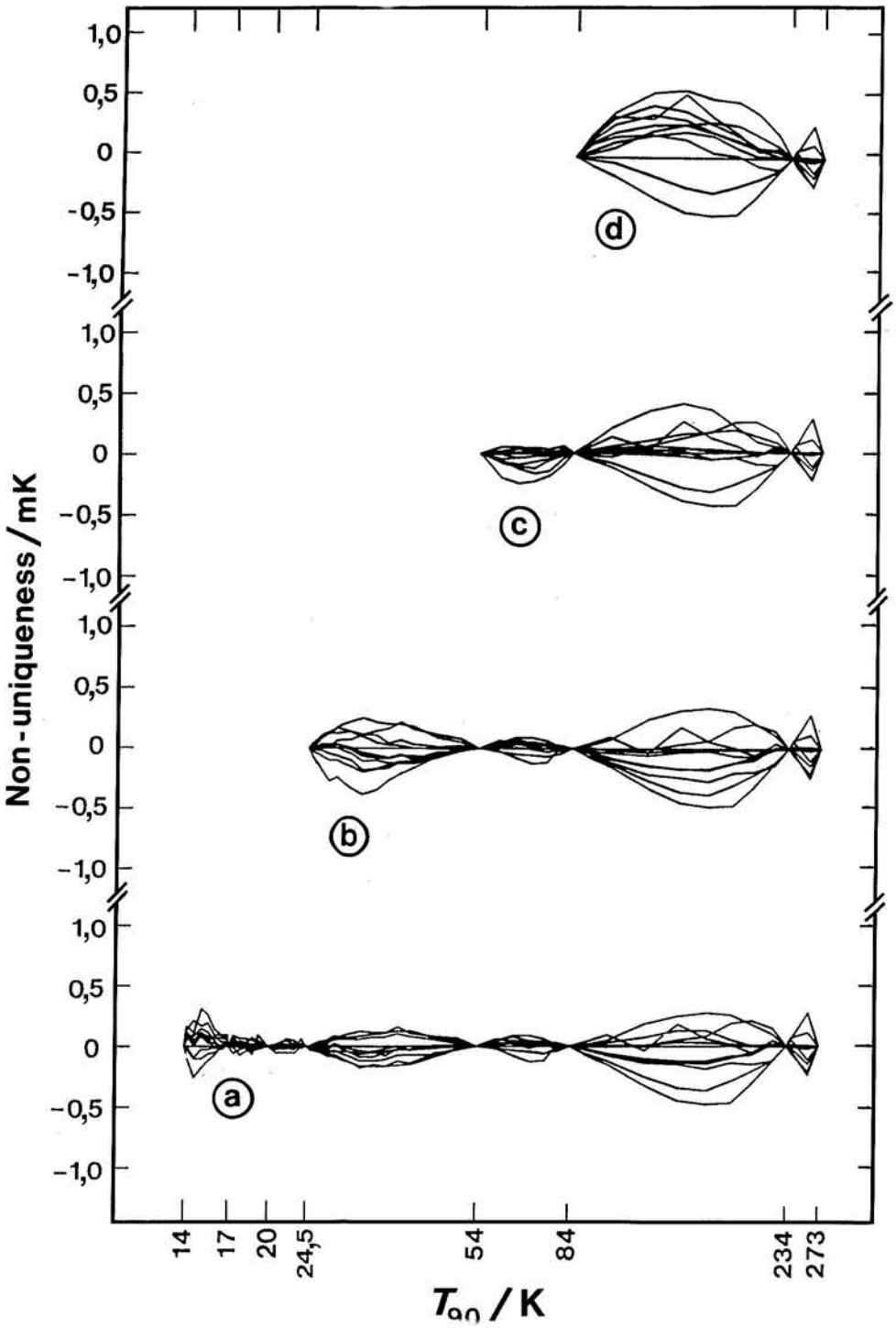

(a) Full range, 13,8033 K to 273,16 K
(b) Sub-range of 24,5561 K to 273,16 K
(c) Sub-range of 54,3584 K to 273,16 K
(d) Sub-range of 83,8058 K to 273,16 K.

Figure 1.6. The sub-range inconsistency of the ITS-90 for a number of platinum resistance thermometers.
Differences ΔT shown are those between temperatures calculated from a full range calibration (13,8033 K to 273,16 K or 0 °C to 660,323 °C, as applicable) and those calculated from the sub-ranges shown, using the same calibration data. (Figures prepared by K. Hill)
Sections 1.2.6, 1.3.2.

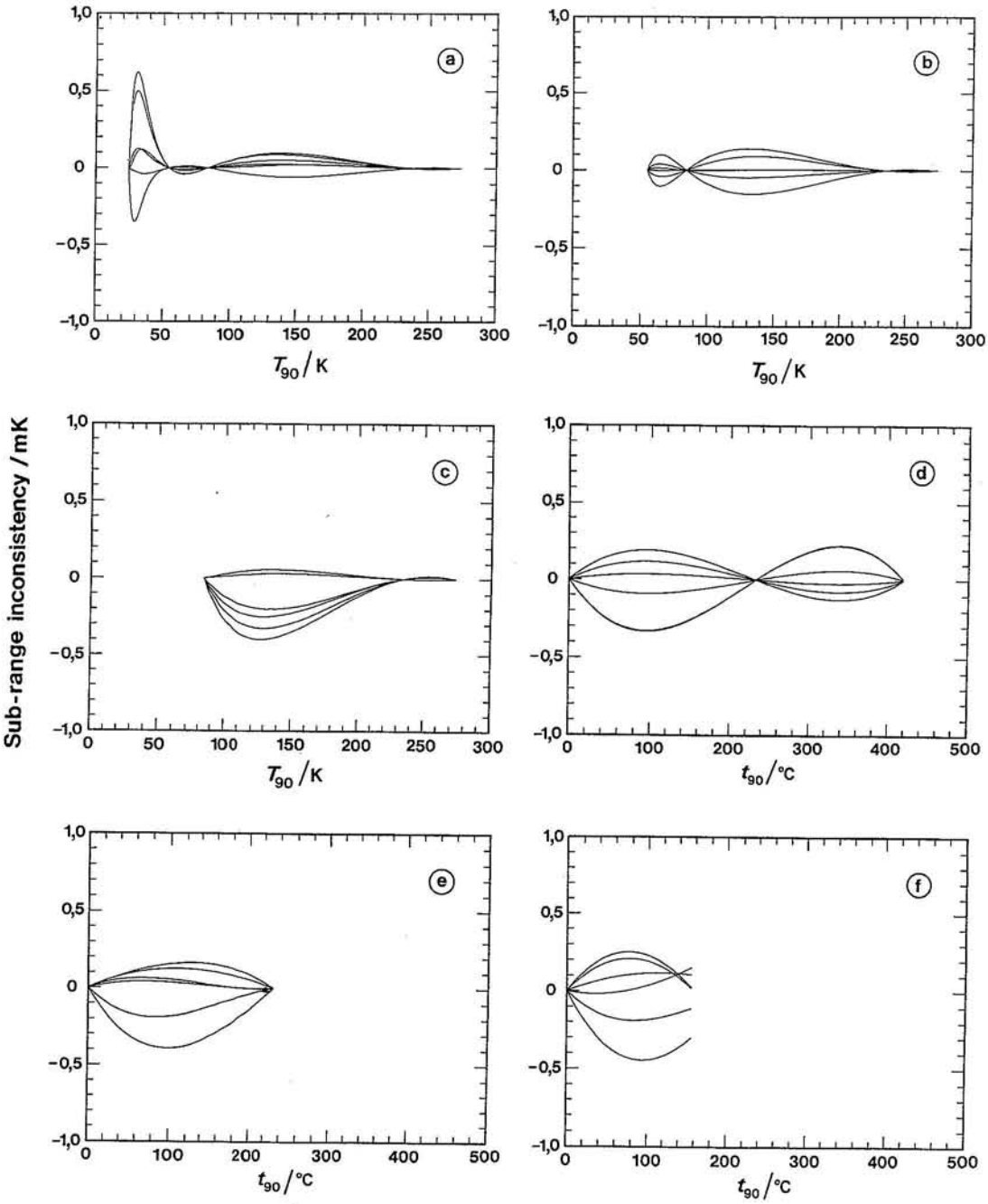

(a)	24,5561 K to 273,16 K	(d)	0 °C to 419,527 °C
(b)	54,3584 K to 273,16 K	(e)	0 °C to 231,928 °C
(c)	83,8058 K to 273,16 K	(f)	0 °C to 156,5985 °C

Figure 1.7 The effect of 1 mK errors (0,1 mK for H_2O triple point) at the calibration points in the platinum resistance thermometer range of the ITS-90. (Figures prepared by K. Hill (a and c to i) and B.W. Mangum (b)) Section 1.3.3.

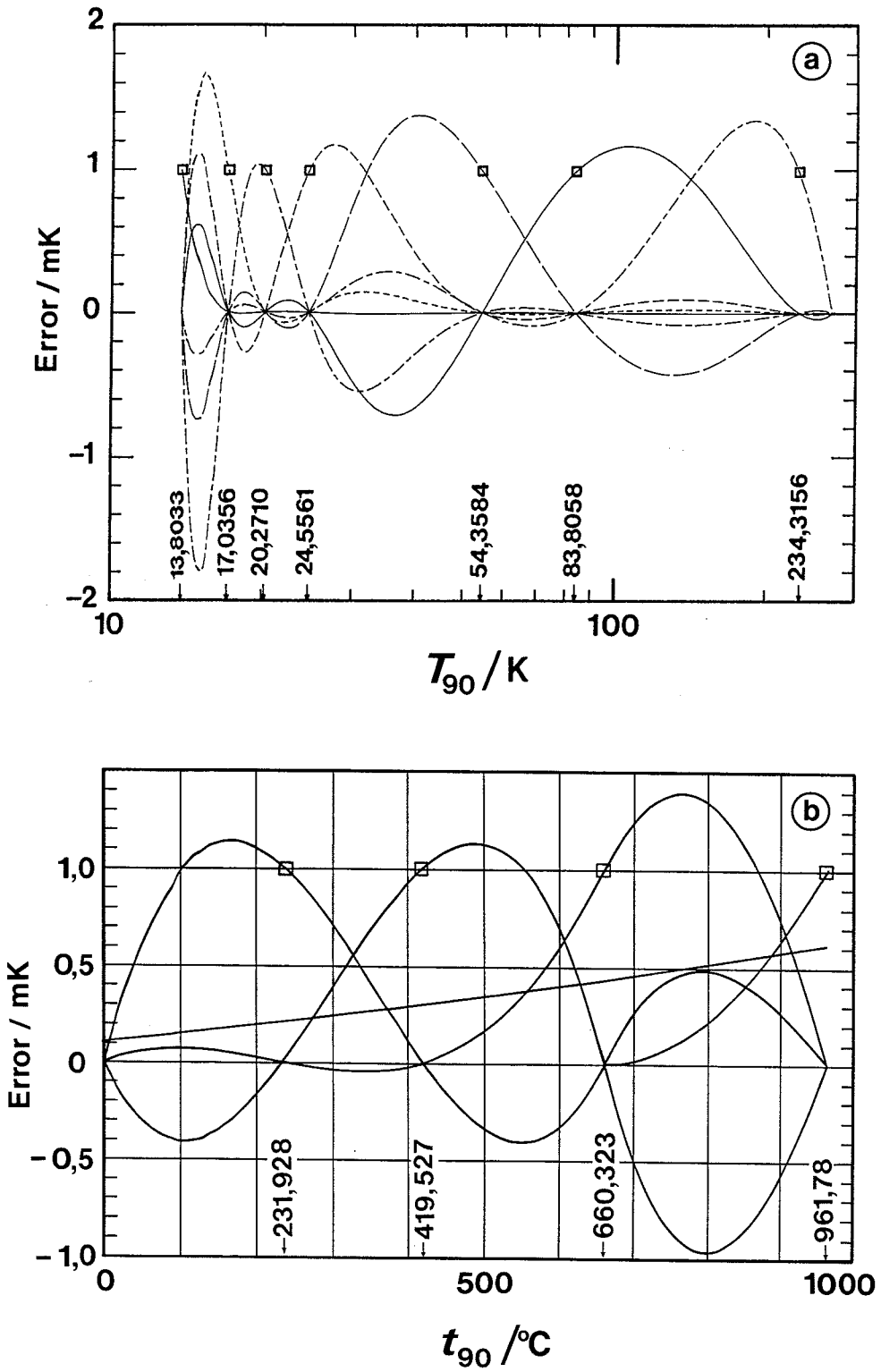

(a) Full range, 13,8033 K to 273,16 K

(b) Full range, 0 °C to 961,78 °C

Figure 1.7 (continued)

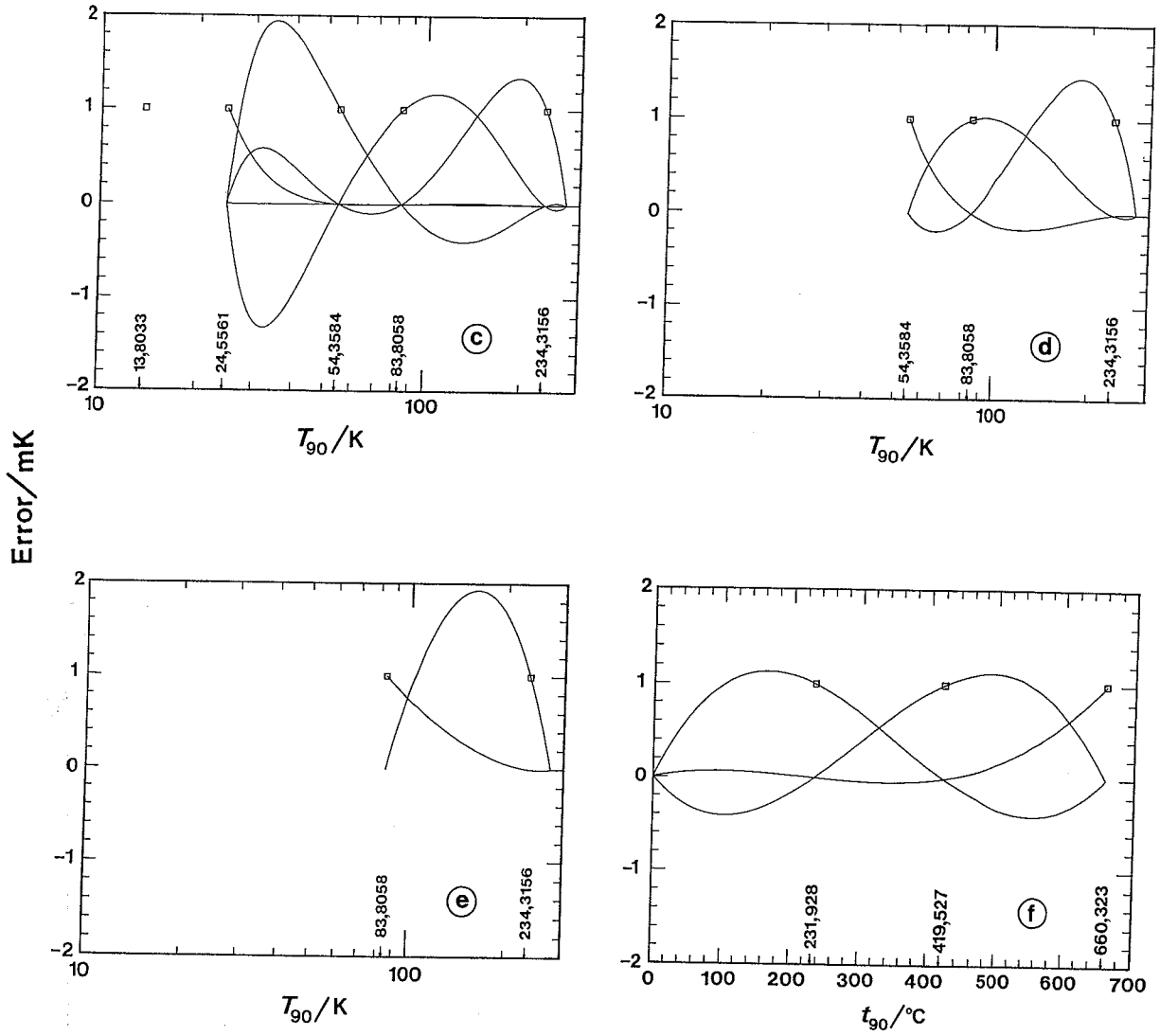

(c) Sub-range, 24,5561 K to 273,16 K
(d) Sub-range, 54,3584 K to 273,16 K
(e) Sub-range, 83,8058 K to 273,16 K
(f) Sub-range, 0 °C to 660,323 °C

Figure 1.7 (continued)

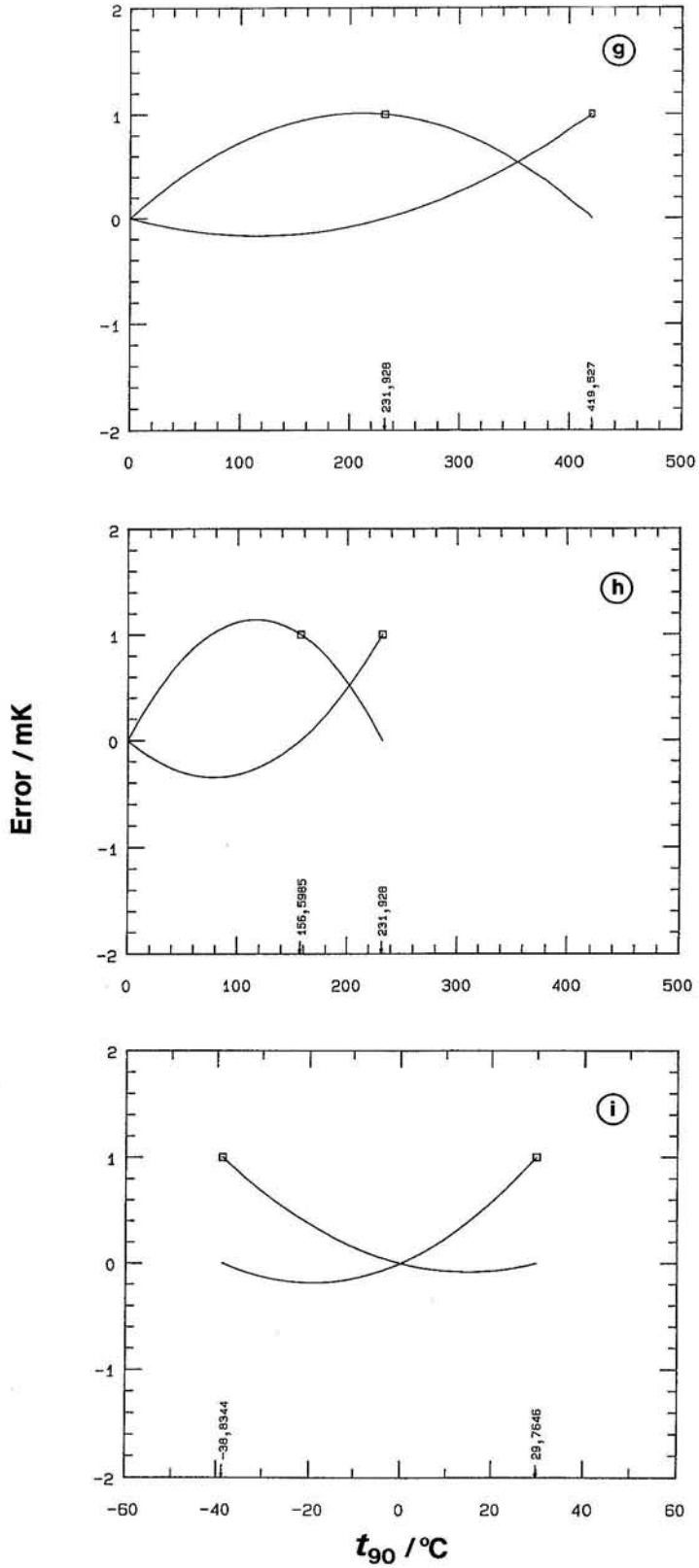

(g) Sub-range, 0 °C to 419,527 °C

(h) Sub-range, 0 °C to 231,928 °C

(i) Sub-range of −38,8344 °C to 29,7646 °C

REFERENCES

Bedford, R.E., Dauphinee, T.M. and Preston-Thomas, H. (1970): Temperature Measurement ; Tools and Techniques in Physical Metallurgy (F. Weinberg ed., Marcel Dekker, New York), Chapter 1, 1-114

Bedford, R.E., Bonnier, G., Maas, H. and Pavese, F. (1984): Recommended Values of Temperature for a Selected Set of Secondary Reference Points ; Metrologia **20**, 145-155

BIPM (1979): EPT-76, The 1976 Provisional 0,5 K to 30 K Temperature Scale ; Metrologia **15**, 65-68

Brickwedde, F.G., van Dijk, H., Durieux, M., Clement, J.R. and Logan, J.K. (1960): The 1958 ^{4}He scale of temperature ; J. Res. NBS **64A**, 1-17

CGPM (1889): Comptes Rendus des Séances de la Première Conférence Générale des Poids et Mesures, 35

CGPM (1927): Comptes Rendus des Séances de la Septième Conférence Générale des Poids et Mesures, 94-99

CGPM (1948): Comptes Rendus des Séances de la Neuvième Conférence Générale des Poids et Mesures, 89-100

CGPM (1960): Comptes Rendus des Séances de la Onzième Conférence Générale des Poids et Mesures, 124-133

CGPM (1967-68): Comptes Rendus des Séances de la Treizième Conférence Générale des Poids et Mesures, A1-A24.

CGPM (1975): Comptes Rendus des Séances de la Quinzième Conférence Générale des Poids et Mesures, A1-A21

CGPM (1987): Comptes Rendus des Séances de la Dix-Septième Conférence Générale des Poids et Mesures, 67-69, 101

CIPM (1887): Procès Verbaux des Séances, 85

CIPM (1989): Procès Verbaux de la 78e Session

De Groot, M.J., Peters, C.M.A.A., Bloembergen, P. (Submitted to Metrologia)

Durieux, M., Astrov, D.N., Kemp, W.R.G. and Swenson, C.A. (1979): The Derivation and Development of the 1976 Provisional 0,5 K to 30 K Temperature Scale ; Metrologia **15**, 57-63

Hall, J.A. (1955): International Temperature Scale ; Temperature, Its Measurement and Control in Science and Industry (Reinhold, New York) **2**, 115-121

Mangum, B.W., Pfeiffer, E.R. and Strouse, G.F. (1990): Non-uniqueness of some Standard Resistance Thermometers over the Temperature Range from 13,8 K to 1235 K ; Tempmeko-90, Finnish Society of Automatic Control, 17-36.

Pfeiffer, E.R. and Kaeser, R.S. (1982): Realization of the 1976 Provisional 0.5 K to 30 K Temperature Scale at the National Bureau of Standards ; Temperature, Its Measurement and Control in Science and Industry (American Institute of Physics, New York) **5**, 159-167

Preston-Thomas, H. (1976): The International Practical Temperature Scale of 1968 Amended Edition of 1975 ; Metrologia **12**, 7-17

Preston-Thomas, H. (1990): The International Temperature Scale of 1990 (ITS-90) ; Metrologia **27**, 3-10 and 107

Quinn, T.J.(1990): Temperature, 2nd edition ; Academic Press (London), 495 p.

Rusby, R.L. (1990): Private communication

Rusby et al. (1991): The Thermodynamic Basis of the ITS-90 ; Metrologia **28** (in press)

Sydoriak, S.G., Sherman, R.H. and Roberts, T.R. (1964): The 1962 He^3 Scale of Temperature, Parts I to IV ; J. Res. NBS **68A**, 547-588

2. FIXED POINTS

This section describes ways of realizing the defining fixed points of the ITS-90. A number of precautions must be taken if the highest accuracy is to be achieved. However, techniques to achieve this accuracy evolve as new measuring instruments become available, as improved thermometers are developed, and as new information is gained on the behaviour of the various fixed points. The information given here was prepared in 1990 and should, therefore, be supplemented in later years by referring to the up-to-date literature. This will include the Working Documents of the most recent meetings of the CCT : these are available from the BIPM.

The defining fixed points of the ITS-90 are given in Table 1-1.

Above the triple point of water the assigned values of temperature are for equilibrium states at a pressure p_0 = 101 325 Pa (one standard atmosphere). Hydrostatic pressures within fixed-point cells produce small but significant temperature effects ; these are summarized in Table 2.1 (and such effects are illustrated in Figures 2.14 and 3.4).

2.1 Triple Point of Water (0,01 °C)

An operating triple-point cell contains ice, water, and water vapour, all of high purity and of substantially the isotopic composition of ocean water. Naturally any water triple-point cell must be assembled with scrupulous attention to the requirement that the water remain free of impurities.

Sealed glass cells for measurements with long-stem thermometers usually contain between 400 and 500 cm^3 of water and are placed in a bath of crushed ice (Figure 2.1). Using this simple apparatus it is possible to achieve a reproducibility better than 0,1 mK [Furukawa and Bigge (1982)]. The same cells are also used for triple-point measurements with capsule-type thermometers with an electrically insulating thermal contact liquid, such as paraffin, in the central well (this is still the most common technique). Cells are available commercially, but for construction details see Barber *et al.* (1954).

Alternatively an all-metal sealed cell containing about 1 cm^3 of water may be used in a cryostat (Figure 2.2). These are not at present

(1990) commercially available but can be readily constructed in the laboratory : *see* Ancsin (1982), Hermier and Bonnier (1987).

2.1.1 Isotopic Composition

Variations in the isotopic content of naturally occurring water can give rise to detectable differences in the triple-point temperature. Ocean water contains about 0,16 mmol of ^{2}H per mole of ^{1}H, and 0,4 mmol of ^{17}O and 2 mmol of ^{18}O per mole of ^{16}O ; this proportion of heavy isotopes is almost never exceeded in naturally-occurring water. Continental surface water normally contains about 0,15 mmol of ^{2}H per mole of ^{1}H ; water coming from polar snow or glacial ice may occasionally contain as little as 0,1 mmol of ^{2}H per mole of ^{1}H.

The purifying of the water may slightly modify its isotopic composition (distillation normally entails a decrease in the ^{2}H content), and the isotopic composition at an ice-water interface is very slightly dependent on the freezing technique.

A decrease of 10 μmol of ^{2}H per mole of ^{1}H corresponds to a decrease of temperature of the triple point of 40 μK ; this is the difference between the triple points for ocean water and the normally occurring continental surface water. The extreme, and quite atypical, difference in the triple-point temperatures of naturally-occurring water is about 0,25 mK and is that between sea water and water obtained from melted old polar ice.

2.1.2 Hydrostatic Pressure Effects

At a depth l metres below the liquid surface (where the true triple point temperature exists) the equilibrium temperature t_{90} at the solid-liquid interface is given by $t_{90} = A + Bl$, where $A = 0{,}01$ °C and $B = -7{,}3 \times 10^{-4}$ m^{-1} °C (*see* Table 2.1).

2.1.3 Preparation of the Triple Point in a Glass Cell

The triple-point temperature of a freshly prepared glass cell can be slightly low (initially of the order of 0,5 mK), *see* Figure 3.4 (c) ; *the cell*

should therefore be prepared at least one day prior to its use. The reason for this low initial temperature and the subsequent gradual increase during one or two days to a steady value is not clearly established but is believed to be connected with structural strains that are produced when the ice is first frozen ; presumably the strains are relieved with time as the ice anneals. The amount by which the initial temperature is too low and the rate of increase to a steady temperature value are to some extent dependent upon the cell preparation technique [Berry (1959)].

2.1.3.1 Standard Cooling Method to Form the Ice Mantle

A glass triple-point cell (Figure 2.1) is prepared for use by first drying thoroughly the re-entrant well and sealing it with a rubber stopper, then cooling the cell (to about 2 °C) by immersion in an ice bath for at least one hour. After the cell has been pre-cooled in an ice bath, it is withdrawn prior to preparing an ice mantle around the re-entrant well. The ice mantle is readily formed by filling the well with crushed solid carbon dioxide up to the level of the water surface in the cell ; alcohol (or some equivalent) may be added to the well along with the CO_2 to promote heat transfer. If solid CO_2 is not available, an immersion cooler may be used for forming the ice mantle: for example, a metal rod precooled in liquid nitrogen that is inserted into the heat transfer liquid in the thermometer well (several insertions will be needed to produce an adequate mantle). However, this method is more likely to lead to a cracked or uneven ice mantle than is the solid CO_2 method [Foster (1972)].

The initial freezing of water within the triple-point cell will occur several degrees below the triple point as a result of supercooling. When the water starts to freeze, fine needle-crystals (dendrites) of ice protrude from the wall of the well into the liquid. The dendrites quickly cover the well but are soon replaced by a clear sheath of ice that thickens to a 4 to 8 mm ice mantle in about 10 to 20 minutes. It is important to keep the solid CO_2 compacted and topped up until the ice is at least 4 mm thick ; this may be accomplished by gently tapping the outside of the cell and from time to time adding more CO_2. If the solid CO_2 level in the well is allowed to fall more than a few centimeters before the well is refilled, the ice mantle is likely to crack: the correct triple-point temperature may not be realized if a crack in the ice mantle extends from the well surface into

the surrounding liquid water. In the process of introducing solid CO_2 into the well some of it may be deposited around the top of the cell, causing the water within the cell to freeze solidly across the top. This top layer of ice should be melted immediately, as any subsequent freezing of water below it can result in sufficient pressure to rupture the cell. The melting can be accomplished by warming its top with the hands while gently shaking it from side to side so as to "wash" the region with the cell water.

A mantle that is thicker at the bottom of the well can be formed by returning the cell to the ice bath before the CO_2 has entirely sublimed or by adding a small amount of CO_2 to the well while watching the mantle grow. A mantle that is thicker at the bottom of the well is advantageous whenever many thermometers must be calibrated: this is because of the consequent relatively high rate of melting of the lower part of the mantle.

2.1.3.2 Alternative Cooling Methods

The probability of encountering the defects mentioned above can be greatly reduced by a minor change in the procedure but at the cost of an increase in the time needed to form the mantle. A glass tube, sealed at the lower end, is placed in the dried reentrant well and crushed carbon dioxide is placed in the inner tube. This reduces the rate of cooling of the ice mantle and reduces the consequent strain in the ice, and also reduces the freezing rate on the free water surface. Precooled alcohol can be used as a heat transfer fluid between the tube and the well. A heat pipe cooling device [Evans and Sweger (1969)] can be used instead of the inner tube, and is especially effective in re-establishing a mantle which has melted excessively at the bottom.

2.1.3.3 Generating the Defining Water-Ice Interface

For either of the above methods, when the ice sheath is fairly uniform and has become 4 to 8 mm thick, any remaining alcohol or CO_2 in the well should be carefully poured out or allowed to sublime completely. Water pre-cooled to 0 °C is then used to flush the alcohol from the well. Finally the well is filled with fresh, precooled water and stoppered, and the cell is placed in its operating position in the ice bath. During the freezing process the magnifying action of the cylinder of water will give

the impression that the cell is, or is about to be, frozen solid with ice even though the coating of ice on the well may still be as little as 1 or 2 mm thick. If the cell is inverted, or temporarily immersed in a large beaker of water, the true thickness of the ice may be seen. (The cell should not be inverted after the "inner-melt", described in the next paragraph, has been made).

After the formation of the ice mantle, a second ice-water interface, the temperature-defining interface, is formed by melting the ice immediately adjacent to the well surface. This "inner melt" can be made, for example, by inserting a glass rod at ambient temperature into the well for a few seconds. A test for the existence of the ice-water interface over the entire interior surface of the mantle is to give the cell a small rotational impulse ; the ice mantle should rotate freely around the axis of the thermometer well. The inner melt should be remade on each occasion on which the cell is used, and the test for the existence of a free mantle should be carried out regularly during the course of a day.

2.1.3.4 Maintenance and Life-Time of a Triple Point Realization

In storage ice will form on the surface of the water in the cell as a result of heat transferred via the vapour to the cold glass, which is often at 0 °C. When a cell is not disturbed for several days the ice will freeze completely across the top surface and must be melted back (for example by warming with the hands) before the cell ruptures. Care must be taken to warm the water as little as possible so as not to melt too much of the mantle.

The ice mantle can stick to the well, and sometimes this recurs very soon after it is initially melted free. This probably is also due to cooling via the vapour, resulting in the freezing of the top of the inner liquid layer. Pressure can then build up in this layer and observed temperatures can be low by as much as 0,1 mK. The mantle must, of course, again be freed by the temporary insertion of a warm rod in the well.

The above effects are much reduced by insulating the cell from the ice bath. This can be done by using a plastic container with foam plastic spacers to ensure that there is an air gap of about 1 cm between the cell and the container wall (*see* Figure 2.1). A cell stored in this way can be used for many months with very little attention beyond maintaining the ice bath (*see* Section 2.1.3.5)

2.1.3.5 Operating Conditions

Figure 2.1 shows a triple-point cell immersed in an ice bath. A cover is placed over the bath to reduce melting of the ice and prevent visible and infra-red radiation from penetrating the ice and reaching the thermometer [McLaren and Murdock (1966)]. Heavy felt cloth is adequate for this ; more effective thermal insulation can be provided by a combination of aluminium foil and several centimetres of foam plastic.

Five centimetres of polystyrene foam is used as a lid when the bath is not being used, and a drain from the bottom continuously removes all melted water. After the bath has been refilled with shaved ice, a layer a few millimetres thick gradually melts away from the walls and the air gap produced then reduces further melting. This type of container needs repacking with ice every two or three days. Any surface contamination on the ice is removed by the water draining from freshly melting ice at the top. Such an ice bath can remain within 1 mK or so of 0 °C with no special precautions about cleanliness as long as the ice is made from reasonably pure water (e.g. most sources of tap-water).

To provide adequate heat transfer to the thermometer, sufficient precooled distilled water should be placed in the well to bring its surface to approximately the same level as that of the free water in the cell when the thermometer is in place in the well. Other heat transfer liquids, such as paraffin, should be used for capsule-type thermometers that have exposed leads.

The thermometer should be precooled for at least 5 minutes in an ice bath before it is inserted in the triple point cell ; it is convenient to keep a clean glass tube containing water in the ice for this purpose, hence avoiding damage to the thermometer and ensuring that no ice particles stick to the thermometer and enter the well. The thermometer current should be switched on as soon as practicable after immersion of the thermometer in the cell to allow the self-heating effects to stabilize. Most thermometers are stable to within 0,1 mK after 5 minutes immersion ; those with larger sensors or poor thermal characteristics may take 10 minutes or more to reach equilibrium.

Self heating effects i.e. effects of Joule heating by the measuring current (Section 3.2.5), for a 25 Ω thermometer are typically of the order of 1 mK/mA^2. Of this amount, about 0,2 mK/mA^2 is external to the thermometer sheath with a 13 mm well containing water and a 7,5 mm

diameter thermometer, and this can be reduced by a factor of 5 by placing a close-fitting aluminium bushing around the thermometer (*see* Figure 3.5).

Routine calibrations of thermometers in triple point cells have an estimated standard deviation of less than 0,15 mK using a single current. Careful measurements using two currents and extrapolating to zero power yield an estimated standard deviation of less than 50 μK. Reproducibility (one standard deviation) for a single cell may approach 10 μK [Furukawa and Bigge (1982)] *see* for example Figure 3.4 (a).

2.1.4 The Realization of the Triple Point in a Sealed Metal Cell

The triple point obtained using a sealed metal cell, such as that shown in Figure 2.2, is highly reproducible and agrees within 0,1 mK with the value obtained in glass triple point cells. Capsule-type thermometers may be measured in glass triple-point cells as described above (with an electrically insulating heat transfer liquid in place of water) and the results can be of a quality similar to that obtained for long-stem thermometers. Capsule-type thermometers may exhibit a higher degree of reproducibility in metal cells such as those described by Ancsin (1982), Pavese and Ferri (1982) and Hermier and Bonnier (1987). An example of a triple-point-of-water realization in a sealed metal cell is shown in Figure 2.3. For general conditions of use and operating parameters *see* Section 2.3.3

2.2 Metal Fixed Points

All metal fixed points must provide a continuous liquid-solid interface that, as nearly as is practical, encloses the sensing element of the thermometer being calibrated. In the special case of radiation thermometry where there is, strictly speaking, no sensing element, the equivalent requirement is the substantially complete enclosure of the blackbody radiator.

As in the case of water triple point cells, for metal fixed points used for resistance thermometry two liquid-solid interfaces are generally induced. In such a situation, the outer interface advances slowly as the liquid continues to solidify. Ideally this generates a shell that continues to be of uniform thickness completely surrounding the liquid, which itself

surrounds the inner liquid-solid interface that is adjacent to the thermometer well. The inner interface is essentially static except when a specific heat-extraction process takes place: e.g. the insertion of a cool replacement thermometer. Uniformity of thickness of the solid shells has been verified by decanting melts after various amounts of freezing at a variety of cooling rates and examining the closed cylindrical shells remaining in the crucible. The existence of these shells attests to, and is sufficient evidence of, the nearly-ideal freezing environment. It is the temperature of the inner liquid-solid interface which is measured by the thermometer. The equipment and the varying techniques required in the generation of these interfaces, together with some methods of checking the quality of the results, are described below.

The particular constructions of apparatus described in Section 2.2.1 and Section 2.2.3 have been successfully employed for measurements of the highest accuracy: it is not suggested, however, that these are the only constructions capable of giving such results [*see* for instance McLaren (1962), Evans and Wood (1971), Chattle (1972), McAllan and Ammar (1972), Furukawa (1974)].

2.2.1 Crucible Assembly

For most metal freezing points for resistance thermometry below 1100 °C, the metal ingot is contained in a cylindrical graphite crucible of high purity. For mercury, however, stainless steel or borosilicate glass is used, while for gallium a container of polytetrafluorethylene (PTFE or Teflon) is generally preferred. Typically (Figure 2.11 and 2.12) the crucible is about 5 cm in diameter and should be more than 20 cm in length ; the liquid metal depth to the thermometer tip should be not less than 20 cm if the highest accuracy measurements are to be possible. For a discussion on thermometer immersion *see* Section 3.2.4. The metal ingots used for resistance thermometer calibration normally have a volume of the order of 100 to 150 cm^3.

The graphite crucible is capped with a graphite lid having a central hole which allows a thermometer well (of pyrex, fused silica, or graphite) to be axially located in the ingot. *After freezing, the ingot should not be allowed to cool significantly (i.e. not more than 50 K) below the freezing point, as this is likely to fracture fused silica or pyrex thermometer wells:*

the ingot should be re-melted and the well in question withdrawn before final cooling. The crucible is contained in a pyrex or fused silica holder long enough to extend to the top of the furnace ; this facilitates control of the atmosphere surrounding the ingot and provides a means for removing the crucible from the furnace. Silica wool insulation (interspersed between graphite disks for temperatures above 400 °C) fills this holder from the top of the crucible to the level of the top of the furnace ; however, in the case of aluminium, graphite wool instead of silica wool has to be used [McAllan and Ammar (1972)].

The holder is sealed at the top with a stainless-steel or brass head that provides for the introduction of a suitable gas: helium or nitrogen may be used for tin and zinc ; argon is used at higher temperatures and may of course be used at any. The oxygen and water content of the gas should in general not exceed ten parts per million, and for metals where reactions are known to occur with these gases (e.g. Al, Ag, Cu) it should preferably be at the one part per million level or better.

Except in the regions alongside and a little above the sensor, the outer surfaces of both the holder and the well should be roughened so as to prevent heat loss by "radiation piping". *See* also Section 3.2.6 for the effects of radiation heat loss down the sheaths of platinum resistance thermometers.

Sealed metal freezing-point-cells [Furukawa (1974), Sostman (1977), Ancsin (1985, 1989), Crovini *et al.* (1987), Nubbemeyer (1990)] are increasingly coming into use. In these cells, *see* Figure 2.13, the fused silica (or Vycor) holder and the re-entrant well of the same material are sealed together, forming one integral part hermetically enclosing the graphite crucible, the graphite re-entrant well, and the metal ingot under pure argon at the appropriate pressure.

A detailed description of the filling procedure for a sealed cell assembly suitable for In, Sn, Zn, Al and Ag is given, in Section 2.2.4.8.

For an optical-pyrometry fixed point the cylindrical graphite crucible is constructed with a re-entrant graphite blackbody cavity of high emissivity immersed in the metal ingot. Typical constructions are shown in detail in Figures 2.5a and 2.5b. The crucible (about 5 cm diameter by 12 cm long) is preferably so formed that the freezing or melting metal extends well forward of the radiating aperture: this is to ensure that the entire cavity, including the region near the aperture, is maintained at the temperature of the freezing metal. The volume of metal required is about

50 cm^3. Because the pyrometer must have an unobstructed view of the cavity aperture, the crucible is not contained in any holder. During operation pure nitrogen or argon (having less than 50 parts per million of O_2) is allowed to flow slowly (0,1 litre per minute) along the core from the rear so as to inhibit oxidation of the graphite.

2.2.2 Metal Ingot Purity

For calibration of a standard platinum resistance thermometer to the highest possible accuracy, all metal ingots should be nominally 99,9999% pure. Freezing-point temperatures below 420 °C should then be within one or two tenths of a millikelvin of that of an ideally pure ingot. Zone-refined Sn and Zn with a purity of 99,999% will usually allow calibration to within 1 mK, but this depends upon the particular impurities present, but *see* Connolly and McAllan (1980) for a discussion on this question. With Al, Ag, Au and Cu a purity of 99,999% will usually result in an error of a few millikelvins.

2.2.3 Furnaces

2.2.3.1 Medium-Temperature Furnace (In, Sn, Zn)

A furnace suitable for metals which freeze below 500 °C is shown schematically in Figure 2.6.

The tube containing the crucible fits into an aluminium block which is centred in an alumina tube heated by a nickel/chromium winding which is powered by a regulated supply. It is useful to have end heaters in addition to the main heater, although these may not be necessary for measurements on a thermometer having good immersion characteristics.

2.2.3.2 High-Temperature Furnace for Resistance Thermometry (Al, Ag)

Figure 2.7 shows a high-temperature freezing-point furnace [McLaren and Murdock (1979)]. It differs from the medium-temperature furnace of Section 2.2.3.1 in the following ways: an inconel lining tube is used or, preferably, a heat pipe ; there may be end-heater windings, each with a

separate regulated power supply ; fused-silica fabrics and sleevings are used as electrical insulations for the heater windings which can be made from chromel or nichrome up to 1000 °C, while Kanthal[2.1] is preferred above this temperature ; there are stainless steel and inconel radiation shields. Bottom and top supports for the furnace block are inconel and the outer and inner insulation materials are Santocel (puffed silica gel) powder and silica-wool respectively ; exterior water cooling is desirable in air conditioned laboratories.

When using resistance thermometers with ac bridges at frequencies above 10 Hz it is advantageous to have non-inductive windings for the heaters. Control systems should be designed so that any switching is done at zero current, to reduce electrical interference ; interference is adequately suppressed if there is no change in the measurement when the furnace power is switched off for a short period. Currently, practical dc regulators are nearly two orders of magnitude more precise in their operation than their ac counterparts, and for thermometry of highest precision a heat-pipe liner is recommended having a single winding (no end heaters) with direct current heating. The temperature ranges over which a heat pipe may be used as an efficient furnace muffle are shown in Table 2.2.

2.2.3.3 High-Temperature Furnace for Radiation Thermometry (Ag, Au, Cu)

The copper, gold, and silver freezing points can be realized in a resistance-heated furnace such as that shown in Figure 2.8 [Ohtsuka and Bedford (1982)]. A suitable winding for the refractory furnace tube would be about 45 turns of 1 cm by 0,04 cm Kanthal ribbon uniformly wound along the length. A cylindrical tube of inconel or, preferably a sodium-filled inconel heat-pipe liner should be placed inside the furnace tube. A graphite blackbody and crucible assembly containing the metal is placed inside the liner. Additional blocks and rings of graphite (scavenger rings) serve to keep oxygen from reaching the crucible. A monitoring platinum 10% rhodium-platinum thermocouple enclosed in a fused-silica sheath extends to the back of the crucible. Except on the axis along which the pyrometer views the blackbody, the front and rear of the crucible

2.1 These are suitable commercial alloys. Equivalent nickel chromium alloys are available and may be substituted.

assembly are insulated with inconel heat shields and quartz wool. The furnace is insulated with quartz wool and is water-cooled.

During operation pure nitrogen or argon (having less than 50 parts per million of O_2) is arranged to flow slowly (0,1 litre per minute) along the tube from the rear so as to inhibit oxidation of the graphite.

Such a furnace will operate continuously above 1000 °C for many weeks with little deterioration of the graphite of the blackbody and with only occasional need for replacement of the graphite scavenger rings.

2.2.4 Realizations of Metal Fixed Points for Resistance Thermometry

The following sections describe ways of obtaining metal fixed points having extended regions of reproducible and virtually uniform temperature. There will be very slight vertical temperature gradients resulting from the effect of hydrostatic pressure on the equilibrium temperatures of the liquid-solid interface being measured [McLaren and Murdock (1960)], *see* Table 2.1 and Figure 2.14. The thermometer must be adequately immersed, *see* Section 2.2.6.3 and 3.2.4 and Figure 3.4.

The most accurate realization of a solid-liquid phase transition in a metal is generally in the liquid-to-solid direction, i.e., a freeezing point. The highest accuracy measurements are greatly facilitated by establishing a second, essentially static, solid-liquid interface immediately surrounding the thermometer well (*see* Section 2.2).

It should also be remembered that for the highest accuracy measurements account must be taken of the fact that neither melting nor freezing plateaus are at a constant temperature over the whole of their length. This may be done, after careful examination of the shape of the melting or freezing plateau, either by excluding the first and last 15% to 20% and taking an average of the remainder or by specifying that the required temperature is that at which a particular fraction, say 50%, of solid is melted or frozen (*see* also Section 2.3.3). Only then are the highest accuracies (often approaching 0,1 mK) attainable.

For many purposes, where very high accuracy is not required, the melting point is a suitable alternative to the freezing point, and because this eliminates effects such as nucleation and supercooling it is often easier to realize. It can be especially useful when large numbers of calibrations must be made and an uncertainty of a few millikelvins is not

excessive [McAllan (1982b)]. (Note, however, that for gallium the melting curve is the preferred alternative : *see* Section 2.2.4.2.)

The construction of fixed point cells and the method of filling them for the high accuracy realization of metal melting, freezing and triple points have been described by many authors. In each of the sections that follow appropriate references will be found. Although a single design cannot be adopted for all defining fixed points of the ITS-90 from the triple point of mercury to the freezing point of silver, for Sn, Zn, Al and Ag a common design is appropriate. This may either be of the open crucible type or of the sealed cell type. The advantages of the sealed cell for the realization of metal freezing points, principally ease of handling and protection from external contamination, are leading to their increased use in high accuracy realizations of the ITS-90 although it should be remembered that once sealed the internal pressure can no longer be checked, which is their one disadvantage. In Section 2.2.4.8 a detailed guide is given to the recommended construction and filling procedures.

2.2.4.1 Triple Point of Mercury (234,3156 K)

Mercury with about 1 part in 10^8 total impurity content can be prepared by chemical washing plus triple distillation. At such high levels of purity both freezing and melting techniques yield triple-point values within ± 0,1 mK over most of the liquid-solid range [Furukawa *et al.* (1982), Chattle and Butler (1988)].

As with the realization of the water triple point, a closely controlled environment, e.g., a stirred liquid bath is desirable. If the surrounding temperature is not controlled precisely, or differs markedly from the triple point, thermal insulation must be interposed between it and the sample.

A sealed cell is convenient, as this avoids moisture condensation and contamination. Figure 2.9 shows such a mercury triple-point cell of borosilicate glass in an insulating stainless-steel holder. Mercury triple-point cells of stainless steel are to be preferred however, as mercury in borosilicate-glass cells has been found to supercool about 6 °C, while that in stainless-steel cells supercools only 0,1 to 0,3 °C. The insulation of either type of cell is controlled by varying the pressure in the annular

space between the holder and the cell. Ethyl alcohol is used in the thermometer well to improve the thermal contact with the thermometer.

A solid-CO_2 ethyl-alcohol mixture can be used for cooling, the stainless steel holder being immersed in the cooling mixture ; when the cell temperature reaches the freezing point the annular space is evacuated. When the mercury has begun to freeze or is in the supercooled state, the thermometer is removed and an auxiliary closed-end thin-wall stainless-steel tube is inserted into the thermometer well. Two liquid-nitrogen-cooled glass rods successively inserted into the stainless-steel tube will produce a solid mercury mantle on the thermometer well. The stainless-steel tube is then withdrawn, taking with it any ice that may have been introduced by the glass cooling rods. Finally, the thermometer, which has been pre-cooled in an auxiliary alcohol-filled tube immersed in the solid-CO_2-ethyl-alcohol cooling mixture, is inserted into the thermometer well. With continuous evacuation of the annular space, freezing times of up to 14 hours have been obtained using about 2 kg of mercury in the cell. The reproducibility of the triple point on freezing is better than ± 0,05 mK.

To obtain a melting point, i.e. triple point on melting, the mercury is first frozen rapidly by admitting air to the annular space or with a heat-pipe cooler in the thermometer well. With either method, about 20 to 25 minutes are required from the start of the freezing to its completion. The melting measurements should be carried out either with an annular space around the ingot evacuated, or with the ingot container placed in a plastic foam box to provide adequate thermal insulation. To start the melting measurements, warming rods are introduced or a small heater is used until an inner melt around the thermometer well is obtained. A monitoring thermometer which has been used in earlier measurements will help in testing for the existence of the melting state. Melts lasting up to 24 hours have been obtained depending upon the thermal insulation. *See* Figure 2.10 for typical results.

2.2.4.2 Melting Point of Gallium (29,7646 °C)

Gallium with about a part in 10^7 total impurity content is commercially available. A sample of this purity allows one to achieve an exceptionally stable melting point [Mangum and Thornton (1979), Chattle

et al. (1982), Mangum (1982), Bonhoure and Pello (1983), Arai and Sakurai (1990)]. Gallium melting point cells are commercially available.

The large expansion at solidification (3,1%) makes it desirable to use a slightly flexible construction, so an all-plastic container is commonly used, with the parts joined together by means of a high-vacuum epoxy or a rubber O-ring seal. The plastic is permeable to air, so it is convenient to store and use the cell with the gallium in an atmosphere of pure argon. Gallium shows substantial supercooling, so the solid-to-liquid transition is used rather than the freezing point. The cell shown in Figure 2.11 contains about 900 g of gallium.

The gallium is solidified completely by placing the cell in a vacuum flask filled with crushed ice for at least one hour. If the gallium is initially molten, nucleation may be induced by the repeated insertion of liquid-nitrogen-cooled copper rods in the well (containing a light oil as contact medium) before placing the cell in the vacuum flask.

The solid gallium is then partially melted, for example by using oil at a temperature of about 40 °C. To ensure that a liquid-solid interface is developing both along the outside of the sample and along the thermometer well, the oil is pumped from a circulator through a tube placed in the thermometer well, is allowed to flow uniformly over the outside of the cell, and is then returned to the circulator. The system is left pumping for 10-15 minutes during which time about 25% of the sample is melted. The cell is then transferred to a stirred oil bath which is controlled at a temperature about 0,1 K above the melting-point temperature, where it is suspended in such a way that the plastic container is well-immersed in the liquid. An alternative procedure is to place the cell containing solid gallium in the bath at about 29,9 °C, and to fit a small electric heater in the thermometer well ; approximately 10 W is applied for about 20 minutes in order to create a liquid-solid interface adjacent to the thermometer well.

A thermometer (pre-heated in the oil bath) is inserted and measurements are started about 20 minutes later. Measurements can be made with several thermometers successively on the same melting plateau. Standard deviations in the range from 25 to 85 μK can be achieved for repeated measurements with an individual thermometer [Mangum and Thornton (1979)].

2.2.4.3 Freezing Point of Indium (156,5985 °C)

Freezing-point cells of conventional graphite pattern containing high purity indium (greater than 99,999%) have been described by McLaren (1958) and Chattle and Pokhodun (1989). Sawada (1982) described a triple-point cell made entirely of glass, while Oleinik *et al.* (1984) and Mangum (1989) reported results obtained from PTFE-encased cells.

Indium supercools by 1 K or less, so outside nucleation (*see* Section 2.2.4.4) is usually unnecessary. After melting the ingot, the furnace temperature is stabilised a degree or so below the freezing point. When the temperature indicated by a thermometer in the cell has fallen close to the freezing point the thermometer is withdrawn and allowed to cool for up to 1 minute before being replaced in the cell. The loss of heat to the thermometer is sufficient to cause rapid nucleation with the formation of a thin mantle of solid indium around the thermometer well ; the plateau temperature is quickly reached. Several thermometers may be calibrated sequentially in the same freeze, each being pre-heated to minimise cooling of the mantle around the thermometer well.

The freezing point of a high purity (99,9999%) sample of indium is reproducible to about 0,1 mK [Mangum (1989)].

2.2.4.4 Freezing Point of Tin (231,928 °C)

A large amount of supercooling occurs when high purity tin freezes. Because of this, in order to obtain a suitable constant temperature plateau, it is necessary to induce an "outside nucleated slow freeze". The procedure [McLaren (1957), McLaren and Murdock (1960)] is as follows:

The melted ingot is allowed to cool slowly (less than 0,1 K per minute) until its temperature approaches the freezing temperature of the tin. At this point the pyrex tube holding the crucible of tin and the thermometer is extracted from the furnace block (Figure 2.6) into the throat of the furnace until the top of the crucible is nearly level with the top of the furnace (or, for quicker results but a shorter operating period, extracted completely from the furnace) and is held in this cooler environment until recalescence occurs. The crucible is then immediately lowered into the block, which will still be close to (or may be automatically controlled about 1 K below) the freezing temperature. The

result of this operation is the formation of a solid shell of tin of approximately uniform thickness at the outer walls of the crucible.

The thermometer is then withdrawn from the well for about 1 minute and then replaced. The loss of heat to the thermometer causes rapid nucleation and growth of a mantle of solid tin about 1 mm thick on the thermometer well, the solid-liquid boundary of which constitutes the tin point interface around the sensing element of the thermometer. Thereafter this interface remains nearly stationary ; the bulk of the metal freezes in a cylindrical shell from the crucible walls.

It is important to achieve a high degree of supercooling (> 4 K) for the attainment of the plateau temperatures by means of outside-nucleated slow freezes. High-purity tin should be kept in an inert atmosphere and the ingot should *not* be topped with graphite powder: when graphite powder becomes distributed throughout a sample, inadequate supercooling (< 4 K) may result.

The extent of the supercool appears to depend on the characteristics of the previous overheating. Ingots that are held 10 K above their liquidus points overnight nearly always supercool more than those that are refrozen less than 2 hours after melting. When ingots are held 2 K or less above the liquidus points for 2 hours or less and then refrozen, the observed supercooling is usually less than 4 K. It has also been reported [Marcarino *et al.* (1989)] that satisfactory inner nucleation can be obtained following nucleation induced by a flow of cold nitrogen into the thermometer well.

The freezing point of high purity (99,9999%) Sn is reproducible to within 0,1 mK.

Depending on the thermometer construction, it may require as little as 13 cm or as much as 25 cm immersion in the constant temperature zone, *see* Figure 2.14(a).

2.2.4.5 Freezing Point of Zinc (419,527 °C)

The freezing temperature is obtained as follows [McLaren (1957), (1958)]:

The melted ingot is allowed to cool until nucleation at the outside of the ingot begins, as evidenced by an initial arrest in the cooling curve. The thermometer is then withdrawn from the well for about 1 minute

(during which time the temperature indication drops below 200 °C) and replaced. If the thermometer is held in the room for much more than 1 minute an unnecessarily large amount of the sample is frozen on re-insertion, and the recovery time is extended. The loss of heat to the thermometer causes rapid nucleation and growth of a mantle of solid zinc about 1 mm thick on the thermometer well, the solid-liquid boundary of which constitutes the zinc point interface around the sensing element of the thermometer. Thereafter this interface remains nearly stationary ; the bulk of the metal freezes in a cylindrical shell from the crucible walls.

When many thermometers are calibrated using the same freeze, the thermometers should be pre-heated close to the zinc point to avoid changing the thickness of the solid zinc mantle on the thermometer well. The apparent reproducibility of the freezing point from sample to sample of 99,9999% Zn is of the order of 0,2 mK ; it has been suggested that about half of this amount arises from variations within the thermometer, and that the intrinsic reproducibility of the Zn point is ≈ 0,1 mK.

Melting curves taken after such freezes reveal a "memory" of the freezing plateaus ; i.e., their form is dependent on the rate and method of induction of the preceding freeze. In general, the melting plateaus are not quite as constant in temperature as freezing plateaus but tend to rise a few tenths of a millikelvin for highest purity zinc and up to 3 mK for zinc of lesser purity.

Depending on the thermometer construction, it may require as little as 17 cm immersion in the constant temperature zone ; others require 25 cm immersion, and for some as much as 33 cm remain inadequate, *see* Figure 2.14(b).

2.2.4.6 Freezing Point of Aluminium (660,323 °C)

The ingot should first be completely melted by keeping it at a temperature about 10 °C above the freezing point for about 2 hours.

The ingot is allowed to cool slowly (≈ 0,1 K per minute) below the freezing point. It usually supercools about 0,4 to 0,6 K. When recalescence is observed, the thermometer is removed and the cooled thermometer or a fused-silica rod is re-inserted in order to generate an inner-solid aluminium mantle on the well. The temperature of the furnace should then be set 0,5 to 1 K below the freezing temperature. Depending

upon the purity of the aluminium sample, the temperature plateau is constant to about 0,2 mK over the first 50 percent of the freeze [McAllan and Ammar (1972), Furukawa (1974)]. Graphite wool rather than silica wool should be used above the graphite crucible (*see* Section 2.2.1 and Figure 2.4). Residual water and oxygen, both highly reactive with molten aluminium, must be removed before melting. In addition, the molten aluminium must not be allowed to come in contact with the fused silica container; it will adhere tenaciously to the silica, and the rapidly following chemical reaction may perforate the container.

The reproducibility of this point in any one laboratory is about 1 mK, the measurements being limited by the stability of the thermometers used. Reported results cover a range of 10 mK; however, most of the variation was probably due to non-uniqueness of the IPTS-68 or variation in thermometer characteristics.

2.2.4.7 Freezing Point of Silver (961,78 °C)

The ingot should first be completely melted by keeping it at a temperature about 10 °C above the freezing point for about 2 hours.

The recommended induced-freezing technique is similar to that used for the freezing point of zinc or aluminium. The ingot is allowed to cool slowly (about 0,1 K per minute) below the freezing point; at such a low cooling rate the supercooling never exceeds 0,5 K. When it is evident that a nucleation is taking place (the temperature rise clearly shows the recalescence) the thermometer is extracted from the well and then reinserted after about 1 minute exposure to ambient temperature.

The temperature of the resulting plateau rises to an equilibrium value after about 20% of the total freezing time has elapsed; thereafter it remains constant to within 1 mK or better for about a further 40% of the total freezing time.

The presence of oxygen in the silver will lower the observed freezing temperature. Experiments with argon-oxygen mixtures (up to 1% oxygen) bubbling through the silver have produced liquidus point depressions that were always less than 5 mK. A slope inversion on a melting curve following a very fast freeze is a reliable indication of contamination by oxygen. However, if the ingot is kept in the molten state in an inert gas

the surrounding graphite will effect the complete removal of the oxygen within a few hours [Bongiovanni *et al.* (1975), Takiya (1978)].

2.2.4.8 The Construction and Filling of Sealed Freezing-point Cells Suitable for In, Sn, Zn, Al and Ag

The following notes give a sufficiently detailed description of the preparation of a sealed cell for it to be used as a guide by someone not experienced in this type of work. The numbers preceding each paragraph refer to the numbered parts of Figure 2.12.

Preliminary phase

1 - Bake the high-purity graphite parts (crucible, lid, and well) at a temperature of 20 K or more above the fixed point under preparation ; evacuate the system down to a pressure of 10^{-4} Pa, cool, and fill with pure Ar at about 10^{5} Pa.

2 - Insert the high-purity metal into the crucible, put the lid on the crucible, insert the graphite well through the hole in the lid, letting it rest on the metal block. A quartz press-rod is fed through a vacuum-tight seal and rests on the top of the graphite well. Evacuate the auxiliary quartz vessel to a pressure of 10^{-4} Pa, then fill with pure Ar at a pressure of about 90 kPa[2.2].

3 - Melt the metal block completely ; heat it to a temperature of 10 K or more above the melting point ; push the quartz press-rod downward, until the graphite well reaches the bottom of the crucible.

Second phase of preparation

4, 5 - Degrease the lower and upper part of the quartz sheath shown using ethanol, etch it (5 % fluoric acid, 5 minutes), and rinse about ten times with high-purity water (conductivity, $\gamma \approx 5 \times 10^{-6}$ S/m).

6, 7 - Assemble the two parts of the quartz sheath and the crucible prepared as above ; fuse the quartz parts together. Evacuate the assembled fixed-point cell to a pressure of $\approx 10^{-4}$ Pa by means of a turbo-molecular pump. Insert a calibrated platinum resistance thermometer into the quartz well of the cell. Melt the fixed-point

---

2.2 Due to the high vapour pressure of zinc at its melting point and the tendency of molten aluminium to bond to graphite in vacuum, both of these metals should be melted only in the presence of about one atmosphere of a gas such as argon.

metal completely, until the graphite well floats up from the base of the crucible. Let the fixed-point metal freeze slowly, filling the cell with argon at a pressure of the order of 95 to 100 kPa. While keeping the cell close to the freezing point temperature, seal off the pump tube directly above the furnace (the actual values of the filling pressures and seal-off temperatures, here and elsewhere, should be such that the pressure at the freezing-point temperature is well within 1% of one standard atmosphere, *see* Table 1.1). Allow the cell to cool and seal off the pump tube at its contraction.

Figure 2.13(a) shows such a final fixed point assembly mounted in an inconel-601 cylinder. The cell can easily be removed from the inconel cylinder by pushing a metal rod up through the hole in the bottom of the cylinder. An alternative design by Crovini *et al.* (1987) is shown in Figure 2.13(b): in this latter design, it is necessary to keep the large gas-filled portion of the cell at an average temperature close to (i.e. well within 3 K) of the freezing point so as to ensure that the pressure is sufficiently close to one standard atmosphere.

2.2.5 Realization of Metal Freezing Points for Radiation Thermometry Silver (961,78 °C), Gold (1064,18 °C), and Copper (1084,62 °C)

Accurate radiation thermometry requires a system with an unimpeded optical path between the blackbody cavity and the thermometer ; solid windows of any kind will introduce uncertainties in transmittance and are sources of systematic errors. In the absence of windows, a small quantity of oxygen is likely to be present in the surroundings of the crucible, but this does not necessarily degrade the accuracy of a silver, gold or copper point. A small flow of pure argon is sometimes used (*see* Section 2.2.3.3) [Ricolfi and Lanza (1977)].

2.2.6 Methods of Analysis

2.2.6.1 Purity Check Using Melting Curves

While the freezing plateau is used to provide the most reproducible fixed point temperature, the melting plateau provides a great deal of qualitative information on the content and distribution of impurities in the ingot [Quinn (1990)]. Chemical analysis is useful in the initial selection of high-purity material, but lack of knowledge of all the necessary phase diagrams in the limit of small dilutions makes the application of the results uncertain. The advantage of the melting curve over the freezing curve as a source of information on impurity content and distribution is that there is no equivalent of the supercooling and nucleation effects which distort the first part of the freezing curve. Also, since the diffusion of impurities within the solid during melting is much too slow to allow proper equilibrium (i.e., uniform distribution) to be attained throughout the bulk of the ingot, it follows that the solid ingot retains information concerning segregation of impurities during freezing ; some of this information can be obtained from a comparison of melting curves following various rates of freezing. Many examples are given by McLaren (1962).

Comparisons between cells, as opposed to measurements on a single cell, can be validly undertaken by this method provided that the cells are geometrically similar and are similarly treated.

2.2.6.2 Freeze Evaluation using Temperature Oscillations

The presence of incomplete shells resulting from improperly induced freezes can be detected by applying temperature oscillations to the crucible, the oscillation period being of the order of 30 minutes and the peak-to-peak amplitude at the crucible wall being about 1 K. Resulting small temperature oscillations during either a freezing or melting plateau constitutes clear evidence of the presence of incomplete shells, ***provided*** that the thermometer is adequately immersed, *see* Section 2.2.6.3. On the other hand, if such oscillations are not observed it is clear that the temperature of the thermometer is determined only by the temperature of the liquid-solid interface, the thermal resistance between the coil and the

interface, and the thermometer stem losses [Bongiovanni *et al.* (1975), Takiya (1978)].

2.2.6.3 Immersion Check

An immersion check consists of measuring the thermometer resistance as a function of depth of immersion of the sensor in the ingot. As the sensor is withdrawn the point at which its temperature begins to diverge significantly from that of the ingot, which provides a quasi-constant temperature zone[2.3], is moderately dependent upon the ambient conditions and strongly dependent upon the thermometer construction. With some thermometer constructions, above some limiting temperature it becomes impossible to achieve adequate immersion in ingots of normal size ; for other constructions a moderately small immersion will suffice. Both of these conditions, together with an intermediate one, are illustrated in Figure 2.14, *see* also Section 3.2.4. Ingots are often, indeed usually, too short to provide adequate immersion (20 cm or more) in themselves for many thermometers at the tin, and zinc points: this drawback can be overcome to a certain extent by so adjusting the furnace as to keep an additional 10 cm above the ingot within a few kelvins of the fixed point temperature.

2.3 Cryogenic Fixed Points (13,8 K to 84 K)[2.4]

Of the six cryogenic fixed points dealt with here : all six (H_2, Ne, O_2 and Ar triple points and two H_2 vapour pressure points) are used for calibrations of capsule-type platinum resistance thermometers (*see* Section 3.1.1) ; two (O_2 triple point very rarely and Ar triple point often) are used for calibrations of long-stem platinum resistance thermometers (*see* Section 3.1.2) ; and two (H_2 and Ne triple points) are two of the three points used for calibrations of gas thermometers (*see* Section 5).

2.3 For the unavoidable deviations due to hydrostatic pressure variations *see* Section 2.2.4 and Table 2.1.

2.4 For the fixed point in the liquid helium range *see* Section 4.

The uncertainties quoted for the best vapour pressure point realizations range from 0,2 to 1 mK ; those quoted for triple points are of the order of 0,2 mK.

2.3.1 Vapour Pressure Systems

Vapour pressure (boiling-point) cryostats have been described by several investigators [Compton (1970), Ancsin (1973a), Kemp and Kemp (1978)] ; an example specifically designed for the realization of the boiling points of equilibrium hydrogen is shown in Figure 2.15.

The temperature of the sample must be precisely controlled so that vapour pressure measurements can be made at stable, uniform temperatures.

The vapour pressure above the sample is usually sensed via a vacuum-jacketed capillary tube of about 2 mm bore (which is sufficient to avoid significant errors arising from the thermomolecular pressure effect) and made of a material having a low thermal conductivity. Net radiant influx down the capillary to the surface of the liquid must be prevented, as this would raise the sample temperature above that of the thermometer. No portion of the capillary can be allowed to be colder than the sample or condensation will give rise to spuriously-low vapour pressure readings. It is recommended that the capillary pass through a radiation trap having a temperature very slightly above that of the sample. The temperature distribution along the capillary should be measured, both to ensure that there are no portions of the capillary colder than the sample and also to allow the aerostatic pressure differential between the ends of the capillary to be calculated.

The vapour pressure above a cryogenic liquid may depend on impurities present in the liquid [Ancsin (1973a) ; Compton and Ward (1976)], and may also, because of impurity or isotopic concentration effects, depend on whether gas has been removed from or added to the sample chamber. It is desirable, therefore, that the purity of the gas be measured and that a gas-handling system be used that enables measured amounts of gas to be removed from or added to the sample chamber.

Errors in pressure measurement may contribute significantly to the uncertainty of the boiling point realization. *See* Section 4.4.

2.3.2 Triple-Point Systems

Triple-point systems have the great advantage over boiling-point systems of requiring no pressure measurements. Cryogenic triple points are almost always obtained from melting, rather than freezing, of the sample.

A cryogenic triple-point cell may be refillable, via a more-or-less-permanently connected gas handling and purifying system, or it may be a more robust, permanently sealed unit. The latter type is now almost universally used for triple point realizations.

A sealed triple-point cell must be designed to withstand the pressure arising at the maximum expected temperature (typical room temperature pressures range from 0,5 to 10 MPa). The heat capacity of the container is not of great importance in determining melting curves: it would be important if one were to measure freezing curves, because of the effects of supercooling. Non-sealed cells need not be particularly robust and therefore can have a heat capacity substantially less than that of a sealed cell of comparable sample size.

Cell design should be such as to reduce as far as possible the thermal resistance between the thermometer and the sample, taking due account of the very low thermal conductivities of liquified gases. Heat conduction to the sample can be made sufficiently good, either by subdividing the chamber by a set of closely spaced (about 0,5 mm) horizontal or vertical copper baffles or by using a horizontal, thin pancake-shaped chamber [Ancsin (1973b)]. Other constructions, perhaps more amenable to a thorough cleaning of the inside of the cell, have been reported [Bonnier and Malassis (1975), Mitsui and Inaba (1978), Pavese and Ferri (1982)]. A wide variety of successful designs for use with capsule thermometers is illustrated in Figure 2.16. Some properties of thermometric substances at their triple point when enclosed in a copper cell are given in Table 2.3.

In order to keep temperature gradients low, heat flows in the cell must be extremely small. To this end, the cell is surrounded by one or more temperature-controlled heat shields, the whole being enclosed in a vacuum jacket which is normally immersed in the cryogenic fluid. Several such triple-point cryostats have been described [Ancsin and Phillips (1969), Ancsin (1970), Pavese (1975), Compton and Ward (1976), Kemp *et al.* (1976)] ; one of these is illustrated in Figure 2.17.

Sealed triple-point cells for long-stem thermometers are similar in principle both in design and in operation to those for capsule-type thermometers but are much longer so as to provide adequate immersion for the thermometer. For details of their design and operation *see* Bonnier (1975), (1987), Ancsin and Phillips (1976) and Figure 2.18.

2.3.3 Realization of a Triple Point

The realization of a triple point proceeds as follows: The sample is frozen, thermally isolated, and a series of measured heat pulses applied. The equilibrium temperature is measured after each pulse. A marked diminution in the temperature change per pulse indicates the onset of melting. The transition is observed by further intermittent heating until melting is completed. This is illustrated in Figure 2.19.

A plot (or least-squares analysis) of the equilibrium temperatures as a function of the fraction F of the sample melted gives a well-defined representation of the melting curve. Most melting curves consist of a curved region at the onset of melting, followed by a flat region over which the bulk of the transformation occurs, and finally a region of rapid temperature rise as melting is completed. The shape and transformation temperature of the melting curve depend on the purity of the sample and on the experimental technique used ; a temperature offset may occur, especially towards the end of the plateau, due to the poor thermal conductivity of the liquid phase. The question of deducing the triple-point temperature from an observed melting curve is a difficult and contentious one [e.g. Pavese (1984)]. There are two widely-used methods of deducing this temperature: the first discards the initial and final 15% of this curve and then takes the mean of the remaining 70% as defining the temperature of the triple point. The second plots the $1/F$ values between about five and two, extrapolates this part of the melting curve to $1/F = 1$ (liquidus point) and defines this as the triple-point temperature. In most cases however for the points specified in the ITS-90 the plateaus are sufficiently flat that the ambiguity is small (0,2 mK or less) as is the case in Figure 2.19.

Sealed triple-point cells have been successfully used with all of the low-temperature fixed triple points of the ITS-90, namely H_2, Ne, O_2, Ar, Hg and H_2O

2.3.4 Triple Point (13,81 K) and Vapour Pressure Points (≈ 17,035 K and ≈ 20,27 K) of Equilibrium Hydrogen

Hydrogen has two molecular modifications designated by the prefixes ortho and para. The equilibrium ortho-para composition is temperature dependent and, at room temperature, is about 75% ortho-hydrogen and 25% para-hydrogen ("normal hydrogen"). The term "equilibrium hydrogen" means that the hydrogen has attained the equilibrium composition corresponding to its temperature. On liquefaction the composition changes slowly with time and there are corresponding changes in the physical properties. At the normal boiling point, the equilibrium composition is 0,21% ortho and 99,79% para-hydrogen and the boiling-point temperature of this equilibrium composition is lower than that for normal hydrogen by about 0,12 K. In order to avoid errors in the realization of these fixed points, it is essential that the hydrogen should have the appropriate equilibrium composition. The easiest way of ensuring this is to place a suitable catalyst such as activated ferric hydroxide in the sample chamber. To activate the ferric hydroxide, it is maintained at 115 °C under vacuum for at least 24 hours. After activation the catalyst must be kept in an atmosphere of pure hydrogen. The normal isotopic composition of hydrogen is 0,15 mmol of deuterium per mole of hydrogen. Isotope fractionation may occur which can result in a difference of 0,4 mK between the dewpoint (vanishingly small liquid fraction) and the boiling point (vanishingly small vapour fraction). In practice the boiling point is used since the catalytic action is more efficient if the free liquid is in contact with the catalyst.

The temperature T_{90} as a function of the vapour pressure p of equilibrium hydrogen is given within the ranges 17,025 K to 17,045 K and 20,26 K to 20,28 K by the relations :

$$T_{90}/\mathrm{K} - 17{,}035 = (p/\mathrm{kPa} - 33{,}3213)/13{,}32 \qquad (2.1)$$

$$T_{90}/\mathrm{K} - 20{,}27 = (p/\mathrm{kPa} - 101{,}292)/30 \qquad (2.2)$$

The influence of impurities on the hydrogen fixed points is fairly small. The only impurity having a lower boiling point, He, is easily removed if the gas is pumped away from the solid. Other impurities having a higher boiling point, such as N_2, are probably cold-trapped in the cryostat. The most troublesome impurity is neon, which lowers the triple-point temperature by about 8 μK and the boiling point temperature by

about 1,5 μK for each part per million of neon [Ancsin (1977), Compton (1972), Kemp and Kemp (1979)].

2.3.5 Triple Points of Neon, Oxygen and Argon

The neon triple point is easily realized and very high quality melting plateaus can be obtained [Kemp and Kemp (1978)]. Ancsin (1978) has reported that the triple point of neon is insensitive to volatile impurities (He, H_2) and to the non-volatile impurities O_2 and Ar. However, he found that N_2 impurity can depress the triple point by as much as 2 mK while not necessarily affecting the melting range. Care should therefore be taken with the purity of the neon. Variations in the isotopic composition of natural neon can lead to differences of up to 0,5 mK between samples [Pavese (1984)].

The oxygen triple point is easily realized and is only moderately sensitive to the presence of impurities [Ancsin (1970), Compton and Ward (1976), Kemp *et al.* (1976), (1979), Pavese (1978)]. The effect of various impurities on the triple point temperature of oxygen is given in Table 2.4. The effect of argon contamination, common in commercial oxygen, is an insidious one as it has no effect on the melting range. The manufacturer's specifications for argon content are frequently wrong by as much as an order of magnitude. Increases of 2 to 3 mK in the apparent oxygen triple-point temperature due to argon impurity have been observed [Pavese *et al.* (1984)].

The argon triple point is very easily realized. It is moderately sensitive to the presence of impurities, the triple-point temperature being lowered by as much as 30 μK per part per million of impurities such as O_2, N_2, CO_2, and CH_4 [Ancsin and Phillips (1969), Pavese and Ferri (1982)]. However, gas with purity better than 99,9999% is readily available.

TABLE 2.1

Effect of pressure on the temperatures of some defining fixed points[2.5]

Substance	Assigned value of equilibrium temperature T_{90}/K	Temperature variation with pressure, p $(dT/dp)/(10^{-8}\ K \cdot Pa^{-1})$[2.6]	Temperature variation with depth, l $(dT/dl)/(10^{-3}\ K \cdot m^{-1})$[2.7]
e-Hydrogen (tp)	13,8033	34	0,25
Neon (tp)	24,5561	16	1,9
Oxygen (tp)	54,3584	12	1,5
Argon (tp)	83,8058	25	3,3
Mercury (tp)	234,3156	5,4	7,1
Waper (tp)	273,16	−7,5	−0,73
Gallium	302,9146	−2,0	−1,2
Indium	429,7485	4,9	3,3
Tin	505,078	3,3	2,2
Zinc	692,677	4,3	2,7
Aluminium	933,473	7,0	1,6
Silver	1234,93	6,0	5,4
Gold	1337,33	6,1	10
Copper	1357,77	3,3	2,6

2.5 The reference pressure for melting and freezing points is the standard atmosphere (p_0 = 101 325 Pa). For triple points (tp) the pressure effect is a consequence only of the hydrostatic head of liquid in the cell.

2.6 Equivalent to millikelvins per standard atmosphere.

2.7 Equivalent to millikelvins per metre of liquid.

TABLE 2.2

Heat pipes

Useful combinations of working fluid, wall material and temperature ranges [after Neuer and Brost (1975)]

Working Fluid	Wall material	Useful temperature range (°C)
Nitrogen	stainless steel	−200 to −163
Methane	copper,aluminium	−170 to −120
Carbon tetrafluoride	copper, aluminium	−170 to −70
Freons	copper, aluminium	−150 to 30
Ammonia	stainless steel, nickel aluminium	−40 to 60
Acetone	copper, stainless steel	−40 to 150
Methanol	copper, nickel	−30 to 150
Water	copper, nickel, titanium, stainless steel	30 to 180
Organic fluids	stainless steel, super alloys, carbon steel	130 to 300
Mercury (with additives)	stainless steel	180 to 500
Caesium	stainless steel, nickel	400 to 600
Potassium	stainless steel, nickel	400 to 200
Sodium	stainless steel, nickel	600 to 1050

TABLE 2.3

Some properties of thermometric substances at their triple points in a copper cell.

Substance	T_{tp} (K)	p_{tp} (kPa)	H_f (J/mol)	d_{tp}/d_{NTP}	λ W m^{-1} K^{-1}	H_f/c_p
e-Hydrogen	13,803	7,034	117	1040	0,103	90
e-Deuterium	18,689	17,079	197	1040	0,123	110
Neon	24,556	43,379	335	1728	0,117	33
Oxygen	54,358	0,1464	444	980	0,196	4,4
Nitrogen	63,151	12,526	720	814	0,161	4,8
Argon	83,806	68,892	1189	980	0,125	6
Krypton	115,776	73	1500	812	0,09	6
Xenon	161,403	81,681	3100	647	0,07	10
Carbon Dioxide	261,590	518	8400	825	0,158	28
Water	273,16	0,61166	6010		5,6	16

T_{tp} = triple point temperature (T_{90}); p_{tp} = triple point pressure; H_f = melting enthalpy; d_{tp}/d_{NTP} = density ratio between the liquid at T_{tp} and the gas at 20 °C and at a pressure of 101 325 Pa; λ = thermal conductivity of the liquid at the triple point, and c_p is the specific heat of copper, so that the last column (H_f/c_p) is a measure of the ability of the melting substance to maintain a mass of copper at the temperature of the melting point.

TABLE 2.4

The change in oxygen triple-point temperature ΔT due to the presence of the more common impurities at a concentration of 1 part in 10^4.

Impurity	ΔT
N_2	−2 mK
Ar	+1
Kr	−0,4
Ne	−0,15
He	+0,15

Figure 2.1 Water triple-point cell, made from glass for use principally with long-stem thermometers, shown in an ice bath.
(1) platinum resistance thermometer, (2) plug of glass wool, (3) water vapour, (4) water, (5) ice, (6) plastic container, (7) crushed ice, (8) opaque cover, (9) thermometer leads, (10) insulating break in stainless-steel container wall, (11) stainless steel containers, (12) polystyrene-foam insulation, (13) air gap (maintained by plastic spacers which are not shown), (14) base containing drain holes, (15) supports, (16) water container.
Section 2.1.

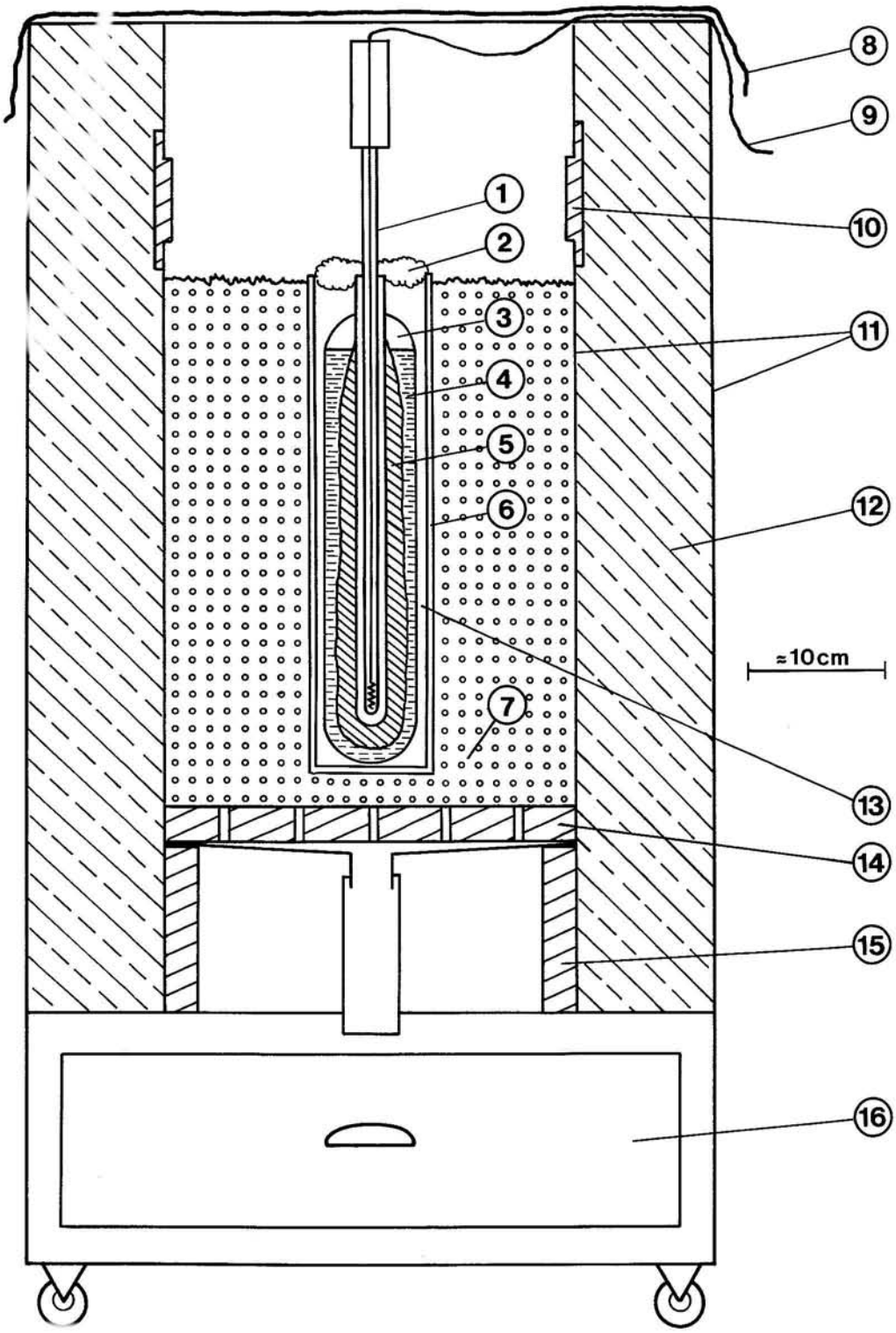

Figure 2.2 A triple-point of water sealed metal cell for use with capsule-type thermometers shown inserted into a multicomponent sealed cell for the realization of the five low-temperature fixed points.
(1) filling tubes, (2) stainless steel multicomponent cell, (3) compartments for samples, (4) copper triple-point-of-water cell, (5) thermometer well [after Hermier and Bonnier (1987)].
Section 2.1.4.

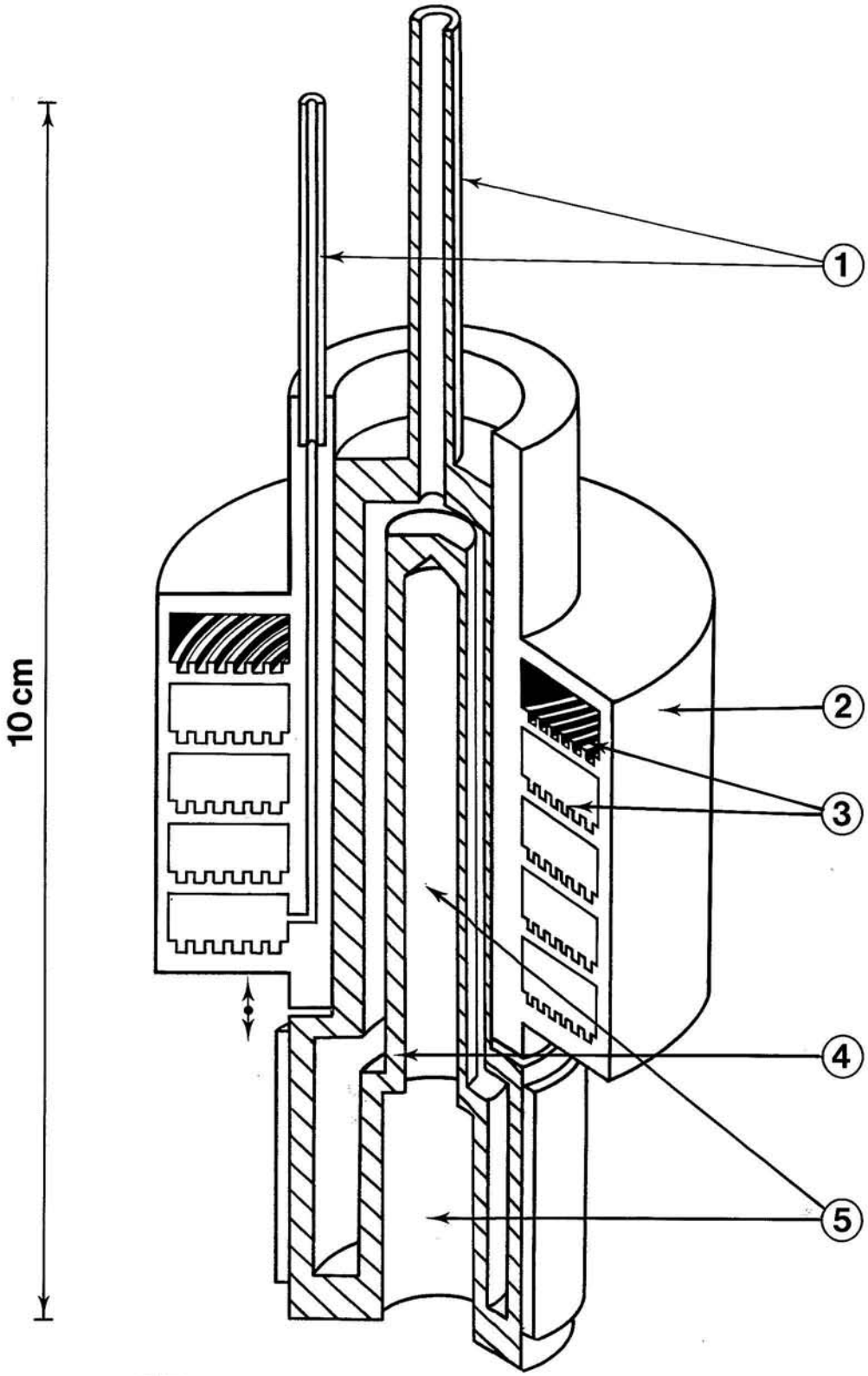

Figure 2.3 A triple-point of water realization using the cell shown in Figure 2.2 [after Hermier and Bonnier (1987)]
Section 2.1.4.

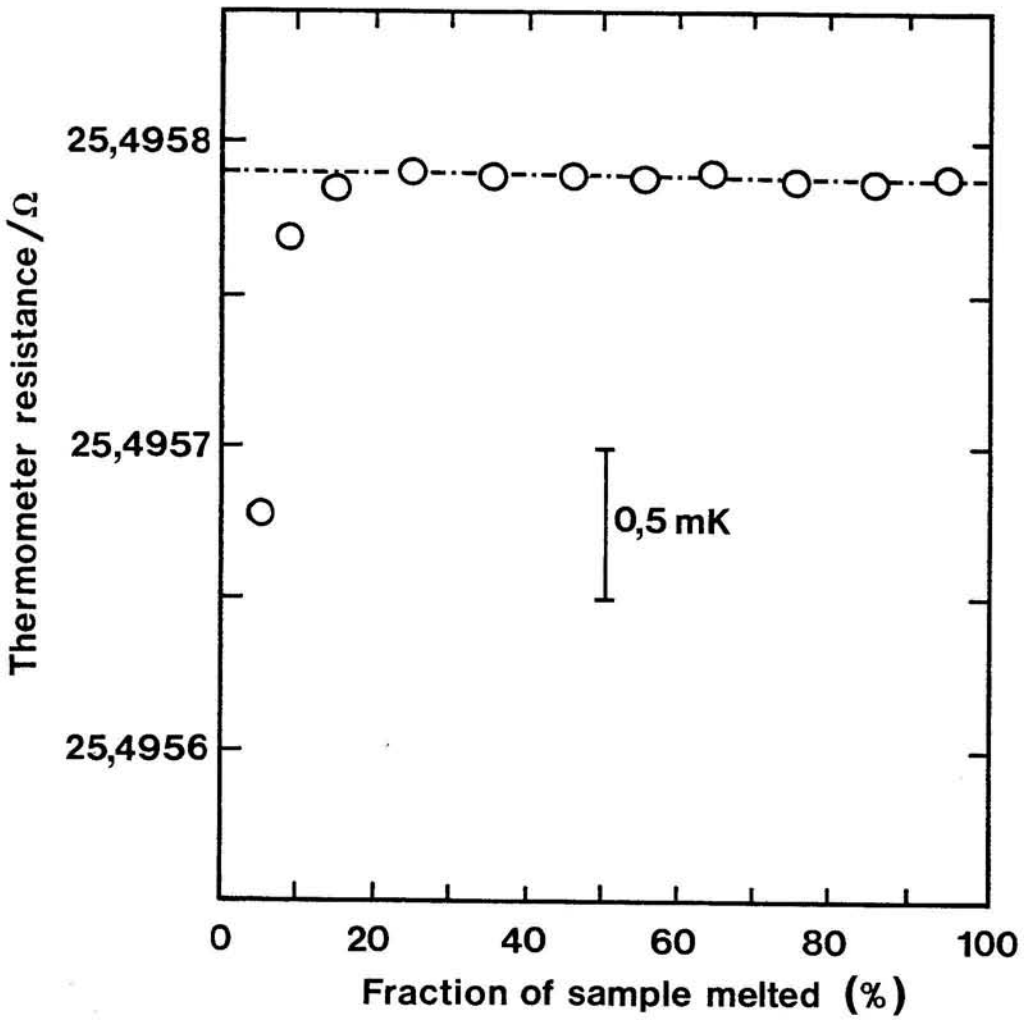

Figure 2.4 Metal freezing-point sample holder for resistance thermometry [Bongiovanni *et al.* (1975)]
Sections 2.2.1, 2.2.4.6.

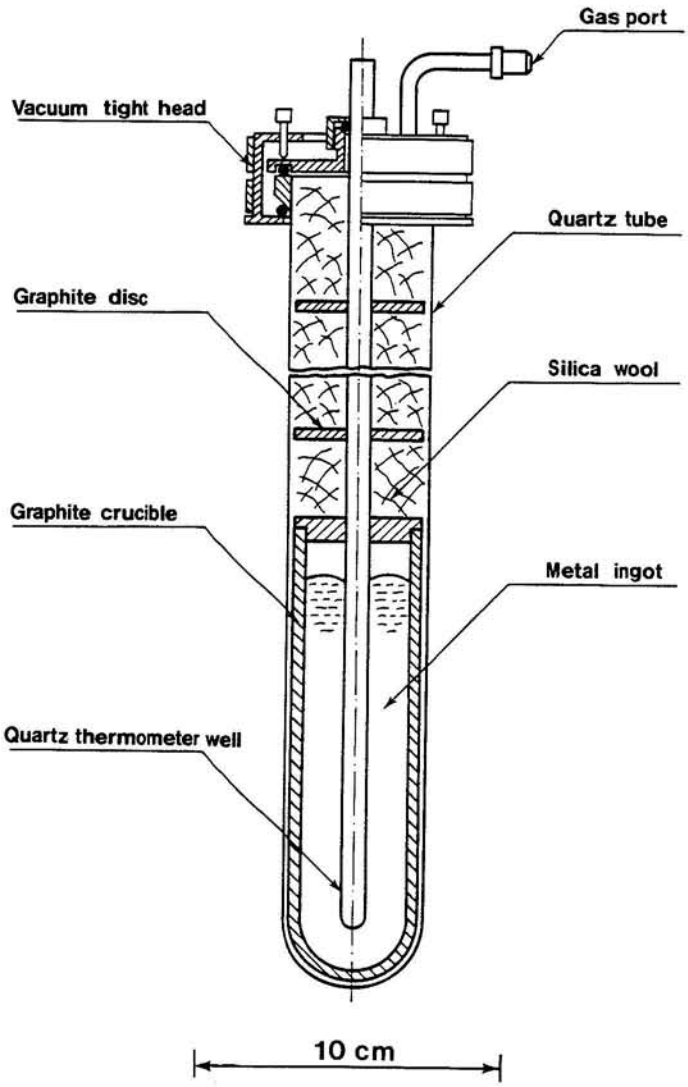

Figure 2.5 Fixed point blackbody assemblies for radiation thermometry [a) Ohtsuka and Bedford (1982), b) Quinn and Ford (1969)]
Dimensions are in millimetres.
Sections 2.2.1, 6.5.1.

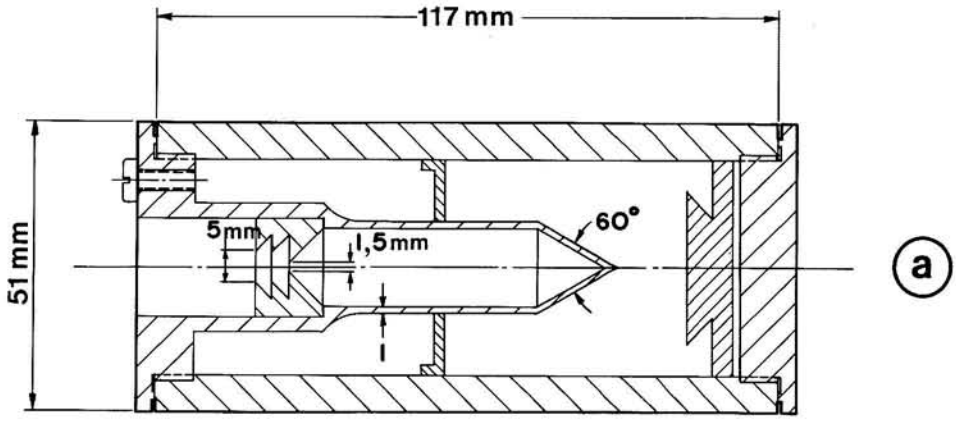

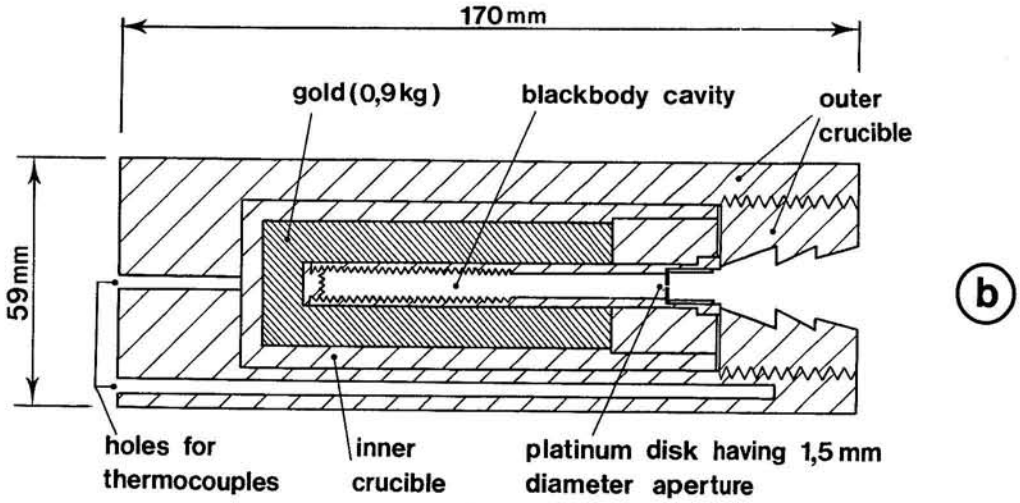

Figure 2.6 Medium-temperature furnace for resistance thermometry metal freezing points [after Chattle (1972)]
1. Silica-wool ; 2. glass tubes ; 3. alternate graphite-ceramic discs ; 4. nickel/chromium heater on alumina former ; 5. thermocouple ; 6. aluminium block with lining tube. The case is filled with mineral wool insulation.
Sections 2.2.3.1, 2.2.4.4.

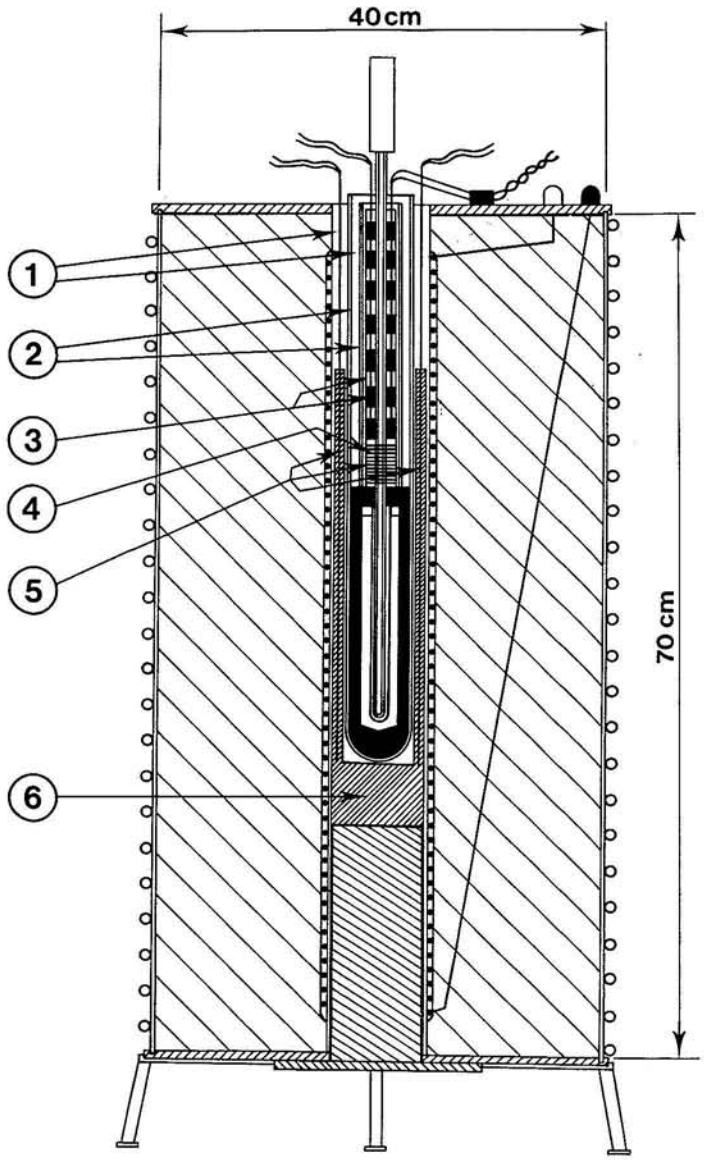

Figure 2.7 High-temperature furnace for resistance thermometry metal freezing points [McLaren and Murdock (1979)]. A heat pipe is preferred, but is a much more costly alternative to the inconel block ; with a heat pipe, the end heaters are omitted. Section 2.2.3.2.

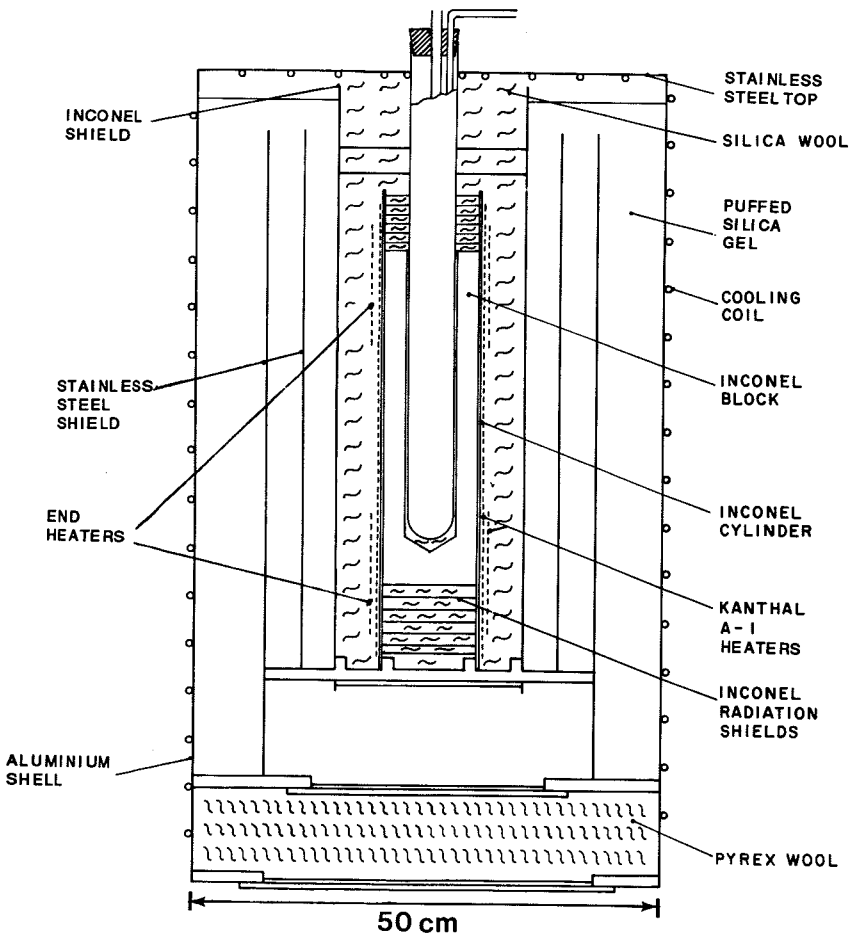

Figure 2.8 High-temperature furnace for radiation-thermometry metal freezing points [Ohtsuka and Bedford (1982)]
Section 2.2.3.3.

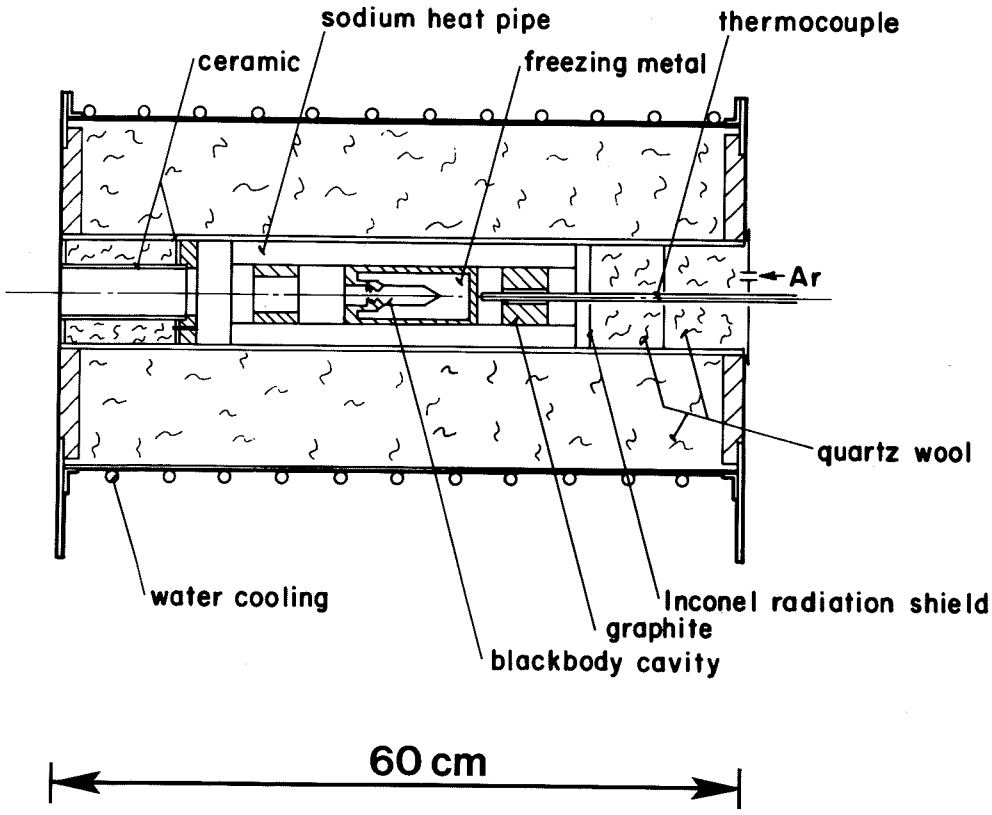

Figure 2.9 Mercury triple-point cell assembly. The sample holder is of borosilicate glass ; stainless-steel cells are also used, and are to be preferred, *see* Figure 2.10. Cooling is started with air in the stainless-steel jacket space. When the mercury cell is adequately cooled, the jacket is evacuated to reduce the cooling, or subsequent heating, rate [Furukawa *et al.* (1982)]

A. "O" ring tube seal ; B. Thermometer well ; C. Ethyl alcohol in well ; D. Indium gasket seal ; E. Insulation, rolled paper tissue ; F. Stainless steel jacket ; G. Tubular connection for cleaning and filling ; H. Insulation, tissue paper rolled around (I) for centering ; I. Copper foil cylinder ; J. Borosilicate glass cell ; K. Mercury ; L. Thermometer cushion (fused quartz wool) ; M. Stand for mercury cell ; N. Insulation (Aluminium silicate wool)

Section 2.2.4.1.

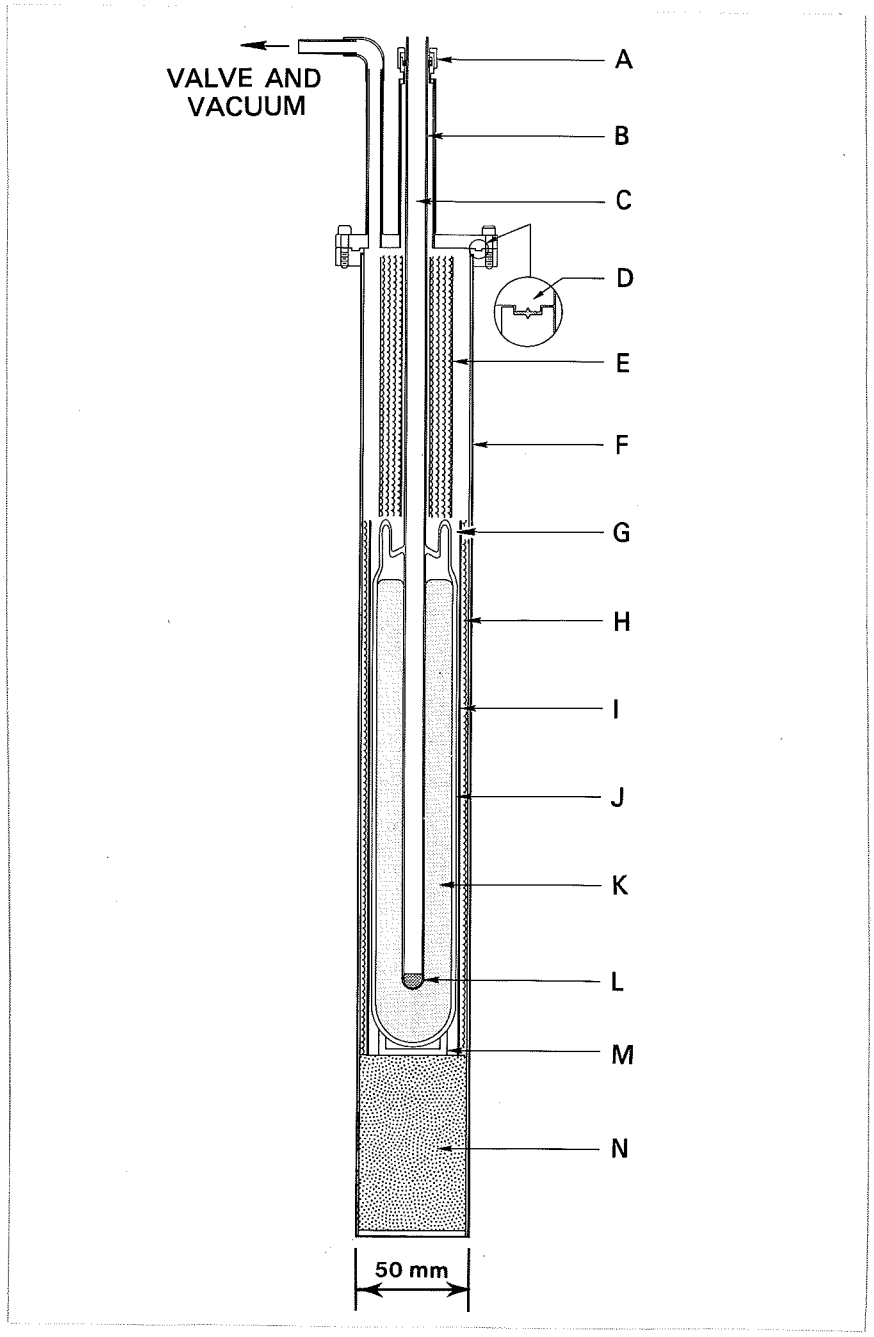

Figure 2.10 Freezing (F) and melting (M) curves for mercury in borosilicate glass (BS) and stainless-steel (SS) cells [Furukawa *et al.* (1982)]
Section 2.2.4.1, Figure 2.9.

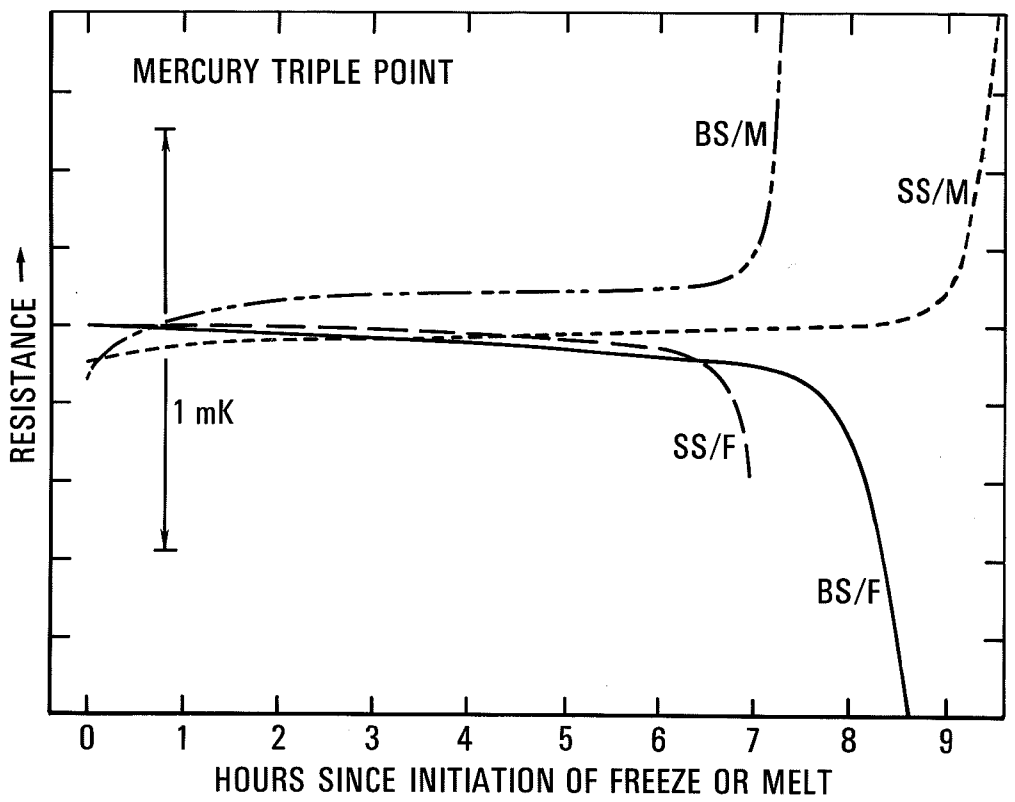

Figure 2.11 Gallium melting and triple-point cell [after Mangum and Thornton (1979)]. N indicates nylon and T indicates teflon.
Section 2.2.4.2.

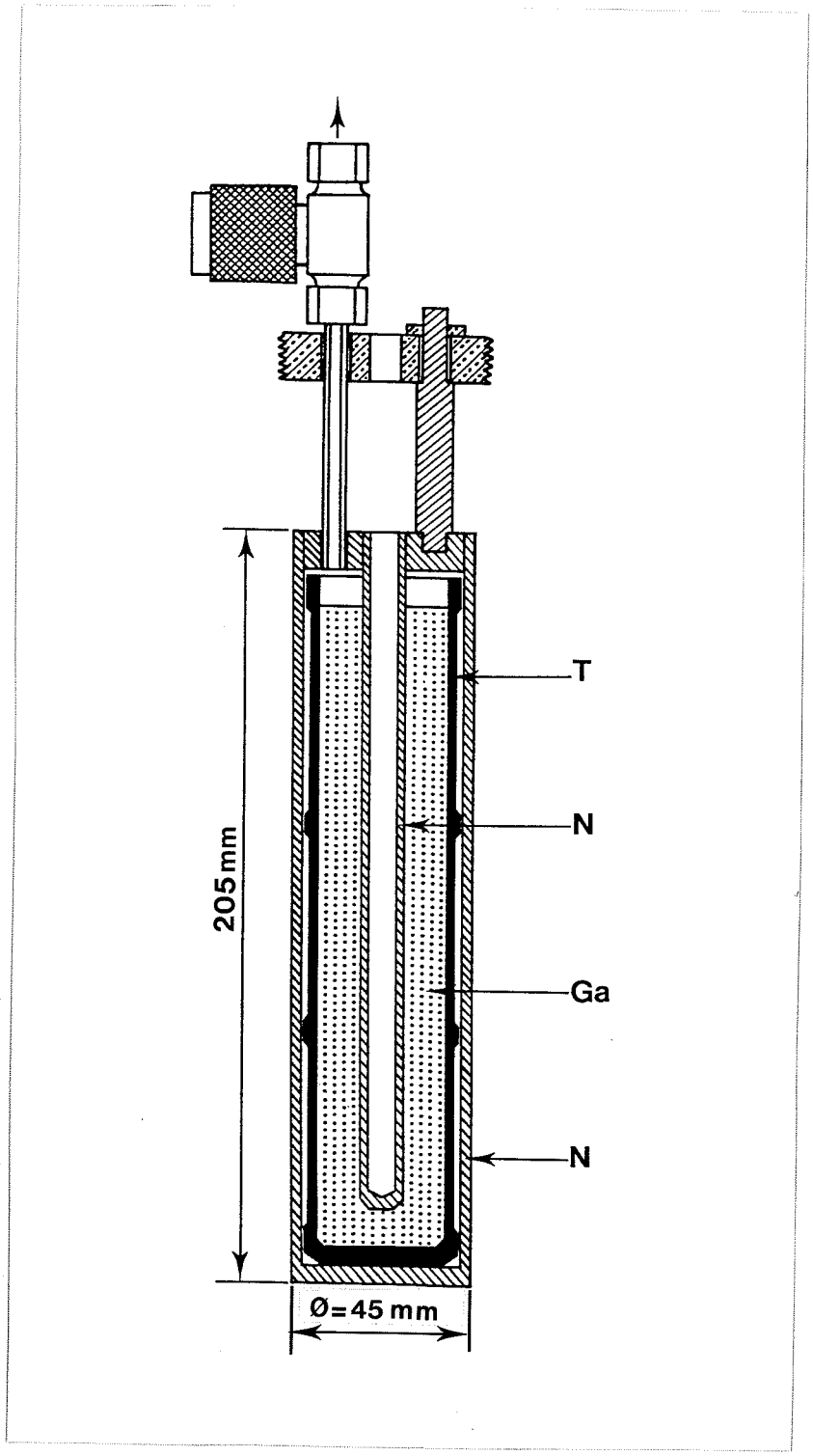

Figure 2.12 Preparation and filling of a sealed cell suitable for the freezing points of In, Sn, Zn, Al and Ag [Nubbemeyer (1990)] : (1) Parts ready for baking in vacuum. (2) Join the graphite parts and the metal block of the fixed-point cell. (3) Melt the metal block and lower the graphite well completely. (4) and (5) Quartz parts ready for degreasing. (6) Assemble crucible and quartz parts, seal the quartz, evacuate and fill with argon. (7) Seal off. A mounted cell is shown in Figure 2.13(a).
Section 2.2.4.8.

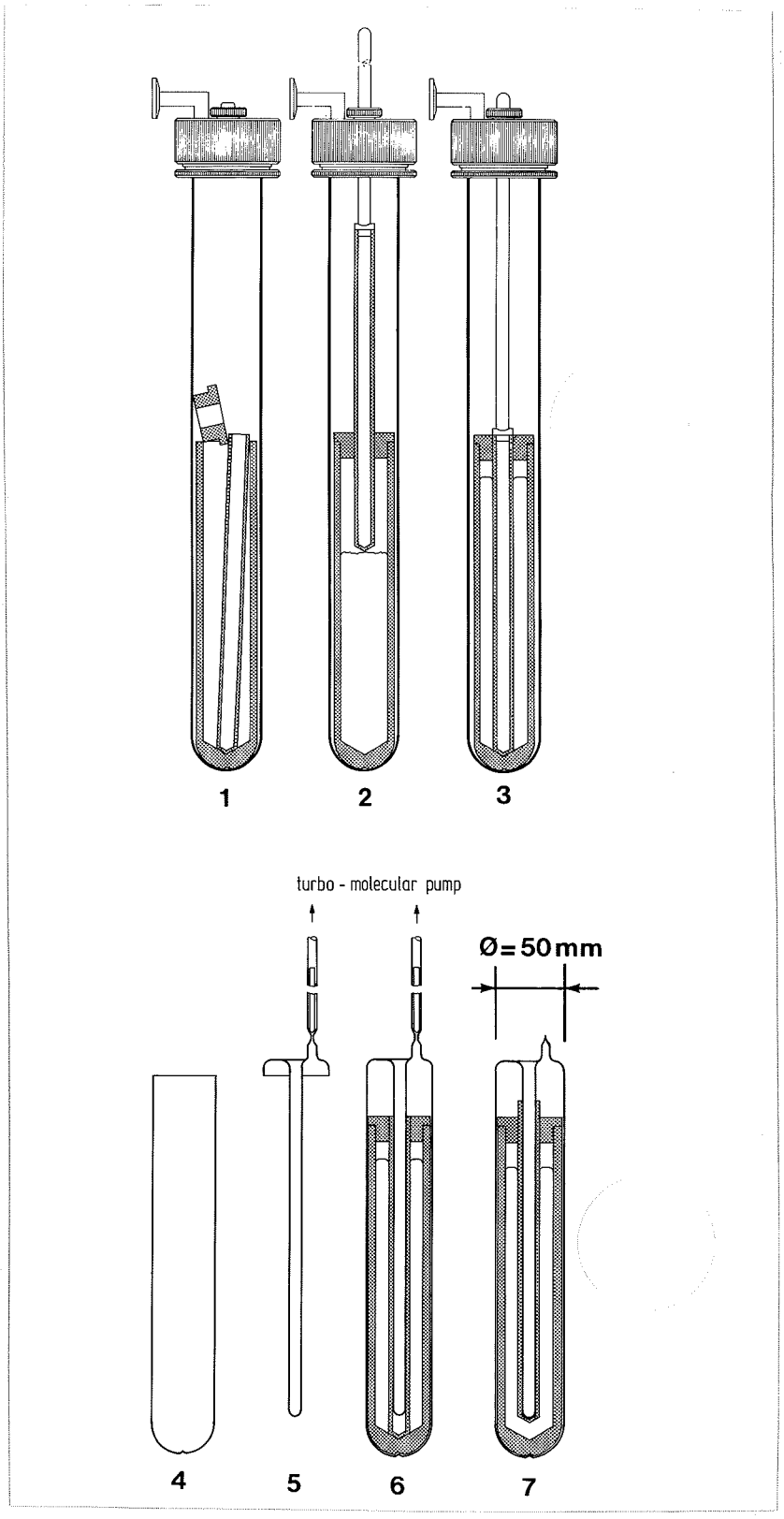

Figure 2.13 (a) Sealed cell in an inconel-601 container for the In-, Sn-, Zn-, Al-, and Ag-fixed point cells. Stainless steel can be used for Sn and Zn fixed-point cells. The quartz is type GE214, the graphite is type UT-6ST [Nubbemeyer (1990)]. (b) an alternative design using a silica outer container, (1) graphite crucible, (2) metal ingot, (3) silica re-entrant well, (4) graphite-disk shields, (5) pure silica wool, (6) argon atmosphere, (7) graphite well [Crovini *et al.* (1987)]. For preparation of this cell *see* Figure 2.12 and Section 2.2.4.8.

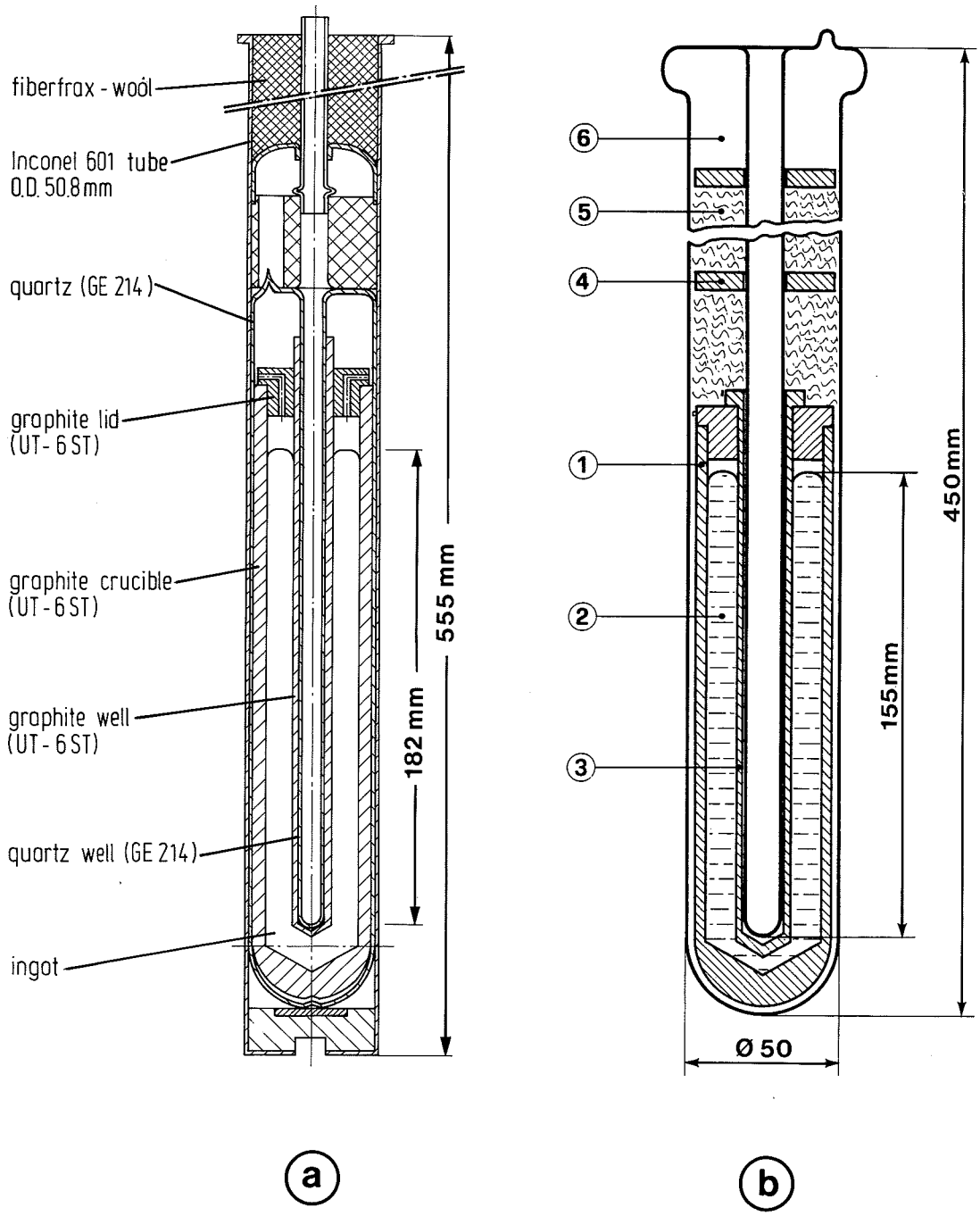

Figure 2.14 Immersion-temperature effects for different thermometers in the same ingot of tin or zinc [after McLaren (1959)]. The solid lines indicate the calculated slopes, i.e. the hydrostatic effect alone. It can be seen that thermometer A-1 in long-discontinued Leeds and Northrup design at the freezing point of zinc never achieves adequate immersion and the immersion of the Tinsley thermometer E-1 is marginal. By contrast the Meyers thermometer S 155 has excellent immersion characteristics at both the tin and the zinc points.
Sections 2, 2.2.4, 2.2.4.4, 2.2.4.5, 2.2.6.3.

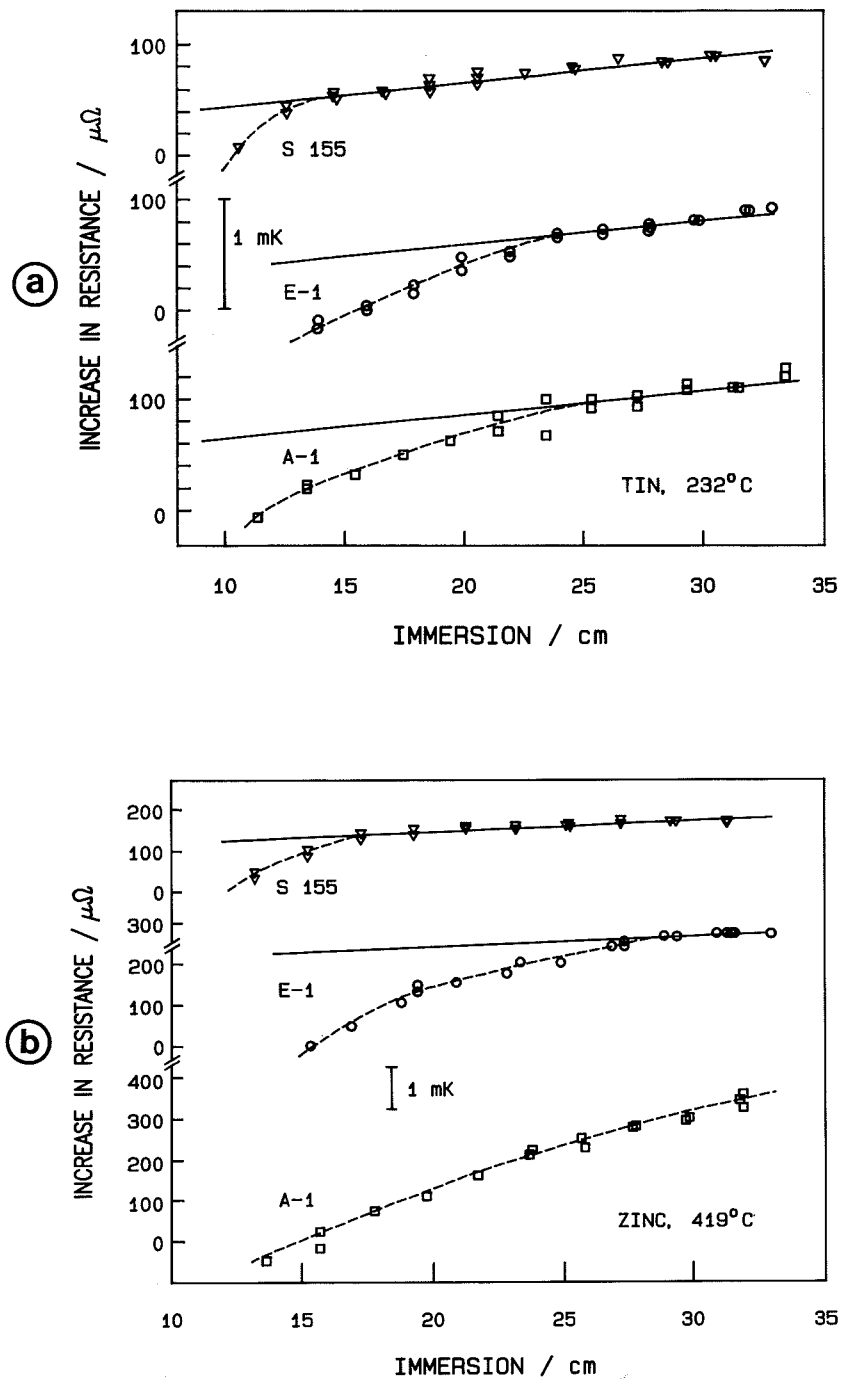

Figure 2.15 Vapour pressure cryostat for equilibrium hydrogen. The sample chamber (1) and thermometer wells (2) are drilled in a block of OFHC copper (3) enclosed in a radiation shield (4) bolted to the base of the block. This assembly is enclosed in another radiation shield (6), connected to a gas-cooled refrigerator (5). Stainless steel shims (7) reduce the thermal contact between the block assembly and the refrigerator. The whole assembly is contained in an evacuated enclosure (8) suspended above a bath of liquid helium by means of a thin-walled stainless steel tube (9) 12,5 mm in diameter. The sample is filled through the stainless-steel tube (10) which enters the sample chamber through the radiation trap (11) and a subsidiary chamber (12) in which catalyst may be placed. Hydrogen passes into the sample chamber through a sintered stainless-steel disc (13). The vapour-pressure-transmitting tube (14) enters the sample chamber through a radiation trap (15). Thermometer leads are anchored at (16) and (17). Temperature control is by means of a carbon resistance heater (19), platinum resistance thermometer (18) and an external electronic controller. The heat sink for the controller is (5) whose temperature is monitored by a carbon resistance thermometer (20). The temperature of the outer case is controlled with the aid of a platinum resistance thermometer (21) and carbon resistance heater (22) [Kemp and Kemp (1979)].
Section 2.3.1.

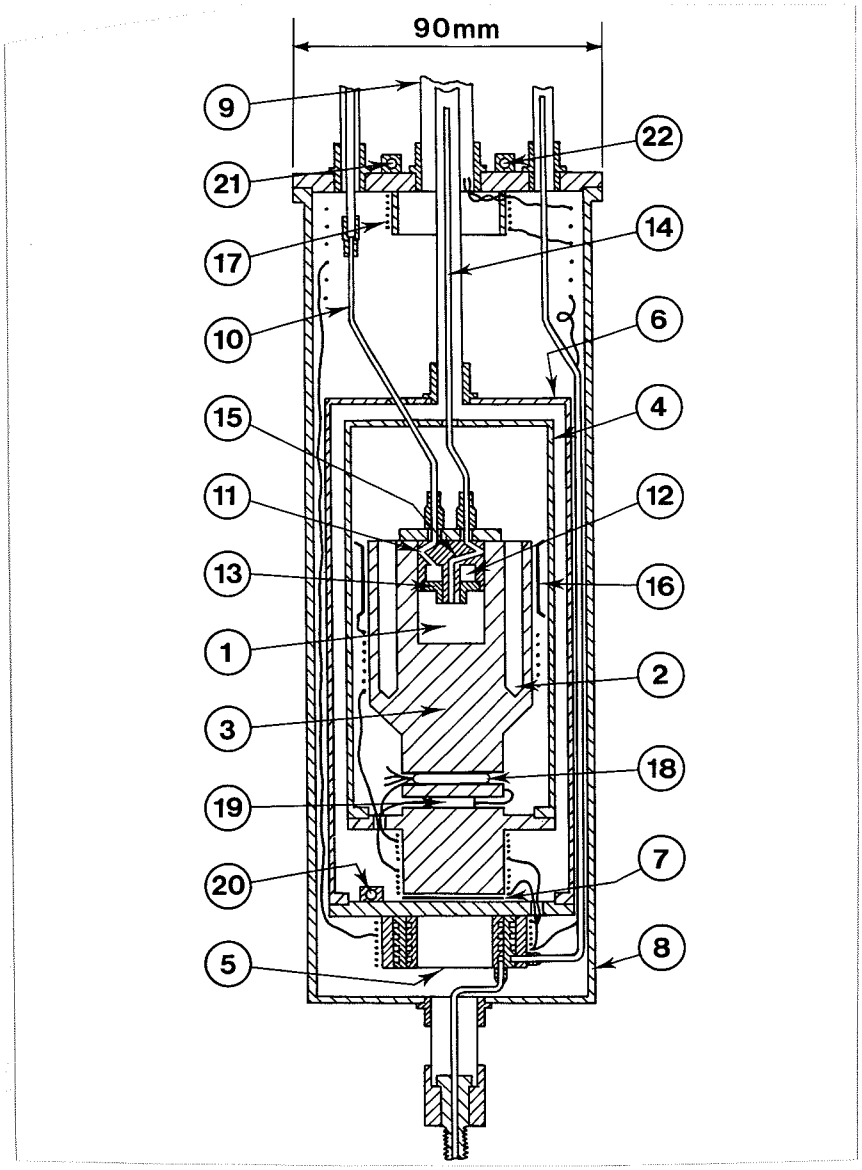

Figure 2.16 A selection of designs for sealed all-metal triple point cells [after Pavese et al (1984)]
Section 2.3.2.

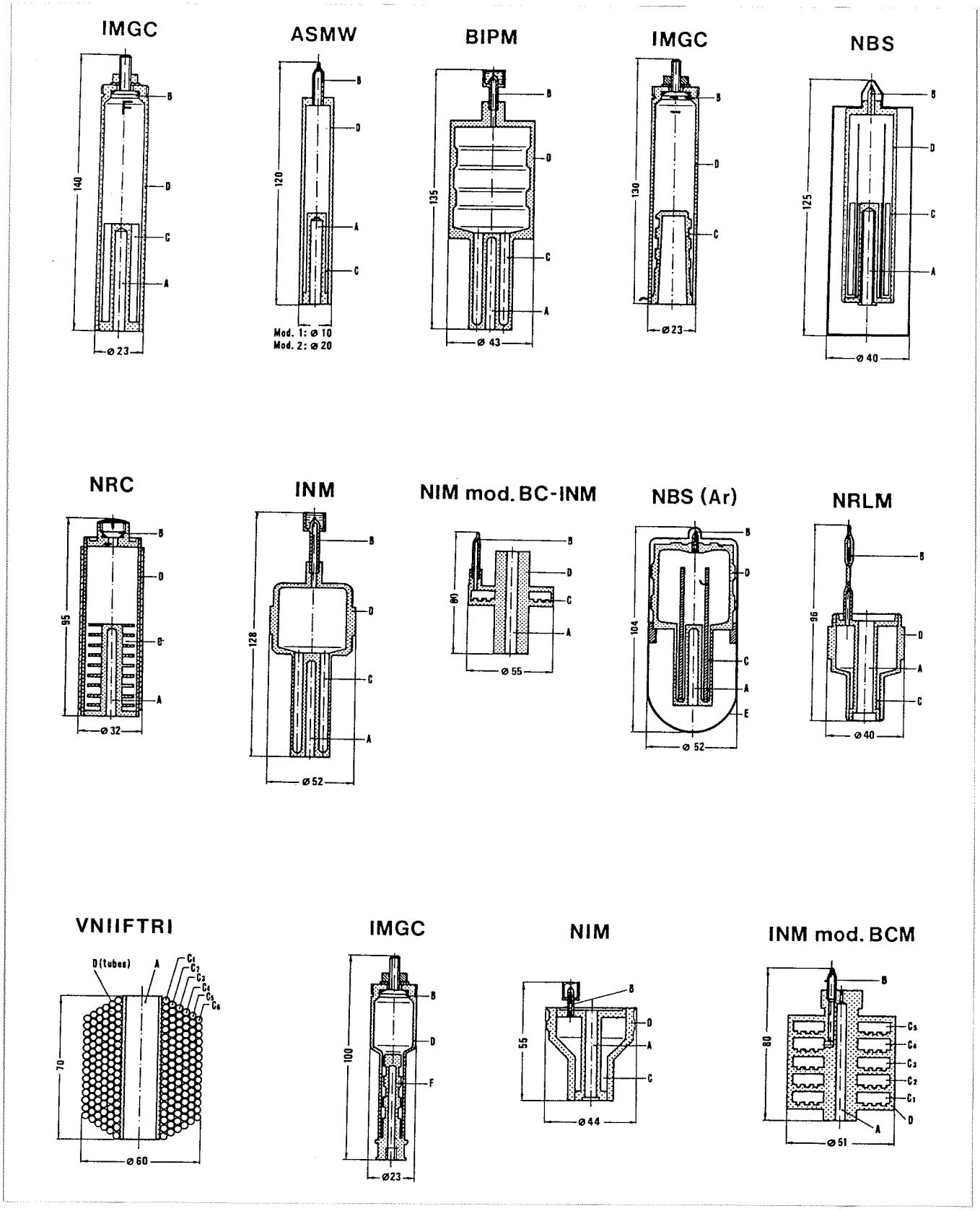

Figure 2.17 Cryostat for the realization of boiling and triple points of Ar and O_2 [Kemp *et al.* (1976)]

For the cryostat shown in the figure, (1) is an outer vacuum case, (2) a temperature controlled outer shield and (3) the cell containing the sample. The cell consists of three parts:

(a) a lower gas-cooled refrigerator (4), to which is soldered a copper tube (5) forming the effective thermal outer wall. This assembly is heated by a carbon heater (6) and its temperature monitored by a miniature platinum resistance thermometer (6a) ;

(b) an upper gas-cooled refrigerator (7) soldered to a thick-walled copper thermometer pocket (8) in which the test thermometer is inserted with Apiezon N grease. The thermometer pocket may be heated by the carbon resistor (10) ;

(c) the outer wall of the cell (11) consists of a thin walled stainless steel tube 25 mm in diameter which isolates the test thermometer from the heated outer wall (5) and the bottom of the cell.

The three parts of the cell are sealed together with indium-wire seals. The radiation shield (2) is controlled adiabatically with respect to the cell using a gas cooled refrigerator (12) as heat sink. The cold gas for the refrigerators is drawn up from the liquid helium through vacuum insulated tubes (13). The cryostat is suspended in a 100 cm deep helium dewar such that the base of the cryostat is some 50 cm above the bottom of the dewar. During operation the level of liquid helium is about 20 cm below the base of the cryostat.

Section 2.3.2.

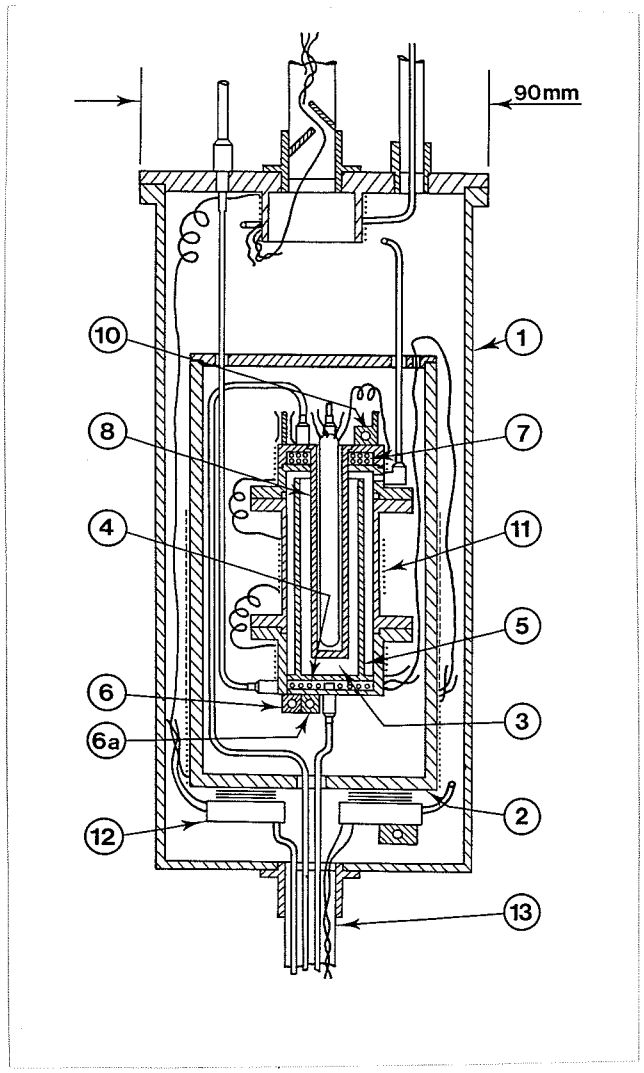

Figure 2.18 Apparatus for the calibration of long-stem platinum resistance thermometers at the argon triple point using a sealed cell : (1) long-stem platinum resistance thermometer ; (2) stainless-steel body of cell ; (3) thermometer tube ; (4) polyurethane foam ; (5) solid-liquid argon ; (6) bath of liquid nitrogen ; (7) helium in ; (8) manometer ; (9) pressure control valve ; (10) filling tube for liquid nitrogen ; (11) cryostat [Bonnier (1987)].
Section 2.3.2.

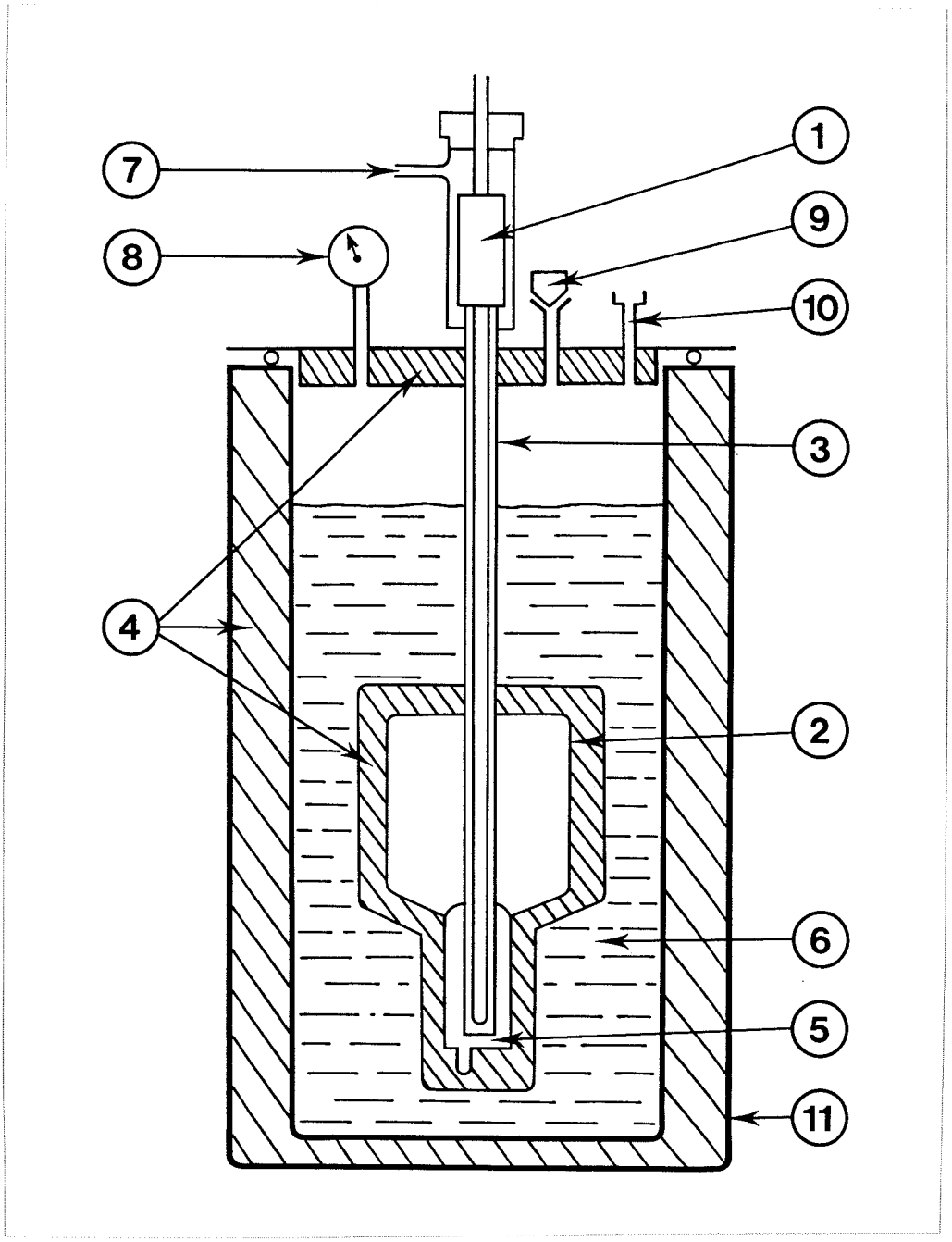

Figure 2.19 A schematic representation of a melt observed in a sealed triple-point cell [after Pavese (1984)].
Section 2.3.3.

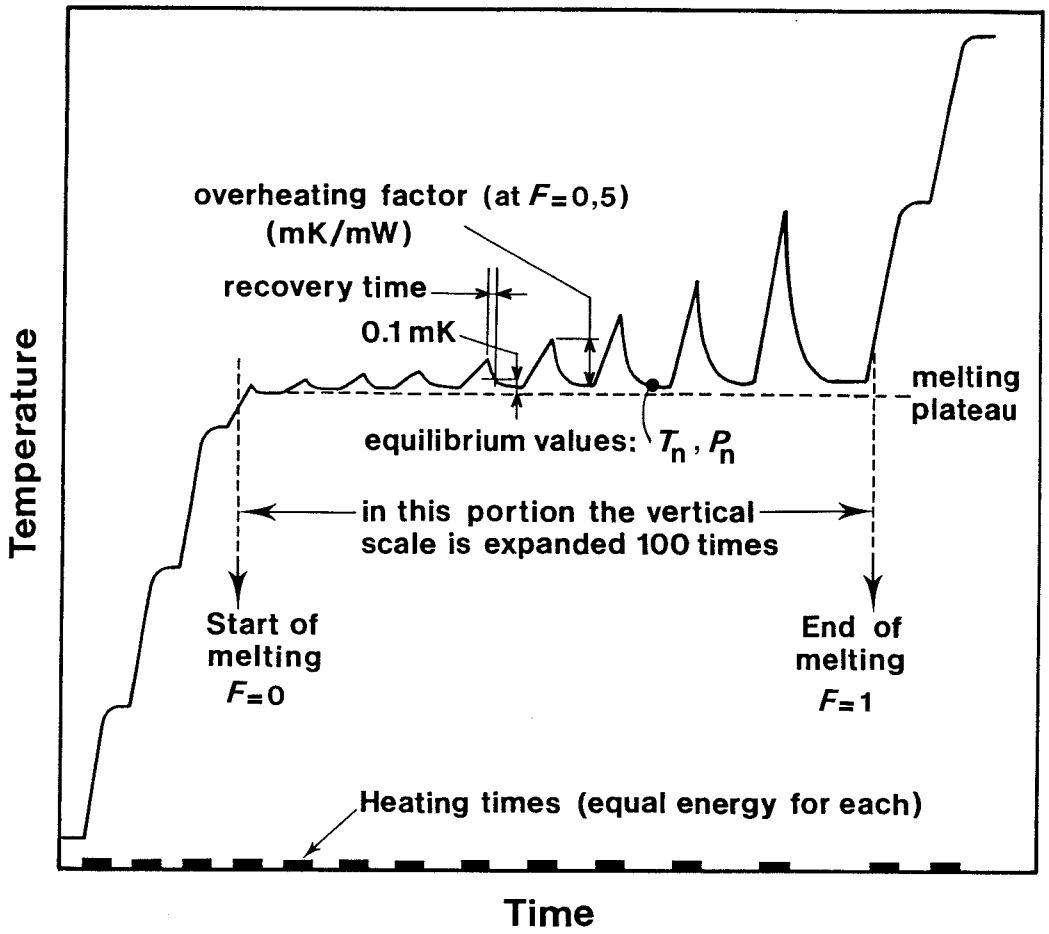

REFERENCES

Ancsin, J. (1970): The Triple Point of Oxygen and its Change by Noble Gas Impurities ; Metrologia **6**, 53-56

Ancsin, J. (1973a): Dew Points, Boiling Points and Triple Points of Pure and Impure Oxygen ; Metrologia **9**, 26-39

Ancsin, J. (1973b): Studies of Phase Changes in Argon ; Metrologia **9**, 147-154

Ancsin, J. (1977): The Thermometric Fixed Points of Hydrogen ; Metrologia **13**, 79-86

Ancsin, J. (1978): Vapour Pressures and Triple Point of Neon and the Influence of Impurities on These Properties ; Metrologia **14**, 1-7

Ancsin, J. (1982): Melting Curves of H_2O ; Temperature, Its Measurement and Control in Science and Industry (American Institute of Physics, New York) **5**, 281-284

Ancsin, J. (1985): Melting Curves and Heat of Fusion of Indium ; Metrologia **21**, 7-9

Ancsin, J. (1989): A Study of the Realisation of the Melting and Freezing Points of Silver ; Metrologia **26**, 167-174

Ancsin, J. and Phillips, M.J. (1969): Triple Point of Argon ; Metrologia **5**, 77-80

Ancsin, J. and Phillips, J. (1976): Argon Triple Point Realization Cryostat for Platinum Resistance Long Stem Thermometers ; Rev. Sc. Instr. **47**, 1519-1521

Arai, M. and Sakurai, H. (1990): Development of a sealed glass cell for gallium triple point; Tempmeko-90 (Finnish Society of Automatic Control), 80-85

Barber, C.R., Handley, R., and Herington, E.F.G. (1954): The Preparation and Use of Cells for the Realization of the Triple Point of Water ; Brit. J. Appl. Phys. **5**, 41-44

Berry, R.J. (1959): The Temperature-Time Dependence of the Triple Point of Water ; Can. J. Phys. **37**, 1230-1248

Bongiovanni, G., Crovini, L. and Marcarino, P. (1975): Effects of Dissolved Oxygen and Freezing Techniques on the Silver Point ; Metrologia **11**, 125-132

Bonhoure, J. and Pello, R. (1983): Température du Point Triple du Gallium ; Metrologia **19**, 15-20

Bonnier, G. (1975): Point triple de l'argon (83,798 K) référence de transfert ; Bulletin du BNM (Paris) **22**, 14-18

Bonnier, G. (1987): Calibration of Temperature Sensors ; Thermal and Temperature Measurement in Science and Industry (Institute of Measurement and Control, London), 57-68

Bonnier, G. and Malassis, R. (1975): Réalisation d'un nouveau type de cellule scellée destinée aux étalonnages cryogéniques ; Bulletin du BNM (Paris) **22**, 19-20

Chattle, M.V. (1972): Platinum Resistance Thermometry up to the Gold Point ; Temperature, Its Measurement and Control in Science and Industry (Instrument Society of America, Pittsburgh) **4**, 907-918

Chattle, M.V. and Butler, J. (1988): Cells for the realization of the triple point of mercury ; NPL Report QU 79

Chattle, M.V. and Pokhodun,.A.I. (1989): An Intercomparison between fixed-point cells made at VNIIM (USSR) and NPL (UK) for the realization of the melting and triple points of gallium and the solidification points of indium and cadmium ; Measurement **7** (4), 146-152

Chattle, M.V., Rusby, R.L., Bonnier, G., Moser, A., Renaot, E., Marcarino, P., Bongiovanni, G. and Frassineti, G. (1982): An Intercomparison of Gallium Fixed Point Cells ; Temperature, Its Measurement and Control in Science and Industry (American Institute of Physics, New York) **5**, 311-316

Compton, J.P. (1970): The Realization of the Normal Boiling Point of Neon.I The Cryostat ; Metrologia **6**, 69-74

Compton, J.P. (1972): The Realization of Low Temperature Fixed Points ; Temperature, Its Measurement and Control in Science and Industry (Instrument Society of America, Pittsburgh) **4**, 195-209

Compton, J.P. and Ward, S.D. (1976): Realization of the Boiling and Triple Points of Oxygen ; Metrologia **12**, 101-113

Connolly, J.J. and McAllan, J.V. (1980): Limitations on Metal Fixed Points Caused by Trace Impurities ; Metrologia **16**, 127-132

Crovini, L., Actis, A. and Galleano, R. (1987): A sealed cell for the copper point ; High Temp. - High Pressures **18**, 697-705

Evans, J.P. and Sweger, D.M. (1969): Immersion Cooler for Freezing Ice Mantles on Triple-Point-of-Water Cells ; Rev. Sci. Instrum. **40**, 376-377

Evans, J.P. and Wood, S.D. (1971): An Intercomparison of High Temperature Platinum Resistance Thermometers and Standard Thermocouples ; Metrologia **7**, 108-130

Foster, R.B. (1972): A Fixed Point Calibration Procedure for Precision Platinum Resistance Thermometers ; Temperature, Its Measurement and Control in Science and Industry (Instrument Society of America, Pittsburgh) **4**, 1403-1414 (or Suyama, Y. (1980): Jap. J. Appl. Phys. 19, 421-426)

Furukawa, G.T. (1974): Investigation of Freezing Temperatures of National Bureau of Standards Aluminum Standards ; J. Research Natl. Bur. Stand. **78A**, 477-495

Furukawa, G.T., Bigge, W.R. (1982): Reproducibility of some triple point of water cells ; Temperature, its Measurement and Control in Science and Industry (American Institute of Physics, New York) **5**, 291-297

Furukawa, G.T., Riddle, J.L. Bigge, W.R. and Pfeiffer, E.R. (1982): Application of Some Metal SRM's as Thermometric Fixed Points ; National Bureau of Standards (U.S.), Special Publication 260-77

Hermier, Y. and Bonnier, G. (1987): A water triple point in a multicompartment cell ; Thermal and Temperature Measurement in Science and Industry (Institute of Measurement and Control, London), **3**, TEMP/MEKO 87, Sheffield, UK, 33-39

Kemp, R.C. and Kemp, W.R.G. (1978): The Realization of the Normal Boiling Point of Neon ; Metrologia **14**, 9-13

Kemp, R.C. and Kemp, W.R.G. (1979): The Triple Point, Boiling Point and 17 K Point of Equilibrium Hydrogen ; Metrologia **15**, 155-159

Kemp, R.C., Kemp, W.R.G. and Cowan, J.A. (1976): The Boiling Points and Triple Points of Oxygen and Argon ; Metrologia **12**, 93-100

Mangum, B.W. (1982): Triple Point of Gallium as a Temperature Fixed Point ; Temperature, Its Measurement and Control in Science and Industry (American Institute of Physics, New York) **5**, 299-309

Mangum, B.W. (1989): Determination of the indium freezing point and triple point temperatures ; Metrologia **26**, 211-218

Mangum, B.W. and Thornton, D.D. (1979): Determination of the Triple-Point Temperature of Gallium ; Metrologia **15**, 201-215

Marcarino, P., Dematteis, R. and Fernicola, V. (1989): Intercomparison of fixed points. Phase I : Measurements related to zinc and tin cells ; IMGC Report S/267, 38 p. + 17 fig.

McAllan, J.V. (1982a): The Effect of Pressure on the Water Triple Point Temperature ; Temperature, Its Measurement and Control in Science and Industry (American Institute of Physics, New York) **5**, 285-290

McAllan, J.V. (1982b): Practical Reference Temperatures using Melting Point Techniques ; Journal of Physics E **15**, 884-885

McAllan, J.V. and Ammar, M.M. (1972): Comparison of the Freezing Points of Aluminium and Antimony. Temperature, Its Measurement and Control in Science and Industry (Instrument Society of America, Pittsburgh) **4**, 275-285

McLaren, E.H. (1957): The Freezing Points of High Purity Metals as Precision Temperature Standards ; Can. J. Phys. **35**, Part II (Zinc, Cadmium and Tin), 1086-1106

McLaren, E.H. (1958): The Freezing Points of High Purity Metals as Precision Temperature Standards ; Can. J. Phys. **36**, Part III (Zinc), 585-598, Part IV (Indium), 1131-1147

McLaren, E.H. (1959): Intercomparison of 11 Resistance Thermometers at the Ice, Steam, Tin, Cadmium, and Zinc Points ; Can. J. Phys. **37**, 422-432

McLaren, E.H. (1962): The Freezing Points of High-Purity Metals as Precision Temperature Standards ; Temperature, Its Measurement and Control in Science and Industry (Reinhold, New York) **3**, 185-198

McLaren, E.H. and Murdock, E.G. (1960): The Freezing Points of High Purity Metals as Precision Temperature Standards ; Can. J. Phys. **38**, Part V (Tin), 100-118

McLaren, E.H. and Murdock, E.G. (1966): Radiation Effects in Precision Resistance Thermometry: II. Illumination Effect on Temperature Measurement in Water Triple-Point Cells Packed in Crushed Ice ; Can. J. Phys. **44**, 2653-2659

McLaren, E.H. and Murdock, E.G. (1979): The Properties of Pt-PtRh Thermocouples for Thermometry in the Range 0-1100 °C, Parts I and II ; NRC Reports NRCC 17407 and NRCC 17408

Mitsui, K. and Inaba, A. (1978): A Sealed Portable Cell Made of Copper for Realizing Triple Points of Condensed Gases ; CCT 12^{e} Session, Annexe T12, T98-T99

Never, G. and Brost, O. (1975): Heat pipes for the realization of isothermal conditions as temperature reference sources Temperature-75 ; Inst. Phys. Conf. Series No 26, 446-452

Nubbemeyer, H.G. (1990): High temperature platinum resistance thermometers and fixed point cells for the realization of ITS-90 (Private communication)

Ohtsuka, M. and Bedford, R.E. (1982): Measurement of the Thermodynamic Temperature Interval Between the Freezing Points of Silver and Copper ; Temperature, Its Measurement and Control in Science and Industry (American Institute of Physics, New York) **5**, 175-181

Oleinik, B.N., Ivanova, A.G., Drinianinov, M.M. and Zamkovets, V.A. (1984): Realization of the indium freezing point ; CCT 15^{e} Session, Doc. CCT/84-1

Pavese, F. (1978): The triple point of argon and oxygen; Metrologia **14**, 93-103

Pavese, F. (1984): An International Comparison of Fixed Points by Means of Sealed Cells (13.81 K to 90.686 K) ; BIPM Monographie 84/4, 221 p.

Pavese, F., Ancsin, J., Astrov, D.N., Bonhoure, J., Bonnier, G., Furukawa, G.T., Kemp, R.C., Maas, H., Rusby, R.L., Sakurai, H. and Ling Shan-Kang (1984): An international comparison of fixed points by means of sealed cells in the range 13.81 K to 90.686 K ; Metrologia **20**, 127-144

Pavese, F. and Ferri, D. (1982): Ten years of research on sealed cells for phase transition studies of gases at IMGC ; Temperature, Its Measurement and Control in Science and Industry (American Institute of Physics, New York) **5**, 217-227

Quinn, T.J. (1990): Temperature, 2nd edition ; Academic Press (London), 495 p.

Ricolfi, T. and Lanza, F. (1977): The Silver and Copper Freezing Points as Accurate Reference Standards for Radiation Pyrometry ; High Temp. - High Pressures **9**, 484-497

Sawada, S. (1982): Realization of the triple point of indium in a sealed glass cell ; Temperature, Its Measurement and Control in Science and Industry (American Institute of Physics, New York) **5**, 343-346

Sostman, H.E. (1977): Melting Point of Gallium as a Temperature Calibration Standard ; Rev. Sci. Instr. **48**, 127-129

Takiya, M. (1978): Mesure Précise du Point de Congélation de l'Argent avec un Thermomètre à Résistance de Platine ; CCT, 12e Session, Annexe T30, T154-T159

3. PLATINUM RESISTANCE THERMOMETRY

3.1. Platinum Resistance Thermometer Construction

To be suitable as a standard platinum resistance thermometer the resistor must be made of platinum of sufficient purity that the finished thermometer will satisfy at least one of the following two relations

$$W(29{,}7646\ °C) \geq 1{,}11807 \qquad (3.1a)$$

$$W(-38{,}8344\ °C) \leq 0{,}844235\ . \qquad (3.1b)$$

A platinum resistance thermometer that is to be used at the silver point must additionally satisfy the relation

$$W(961{,}78\ °C) \geq 4{,}2844 \qquad (3.2)$$

There are three types of standard platinum resistance thermometers in common use: (a) capsule thermometers, (b) long-stem low- or medium-temperature thermometers (often referred to as either standard long-stem thermometers or simply long-stem thermometers, terms which, used on their own, are usually meant to exclude the high-temperature long-stem thermometers), and (c) high temperature long-stem thermometers (usually referred to as high temperature thermometers).

The capsule-type thermometers are principally intended for use at low temperatures (down to 13,8 K) ; they are often used up to 156 °C, and sometimes up to 232 °C. The standard long-stem thermometers are intended for the range 84 K (occasionally down to 54 K) to about 660 °C (although those with mica insulation should not be used above 500 °C unless the necessary steps are taken, at suitable intervals, to remove water of crystalization from the mica, *see* also Section 3.1.2). The high temperature thermometers are specifically designed for use at temperatures up to the silver point.

Capsule and standard long-stem thermometers have ice-point resistances of about 25,5 Ω, giving a sensitivity of about 0,1 Ω/K. High temperature thermometers have ice point resistances that typically are between 0,2 Ω and 2,5 Ω.

The platinum wire for all thermometers is obtained "hard drawn", as it is somewhat easier to handle in this condition, but it is annealed after the resistor is formed. The sensing elements of all standard resistance thermometers have four leads. The resistor winding is usually bifilar, but occasionally other low inductance configurations are used. A low inductance is always advantageous, and is particularly important if the thermometer is to be used in ac circuits.

Platinum-to-glass seals provide the hermetic seal for the platinum leads. Externally the platinum leads are soft-soldered to copper leads that are mechanically secured to the head. For dc measurements, satisfactory external copper leads can be made from commercially available cable. Stranded leads which do not have individually-insulated strands should not be used in dc measurements, as a single broken strand may cause "noise" in the resistance thermometer circuits which is difficult to locate and eliminate. For ac measurements PTFE or polyethylene insulated leads should be used.

Use of a thermometer above its designated temperature range may give rise to measurement errors resulting from electrical leakage ; this will in general disappear on cooling. Irreversible faults are usually due to loss of filling gas by diffusion through the glass seal, but may occasionally result from overheating that has led to sagging of the platinum coil or contamination of the platinum. The overheating may also affect the calibration, particularly at low temperatures. It is not advisable to use the same thermometer as a standard at high as well as at low temperatures.

3.1.1 Capsule Platinum Resistance Thermometer

The capsule-type platinum resistance thermometer constitutes a standard interpolating instrument between 13,8 K and 273,16 K (0,01 °C) ; it is also extensively used up to 30 °C, sometimes to 157 °C and occasionally to 232 °C. The platinum resistor is mounted much as in a long-stem thermometer, but is inserted in a closed-ended platinum sheath (typically of 5 mm diameter). The short (30 to 50 mm) platinum leads emerge through a glass seal to the sheath. The filling gas is usually helium at a pressure of about 30 kPa at room temperature. A typical design of a capsule-type, 25 Ω thermometer is shown in Figure 3.1. The electrical connections can be made with ordinary soldering techniques ; the user should take care never to strain the leads where they emerge from the glass seal.

Capsule-type platinum resistance thermometers are usually used "totally immersed", meaning that they are generally inserted into a well in a copper block. The connections are made to long fine copper wires insulated with varnish or a similar coating, and these are thermally

anchored to the block and to at least one other point within the cryostat so as to reduce or eliminate heat flow into or from the thermometer. When this is done correctly, the heat leaks through the leads produce an effect that is much less than 0.1 mK [Hust (1970), Kemp *et al.* (1976)].

The ITS-90 lower limit for the platinum resistance thermometers has been set at 13,8 K because at lower temperatures their resistance and sensitivity becomes inconveniently small, and the low-temperature characteristics become increasingly strain-dependent. To compensate for the loss of sensitivity, measuring currents below 24,5 K are generally increased from the 1 mA usually used above that temperature, up to about 5 mA at 13,8 K. Even at this level, because of the low values of resistance $\approx 10^{-2}$ $\approx 10^{-3}$ of R_{tp} in this range, the self-heating effect should not exceed 0,2 mK.

There are no other special requirements for maintaining calibrated capsule thermometers, beyond normal careful handling and measurements at the triple point of water before and after use. The use of capsule-type thermometers at high temperatures is limited by electrical leakage through the glass seal, and diffusion of helium, also through the glass. Calibrations up to 505 K (the freezing point of tin) are possible, especially with air-filled thermometers, though the results at this temperature are not likely to be of the best quality.

3.1.2 Standard Long-Stem Platinum Resistance Thermometer

Standard long-stem thermometers may readily be used at temperatures down to the argon triple point ($\approx$ 84 K) and are sometimes used down to 54 K. The thermometers normally designated by this term are usually not designed for use above 660 °C, while a number of them will deteriorate or fail if taken above 500 °C (*see* Section 3.2.2). Typical designs of the resistance elements of 25 Ω long stem thermometers are shown in Figure 3.2. These are ususally mounted in silica tubes about 7 mm in diameter and filled with dry air at a pressure of about 30 kPa at room temperature. Note that the self-heating (Section 3.2.5) and immersion (Section 3.2.4) effects encountered using the design shown in Figure 3.2 (b) are very much worse than those for the design shown in Figure 3.2 (a).

The insulation resistance between the leads of a 25 Ω thermometer must be greater than 70 MΩ at 500 °C if the error introduced by insulation leakage is to be less than the equivalent of 1 mK[3.1]. For thermometers for use up to 500 °C mica is often used as the insulation material; for thermometers to be used at higher temperatures the insulation will be vycor, fused silica or alumina. The primary objections to the use of mica at high temperatures are dehydration resulting in the evolution of water vapour which leads to insulation breakdown, and the presence of iron oxide impurity which, if reduced, leaves free iron that will contaminate the platinum. The dehydration may start at a temperature as low as 450 °C, and is usually encountered at approximately 540 °C. Significant dehydration will render the mica more susceptible to deterioration from mechanical shock.

3.1.3 High-Temperature Platinum Resistance Thermometer

In the ITS-90 the upper limit to the range in which the platinum resistance thermometer is the defining instrument is the freezing point of silver, 961,78 °C. This is some 300 °C higher than the upper limit for resistance thermometers in the 1927, 1948 and 1968 international scales.

The critical factors in the successful operation of a platinum resistance thermometer at high temperatures are reducing effects of electrical leakage, achieving and maintaining the cleanliness of the sheath and preventing metallic contamination of the sensor. The detailed design of the thermometer seems to be of secondary importance as two or three quite different but equally successful designs have been made.

A fundamental requirement for such a thermometer is that the electrical resistance of the sensor be low enough to reduce the effect of the electrical leakage across the insulators at high temperatures to a tolerable level, yet be high enough to provide adequate measurement sensitivity. These competing requirements have sharply limited the range of suitable thermometer resistances : at present the acceptable range for R_{tp}, the resistance at the triple point of water, is roughly from 0,25 Ω to 2,5 Ω, these two figures are used for the two thermometers in Figure 3.3a

---

3.1 A leakage equivalent to 1 mK does not imply a measurement error of that amount. If leakages are exactly repeatable at all temperatures, much of the effect is compensated in the calibration procedures. However, in general leakage resistance is variable with time, and a substantial part of the effect emerges as an error.

and b. In recent years, advances in commercial resistance-measuring bridges have substantially reduced the problems of high-accuracy measurement of low-value resistors, so that, even for the low-resistance thermometer, measurements can now be made easily and accurately. In consequence of this and their reduced electrical leakage errors these low resistance thermometers are now the recommended instruments. Experiments by Li Xumo (1989) indicate that the effects of leakage resistance across the insulators at the silver point amount to no more than one or two millikelvin for the 2,5 Ω thermometer and one tenth of this for the 0,25 Ω thermometer. For cleanliness of the sheath, *see* Section 3.2.3.

As regards the protection of the platinum elements from metallic contamination, Marcarino *et al.* (1989) have shown that Ni, Cr and Fe ions can permeate fused silica at temperature above about 960 °C. Their experiments suggest that the metal ions can be prevented from contaminating the sensor by flushing with a slow gas flux along the thermometer surface. Jung *et al.* (1989) have concluded that for operation at temperatures above about 800 °C the only reliable method of protection is to enclose the thermometer in a platinum sheath. The thickness of the sheath need not be great, they found that a platinum tube with a wall thickness of only 0,1 mm was adequate, but that it was essential to clean the inside of the platinum sheath very carefully. They recommend flushing with a hot solution of 50% fuming nitric acid and water. Precautions should be taken to prevent excessive heat loss along the platinum sheath at high temperatures. Furnaces should be designed to include an additional barrier of graphite or alumina about 1 cm thick between any metal liner or heat-pipe and the central block containing the thermometer well. The central block itself should of course be made of ceramic material or graphite.

3.2. Platinum Resistance Thermometer Use

3.2.1 Mechanical Treatment and Shipping Precautions

A standard platinum-resistance thermometer is a delicate instrument. Shock, vibration, or any other form of acceleration may cause the wire to bend between and around its supports, thus producing

strains that change its temperature-resistance characteristics. Strains in the platinum resistor normally will both increase the resistance and decrease the values of W above 0,01 °C (or increase the values of W below 0,01 °C). Careless day-to-day handling of a thermometer over a one year period has been observed to increase its resistance at the triple point of water by an amount equivalent to 0,1 K. Depending on the reason for this change in R_{tp}, unless the thermometer is then recalibrated it could lead to temperature errors as high as 10 mK. Similar changes may be caused by an apparatus that transmits vibrations to the thermometer, or by shipping the thermometer in an unsuitable container. For capsule resistance thermometers, the existence of small changes in W can readily be detected by checking for accompanying changes in low temperature (e.g., liquid helium temperatures) residual resistance.

It is advisable to hand-carry a thermometer to maintain the integrity of its calibration. If a thermometer must be shipped, it should first be placed in a rigid and moderately massive container that has been lined with soft material which conforms to the thermometer shape and protects it from mechanical shocks or vibrations. This container should then be packed in an appreciably larger box with room on all sides for soft packing material that will substantially attenuate the shocks that might occur during shipment.

A thermometer should, of course, be stored in a way that minimizes the likelihood of its receiving appreciable mechanical shock.

3.2.2 Thermal Treatment

If properly used and constructed, standard platinum resistance thermometers are not greatly susceptible to permanent damage from cycling within their intended operating temperature range. However, it should be noted that the metal-to-glass seals of capsule-type thermometers may be broken by extremely rapid cooling, e.g., when a capsule thermometer that has been at room temperature is suddenly immersed in liquid nitrogen.

The upper temperature limit of a long-stem resistance thermometer is determined by the softening point of any of the material, usually the protecting sheath, used in its construction ; by the temperature at which the thermometer was annealed before calibration ; by the evolution of

water and other contaminants from the sheath and insulators ; or by grain growth in the platinum wire. Changes resulting from operation at too high a temperature are a function of time and temperature and in general are predictable in only a qualitative way. Thermometer sheaths of borosilicate glass soften noticeably at temperatures above 500 °C ; their use even at 500 °C is limited to a few hours unless they are specially supported to prevent deformation. Fused-silica sheaths can be used for measurements up to 960 °C. Platinum grain growth has been observed in thermometers that have been used over a period of several hundred hours at 420 °C ; growth is, of course, more rapid at higher temperatures. The larger grains are undesirable in that they result in greater susceptibility to changes in resistance and in the value of W that are caused by mechanical shock, or even by repeated thermal cycling. Also, coiled-coil platinum resistance thermometers can short-circuit one or more turns after repeated thermal cycling to high temperatures.

Most long-stem thermometers are annealed during manufacture at 450 °C or higher. However, if this anneal was inadequate, or if the thermometer has been strained by mechanical shock since it was last annealed, then operation at temperatures above 450 °C may result in resistance changes due to further annealing. If strains are sufficiently severe noticeable annealing will occur at temperatures as low as 100 °C. This further annealing process has some beneficial aspects in that the thermometer sensor will tend to return to the metallurgical state that it was in during its previous calibration. Prior to their calibration, long-stem thermometers are typically annealed at about 450 °C or at their upper working temperature limit, whichever is higher, for up to 4 hours. The comparison of the resistance values of an originally-strained thermometer at a fixed point before and after annealing will show a shift downward in resistance and, usually, a shift upward (or down far for points below 0,01 °C) in W.

In measurements using platinum resistance thermometers at temperatures above 500 °C the difficulties discussed above are likely to be aggravated or their onset accelerated, and care should be taken at the manufacturing stage in baking and evacuating (where possible) the thermometer after assembly but before final annealing. Also, care should be exercised to avoid too rapid cooling. Rapid quenching from 660 °C may freeze in high-temperature dislocations or other crystal defects, resulting in an increase in R_{tp} that may amount to the equivalent of 1 mK or even

more. Provided that the cooling rate between 660 °C (after 15 minutes annealing at that temperature) and 450 °C does not exceed 100 °C/h, no detectable freezing in of defects occurs.

After using a high-temperature resistance thermometer at temperatures above about 700 °C, the thermometer should be annealed before making measurements at lower temperatures, in particular before making the measurements of R_{tp}. A suitable annealing procedure is a 2 hour anneal at 700 °C at the end of which the furnace containing the thermometer is allowed to cool naturally over a period of a few hours to 450 °C where it is held for a further 30 minutes to one hour, after which the thermometer may be removed and allowed to cool quickly to room temperature. Thermometers used at temperatures above 450 °C but less than 700 °C should first be annealed for one to two hours at the maximum temperature of operation, and then the above procedure for cooling to 450 °C and then to room temperature should be followed.

Thermometers that are used at temperatures above 600 °C will in time become very fragile, especially when hot. Great care must then be taken in removing them from the furnace; the removal, nevertheless, should be done reasonably quickly and they should be stored hanging from their heads in vertical protection tubes.

If the precautions outlined in this Section and in Section 3.2.3 are taken, particularly as regards cleanliness (Section 3.2.3) and protection from metallic contamination, a high-temperature resistance thermometer should allow measurements to be made having a reproducibility of a few millikelvins at all temperatures up to the silver point.

3.2.3 Devitrification

Protection from contamination of the element and from devitrification of the sheath becomes increasingly difficult at higher temperatures. Before using a quartz or silica-sheath platinum resistance thermometer above 100 °C it should be carefully cleaned with pure ethanol and dried with clean paper or cloth. This serves to remove all traces of finger prints that would otherwise be fixed as patterns of devitrification at high temperatures. Devitrification is an irreversible phase transition that converts quartz glass to a milky, brittle and gas-permeable substance. It may occur at high temperatures and is catalytically enhanced by alkali. First significant traces of devitrification

of the outer surface of the sheath should be removed by sandblasting with alumina powder in order to stop this process.

3.2.4 Thermometer Immersion

A thermometer is sufficiently immersed when there is no change in indicated temperature with additional immersion in a constant temperature environment. Checking the adequacy of immersion is a simple matter provided that the measured temperature is uniform along the immersed length of the thermometer[3.2] and is constant in time, as for instance, in the case of the fixed point cells designed to be used with long-stem thermometers (Section 2.2) ; in addition the thermometer must be protected from intrusive, or escaping, radiation. Although simple, these requirements are exacting and the checking process is, in practice, a lengthy one (several hours for measurements at a single temperature). A prior knowledge of what is likely to be an adequate immersion is frequently necessary and always desirable.

The immersion required to exploit the full accuracy of the thermometer is highly dependent both on the temperature being measured and on the thermometer design. The latter should, of course, facilitate radial and inhibit longitudinal thermal radiation by use of a series of radiation baffles, and in addition to prevent radiation piping (Section 3.2.6) by roughening or, in severe cases, by blackening one of the surfaces (normally the outer one) of those thermometers that have transparent (glass, quartz or saphire) sheaths.

Where radiation piping has been inhibited, the remaining longitudinal heat flow is likely to be roughly the same for all standard thermometers at a given immersion and temperature. At low temperatures (<420 °C) the required immersion is then a function of the radial thermal conductivity between the sensing element and the sheath (assuming adequately high conductivity in the measured substance), and this radial conductivity is inversely proportional to the self heating arising from the thermometer measuring current. This self heating can be easily and quickly determined (Section 3.2.5). At the triple point of water, using a 1 mA measuring current in a 25 Ω thermometer, it can vary from about

3.2 This discussion assumes the use of a long-stem thermometer. For capsule thermometers the requirement is that the entire thermometer be at the temperature being measured and that its leads be adequately thermally-anchored to that temperature.

0,35 mK (Meyers thermometer) through 0,65 mK (Leeds and Northrup thermometer) to over 3 mK (Tinsley thermometer). The required immersion depths vary accordingly.

Although at temperatures above room temperature the required immersion depth initially increases with temperature, a maximum is reached at temperatures in the region of 400 °C to 500 °C, after which the rapidly rising radial heat transfer by radiation causes it to fall slightly ; this is still on the assumption of the presence of adequate longitudinal radiation baffles and the inhibition of radiation piping. Data on this, and other, immersion effects are in short supply, *see* below ; for the admirable Meyers platinum resistance thermometer (now no longer made, but somewhat akin to recent Leeds and Northrup thermometers) adequate immersions (of the thermometer tip) at 0 °C, 230 °C, 420 °C and 630 °C are about 11 cm, 14 cm, 17 cm and 14 cm respectively. (These are for measurement precisions of the order of or better than 0,05 mK, 0,1 mK, 0,2 mK and 0,5 mK, also respectively). A Tinsley thermometer requires about 23 cm immersion at 230 °C and about 27 cm at 420 °C. An old and long-discontinued Leeds and Northrup design is not adequately immersed even at a depth of 32 cm at 420 °C (Figure 2.14, thermometer A-1).

A large number of measurements on the effects of immersion depth have been published ; unhappily many of these are unreliable. Much of this unreliability is because radiation piping is still only infrequently eliminated ; some results from anomalous temperatures in that part of the thermometer body that is outside the uniform temperature zone (e.g. close to the ice point, rather than at room temperature, for triple point of water measurements) ; many measurements show an internal inconsistency that strongly suggests inadequate measuring techniques. Immersion data are as yet almost entirely lacking for the recently developed high-temperature (960 °C) platinum resistance thermometers.

Advice for those wishing to be assured of being able to obtain precisions within a factor of two or three of those quoted above, is roughly as follows. Obtain a thermometer of good design that can be adequately immersed ; in general the larger the self heating effect the greater the immersion required for a given precision and the longer the time constant. Ensure that it is not subject to radiation piping (Section 3.2.6) unless it is to be used only at 100 °C or less, in which case it *must* be shielded from all natural or artificial light. (Metal-sheathed thermometers obviously need no further radiation shielding but the

conduction down the sheath is usually such as to require deeper immersion.). Immerse the thermometer from 15 cm to 20 cm between −50 °C and 50 °C, and from 20 cm to 27 cm at 200 °C and above.

3.2.4.1 Hydrostatic Pressure Effects

Adequate immersion in practice implies an error due to the hydrostatic pressure effect of the molten liquid[3.3], *see* Table 2.1. This effect can provide a useful check both of overall measurement sensitivity and of adequate immersion. If the thermometer can be shown to provide a linear portion of the immersion curve having the slope deduced from Table 2.1, as is the case in Figures 2.14 and 3.4, the measurement system has both adequate immersion and adequate (≈0,1 mK) discrimination ; the latter would not be evident in the absence of the hydrostatic pressure effect, as the resulting constant reading might, particularly in automated systems, result from a system fault.

For fixed point cells that provide less than 20 cm of immersion within the liquid-solid interface for a long-stem thermometer (this includes all of those illustrated in Section 2.4, which show maximum immersions varying from ≈12 cm to ≈19 cm), it is necessary either to restrict their use to the calibrations of thermometers known to have excellent immersion characteristics, or else to extend, though with a much reduced precision, the effective immersion length. This extension can often be easily accomplished by controlling the furnace temperature at the level of the emergent stem of the thermometers to within a few kelvins of the fixed point temperature. Such control is facilitated by the existence of end heaters on the furnace, the use of a heat pipe, or, in particular, the existence of a specially-provided heater for the emergent stem (Figure 2.6, Item 4) monitored by thermocouples (Item 5). The effectiveness of such a system can be checked in the standard way: by taking careful measurements to confirm that the hydrostatic pressure effect (Table 2.1) is being accurately tracked.

3.3 In theory, a horizontal well would effectively obviate this and hydrostatic head tracking has in fact been confirmed by tilting fixed point cells away from the vertical position.

3.2.5 Self Heating Effects

The measurement of resistance necessarily involves passing a current through the resistor, with a consequent dissipation of heat that results in a heating of the sensor wire above the environmental temperature. Typical steady-state profiles of the radial temperature distribution caused by currents of 1 mA flowing in two 25 Ω platinum resistance thermometers of differing construction and inserted in a water triple-point cell are shown in Figure 3.5. The internal self heating effect of a thermometer (i.e., the value of ΔT, the temperature difference between the platinum resistor and the outside of the wall of the protecting sheath) at a given environmental temperature is a function only of the thermometer construction and the current. It is, therefore, the same during calibration and use (assuming that the thermometer resistor does not move within its protecting sheath). At the triple point of water the internal heating effect is typically between 0,3 and 1,2 mK/mA^2 and can range up to 4,5 mK/mA^2. It should be noted that variations in self-heating effects can be 0,2 mK/mA^2 or more between thermometers of the same design. If the thermometer is used with the same current that was used during its calibration, the same *internal* heating effect occurs and hence the same temperatures (at the calibration temperatures) appear at the outside of the sheath wall (neglecting any radiation effects, *see* Section 3.2.6).

There is also an *external* self heating effect (also illustrated, both for water and for a close-fitting aluminium sheath, in Figure 3.5) outside the thermometer sheath. This arises because the generated joule heat must flow to some external heat sink. The total heating effect (combined internal and external) can easily be determined by extrapolating to the resistance that would be measured at zero current. To determine the internal heating effect only, the experimental conditions must be such that the external heating effect is negligible ; this condition can be closely approximated by directly immersing the thermometer in an ice bath wherein the solid ice particles are in contact with the thermometer sheath, or (if one cares to risk breaking a brittle thermometer) in a tin or zinc freezing-point apparatus in which the metal freezes directly on the thermometer. (The metal must be remelted and the thermometer removed before cooling many degrees below the freezing point or the thermometer will be crushed.) For precise work, the zero-current

resistance is normally calculated from resistance measurements at two currents in the ratio of 1 to $\sqrt{2}$ (to take account of the square law relationship). A slight improvement in precision and a degree of internal checking may be achieved by making three measurements at current ratios of $1 : \sqrt{2} : 1$.

Any material that intervenes between the thermometer well and the region to be measured should preferably be highly conductive (compare the results for water and glass, and those for aluminium, water and glass shown in Figure 3.5). It is essential that this intervening material does not undergo an exothermic or endothermic reaction at the temperatures involved ; such reactions are more common than may generally be supposed, and should be carefully checked for.

In many applications at high temperatures a thermometer must be used in a protective well with air as the transfer medium. In such cases heating effects can be quite different from those which exist during calibration, and their measurement is essential if the instrument is to be used to its full precision.

3.2.6 Radiation Effects

Another source of heat flux to and away from the platinum coil, and consequently a possible source of error, is thermal radiation. If the sensor can "see" a surface that is appreciably hotter or colder than that being measured, the power gained or lost by the resistor will result in its temperature's being changed. In triple point of water measurements, thermal radiation from lights in the room which is incident upon the emergent stem of the thermometer or which has access to the inner wall of the triple point cell can easily produce an error of up to 0,2 mK. The water triple-point cell should, therefore, be immersed in an ice bath in which no extraneous radiation from sources above room temperature can reach the sensor of the thermometer (*see* Figure 2.1). If this precaution is omitted, even with radiation entry restricted to the top of the cell a thermometer may require an immersion below the vapour-liquid level of 35 cm (which is seldom available) instead of the less than 15 cm that for a thermometer with excellent immersion characteristics, otherwise suffices for it to achieve an accuracy approaching 0,05 mK, *see* Figure 3.4 (a). At higher temperature (630 °C) escaping radiation can result in an error as

large as 35 mK can occur (Figure 3.4 (b)) for a thermometer with a clear fused-silica thermometer sheath.

This heat loss or gain is due to "light piping". In this process radiation losses occur due to total internal reflections within the wall of the thermometer sheath. This error can be very substantially reduced by roughening by sand blasting, or effectively eliminated by coating with graphite paint, the lower part of thermometer sheath from just above the sensor for some 15 to 20 cm. The same mechanism can affect the apparent temperatures of fixed point cells having transparent, polished, inner walls. These are less easily dealt with by sand blasting or painting, but it is a fairly simple matter to arrange that they 'see' only opaque surfaces substantially at their own temperature, and they suffer no net loss or gain of heat.

3.2.7 Effect of Oxidation, Partial Pressure of Oxygen

The partial pressure of oxygen in a platinum resistance thermometer should be of the order of 2 kPa. Changes in resistance of a thermometer due to oxidation of the platinum will occur if the surface of the platinum sensor is clean and the partial pressure of oxygen contained in the thermometer is in the commonly-used range of 5 to 11 kPa [Berry (1980, 1982a, b)]. Under these conditions the changes are roughly as follows: A surface film of platinum oxide forms in the range −40 to 300 °C that can cause $R(t)$ to increase at rates of up to the equivalent of 0,5 mK per hour initially ; platinum oxide forms in the body of the wire in the range 300 to 500 °C that can cause $R(t)$ to increase by up to the equivalent of several mK per hour. When the oxides dissociate (above 450 °C for the two dimensional and above 520 °C for the three dimensional case) $R(t)$ will decrease (often in an abrupt manner) to about its original value. The ratio $W(t)$ changes very much less (in equivalent temperature) than either $R(t)$ or R_{tp} individually ; however, this requires that $W(t)$ be calculated from a pair of resistance measurements with the sensor in substantially equivalent states of oxidation. An example of this reduced apparent error is a thermometer that had its R_{tp} increased by the equivalent of 100 mK exhibited corresponding *decreases* in $W(t)$ at 100 °C, 23 °C and 420 °C equivalent to only 2 mK, 8 mK, and 25 mK respectively. To restore full accuracy in such a case, the oxide layers must be dissociated.

The moderately good stability of the resistance ratio during platinum oxide formation (and dissociation) reduces the problem to a manageable level in most cases. The main difficulty in high precision work is that both $R(t)$ and R_{tp} must correspond to the same oxidation state, and hence R_{tp} must be remeasured frequently if the oxidation or dissociation are causing substantial resistance drifts. Particular care may be necessary when the thermometer passes from an oxidizing to a dissociating temperature zone.

Fortunately, good construction practice can effectively eliminate this problem. Difficulties due to oxidation are greatly aggravated if the partial pressure of oxygen is in excess of 10 kPa, so that air at atmospheric pressure should never be used. Oxygen pressures lower than 3 kPa, on the other hand, reduce the oxidation problem to negligible proportions (because internal oxidation does not then occur). These must, however, be at least 1 kPa partial pressure of oxygen in the thermometer in order to prevent contamination of the sensor by metallic impurities reduced from their oxides. A filling pressure of 2 kPa is an excellent compromise, satisfying both requirements.

3.3 Mathematics

The mathematics associated with calibrating a platinum resistance thermometer and measuring temperatures on the ITS-90 with it are relatively simple and need not involve iterative calculations.

The equations given in the text of the ITS-90 relate a resistance ratio W to T_{90} or to t_{90} where

$$W(T_{90}) = R(T_{90})/R(273{,}16\ \mathrm{K}). \tag{3.3a}$$

$$W(t_{90}) = R(t_{90})/R(0{,}01\ ^{\circ}\mathrm{C}). \tag{3.3b}$$

The denominator in equation (3.3), the reference resistance i.e. the resistance of the thermometer at the reference temperature, is *the resistance at the triple point of water and not that at the ice point.* (The reference resistances *were* those at the ice point for the 1927, 1948 and 1968 international scales.)

The relationship between the resistance ratio (W) and the temperature (T_{90}) for a thermometer under calibration is determined in terms of its deviation from the corresponding relationships of two reference thermometers, one covering the temperature range of 13,8033 K to 273,16 K, the other that from 0 °C to 961,78 °C. The reference thermometer relationships are defined by two reference functions of $W_r(T_{90})$ against T_{90} (*see* equations (3.6), (3.7), (3.9) and (3.10)). The deviation of the calibrated thermometer is defined by deviation functions covering the two ranges given above, and a number of subranges (*see* equations (3.4), (3.8), (3.11) and Table 3.1). The subranges have been made available for users requiring, or perhaps having only thermometers capable of, restricted temperature excursions.

The existence of the subranges implies the existence of a variety of values of T_{90} for a given value of W for a given thermometer. For nearly all cases, this variation in T_{90} does not greatly exceed the intrinsic imprecision of a thermometer and associated measurement uncertainties, *see* Section 1.3.2 and Figure 1.6. It is believed that these sub-range differences do not exceed the differences between measured values of T_{90} that may result from the use of two thermometers used to measure a given temperature T on either a single sub-range of the ITS-90 or on any one of the earlier international scales (*see* Figure 1.5).

$W_r(T_{90})$ is continuous in its first and second derivatives throughout the whole range 13,8 K to 1235 K. The deviation function for a particular range or subrange gives continuity of the first two derivatives except in the case of the range 0 °C to 961,78 °C, in which the second derivative continuity is lost at 660,323 °C. However, practically speaking this second-derivative discontinuity at 660,323 °C is smaller than the uncertainty of the second derivative of $W(T_{90}) - W_r(T_{90})$ resulting from the calibration uncertainties. Somewhat similarly, the first and second derivatives at 0,01 °C as given by equations (3.4) or (3.5) are equal to those given by equation (3.8) to within the uncertainties stemming from the ITS-90 non-uniqueness (*see* Section 1.3.2). No discontinuity in the first two derivatives is caused by equation (3.11).

The alternative definitions provided by equations (3.6) and (3.7) and by equations (3.9) and (3.10) allow the temperature to be obtained from a measured resistance or the resistance to be obtained from a given temperature in a direct way, i.e. without iteration.

3.3.1 Temperature Range From 13,8033 K to 273,16 K

From 13,8033 K to 273,16 K the following deviation functions are used:

$$W(T_{90}) - W_r(T_{90}) = a[W(T_{90}) - 1] + b[W(T_{90}) - 1]^2 + \sum_{i=1}^{m} c_i \, [\ln W(T_{90})]^{i+n} \tag{3.4}$$

or

$$W(T_{90}) - W_r(T_{90}) = a[W(T_{90}) - 1] + b[W(T_{90}) - 1]\ln W(T_{90}) \, . \tag{3.5}$$

Equation (3.4) is used in the following subranges:

13,8033 K to 273,16 K : $m = 5$, $n = 2$;
24,5561 K to 273,16 K : $m = 3$, $n = 0$; and
54,3584 K to 273,16 K : $m = 1$, $n = 1$.

Equation (3.5) is used from 83,8058 K to 273,16 K.

In the temperature range from 13,8033 K to 273,16 K the reference function $W_r(T_{90})$ is defined by the following equations:

$$\ln[W_r(T_{90})] = A_o + \sum_{i=1}^{12} A_i \left[\frac{\ln(T_{90}/273{,}16\ \mathrm{K}) + 1{,}5}{1{,}5} \right]^i \tag{3.6}$$

or

$$T_{90}/273{,}16\ \mathrm{K} = B_o + \sum_{i=1}^{15} B_i \left[\frac{W_r(T_{90})^{1/6} - 0{,}65}{0{,}35} \right]^i . \tag{3.7}$$

The coefficients A_o, A_i and B_o, B_i are set out in Table 4 of the text of the ITS-90. Equations (3.6) and (3.7) represent the same relation to within ± 0,1 mK.

<u>Note:</u> In equations (3.4) and (3.5), $W_r(T_{90})$ can replace $W(T_{90})$ in the right-hand side but, of course, different coefficients will then be found.

3.3.2 Temperature Range From 0 °C to 961,78 °C

From 0 °C to 961,78 °C the following deviation function is used

$$W(T_{90}) - W_r(T_{90}) = a[W(T_{90}) - 1] + b[W(T_{90}) - 1]^2 + c[W(T_{90}) - 1]^3$$

$$+ d[W(T_{90}) - W(660{,}323\ °C)]^2 \qquad (3.8)$$

where $d = 0$ for $W(T_{90}) < W(660{,}323\ °C)$. The number of terms in the right-hand side of equation (3.8) depends on the particular subrange as follows, with a, b, c being calculated with $d = 0$:

0 °C to 961,78 °C :	all terms are used (Table 3.1)
0 °C to 660,323 °C :	$d = 0$
0 °C to 419,527 °C :	$d = c = 0$
0 °C to 231,928 °C :	$d = c = 0$
0 °C to 156,5985 °C :	$d = c = b = 0$
0 °C to 29,7646 °C :	$d = c = b = 0$

In the temperature range from 0 °C to 961,78 °C the reference function $W_r(T_{90})$ is defined by the following equations:

$$W_r(T_{90}) = C_o + \sum_{i=1}^{9} C_i \left[\frac{T_{90}/K - 754{,}15}{481} \right]^i \qquad (3.9)$$

or

$$T_{90}/K - 273{,}15 = D_o + \sum_{i=1}^{9} D_i \left[\frac{W_r(T_{90}) - 2{,}64}{1{,}64} \right]^i . \qquad (3.10)$$

The coefficients C_o, C_i and D_o, D_i are set out in Table 4 of the text of the ITS-90. Equations (3.9) and (3.10) represent the same relation to within ± 0,08 mK from 0 °C to 660,3 °C and to within ± 0,13 mK from 660,3 °C to 961,8 °C.

Equations (3.6) and (3.7) coincide with the equations (3.9) and (3.10) from −10 °C to 10 °C to within ± 0,1 mK. They are practically indistinguishable from 0 °C to 0,01 °C.

<u>Note:</u> In equation (3.8) $W_r(T_{90})$ can replace $W(T_{90})$ in the right-hand side but, of course, different coefficients will then be found.

3.3.3 Temperature Range From −38,8344 °C to 29,7646 °C

From −38,8344 °C to 29,7646 °C the following deviation equation is used:

$$W(T_{90}) - W_r(T_{90}) = a[W(T_{90}) - 1] + b[W(T_{90}) - 1]^2 . \qquad (3.11)$$

$W_r(T_{90})$ is given directly either by equation (3.6) or equation (3.9) depending on the value of T_{90}. For this range the differences between equations (3.6) and (3.7) below 0 °C, and between (3.9) and (3.10) above 0 °C are less than 0,06 mK.

<u>Note:</u> In equation (3.11) $W_r(T_{90})$ can replace $W(T_{90})$ in the right-hand side but, of course, different coefficients will then be found.

TABLE 3.1

Deviation functions and calibration points for platinum resistance thermometers in the various ranges in which they define T_{90}

(a) Ranges with an upper limit of 273,16 K

Section[3.4]	Lower limit	Deviation functions[3.5]	Calibration points[3.6]
3.3.1	13,803 3 K	$a[W(T_{90}) - 1] + b[W(T_{90}) - 1]^2 + \sum_{i=1}^{5} c_i[\ln W(T_{90})]^{i+n}$, $n=2$	2 to 9
3.3.1.1	24,556 1 K	As for 3.3.1 with $c_4 = c_5 = 0$ and $n = 0$	2, 5 to 9
3.3.1.2	54,358 4 K	As for 3.3.1 with $c_2 = c_3 = c_4 = c_5 = 0$ and $n = 1$	6 to 9
3.3.1.3	83,805 8 K	$a[W(T_{90}) - 1] + b[W(T_{90}) - 1] \ln W(T_{90})$	7 to 9

(b) Ranges with a lower limit of 0 °C

Section	Upper limit	Deviation functions[3.5]	Calibration points[3.6]
3.3.2[3.7]	961,78 °C	$a[W(T_{90}) - 1] + b[W(T_{90}) - 1]^2 + c[W(T_{90}) - 1]^3 + d[W(T_{90}) - W(660{,}323\ °C)]^2$	9, 12 to 15
3.3.2.1	660,323 °C	As for 3.3.2 with $d = 0$	9, 12 to 14
3.3.2.2	419,527 °C	As for 3.3.2 with $c = d = 0$	9, 12, 13
3.3.2.3	231,928 °C	As for 3.3.2 with $c = d = 0$	9, 11, 12
3.3.2.4	156,5985 °C	As for 3.3.2 with $b = c = d = 0$	9, 11
3.3.2.5	29,7646 °C	As for 3.3.2 with $b = c = d = 0$	9, 10

(c) Range from 234,3156 K (−38,8344 °C) to 29,764 6 °C

3.3.3		As for 3.3.2 with $c = d = 0$	8 to 10

3.4 These numbers refer to sections in the text of the ITS-90 (see Appendix 1).

3.5 Note that the values of the coefficients a, b, c, c_i and d in the deviation functions depend upon the range or sub-range in which they were obtained.

3.6 *See* Table 1.1.

3.7 Calibration points 9, 12 to 14 are used with $d = 0$ for $t_{90} < 660{,}323$ °C ; the values of a, b and c thus obtained are retained for $t_{90} > 660{,}323$ °C, with d being determined from calibration point 15.

Figure 3.1 A typical 25 Ω capsule-type platinum resistance thermometer: A platinum sheath 5 mm in diameter and 50 mm long ; B the two glass tubes containing the 0,07 mm diameter coiled Pt wire ; C flame welds to platinum leads ; D glass/platinum seal.
Section 3.1.1.

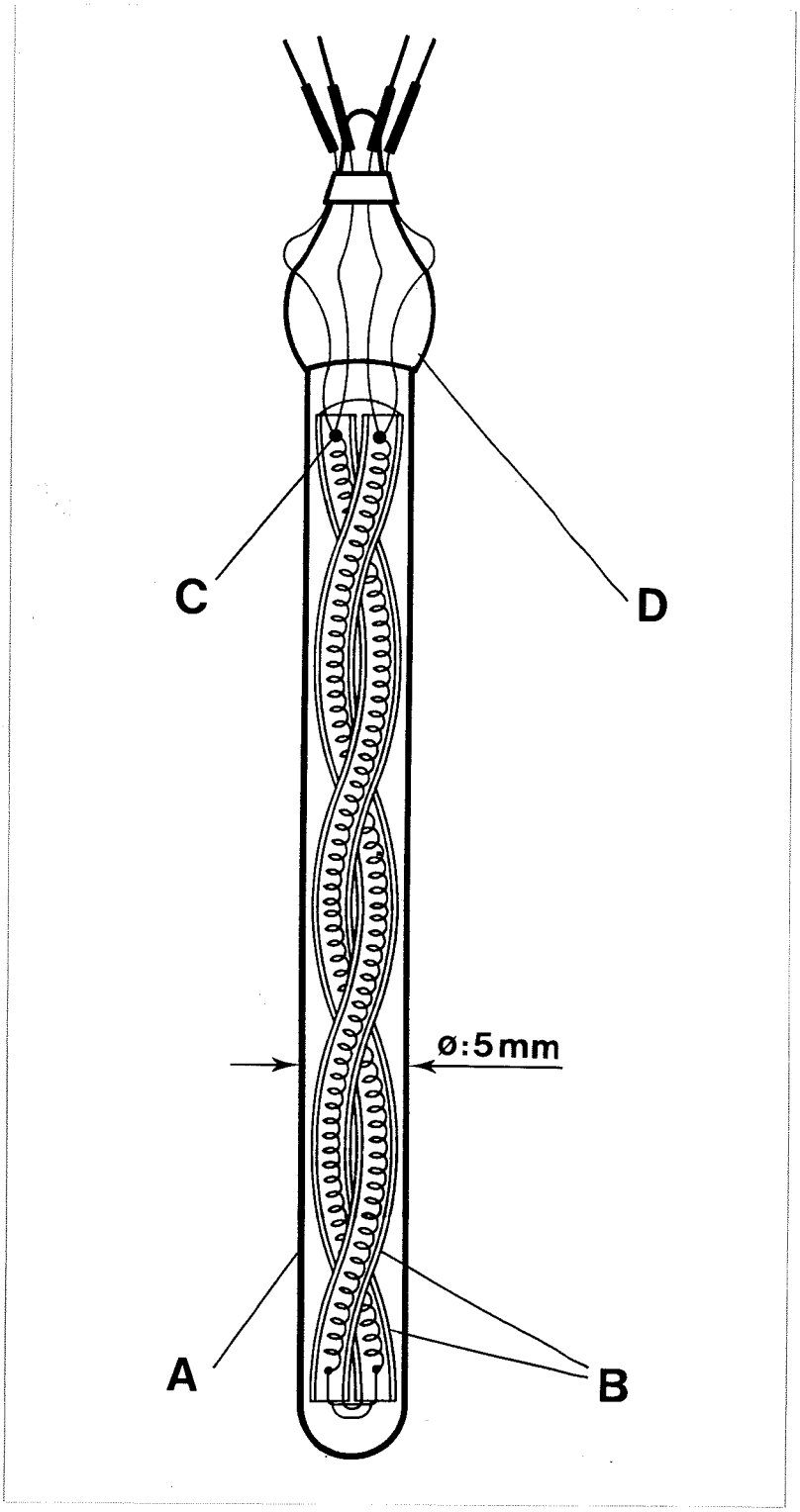

Figure 3.2 Typical designs of 25 Ω long-stem platinum resistance thermometers.
Section 3.1.2.

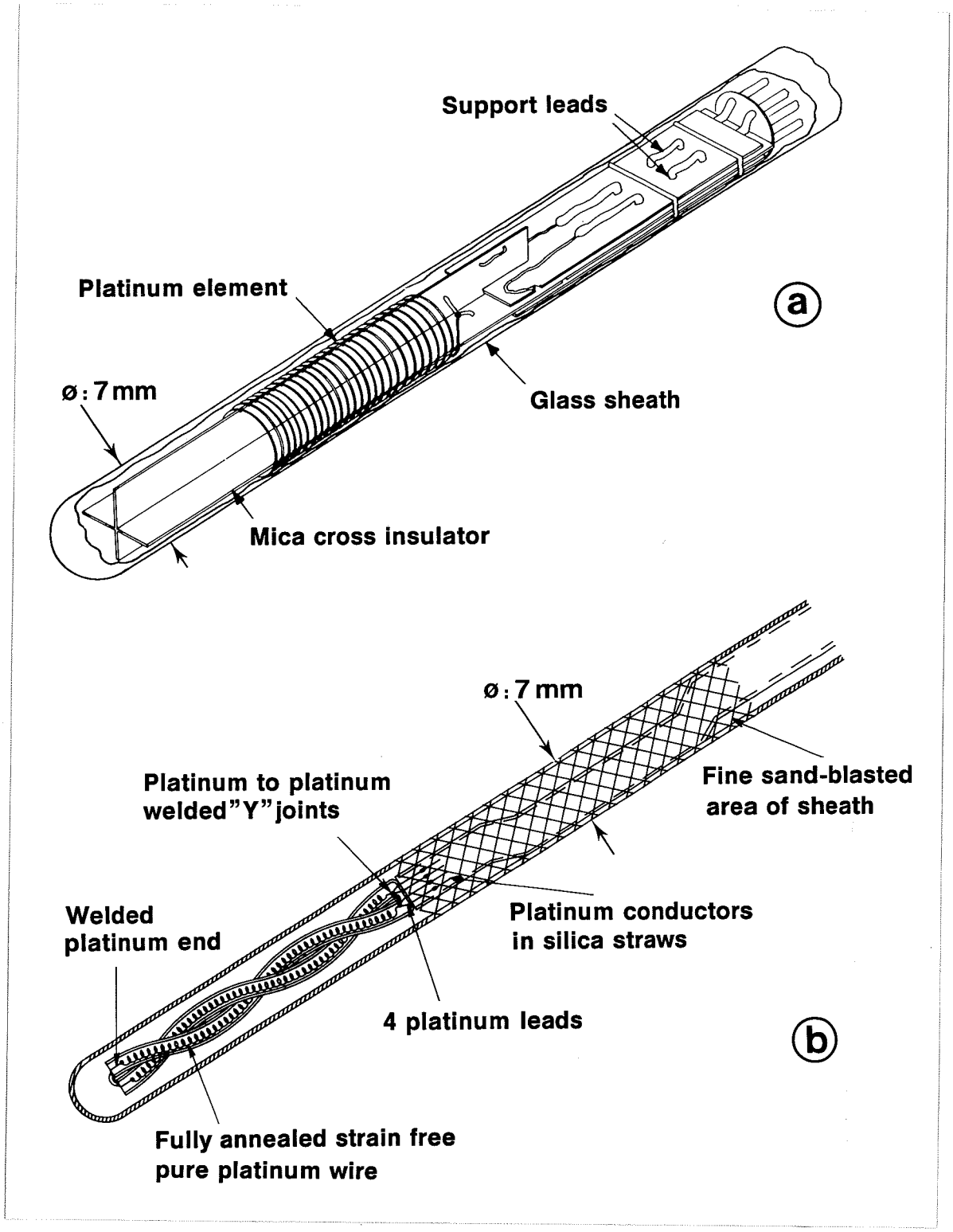

Figure 3.3 Typical designs of high temperature platinum resistance thermometers (a) R_{tp} = 0,25 Ω, (b) R_{tp} = 2,5 Ω.
Section 3.1.3.

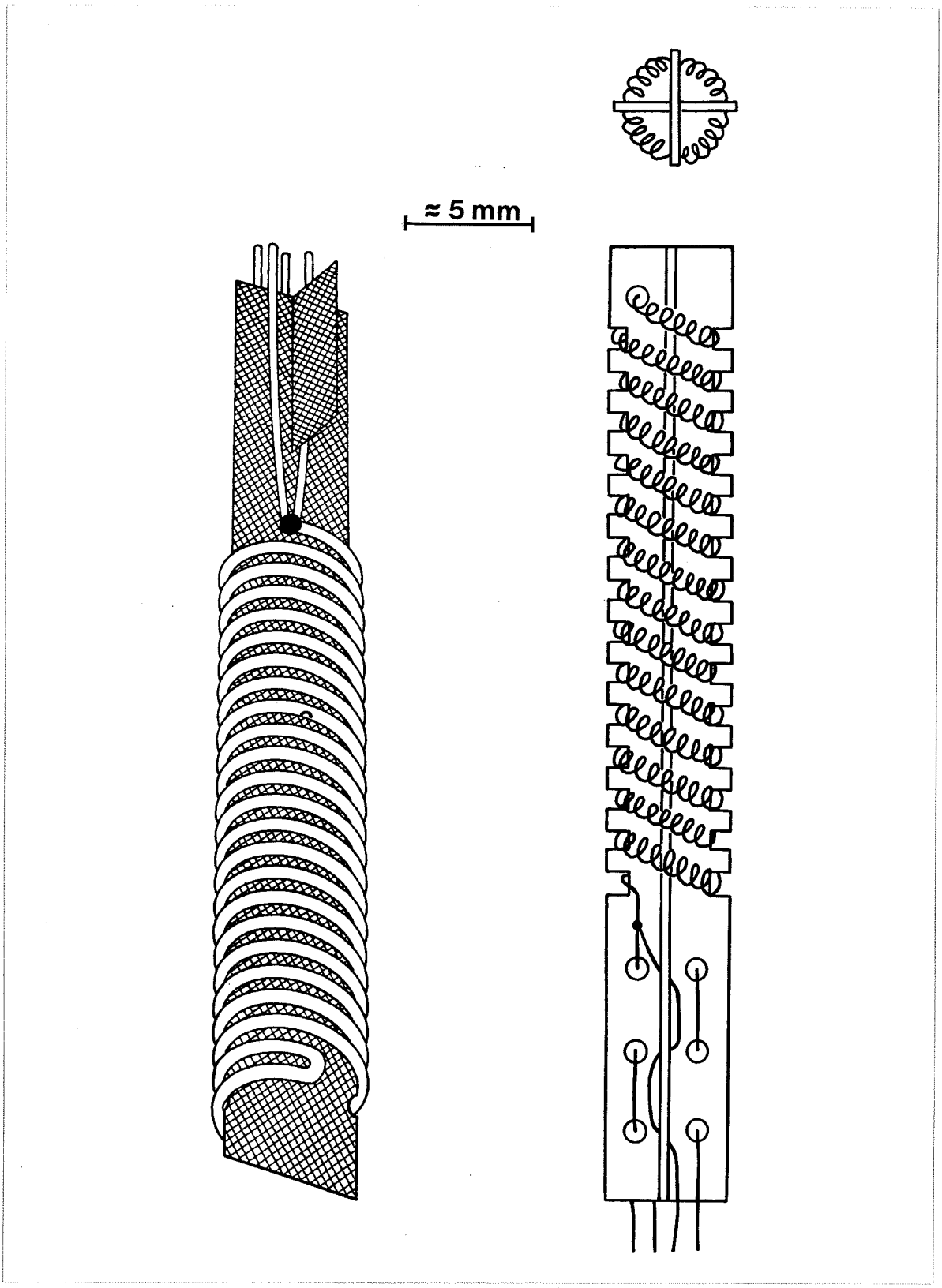

Figure 3.4 (a) Depth-of-immersion effect in a triple point of water cell for a well-designed (Meyers) platinum resistance thermometer with the emergent stem substantially at room temperature [after Ancsin and Murdock (1990)] Section 3.2.4. (b) Depth-of-immersion effect at 631 °C for a well-designed (Meyers) platinum resistance thermometer with the emergent stem exposed to room temperature and with the stem clear, permitting radiation piping and with the stem blackened to prevent such piping [after McLaren and Murdock (1966)] Sections 3.2.4 and 3.2.6. (c) Progress to equilibrium of a typical glass water triple-point cell [Ancsin and Murdock (1990)] Section 2.1.3.

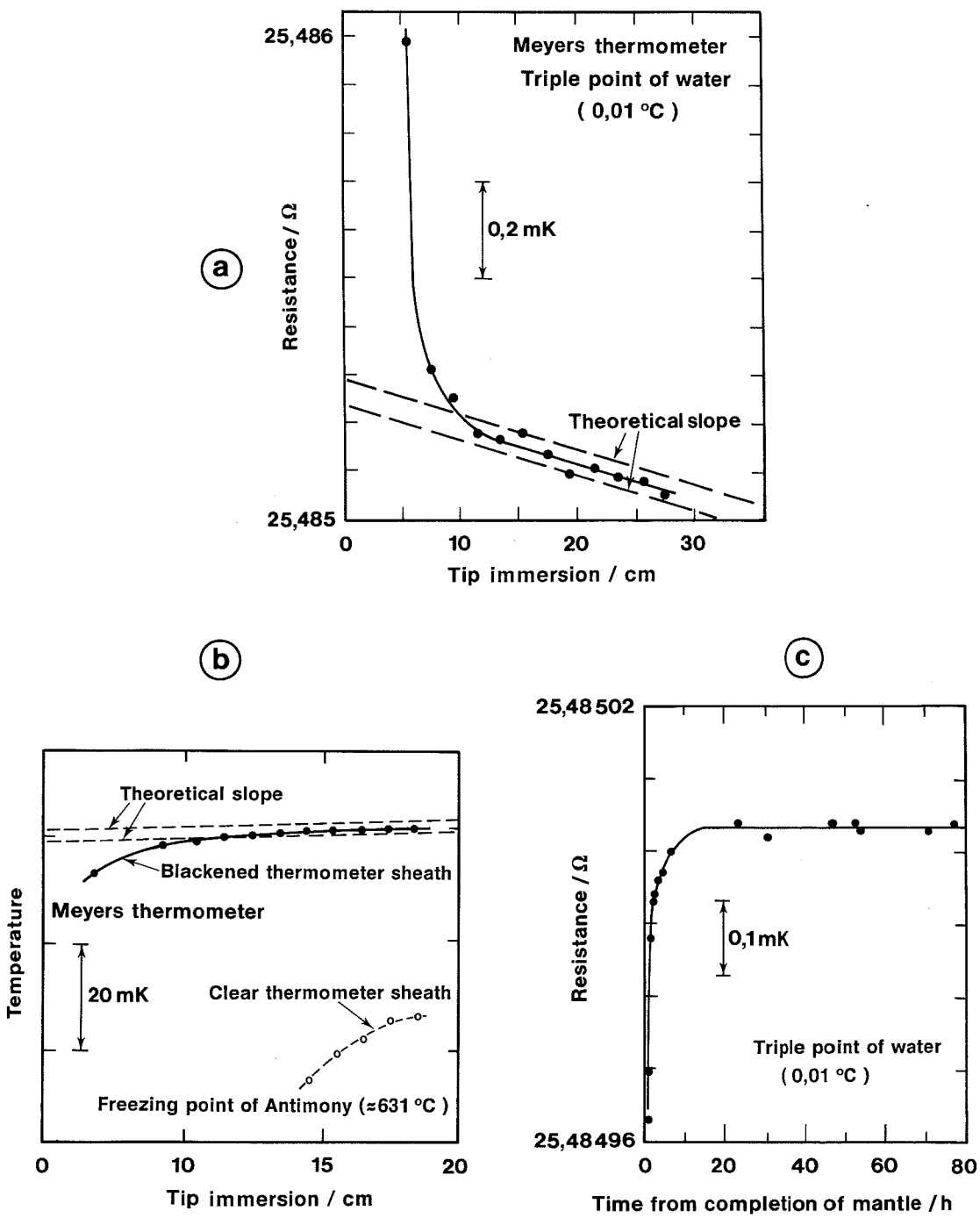

Figure 3.5 Calculated self-heating effects in water-triple-point cell [after Riddle *et al.* (1973)]
Platinum resistance thermometers at 33 cm immersion in a water-triple-point cell
A. Platinum coils of coiled filament thermometer ; only coils of one side are indicated ; B. Platinum coils of single layer helix thermometer ; only turns of one side are indicated ; C. Borosilicate glass thermometer envelope ; D. Water from ice bath ; E. Aluminium bushing (length not to scale) ; F. Borosilicate glass thermometer well ; G. Ice mantle ; H. Inner melt ; J. Water in cell ; K. Cell well (borosilicate glass) ; L. Outside ice-water bath ; N. Polyurethane sponge.
Sections 2.1.3.5, 3.2.5.

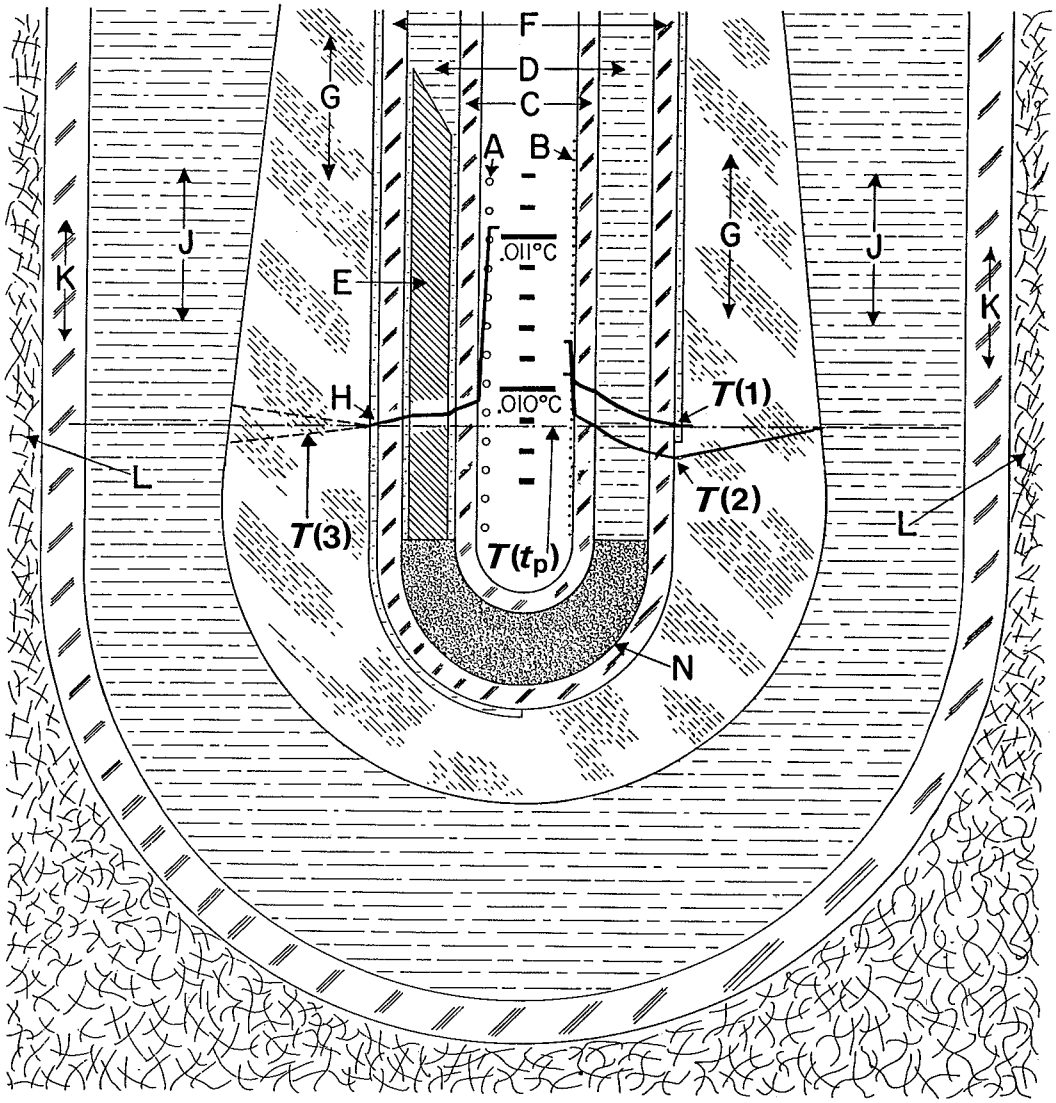

T_1 Temperature profile for thermometer B with an inner ice-water interface and the thermometer immersed in water.
T_2 Temperature profile for thermometer B with no inner interface, thermometer immersed in water.
T_3 Temperature profile for thermometer A with an inner ice-water interface and an aluminium bushing.
T_{tp} Triple-point temperature corrected for hydrostatic pressure.

REFERENCES

Ancsin, J. and Murdock, E.G. (1990): Comparison of water triple-point cells (private communication)

Berry, R.J. (1980): Effect of Pt Oxidation on Pt Resistance Thermometry ; Metrologia **16**, 117-126

Berry, R.J. (1982a): Evaluation and Control of Platinum Oxidation Errors in Standard Platinum Resistance Thermometers. Temperature, Its Measurement and Control in Science and Industry (American Institute of Physics, New York) **5**, 743-752

Berry, R.J. (1982b): Oxidation, Stability and Insulation Characteristics of Rosemount Standard Platinum Thermometers. Temperature, Its Measurement and Control in Science and Industry (American Institute of Physics, New York) **5**, 753-762

Hust, J.G. (1970): Thermal Anchoring of Wires in Cryogenic Apparatus ; Rev. Sci. Inst. **41**, 622-624

Jung, H.J., Li, Xumo and Fischer, J. (1989): An accurate determination of the relationship between the resistance ratio of the high temperature platinum resistance thermometers and thermodynamic temperature in the range from 903 K to 1263 K by infrared pyrometry ; CCT 17^{e} Session, Doc. CCT/89-10

Kemp, R.C., Kemp, W.R.G. and Cowan, J.A. (1976): The Boiling Points and Triple Points of Oxygen and Argon ; Metrologia **12**, 93-100

Li, Xumo (1989): Some remarks on the ITS-90 draft ; CCT 17^{e} Session, Doc. CCT/89-40

Marcarino, P., Dematteis, R., Gallorini, M. and Rizzio, E. (1989): Contamination of Platinum Resistance Thermometers at High Temperature Through Their Silica Sheaths ; Metrologia **26**, 175-181

McLaren, E.H. and Murdock, E.G. (1966): Radiation Effects in Precision Resistance Thermometry ; Can. J. Phys. **44**, 2631-2659

Riddle, J.L., Furukawa, G.T. and Plumb, H.H. (1973): Platinum Resistance Thermometry ; NBS Monograph 126

4. THE ^{3}He AND ^{4}He VAPOUR-PRESSURE SCALES AND PRESSURE MEASUREMENT

4.1 Vapour Pressures of Helium (0,65 K to 5,0 K)

In the range 0,65 K to 5,0 K the ITS-90 is defined using equations relating the vapour pressures of ^{3}He and ^{4}He to T_{90} (*see* Equation 3 and Table 3 of the text of ITS-90). The techniques by which helium vapour pressures can be set up and measured are described in this section.

There are three principal requirements for any vapour pressure thermometer: to arrange for a volume of the pure liquid and vapour phases to come to thermal equilibrium; to measure absolutely the pressure at the (plane) interface; and to know the vapour pressure-temperature relationship. The following sections address these requirements.

4.2 Vapour Pressures Relations For Helium

The vapour pressure relations for helium are of the form:

$$T_{90}/\mathrm{K} = A_0 + \sum_{i=1}^{9} A_i \left[(\ln(p/\mathrm{Pa}) - B)/C \right]^i \qquad (4.1)$$

Values of the constants A_0, A_i, B and C are given in Table 3 of the text of the ITS-90 for the three ranges: 0,65 K to 3,2 K for ^{3}He; 1,25 K to 2,1768 K for ^{4}He (^{4}He II)[4.1]; and 2,1768 K to 5,0 K also for ^{4}He (^{4}He I)[4.1]. The ^{4}He equations coincide at the lambda point (2,1768 K, 5041,8 Pa) with a first derivative $\mathrm{d}\ln p/\mathrm{d}T_{90}$ of 2,461 K^{-1}. In deriving these equations no constraints were placed on the second derivative, which physically is discontinuous at this point.

The upper temperature limits for the use of the two isotopes were chosen to be somewhat below the critical points, since the specification of the relationships and the measurement of vapour pressures become matters of some difficulty as the critical point is approached. The lower temperature limits are such that the vapour pressures are still not less than 100 Pa; at pressures below 100 Pa the inaccuracies of the vapour pressure thermometers are likely to be more than the ± 0,5 mK which was

---

4.1 In the phase equilibrium diagram of ^{4}He the liquid phases of ^{4}He above and below the lambda line are distinguished by referring to them as to He I and He II respectively. The properties of ^{4}He II are very different from those of ^{4} He I.

considered appropriate for the ITS-90, *see* Figure 4.1. It was also the intention to keep open the option of extending the scale to lower temperatures by other means.

The equations adopted in the ITS-90 are a restricted set of those derived by Rusby and Durieux (1984), which themselves were simplified forms of the equations of Durieux and Rusby (1983) that were approved by the CIPM (1982) following the introduction of the EPT-76 [BIPM (1979)]. The unrestricted forms are useful for those choosing to use them at temperatures close to the critical points or below 0,65 K.

4.3 Helium Vapour-Pressure Thermometry

4.3.1 ^{4}He

In its simplest form a vapour-pressure thermometer consists of a vessel containing the liquid in equilibrium with its vapour.

For ^{4}He (both ^{4}He I and ^{4}He II) the liquid is typically contained in a cryostat or storage vessel with appropriate precautions for reducing heat influx and hence the rate of evaporation. A schematic illustration of a cryostat for calibrating capsule thermometers is given in Figure 4.2a.

In this cryostat the refrigerating liquid is also the thermometer liquid. The manometer (not shown) senses the vapour pressure via a tube inserted into the vapour space and terminating close to the liquid surface. The pressure is usually regulated by means of a throttling valve in the pumping line. The pressure, and hence the temperature, is progressively reduced so as to prevent temperature stratification. An electrical heater at the bottom of the liquid (not shown) can be used for reheating and, at low power levels, will promote mixing.

The convection mechanism is a feeble one at these temperatures, and significant temperature gradients can be present in the liquid. Such gradients occur even when the temperature monotonically decreases with time, their magnitude being likely to increase as the temperature is lowered, perhaps becoming as high as 5 mK at the lambda point [Cataland *et al.* (1962)]. On re-heating, the temperature of the bulk liquid may respond only slowly if the pressure is allowed to rise, and gross gradients can then result.

Such difficulties can be avoided by mounting the artifacts in a copper block containing a vapour-pressure bulb (Figure 4.2b) that is independently supplied with helium so that a liquid-vapour interface is contained within it. In a closed system the liquid fraction will increase when the temperature is reduced, and the total mass of helium must be such that the bulb does not overfill. The supply tube (of stainless steel or another material of low thermal conductivity, and typically 2 mm in diameter) is also the pressure sensing tube, and where it passes through the surrounding liquid it must be insulated sufficiently well to avoid condensation within it. Light insulation is reported as being sufficient for this purpose, since cold spots tend to be self-stifling by virtue of the heat of condensation [Ambler and Hudson (1956)] ; however, a stainless-steel vacuum jacket is often used and may extend up to room temperature. In addition, copper cladding or electrical heaters on the sensing tube can be used. These have the advantage of keeping the sensing tube and vapour within it relatively warm, only reaching the liquid temperature just above the bulb thereby reducing the aerostatic head correction. For an exposed tube and a bulb at 4,2 K this correction may be about 0,5 mK, compared with 0,1 to 0,2 mK that is typical for a vacuum-jacketed tube (for which, however, the temperature distribution needed for calculating the pressure head, can be difficult to ascertain). At the lower temperatures aerostatic head corrections are smaller in terms both of pressure and of the temperature equivalents because of the rapid decrease of vapour density with decrease in temperature.

No radiation trap is shown inside the pressure sensing tube of Figure 4.2b. If this is 2 mm in diameter the maximum radiative heat transfer down the tube (assuming that all the radiation emitted at room temperature is absorbed in the bulb) would be about 1,4 mW. The helium in the bulb is not likely to absorb much of this, while the copper block could easily do so without setting up significant temperature gradients. A trap could be included near the bottom of the tube, but it would need careful design. A simple bend in the tube is unlikely to be effective, while any other system must be so constructed that no liquid can be held at that point. Even with a straight tube it is possible for liquid to block the tube just above the bulb, leading to substantial measurement errors. A pressure pulse may dislodge such a block, but as a matter of design the portion of the tube exposed to low temperatures should be short, or the vacuum jacket can be extended right down to the bulb. In the latter case

the heat conducted down the sensing tube, perhaps 0,1 mW, can be readily absorbed in the block but a baffle must be included in the vacuum jacket to intercept the radiation from room temperature components of the jacket.

There will be some differential contraction between the sensing tube and the vacuum jacket. These must not touch, and an insulating spacer, which can also serve as the radiation trap, should be used to prevent this. Alternatively bellows or a sliding seal at the upper end of the tube can prevent touching.

While a vapour-pressure bulb is preferable for normal helium, He I, this is not the case for the superfluid He II. With He II in the bulb, a superfluid film would creep up the walls of the sensing tube, would evaporate at some higher temperature, and would then reflux back to the bulb. This action can result in a measurement error of several millikelvins [Sydoriak and Sherman (1964)] due in part to pressure gradients in the tube and in part to temperature gradients in the bulb. Continuity of measurements (thermometers calibrations or other) on passing through the lambda point is a good test of any design.

By contrast, the system of Figure 4.2a works well below the lambda point. In this system the superfluid film evaporates as part of the cooling process and never affects the pressure sensing. Furthermore, the phenomenal thermal diffusivity of He II ensures that no temperature gradients exist within the liquid. The only limitations are the ability of the pump to reduce the temperature as far as is required and, possibly, the appearance of thermomolecular effects at low pressures. The latter limitation is eliminated by use of a tube of diameter 10 mm or more equipped with appropriate radiation baffles. Clearly a dual system, in which both a vapour pressure bulb and a bath pressure-sensing tube are provided, would enable the complete ^{4}He range to be covered, and would also allow investigations of the differences between the two realizations to be made.

4.3.2. ^{3}He

Extensive vapour-pressure comparisons were carried out with ^{3}He by Sydoriak *et al.* (1964) prior to the derivation of the 1962 ^{3}He vapour-pressure scale and equation. Problems with ^{3}He are its high cost, of the order of 1000 times that of ^{4}He, and the need to take account of

contamination with ^{4}He (there is negligible natural occurrence of ^{3}He, so the reverse does not generally apply, and other impurities are frozen out).

Because of its cost, ^{3}He is usually kept in a closed system and repeatedly used. It is condensed into a small chamber (or pot) in the cryostat as needed for cooling, experimentation, or measurement. The vapour pressure can be measured using a second tube leading to the pot.

Condensation of, typically, up to 10 cm^3 of liquid ^{3}He is effected using a pumped ^{4}He pot (or bath of ^{4}He) at 1,5 K or below. The ^{4}He pot is then boiled dry (or the bath is isolated from the interior assembly), and further cooling is achieved by evaporation of ^{3}He. The heat of vaporisation of this is large compared with the amount of cooling typically required, so the lowest temperature reached will be limited by the pumping speed and heat leaks: 0,5 K can be readily achieved.

Sufficient heat-exchange area must be provided to ensure that the liquid is approximately isothermal and is in equilibrium with the experimental artifacts (including thermometers) despite the heat flows resulting from heat leaks into the pot and from the evaporation of the liquid.

A serious complication is that normal-grade ^{3}He may contain 0,1 % ^{4}He which would cause an error of as much as 0,6 mK at 3 K [Sydoriak *et al.* (1964)]. To overcome this, a second pot of perhaps 1 cm^3 using a small quantity of ^{3}He purified to about 0,01 % is often employed for the vapour-pressure measurement.

4.3.3 Combined ^{4}He, ^{3}He System

A combined ^{4}He and ^{3}He vapour pressure cryostat, somewhat simpler than that of Sydoriak *et al.*, has been described by Rusby and Swenson (1980) and was used by them for the re-determination of the vapour-pressure relations, *see* Figure 4.3. The copper thermometer block containing the helium pots was suspended inside a vacuum jacket which was surrounded by liquid ^{4}He at 4,2 K. A single 50 cm^3 pot of ^{4}He was used for cooling and for sensing the vapour pressure. The problem of film flow was avoided by including an orifice of 0,6 mm diameter in the lid of the pot. Such film as flowed through this was soon evaporated (and thereby contributed to the cooling). The pressure sensing tube joined the 6 mm diameter pumping tube some 4 cm higher up and so was not affected by film refluxing. The pressure gradient across the orifice and

along this section of the tube was negligible at temperatures above 1,4 K. A larger orifice could have permitted accurate measurements to still lower temperatures. The ^{4}He pot contained a spiral of copper foil to promote temperature uniformity (*see* the authors' discussion of measurements above and below the lambda point).

A ^{3}He cooling chamber was provided, and measurements of ^{3}He vapour pressures were made with a small bulb and a sample of purified gas. Pumping tubes were about 20 mm in diameter between the ^{4}He bath and room temperature (with appropriate traps to intercept radiation). The vapour-pressure tubes were 2 mm in diameter at temperatures up to 4,2 K, and 6 mm (for ^{4}He) and 5 mm (for ^{3}He) above this. These dimensions give thermomolecular effects, calculated from the Weber-Schmidt equation (*see* Section 4.4.5), equivalent to 1 mK at 1,25 K and 0,65 K for ^{4}He and ^{3}He respectively, with the effects increasing rapidly at lower temperatures. Larger tubes may be desirable, especially for ^{3}He, though this would require a substantial quantity of gas to be available if ^{3}He vapour-pressure measurements are also to be made up to 3,2 K.

A way of reconciling the requirement for a small thermomolecular effect at lower pressures with the requirement that the amount of gas needed to fill the system at high pressures should not be too large is to increase the diameter of the tube some distance up the cryostat. The temperature of the junction must, of course, be known, but this is desirable in any case for the calculation of the aerostatic head effect. The vapour-pressure sensing tubes used by Rusby and Swenson passed through the ^{4}He bath and the aerostatic head was consequently quite large (equivalent to values as large as 0,6 mK). Steps also had to be taken to damp out thermal oscillations in the ^{4}He pumping tube (a woollen plug at room temperature, or an enlargement of the tube, usually suffices for this purpose). Cold spots were not evident in measurements at 4,2 K, but measurements of pressures above atmospheric were made only when the liquid level in the main helium bath had fallen below the top of the vacuum jacket, and with the bath pressurised to a maximum of 2 atmospheres (absolute).

In this or any similar system the tubing that is at room temperature but is open to the cryogenic area must be clean, as any desorbed vapours will diffuse into the cryostat and be re-adsorbed there. The pressure gradient due to this diffusion can be significant at low pressures.

4.4 Pressure Measurements

Pressure measurements are required for the realization of the boiling points of hydrogen, the helium vapour pressure scales and the gas thermometer.

Table 4.1 summarises hydrogen and helium vapour pressure data and allows the measurement requirements to be calculated. It shows that in order to cover the complete range it is necessary to measure absolute pressures from 100 Pa to 200 000 Pa, with accuracies of 0,5 Pa to 75 Pa, respectively, to achieve 0,5 mK accuracy in T_{90}. The relative sensitivities (from column 4) are less wide ranging, varying from 0,03%/mK for hydrogen at 20,3 K to 0,9 %/mK for ^{3}He at 0,65 K. A measuring instrument with a constant relative uncertainty is thus more suitable than one with a constant absolute uncertainty.

For much of the range the requirements (in terms of room-temperature capability for pressure measurement) are not overly stringent. A mercury manometer of 10 Pa accuracy (achievable with simple optical aids) is sufficient to give 1 mK accuracy in T_{90} down to 2 K (with ^{4}He) or 1,2 K (with ^{3}He), and oil manometers with about 15 times greater sensitivity (though not accuracy) have often been used to lower temperatures.

Where 0,1 mK accuracy is sought, however, more sophisticated systems are needed. Superior mercury instruments are available but tend to be inconvenient to use. Quartz-spiral bourdon gauges and capacitance diaphragm gauges are adequately sensitive and convenient to use, but have constant pressure sensitivity and require comprehensive calibrations. Moreover, quartz is permeable to helium.

Pressure balances operated with air or helium in the 'absolute' mode, i.e. with the space above the assembly evacuated, are much more suitable. They retain essentially the same relative accuracy over their operating range, and this can be 20 parts in 10^6 (equivalent to less than 0,025 mK in the measurement of the vapour pressure of helium) without undue difficulty.

4.4.1 Mercury Manometer

The classical method employs a cathetometer to determine the position of the mercury levels in a U-tube manometer, and has a limit of accuracy of about 3 Pa. For pressures up to 100 kPa higher accuracy can be attained if the levels are sensed by capacitive [Preston-Thomas and Kirby (1968), Guildner *et al.* (1970)] or interferometric [Bonhoure and Terrien (1967), Mitsui *et al.* (1972)] techniques: for pressures of the order of 1 standard atmosphere, such instruments can measure absolute pressures to about 3 in 10^6 or pressure ratios to about 1 in 10^6.

At these levels of accuracy, uncertainties in length, density of mercury (which is pressure and temperature dependent), aerostatic head, mercury vapour pressure and capillary depression may become critical. For absolute pressure measurements (which are required for hydrogen vapour-pressure points and helium vapour pressure temperature measurements) a knowledge of the local value of the acceleration due to gravity (g) is required. However, for gas thermometry, in which pressure ratios only are measured, constant errors in the average density of the mercury or in the value of g cancel out.

The mean density of pure mercury at t_{90} in a barometric column supported by the pressure p being measured is given with sufficient accuracy, over the temperature range from 0 °C to 40 °C and for the pressures relevant to these measurements, by the relation

$$\rho\left(t_{90}, \frac{p}{2}\right) = \frac{\rho(20\ ^\circ\mathrm{C}, p_0)}{\left[1 + A(t_{90} - 20\ ^\circ\mathrm{C}) + B(t_{90} - 20\ ^\circ\mathrm{C})^2\right] \times \left[1 - \chi\left(\frac{p}{2} - p_0\right)\right]} \quad (4.2)$$

where $A = 1{,}8120 \times 10^{-4}\ ^\circ\mathrm{C}^{-1}$, $B = 8 \times 10^{-9}\ ^\circ\mathrm{C}^{-2}$, $\chi = 4 \times 10^{-11}\ \mathrm{Pa}^{-1}$, $p_0 = 101\ 325$ Pa and $\rho\ (20\ ^\circ\mathrm{C}, p_0) = 13\ 545{,}854\ \mathrm{kg\ m^{-3}}$ [Ambrose (1990)]. A sufficiently accurate local value of g may be obtained by using the Réseau Gravimétrique International Unifié 1971 (IGSN-71) de l'Union Géodésique et Géophysique Internationale.

Corrections for the errors mentioned above are straightforward, except for the capillary depression of mercury surfaces of less than several centimetres diameter which remains a potential source of uncertainty in high-precision manometry [Brombacher et al. (1960)]. Tables for the capillary correction in terms of bore diameter and meniscus

height based upon experimental data are given by Kistemaker (1944-1946) and Cawood and Patterson (1933). Gould and Vickers (1952) computed similar tables for values of the coefficient of surface tension (σ), ranging from 0,4 to 0,5 Nm^{-1} ; within this range, for a given meniscus height, the capillary depression is practically linearly dependent on σ.

In practice, σ appears to vary from 0,4 to 0,58 Nm^{-1} depending upon the degree of surface cleanliness of the mercury and the surface conditions of the container ; there is frequently a degree of hysteresis in the relation between meniscus height and pressure. The lack of a precise knowledge of σ is such that if an accuracy within 10 Pa is desired, a tube of diameter not less than 15 mm should be used. To achieve the highest levels of accuracy the diameter of the mercury surfaces should be so large ($\geq$ 30 mm) that the uncertainty in the capillary depression will be negligible ($\leq$ 0,15 Pa).

4.4.2 Pressure Balance

For this instrument the pressure is defined by the mass, the local value of g and the effective area of a piston freely rotating in a closely-fitting cylinder. Pressure settings for a given piston are changed by changing its mass, i.e. by adding additional weights [Dadson *et al.* (1982)].

The principal limitation here is the accuracy with which the effective area is known. This may be obtained from direct dimensional measurements or, more usually, by calibration against another pressure balance, or against a mercury instrument near standard atmospheric pressure (where this too has high relative accuracy). For stainless steel the temperature and pressure coefficients of the effective area amount to 2 to 3 $\times$ 10^{-5} K^{-1} and -5×10^{-6} MPa^{-1}, respectively.

The calibration of the weights should not be a problem, even allowing for the need for buoyancy corrections (if the weighing is performed in air). The buoyancy of the floating member of the piston-cylinder assembly should be assessed carefully, however, as some parts may be made of aluminium, rather than stainless steel, to reduce the weight (which limits the lowest pressure at which the device can be operated). Some approximate means of measuring the temperature of the assembly should be included, as the temperature coefficient is likely to be more than 2×10^{-5} K^{-1}.

In the measurement of absolute pressure (as required in vapour-pressure thermometers) the bell jar containing the piston assembly is evacuated and the local value of g must be known. Small corrections must be applied to take account of the effects of the gas streaming between the piston and the cylinder, and of the resulting residual pressure (which must therefore be measured) in the evacuated space above the piston. The gas head may vary by about 2 cm as the piston sinks in use, which (for argon) is equivalent to a few parts in 10^6 at standard atmospheric pressure.

Pressure balances are not so much *gauges* of pressure as *generators* of a series of pressures whose values are determined by the (fixed) effective area and the (variable) loading. The minimum value is that with the assembly unloaded. Since a continuum of pressures is not available, and because the assembly will need to be taken apart for occasional cleaning, it is usual to apply the generated pressure to the reference port of a differential capacitance-sensed diaphragm gauge (*see* Section 4.4.4). The vapour pressure to be measured is fed to the other port and the gauge output gives the difference between the two. The diaphragm gauge needs to be calibrated, and this can be done (at various line pressures) using two pressure balances, or one pressure balance and a temperature-controlled reference volume, or even with a temperature-controlled (or monitored) vapour pressure bath itself as the reference. The first is preferable, but in the measurement of helium vapour pressures the problem can be avoided by so adjusting the helium temperature that the diaphragm gauge reads zero - i.e. that the pressure to be measured exactly equals the pressure generated by the balance. The true zero of the diaphragm gauge can be simply checked by cross connecting the two sides of the diaphragm.

For measurements of ^{4}He vapour pressures it is convenient to operate the balance with helium, drawing gas from the vapour pressure system as needed. For ^{3}He, however, the cost of the gas usually precludes this, while ^{4}He should not be used for fear of contaminating the ^{3}He. Air, nitrogen or argon will be convenient, but once ^{3}He is admitted to the diaphragm gauge care must be taken not to allow air into the ^{3}He line. Cross-connection to check zero entails some wastage of gas and so for ^{3}He should preferably be carried out only immediately before and after a series of measurements, the minimum requirement.

As was mentioned earlier, the lower limit of operation of the pressure balance is that which supports just the unloaded floating member (which may be the piston or the cylinder, according to design). This can be reduced by choosing a light assembly with a large effective area, and a typical minimum pressure is 2 kPa.

The pressure balance can achieve an accuracy within 1 part in 10^5 and a resolution of 1 part in 10^6 between about 200 kPa and 2 kPa. Below the latter value an alternative device must be used.

Unless a gas-injection system is available, the measuring time available ($\approx$ 5 min) is determined by the downward movement of the piston resulting from the inevitable gas loss through the annular gap between piston and cylinder. Elegant solutions to this problem are reported in the literature [Neubert (1977)].

4.4.3 Quartz Pressure Gauge

The modern quartz bourdon-tube pressure gauge can be used as a pressure transfer and interpolating device. To avoid hysteresis, the pressure-sensing quartz element is restrained from making large excursions by a servo feedback system. The gas volume of such a gauge is very much smaller than that of a pressure balance ; however, the quartz is highly permeable to helium, so care must be taken to prevent helium-rich gases for coming into contact with it. This type of gauge is usually calibrated directly against a pressure balance ; regular checks are necessary although it may retain its calibration for very long periods. Accuracy can be within one part in 10^5 of full scale, the latter usually being somewhere in the range of 100 Pa to 100 kPa.

As in the case of the diaphragm gauge described in Section 4.4.4, the advantages are that the instrument has a direct read-out and that changes in pressure can readily be accommodated.

4.4.4 Diaphragm and Capsule Pressure Transducer

The diaphragm transducer consists of a thin, usually metal, membrane under tension located between two electrodes. Deflection of the membrane caused by a pressure difference across it can be accurately

detected by capacitance-bridge techniques. High accuracies require precise temperature control and isolation from vibrations. For absolute measurements diaphragm gauges are available with 0,1 kPa to 1 MPa ranges. Calibration can be readily carried out using a pressure balance and accuracies within 1 to 5 parts in 10^4 of full scale are possible provided periodic recalibrations of the instrument are carried out.

In the null mode, temperature and pressure dependence, hysteresis, and stability of the zero are the limiting factors ; high linearity is desirable for ease of calibration but it is not essential. In this mode the resolution may approach 1 in 10^7 of 100 kPa and the temperature coefficient of the zero about 1 Pa/°C. Reproducibility is improved by prestressing the diaphragm in a given direction at a pressure corresponding to full scale deflection and taking care that afterwards the pressure never exceeds this value nor changes sign [Pavese (1981)].

As a null instrument the diaphragm gauge has found wide application in gas thermometry, where it is used primarily to isolate the gas bulb from the manometer system. This allows a large reduction of the dead space and its associated errors, and also a greater flexibility in the application of pressure-measuring systems. For example, a pressure balance can be employed despite its inevitable gas leak [Berry (1979)]. Using the diaphragm to measure residual pressure differences between the bulb and the pressure balance, rather than merely as a null instrument, compensates to some extent for the drawback that the balance can be operated only at discrete pressures.

In its absolute mode of operation (i.e., at zero backing pressure) the diaphragm gauge can fill the gap left by the conventional pressure balance below 2 kPa where it offers a high enough accuracy for low-temperature thermometry, such as the realization of the ^{3}He vapour pressure scale below 1 K. Finally, whenever the purity of a gas being used for thermometric purposes is a matter of concern - which is usually the case - it is worthwhile considering the use of an isolating diaphragm.

The capsule transducer consists of a gas-filled flexible capsule the moveable face of which can apply pressure to a quartz resonating crystal. The resonating frequency is a function of applied mechanical stress and hence of the pressure in the capsule. At about atmospheric pressure the accuracy of a calibrated capsule transducer can be about 10 Pa.

4.4.5 Thermomolecular Pressure Difference

A thermomolecular pressure difference will result from a temperature gradient along a tube if the diameter of the tube is not large compared with the mean free path of the gas molecules.

The pressure at the higher-temperature end (frequently at room temperature) will be greater than the cryogenic bulb pressure due to the thermomolecular pressure difference. The magnitude of this pressure difference in a uniform diameter tube depends on the temperatures of the ends of the tube, on the tube diameter, on the pressure of the gas, and also on the accommodation coefficient of the surface which is a function of both the material and its surface state. Unfortunately, a straightforward and elementary discussion of these effects does not exist. Weber and Schmidt (1936) give an expression for the thermomolecular pressure difference which represents data for pyrex tubes. These calculations have been extended and generalized by McConville (1972) to represent data for both pyrex and stainless-steel tubes ; thermomolecular effects are reported to be 10 % to 15 % greater for stainless-steel than for pyrex, but note the effect of contact time mentioned below. McConville's differential equation can be simplified (to give the Weber-Schmidt relation) using a reasonable long mean free path approximation, and then can be integrated directly. The resulting equation is as complex and awkward to use as is that of Weber and Schmidt. However, the results can be approximated [Swenson (1989)] to within a few percent for pyrex by the relation

$$(p_H - p_L)/p_L = (2.10^{-9})\,(Rp_L/\mathrm{m{\bullet}Pa})^{-1,99}[(T_H/\mathrm{K})^{2,27} - (T_L/\mathrm{K})^{2,27}] \qquad (4.3)$$

where p_H, p_L, T_H and T_L refer to the pressures and temperatures at the high and low temperature extremities respectively of a tube of radius R.

Values calculated from equation (4.3) differ from those obtained using McConville's equation by less than 1 percent for $Rp_L \geq 2$ m•Pa, and by 4% for $Rp_L = 1{,}0$ m•Pa, for $T_H = 293$ K. According to McConville, the calculated pressure differences should be multiplied by roughly 1,1 if the pyrex is replaced by stainless steel. This difference may not be real, however, since there is evidence that the thermomolecular effect for these two surfaces become identical when the gas has remained in contact with the surface for an extended period of time, as is the case for a gas thermometry experiment for example. Equation (4.3), which refers to

pyrex, perhaps should be used for estimating the magnitude of these effects, but the design should be such that they need not be relied upon to better than about 10%.

Typical values for the thermomolecular pressure differences in a gas thermometer that meets the requirement of the ITS-90 are given in Tables 5.3 and 5.4 and are discussed in Section 5.5.2.

In the case of ^{3}He or ^{4}He vapour-pressure measurements, for a tube of constant diameter most (more than 90%) of the pressure difference occurs between 70 K and 300 K ; the magnitude of the effect can therefore be considerably reduced by employing a tube with two or more sections increasing in diameter from cold to hot [Sydoriak *et al.* (1964)]. However, in the extreme case of ^{3}He vapour-pressure measurements at 0,65 K the correction remains considerable: at this temperature, a uniform diameter of 5 mm would still necessitate a correction of about 1 mK.

TABLE 4.1

Pressure and pressure sensitivity of some hydrogen and helium vapour pressure points that are used as defining fixed points or secondary reference points.

Substance	Temperature T_{90}/K	Pressure p/Pa	Sensitivity (dp/dT_{90})/Pa K^{-1}	$(d\ln p/dT_{90})/K^{-1}$
H_2	17,035	33 321,3	13 320	0,400
	20,27	101 292	30 009	0,296
^4He	1,25	114,73	757	6,598
	1,5	471,54	2 289	4,854
	2,0	3 129	9 200	2,939
	2,176 8	5 041,8	12 408	2,461
	2,5	10 227,8	20 062	1,962
	3,0	24 046,4	36 018	1,498
	3,5	47 045,4	56 773	1,207
	4,0	81 616,2	82 330	1,009
	4,222 1	101 325	95 329	0,941
	4,5	130 260	113 235	0,869
	5,0	196 016	151 189	0,771
^3He	0,65	115,91	1 081	9,325
	1,0	1 160,11	5 501	4,741
	1,5	6 709,28	17 797	2,653
	2,0	19 999,2	36 348	1,817
	2,5	44 018,4	60 715	1,379
	3,0	81 825,7	91 831	1,122
	3,196 8	101 321	106 571	1,052
	3,2	101 662	106 826	1,051

Figure 4.1 Examples of uncertainties in pressure measurements using a capacitance diaphragm pressure gauge below 1,3 kPa, and the equivalent uncertainties δT_3 and δT_4 in temperatures T_3 and T_4 for ^{3}He and ^{4}He vapour pressure measurements, respectively [Rusby and Swenson (1980)]. Section 4.2, 4.4.

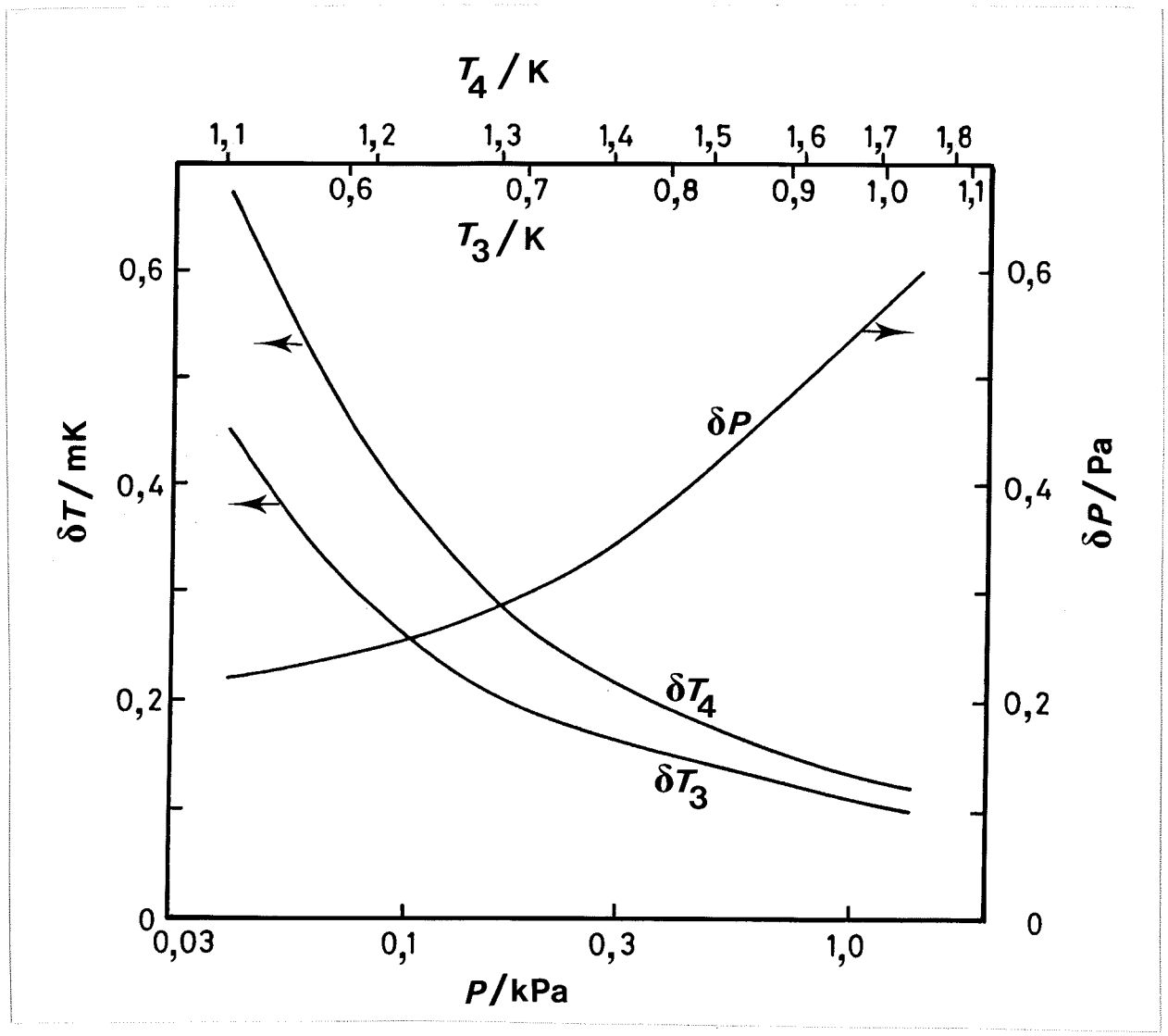

Figure 4.2 Schematic illustrations of systems for realizing ^{4}He vapour pressures: using a bath of liquid (a), suitable only for ^{4}He II ; and a bulb (b), for ^{4}He I, unsuitable for ^{4}He II. Thermal shields around the helium bath are not shown.
Section 4.3.1.

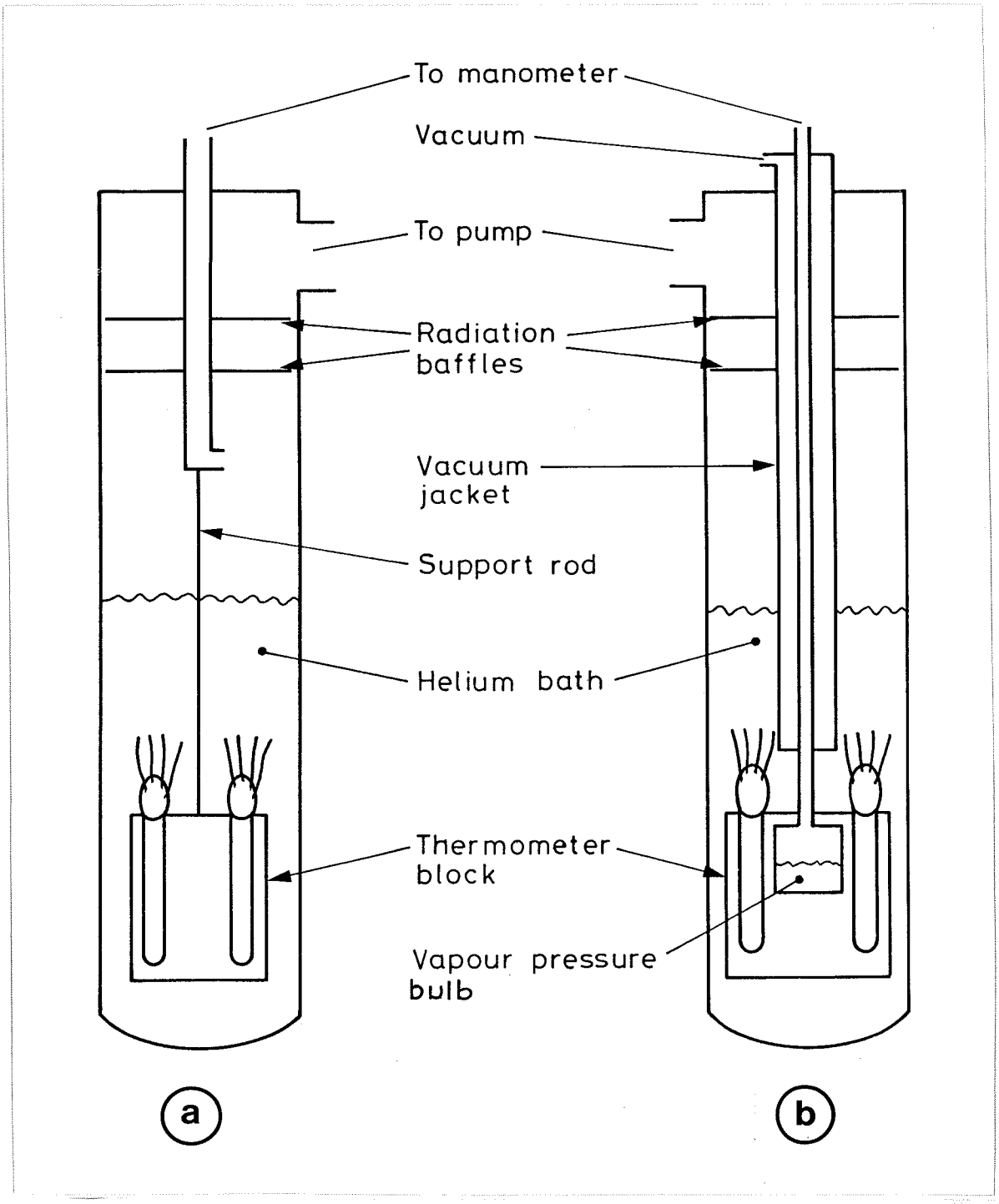

Figure 4.3 A schematic diagram of the cryostat used by Rusby and Swenson (1980) for CMN magnetic thermometry and for ^{3}He and ^{4}He I and ^{4}He II vapour-pressure measurements.
Section 4.3.3.

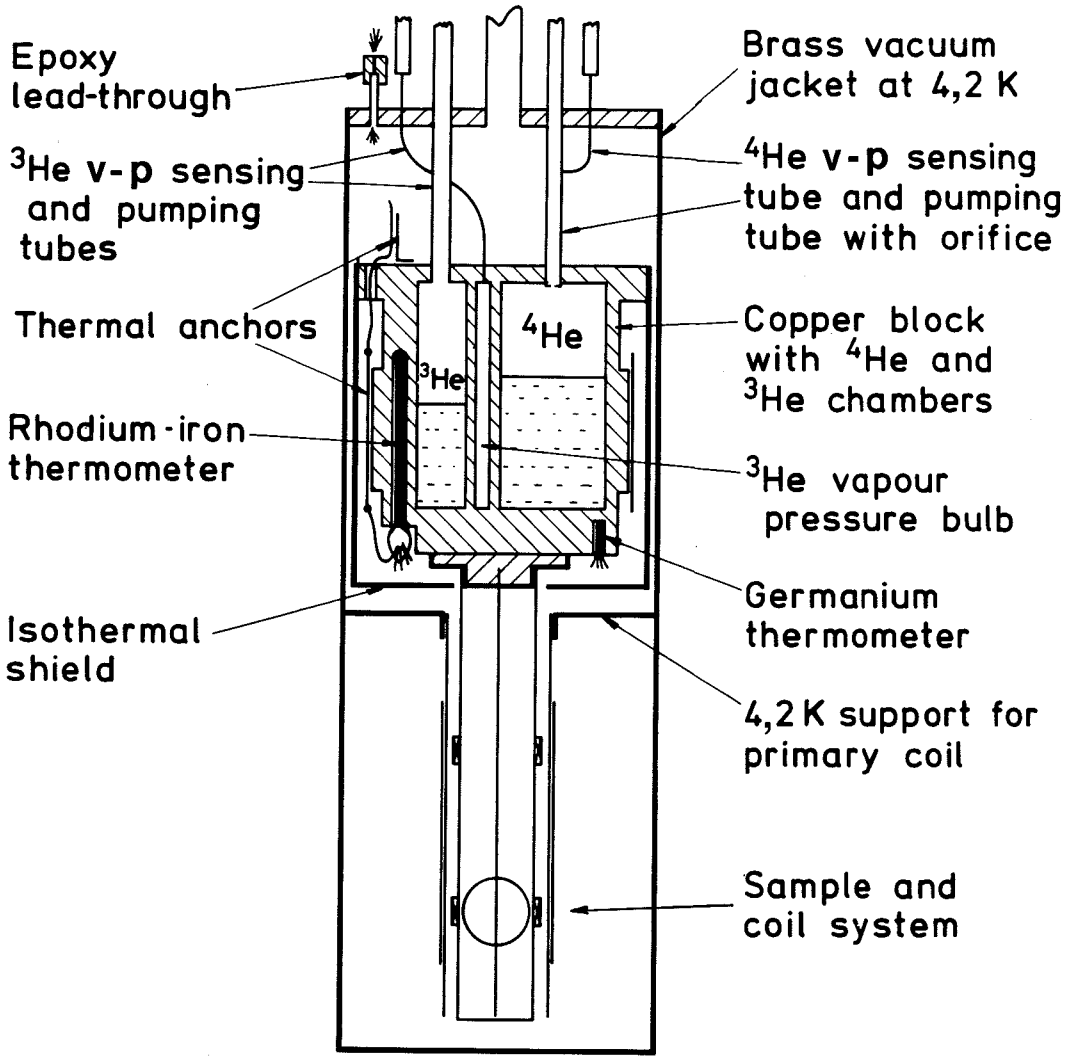

REFERENCES

Ambler, E. and Hudson, R.P. (1956): An Examination of the Helium Vapor-Pressure Scale of Temperature Using a Magnetic Thermometer ; J. Res. Natl. Bur. Stand. **56**, 99-104

Ambrose, D. (1990): The density of mercury ; Metrologia **27**, 245-247

Berry, K.H. (1979): A Low Temperature Gas Thermometer Scale from 2,6 K to 27,1 K ; Metrologia **15**, 89-115

BIPM (1979): The 1976 Provisional 0.5 K to 30 K Temperature Scale ; Metrologia **15**, 65-68

Bonhoure, J. and Terrien, J. (1967): The new standard manobarometer of the Bureau International des Poids et Mesures ; Metrologia **4**, 59-68 and 148.

Brombacher, W.G., Johnson, D.P. and Cross, J.L. (1960): Mercury Barometers and Manometers ; NBS Monograph **8**, 1-59

Cataland, G., Edlow, M.H. and Plumb, H.H. (1962): Recent Experiments on Liquid Helium Vapor Pressure Measurements from 2° to 4°K ; Temperature, Its Measurement and Control in Science and Industry **3**, 413-417

Cawood, W., Patterson, H.S. (1933): The Capillary Depressions of Mercury in Cylindrical Tubes and Some Errors of Glass Manometers ; Trans. Far. Soc. **29**, 514-523

CIPM (1982): Procès verbaux des séances, 8 and T5-6

Dadson, R.S., Lewis, S.L. and Peggs, G.N. (1982): The Pressure Balance, Theory and Practice ; HMSO (London)

Durieux, M. and Rusby, R.L. (1983): Helium Vapour Pressure Equations on the EPT-76 ; Metrologia **19**, 67-72

Gould, F.A. and Vickers, T (1952): Capillary Depression in Mercury Barometers and Manometers ; J. Sci. Instrum. **29**, 85-87

Guildner, L.A., Stimson, H.F., Edsinger, R.E. and Anderson, R.L. (1970): An Accurate Mercury Manometer for the NBS Gas Thermometer ; Metrologia **6**, 1-18

Kistemaker, J. (1944-46): The Capillary Depression of Mercury and High Precision Manometry ; Physica **11**, 277-286

McConville, G.T. (1972): The Effect of the Measuring Tube Surface on Thermomolecular Corrections in vapour pressure thermometry; Temperature, Its Measurement and Control in Science and Industry (Instrument Society of America, Pittsburgh) **4**, 159-165

Mitsui, K., Sakurai, H. and Mochikwai, T. (1972): A Gas Thermometer Measurement Below IPTS Range; Temperature, Its Measurement and Control in Science and Industry (Instrument Society of America, Pittsburgh) **4**, 333-338

Neubert, W. (1977): Piston Manometer With Electronic Indication of the Piston Level for Low-Temperature Control; PTB-Mitteilungen **87**, 369-370

Pavese, F. (1981): The Use of Triple Point of Gases in Sealed Cells as Pressure Transfer Standards : Oxygen (146,25 Pa), Methane (11,696 Pa) and Argon (68,890 Pa) ; Metrologia **17**, 35-42

Preston-Thomas, H. and Kirby, C.G.M. (1968): Gas Thermometer Determinations of the Thermodynamic Temperature Scale in the Range -183 °C to 100 °C ; Metrologia **4**, 30-40

Rusby, R.L. and Durieux, M. (1984): Inverted forms of the new helium vapour pressure equations ; Cryogenics **24**, 363-366

Rusby, R.L. and Swenson, C.A. (1980): A New Determination of the Helium Vapour Pressure Scales Using a CMN Magnetic Thermometer and the NPL-75 Gas Thermometer Scale ; Metrologia **16**, 73-87

Swenson, C.A. (1989): Supplementary Information for ITS-90 - Interpolating gas thermometer ; CCT 17^{e} Session, Doc. CCT/89-27, 7 p.

Sydoriak, S.G., Roberts, R.T. and Sherman, R.H. (1964): The 1962 He_3 Scale of Temperatures. I. New Vapor Pressure Comparisons II. Derivation III. Evaluation and Status IV. Tables ; J. Res. Natl. Bur. Stand. **68A**, 547-588

Weber, S. and Schmidt, G. (1936): Experimentelle Untersuchungen über die thermomolekulare Druckdifferenz in der Nähe der Grenzbedingung $p_1/p_2 = \sqrt{(T_1/T_2)}$ und Vergleichung mit der Theorie ; Leiden Commun. **246C**, 1-13

5. GAS THERMOMETRY

In the range 3 K to the triple point of neon (≈ 24,6 K), the ITS-90 is defined in terms of a ^{3}He or ^{4}He gas thermometer calibrated at three temperatures.

Background information on absolute gas thermometry can be found in the reports of four modern gas thermometry experiments [Berry (1979), Steur and Durieux (1986), Kemp *et al.* (1986/87) and Astrov *et al.* (1989)] which provide details of current good practice, and form the basis for the numerical values assigned to the low temperature portions of ITS-90. These experiments demonstrate in different ways the very great care required in apparatus design and data analysis when a helium gas thermometer is used to determine thermodynamic temperatures in terms of a single reference temperature.

Measurement difficulties can be reduced to trivial levels, however, if the single reference temperature is replaced by two or three designated calibration temperatures, provided that these calibration temperatures lie within the measurement range, and that the measurement range itself be not overly wide. These requirements are met in the case of the ITS-90 gas thermometer: with appropriate design (and the criteria are not too restrictive) measurements accurate to within 0,1 mK can be easily made, there being no requirement for the many corrections that accompany absolute gas thermometry. Two suitable, and typical, designs are described here together with analyses of contributions to the overall thermometric behaviour of the various elements in each of the designs.

5.1 Definition of the Scale

In the range from 4,2 K to 24,6 K using ^{4}He, T_{90} is defined by the relation

$$T_{90} = a + b\,p + cp^2, \qquad (5.1)$$

where p is the measured pressure and a, b and c are coefficients the numerical values of which are obtained from measurements made at the three defining fixed points given in Section 3.2 of the ITS-90, but with the further restriction that the lowest one of these points lie between 4,2 K and 5,0 K.

For a ^{3}He gas thermometer in the range from 3,0 K to 24,6 K, and for a ^{4}He gas thermometer when the lowest defining fixed point is at a

temperature below 4,2 K, the non-ideality of the gas must be accounted for explicitly, using the appropriate second virial coefficient $B_3(T_{90})$ or $B_4(T_{90})$; values calculated for these coefficients in the appropriate temperature range are given in Tables 5.1 and 5.2. In these two cases T_{90} is defined over the whole range from 3 K (or from the lowest defining fixed point) to 24,6 K by the relation:

$$T_{90} = \frac{a + b\,p + c\,p^2}{1 + B_x\,(T_{90})\,N/V_B}\,, \tag{5.2}$$

where p is the measured pressure, a, b and c are coefficients the numerical values of which are obtained from measurements at the three calibration temperatures as given in Section 3.2 of the ITS-90, N/V_B is the gas density with N being the quantity of gas and V_B the volume of the bulb, x is 3 or 4 according to the isotope used, and the values of the second virial coefficients are given by the relations 6a and 6b of the text of the ITS-90, from which the values given here in Tables 5.1 and 5.2 were calculated.

5.2 General Design Criteria[5.1]

It has been shown [Pavese and Steur (1987), Swenson (1989)] that for an interpolating gas thermometer the major low temperature deviations from a quadratic interpolation function are associated with the temperature dependence of the second virial coefficient, $B(T)$, of helium. However, in the ITS-90 these deviations are not significant (< 0,02 mK) for ^{4}He between 4,2 K (if this is one of the three calibration points) and 24,6 K. For ^{3}He and ^{4}He when used below 4,2 K this problem is dealt with in the ITS-90 by departing from the simple quadratic equation, and including in the scale definition explicit corrections for $B(T)$, equation (5.2), which are based on recent results for ^{4}He [Steur *et al.* (1987)] and ^{3}He [Matacotta *et al.* (1987)].

Figure 5.1 and Tables 5.3 and 5.4 constitute between them a schematic representation, list of parameters, and analyses of the operation of two typical interpolating gas thermometers used in the realization of the ITS-90. The magnitudes of the various contributions to non-ideal behaviour of the thermometer including dead space, aerostatic

5.1 Column numbers in section 5.2 to 5.7 refer to (similarly) numbered columns in tables 5.3 and 5.4.

head, thermomolecular pressure and virial effects of the working gas (either ^{3}He or ^{4}He) are shown in Table 5.3 for one set of typical design parameters of the thermometer shown in Figure 5.1(a), and in Table 5.4 (applicable to ^{3}He only) for a different set (Figure 5.1(b)). Tables 5.3 and 5.4 also show the magnitude of the residual errors resulting from imperfect compensation by the three point calibration procedure of all these effects. The results are expressed as temperature differences, $\Delta T(X) = T - T_g$, where T is the assumed thermodynamic temperature of the thermometer bulb[5.2], $T_g = p(\text{meas})\, V_B/NR$, and p(meas) is the pressure which is measured at room temperature, R is the gas constant, and (N/V_B) is the gas density in mol m^{-3}. The p(meas) values in column (2) are the result of an explicit calculation of the room temperature pressures which would be measured for this model for a ^{4}He gas thermometer when all of these contributions [including those from the virial coefficients in columns (11) and (12)] are included. The values of p(meas) at three fixed points (4,2 K, 13,8 K and 24,6 K) were used as described in the ITS-90 to generate a quadratic interpolation function (equation 5.2), giving T_{90}. For a ^{3}He gas thermometer for which the virial coefficient contribution is that in column (13), the residuals ΔT(Fit) in column (13) will be identical with those for ^{4}He in spite of small differences in some columns. The taking account of the individually large contributions, $\Delta T(X)$, by the three-point fitting procedure[5.3] and the inclusion of the second virial coefficient correction in equation 5.2 is not perfect, but the residuals ΔT(Fit), column (3), are all very small (0,02 mK or less between 3,2 K and 24,6 K).

The essentials of gas thermometry can be classified under four headings ; (1) the working fluid, (2) the thermometer bulb, (3) the determination of the pressure of the gas in the bulb, and (4) the effect of the volumes of the pressure-sensing tube and the room temperature manometer system. These will be considered in turn.

5.3 The Working Fluid

The very large, non-quadratic, contribution of the second virial coefficient, $B(T)$ (column (11) for ^{4}He, column (13) for ^{3}He), which is of paramount importance in primary gas thermometry, is removed ***explicitly***

5.2 For the purposes of this discussion we assume that at the three fixed points $T_{90} = T$.
5.3 A two point fitting is quite inadequate for this purpose [*see* Pavese and Steur (1987)].

in the gas thermometer calibration procedure for ITS-90 based upon equation 5.2. At low temperatures and for large gas densities, the temperature dependence of the third virial coefficient, $C(T)$ (column (12)) [Steur *et al.* (1987)], can become significant. For this reason, the gas density (N/V_B) for ^{4}He should be less than 300 mol m^{-3} for the highest accuracy thermometry. A similar limit probably applies to ^{3}He in the temperature regions especially below 4 K where the third virial coefficient is likely to become significant [Matacotta *et al.* (1987)]. The calculations in Tables 5.3 and 5.4 are for 160 mol m^{-3}; the contributions in columns (11) and (13) (for $B(T)$) are proportional to N/V_B, while those in column (12) (for $C(T)$) vary as $(N/V_B)^2$. The extent to which the choice of ^{3}He or ^{4}He as working fluid leads to different values of T_{90} depends upon the accuracy of the expressions adopted for $B_3(T)$ and $B_4(T)$ and on the gas density used in the thermometer. Calculations by Aziz and Slaman (1990) suggest that the expression in the ITS-90 for $B_4(T)$ is accurate, but that there are small discrepancies in that for $B_3(T)$ at the lowest temperatures. These are unlikely to cause errors greater than 0,05 mK.

Gas purity also is important, with hydrogen and neon impurities most significant for ^{4}He, and, in addition, ^{4}He impurities for ^{3}He. While impurity levels of less than 1 atomic part per million are the goal in primary gas thermometry, the gas thermometer calibration at three points allows perhaps 10 atomic parts per million, while 100 parts per million of ^{4}He in ^{3}He would be acceptable [Pavese and Steur (1987)].

5.4 The Thermometer Bulb

The volume of the bulb, V_B, is generally large, (typically one litre) to reduce dead space effects (*see* Section 5.6) and to render adsorption effects negligible. The bulb is made of high purity copper, and is surrounded by an isothermal shield that is maintained at the bulb temperature so as to minimize temperature gradients. The thermal expansion of the copper bulb has only a very small effect [Kroeger and Swenson (1977)] (column (7)). The bulb volume also will increase with the gas pressure, an effect which is proportional to the pressure (and hence the temperature) but which is entirely compensated for in the calibration procedure. Only small effects due to gas adsorption have been detected in the gas thermometry experiments involving either gold-plated

copper surfaces [Berry (1979)], or clean copper surfaces which were baked at high temperature [Astrov *et al.* (1989)]. In each instance, the systems were evacuated thoroughly to remove adsorbed surface layers, and this practice is always advisable.

5.5 Pressure Measurement

The pressure-measuring system[5.4] is isolated from the working gas by a calibrated flexible diaphragm (a capacitance manometer) which may be at room temperature or at the bulb temperature. The considerable advantages of a diaphragm at the lower temperature are to some extent offset by the need for a design which will be stable despite temperature cycling. Pressure measurement at room temperature (*see* Section 4.4) can be based on pressure balances or, with higher accuracy, on a mercury manometer using optical interferometry to measure differences in the heights of mercury columns. The pressure sensitivity of a gas thermometer is proportional to the filling density, with the results in Tables 5.3 and 5.4 corresponding to 1330 Pa/K (10 Torr/K) for 160 mol m^{-3}. Results have been reported for gas densities as small as 44 mol m^{-3} (366 Pa/K) and as large as 234 mol m^{-3} (1945 Pa/K). Pressure measurement sensitivities typically are 0,01 Pa, with accuracies closer to 0,1 Pa at low temperatures.

5.5.1 Aerostatic Head Correction

The hydrostatic pressure generated by the column of gas in the sensing tube (the aerostatic head) causes the room temperature pressure to be less than that in the bulb. To evaluate the aerostatic head correction (column (4)) the temperature distribution along the capillary must be known. This can be measured directly, or it can be calculated from a knowledge of the temperature dependence of the thermal conductivity of the capillary material, or it can be estimated from the expressions given in Figure 5.1 for temperatures above and below T_M [Kemp *et al.* (1986/87)]. Astrov *et al.* (1989) have simplified the

5.4 Figure 5.1 depicts a diaphragm manometer reading p(meas) directly. This is for illustration only. In practice p(meas) is the sum of measurements made with some absolute manometer and a differential (diaphragm) manometer (see Section 4.4.4).

calculation of aerostatic head effects with a design in which temperature gradients occur only in horizontal tubes. In practice, it is preferable to monitor the actual temperature distribution to ensure consistency and reproducibility during an experiment. The aerostatic head correction is proportional to the isotopic mass of the gas, so the values given in column (4) will be 25 % smaller if the working gas is ^{3}He rather than ^{4}He for the same design of gas thermometer. It also will be (in this simple model with vertical tubes) proportional to the length of the sensing tube. A pressure gradient also will occur in the bulb, with T_B corresponding to the average (midpoint) pressure. This correction is independent of temperature (or pressure) and does not affect the calibration.

5.5.2 Thermomolecular Pressure Correction

A thermomolecular pressure difference will result from a temperature gradient along a tube if the diameter of the tube is not large compared with the mean free path of the gas molecules. This has already been discussed in relation to the measurement of helium vapour pressures in Section 4.4.5 and equation 4.3 allows the magnitude of the thermomolecular pressure effect to be calculated.

For a typical ITS-90 gas thermometer (such as those shown in Figure 5.1) the effects of thermomolecular pressure differences are shown in Tables 5.3 and 5.4 in columns (5) and (6) for the upper (hi, 2 mm diameter) and lower (lo, 1 mm diameter) portions of the sensing tube. Since more than 90% of the thermomolecular pressure difference for a uniform capillary occurs between 295 K and 80 K (a somewhat arbitrary choice for T_M) the total contribution is reduced by using a sensing tube that is wider above T_M than below, Δp being proportional to $(Rp)^{-2}$. The same result could be achieved by doubling the pressure (the gas density) for a uniform 1 mm diameter tube, but with increased non-ideality contributions. The total thermomolecular pressure difference for the gas thermometer depends on the bulb temperature, T_B, primarily through the pressure dependence in Equation (4.2). The use of a smaller diameter tube at low temperature results in smaller dead space effects (*see* Section 5.6), but also longer equilibrium times. In contrast with a primary gas thermometry experiment, corrections for the thermomolecular

pressure difference need not be made provided its magnitude is small enough for the quadratic interpolation to be valid.

5.6 Dead Space Correction

Temperature-dependent changes occur in the quantity of gas in the bulb if the diaphragm separating the thermometer and the manometer is not at the bulb. The effects of the room temperature volume, V_R (column (8)) are most important for the highest bulb temperatures. For a vertical sensing tube the effect of the sensing tube dead space depends on the temperature distribution, and the length and cross-sectional area of the pressure sensing tube. For a uniform bore (and vertical tube), these contributions would be proportional to the aerostatic head correction. The values given in columns (9) and (10) were calculated using the temperature distributions of Figure 5.1, and show typical magnitudes. Again, the important requirement is that these effects be not so large that changes in the temperature distribution (due to refrigerant levels changing with time, for instance) can introduce significant systematic errors.

5.7 Design of the Gas Thermometer

There are very few explicit restrictions on the design of an interpolating gas thermometer to implement the ITS-90. The implicit requirement in the above discussion, that the calculated quadratic interpolation errors (column (3)) should be less or even substantially less than 0,1 mK, can be achieved for a wide range of gas densities, bulb volumes and capillary geometries. The designs of Figure 5.1 (a) and (b) (Figure 5.1(a) from Swenson (1989) and Figure 5.1(b) based upon Steur and Pavese (1989)) and the operating conditions used for the thermometers in Tables 5.3 and 5.4 are simply illustrations of how the conflicting requirement that the thermomolecular pressure differences and dead space effects should both be small may be satisfied. Note that in Figure 5.1(b) the temperature gradient from room temperature to low temperature occurs along a relatively wide (2 mm diameter) but short (10 cm) capillary ; temperature-dependent dead space effects are

minimized by thermally anchoring the low temperature end of this capillary to the liquid helium bath.

Any design for an interpolating gas thermometer should be tested with model calculations such as those used for Tables 5.3 and 5.4 so that the magnitudes and temperature dependencies of the various contributions can be assessed. On the experimental side, good practice also requires adequate thermal isolation (small heat leaks, good vacuums) and stability, as well as careful monitoring of various system temperatures to ensure that they are reproducible as the bulb temperature is cycled.

TABLE 5.1

Values of the second virial coefficient, for ^{3}He between 3 K and 24,5561 K calculated using equation 6a of the ITS-90.

T_{90}/K	$B_3(T_{90})$/cm^3 mol^{-1}
3	−86,03
3,5	−72,48
4,2221	−58,2
5	−47,17
7	−29,63
10	−16,11
13,8033	−7,25
15	−5,37
17,0357	−2,78
20,2711	0,29
24,5561	3,12

TABLE 5.2

Values of the second virial coefficient of ^{4}He between 3 K and 24,5561 K calculated from equation 6b of the ITS-90.

T_{90}/K	$B_4(T_{90})$/cm^3 mol^{-1}
3	−120,36
3,5	−100,19
4,2221	−79,76
5	−64,46
7	−40,80
10	−23,10
13,8033	−11,82
15	−9,48
17,0357	−6,25
20,2711	−2,49
24,5561	+0,95

TABLE 5.3

Calculations for an interpolating ^{3}He or ^{4}He gas thermometer

This table is applicable to the gas thermometer of the design shown in Figure 5.1(a) with either ^{3}He or ^{4}He as the working gas and operating parameters shown in Figure 5.1.

Column (1) is the temperature T_{90} of the bulb (assumed to be identical with the thermodynamic temperature T at the three calibration points of 4,2 K, 13,8 K and 24,6 K); column (2), p(meas), is the pressure, measured at room temperature; column (3), ΔT(Fit), is the estimated difference $T - T_{90}$ where T_{90} is obtained from the ITS-90 gas thermometer quadratic equation (equation (5.2)). The small but non-zero temperature differences of column (3) are the residual errors resulting from the imperfect cancellation by the ITS-90 three point calibration procedure of errors. The various significant departures from ideality for these particular design and operating conditions are given in columns (4) to (13).

Columns (4) to (13)[5.5] list the component departures $\Delta T(x) = T - T_g$ of this system from the "apparent" gas thermometer temperature $T_g = p(\text{meas})V_B/NR$.

Column (4), ΔT(A) is the aerostatic head departure; columns (5) and (6) ΔT(TM) give the thermomolecular pressure departure in each of the capillary tubes Cap_{hi} and Cap_{lo}; column (7) is the departure due to the thermal expansion of the copper bulb; column (8), (9) and (10) are the departures resulting from the deadspaces ($V(\text{Cap}_{hi})$ and $V(\text{Cap}_{lo})$ in Figure 5.1) of the two capillary tubes and the room temperature volume; columns (11), (12) and (13) are the departures resulting from the second and third virial coefficients for ^{4}He or the second virial coefficient for ^{3}He.

The dotted lines are at the ITS-90 temperature limits for the gas thermometer.

				ΔT(TM)			ΔT(deadspace)			ΔT(virial)		
T	p(meas)	ΔT(Fit)	ΔT(A)	Cap_{hi}	Cap_{lo}	ΔT(TE)	V_R	Cap_{hi}	Cap_{lo}	^{4}He(B)	^{4}He(C)	^{3}He(B)
K	Pa	mK	mK	mK	mK	mK	mK	mK	mK	mK	mK	mK
2,50	3246,4	−0,13	0,09	−0,18	−0,04	0,00	0,11	0,03	0,03	59,63	0,08	41,77
3,00	3913,9	−0,04	0,11	−0,15	−0,03	0,00	0,16	0,05	0,05	57,77	−0,03	41,30
3,20	4181,0	−0,01	0,11	−0,14	−0,03	0,00	0,17	0,05	0,05	57,09	−0,08	41,04
4,20	5515,1	0,00	0,15	−0,11	−0,02	0,00	0,30	0,08	0,08	53,95	−0,12	39,36
6,00	7916,0	−0,01	0,21	−0,08	−0,02	0,00	0,61	0,17	0,16	48,63	−0,13	35,53
8,00	10583,3	−0,02	0,27	−0,06	−0,01	0,00	1,08	0,31	0,29	42,77	−0,14	30,77
10,00	13250,4	−0,01	0,33	−0,04	−0,01	0,00	1,69	0,48	0,44	36,97	−0,14	25,78
12,00	15917,0	−0,01	0,39	−0,04	−0,01	0,01	2,44	0,69	0,61	31,23	0,14	20,67
13,80	18316,7	0,00	0,45	−0,03	−0,01	0,01	3,23	0,91	0,80	26,13	−0,15	16,02
16,00	21249,4	0,01	0,51	−0,03	−0,01	0,02	4,34	1,22	1,05	19,94	−0,15	10,29
18,00	23915,1	0,02	0,56	−0,02	0,00	0,04	5,49	1,54	1,30	14,36	−0,16	5,05
20,00	26580,4	0,02	0,61	−0,02	0,00	0,07	6,78	1,91	1,57	8,81	−0,16	−0,21
22,00	29245,5	0,02	0,67	−0,02	0,00	0,11	8,20	2,31	1,86	3,29	−0,17	−5,49
24,60	32709,5	0,00	0,73	−0,02	0,00	0,20	10,26	2,88	2,27	−3,85	−0,17	−12,36
26,00	34574,7	−0,02	0,76	−0,02	0,00	0,26	11,46	3,22	2,50	−7,68	−0,18	−16,07
28,00	37238,7	−0,07	0,81	−0,02	0,00	0,38	13,29	3,74	2,85	−13,15	−0,18	−21,37
30,00	39902,5	−0,15	0,86	−0,02	0,00	0,54	15,25	4,29	3,21	−18,60	−0,19	−26,68
32,00	42566,0	−0,27	0,90	−0,01	0,00	0,75	17,36	4,88	3,59	−24,04	−0,19	−31,99
(1)	(2)	(3)	(4)	(5)	(6)	(7)	(8)	(9)	(10)	(11)	(12)	(13)

5.5 Columns (2) to (12) are for the case of ^{4}He as the working gas. If ^{3}He is used in place of ^{4}He, column (2) and columns (3) to (10) will be slightly different, while column (13) replaces columns (11) and (12); the critically important column (3), ΔT (Fit), however, remains virtually unchanged.

TABLE 5.4

Calculations for an interpolating ^{3}He gas thermometer

This Table (which is a complement to Table 5.3) is applicable to the gas thermometer shown in Figure 5.1(b), the conditions of operation and some elements of the design differ from those applicable to Table 5.3. In this Table the values are calculated for ^{3}He as working gas and the thermomolecular pressure effects and capillary dead space corrections are each calculated for the upper and lower parts of the capillary tubes combined. They are indicated in the Table as ΔT(TM) and ΔT(deadspace) in the columns (5 + 6) and (9 + 10) respectively in order to be comparable with the values shown in Table 5.3. Other columns have the same numbering as in Table 5.3, column 7 of Table 5.3 is not repeated here.

					ΔT(deadspace)		
T	p(meas)	ΔT(Fit)	ΔT(A)	ΔT(TM)	V_R	Cap$_{(hi+lo)}$	ΔT(virial)
K	mK	mK	mK	mK	mK	mK	mK
2,5	3269,77	0,07	0,30	−0,18	0,07	0,18	41,77
3,0	3935,34	0,04	0,34	−0,15	0,11	0,24	41,30
3,2	4201,63	0,03	0,35	−0,14	0,12	0,26	41,04
4,2	5533,73	0,00	0,42	−0,10	0,21	0,42	39,36
6,0	7932,57	−0,02	0,50	−0,07	0,43	0,73	35,53
8,0	10598,44	−0,03	0,58	−0,05	0,76	1,14	30,77
10,0	13264,45	−0,03	0,64	−0,03	1,19	1,59	25,78
12,0	15930,45	−0,02	0,69	−0,02	1,72	2,08	20,67
13,8	18329,76	0,00	0,73	−0,02	2,27	2,56	16,02
16,0	21262,17	0,02	0,77	−0,01	3,05	3,19	10,29
18,0	23927,83	0,03	0,81	0,00	3,86	3,80	5,05
20,0	26593,33	0,04	0,84	0,00	4,77	4,46	−0,21
22,0	29258,65	0,03	0,88	0,00	5,77	5,16	−5,49
24,6	32723,31	0,00	0,93	0,00	7,22	6,16	−12,37
26,0	34588,76	−0,04	0,96	0,00	8,06	6,74	−16,08
28,0	37253,51	−0,12	1,00	0,00	9,35	7,62	−21,39
30,0	39918,04	−0,23	1,05	0,00	10,73	8,57	−26,70
(1)	(2)	(3)	(4)	(5+6)	(8)	(9+10)	(13)

FIGURE

Figure 5.1. A schematic representation (not to scale) of a typical gas thermometer experiment, with T_B the temperature of the bulb. The surrounding thermal shields and vacuum jacket are not shown. If, as is true for many metallic alloys, the thermal conductivity is roughly constant above T_M ($\approx$ 80 K) and is approximately proportional to T at lower temperatures, the temperature distributions for the high and low temperature portions of the capillary are given by:

$$T = T_R + (T_M - T_R)\,(L/L_{hi}) \qquad T > T_M$$

and

$$T^2 = T_M^{\,2} + (T_B^{\,2} - T_M^{\,2})\,(L/L_{lo}) \qquad T < T_M$$

where L is measured from T_R and T_M, respectively.

For the calculation of the data shown in both Tables 5.3 and 5.4 V_B = 1000 cm^3 (filling density 160 mol m^{-3}), T_R = 295 K, R_{hi} = 1,0 mm and R_{lo} = 0,5 mm ; for Table 5.3 (Figure 5.1(a)), V_R = 5 cm^3, $L_{hi} = L_{lo}$ = 25 cm and T_M = 80 K ; for Table 5.4 (Figure 5.1(b)), V_R = 3,5 cm^3, $L_{hi} = L_{lo}$ = 10 cm and T_M = 4,2 K.

Sections 5.5.2 to 5.7, Tables 5.3 and 5.4.

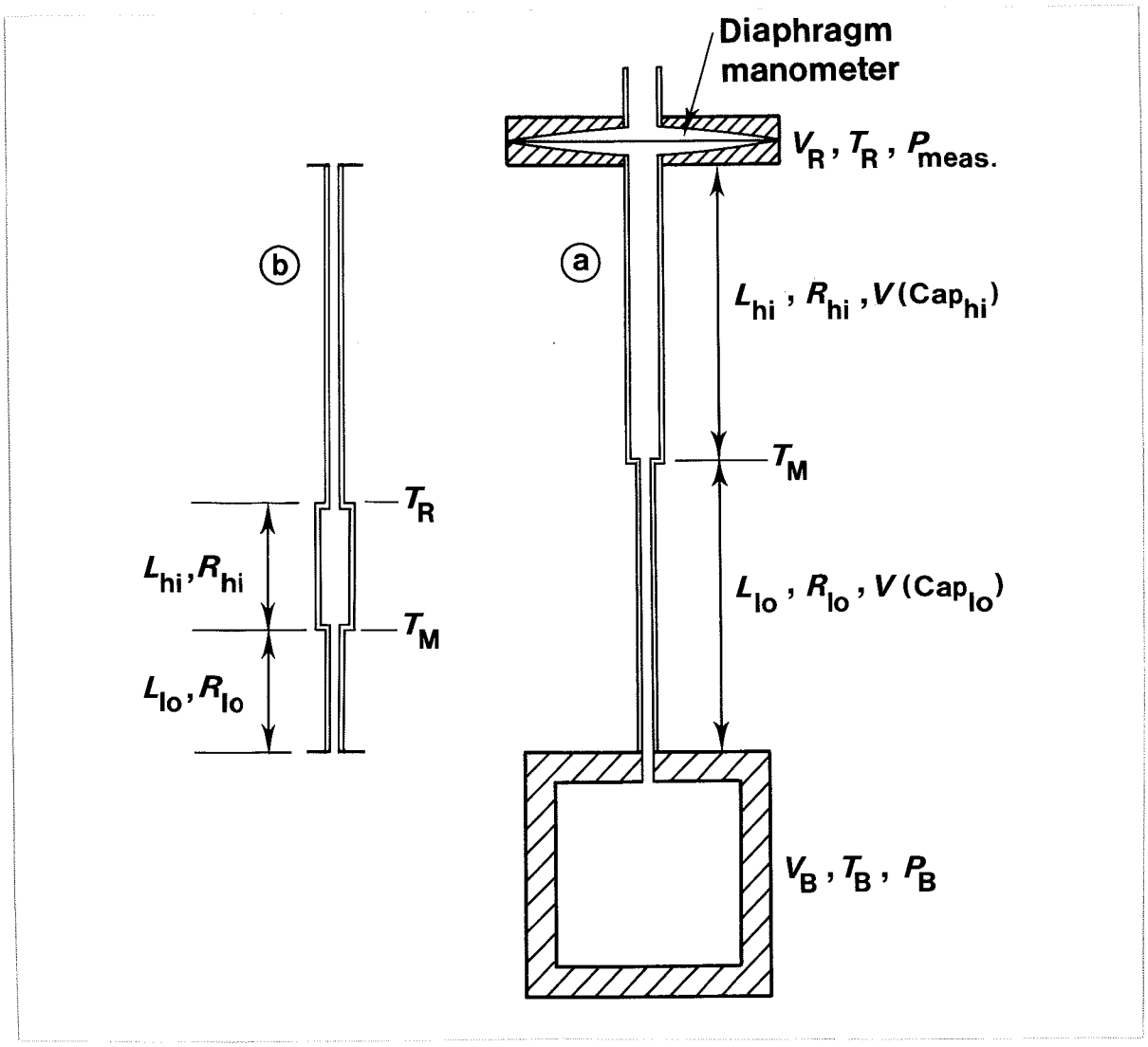

REFERENCES

Astrov, D.N., Beliansky, L.B., Dedikov, Y.A., Polunin, S.P. and Zacharov, A.A. (1989): Precision gas thermometry between 2,5 K and 308 K ; Metrologia **26**, 151-166

Aziz, R.A. and Slaman, M.J. (1990): An analysis of the ITS-90 relations for the non-ideality of ^{3}He and ^{4}He: recommended relations based upon a new interatomic potential for helium ; Metrologia **27**, 211-219

Berry, K.H. (1979): NPL-75 A low temperature gas thermometer scale from 2.6 K to 27.1 K ; Metrologia **15**, 89-115

Kemp, R.C., Kemp, W.R.G. and Besley, L.M. (1986/87): A determination of thermodynamic temperatures and measurements of the second virial coefficients of ^{4}He between 13.81 K and 287 K using a constant volume gas thermometer ; Metrologia **23**, 61-86

Kroeger, F.R. and Swenson, C.A. (1977): Absolute linear thermal-expansion measurements on copper and aluminum from 5 to 320 K ; J. Appl. Phys **48**, 853-864

Matacotta, F.C., McConville, G.T., Steur, P.P.M. and Durieux, M. (1987): Measurements and calculations of the ^{3}He second virial coefficient between 1,5 K and 20,3 K ; Metrologia **24**, 61-67

Pavese, F. and Steur, P.P.M. (1987): ^{3}He Constant-Volume Gas Thermometry: Calculations for a Temperature Scale between 0.8 and 25 K ; J. Low Temp. Phys. **69**, 91-117

Steur, P.P.M. and Durieux, M. (1986): Constant volume gas thermometry between 4 K and 100 K ; Metrologia **23**, 1-18

Steur, P.P.M., Durieux, M. and McConville, G.T. (1987): Analytic expressions for the virial coefficients $B(T)$ and $C(T)$ of ^{4}He between 2,6 K and 300 K ; Metrologia **24**, 69-77

Steur, P.P.M. and Pavese, F. (1989): He-3 constant volume gas thermometer as interpolating instrument: calculations of the accuracy limit versus temperature range and design parameters ; Cryogenics **29**, 135-138

Swenson, C.A. (1989): Supplementary Information for ITS-90 - Interpolating gas thermometer ; CCT 17^e Session, Doc. CCT/89-27, 7 p.

6. RADIATION THERMOMETRY

Above the freezing point of silver 1234,93 K (961,78 °C) the temperature T_{90} is defined by the equation

$$\frac{L_\lambda(T_{90})}{L_\lambda(T_{90}(X))} = \frac{\exp(c_2(\lambda T_{90}(X))^{-1}) - 1}{\exp(c_2(\lambda T_{90})^{-1}) - 1} \tag{6.1}$$

where $T_{90}(X)$ refers to any one of the silver $\{T_{90}(\mathrm{Ag}) = 1234{,}93\ \mathrm{K}\}$, the gold $\{T_{90}(\mathrm{Au}) = 1337{,}33\ \mathrm{K}\}$ or the copper $\{T_{90}(\mathrm{Cu}) = 1357{,}77\ \mathrm{K}\}$ freezing points and in which $L_\lambda(T_{90})$ and $L_\lambda[T_{90}(X)]$ are the spectral concentrations of the radiance of a blackbody at the wavelength (in vacuo) λ at T_{90} and at $T_{90}(X)$ respectively, and $c_2 = 0{,}014\ 388\ \mathrm{m{\bullet}K}$. The text of the scale neither recommends a method by which, nor restricts the wavelength at which, the ratio of radiances is to be experimentally determined.

6.1 Monochromatic Radiation Thermometer

The only requirements embodied in Equation (6.1) are that the instrument used, a radiation thermometer, be effectively monochromatic and that at least the reference source at the temperature $T_{90}(X)$ be a blackbody (*see* Section 6.2.2). A monochromatic radiation thermometer consists of an optical system that includes a wavelength limiting device and focuses an image of a source of radiation onto a photodetector. To measure temperatures as prescribed by Equation (6.1), it is necessary to provide some means (e.g. moving the sources or the pyrometer, or altering the optical path) for alternately focusing the two sources onto the detector. The ratio of the two corresponding detector outputs, suitably corrected or interpreted, is then the ratio of the radiances of the two sources at the effective wavelength of the thermometer.

6.1.1 Optical System

The optical system of a radiation thermometer typically is constructed from standard, readily obtainable components. Most radiation thermometers use refracting systems (Figure 6.1) but some, especially if operating beyond the visible region, use reflecting systems

(Figure 6.2). There seems to be no fundamental advantage of one over the other. Reflecting systems are likely to be more costly, but are less absorbing and have focusing distances which are independent of wavelength ; the last quality can be useful in view of the increasing practice of realizing the scale both at visible and near-infrared wavelengths.

Radiation thermometry does not demand a large numerical aperture of the optical system ; it is typically in the range f/10 to f/20. Targets, i.e. that part of the source actually viewed by the detector, are nearly always small, as such targets can more readily be arranged to be approximately isothermal and black. It may be noted (*see* Sections 6.2.2 and 6.4) that tungsten strip lamps, although not blackbodies, can be calibrated so as to allow for their departure from blackness using the concept of spectral-radiance temperature. Typically a target is circular and about 0,5 mm to 1 mm in diameter. For this reason, and because the radiation thermometer is monochromatic, the only lens aberration of consequence is spherical aberration, and even here the demand is not severe. The lenses (or mirrors) of the radiation thermometer should be corrected for spherical aberration to a level such that they become essentially diffraction limited at all apertures at which they will be used. It is convenient if the lenses are achromatic, especially if the radiation thermometer works at a wavelength in the infrared, so as to allow for visual focusing via an auxiliary viewing system. All lenses and mirrors in the system should be of high optical quality and kept scrupulously clean to minimize the amount of radiation scattered by imperfections and surface contamination.

A further point to consider in designing an optical system is that of stray radiation from outside the target that can propagate through the system by diffraction, reflection or scattering from the mechanical or optical elements. Baffles and grooves are effective in suppressing unwanted radiation. Good results are also obtained by the use of a glare stop and by careful positioning of the aperture stop [Fischer and Jung (1989)]. *See* also, size-of-source effect, Section 6.5.1.

6.1.2 Filters

A radiation thermometer can be made effectively monochromatic in several ways, but at present interference filters are used almost exclusively. High-quality interference filters with high peak transmittances, narrow bandwidths and high degrees of blocking outside the passband are available from many commercial sources.

For a given type of filter (Gaussian, rectangular or other) the smallest detectable temperature difference and the wavelength error $\Delta\lambda$ resulting from imperfect blocking outside the passband are inversely proportional to the half width: this suggests that a wide-band filter is desirable. However, the use of such a filter requires an accurate knowledge of the spectral responsivity $S(\lambda)$ of the thermometer[6.1], and the uncertainty $\Delta\lambda$ due to imperfect knowledge of $S(\lambda)$ is proportional to the square of the half width of the filter: this suggests that a narrow-band filter is desirable. The choice of bandwidth must be a compromise between these two conflicting considerations, and in practice half widths of about 10 nm are preferred, although narrower half widths down to 1 nm have also been used [*see* e.g. Bedford and Ma (1983)].

The uncertainty $\Delta T_{90}(\lambda)$ generated by an uncertainty $\Delta\lambda$ in the wavelength is given by

$$\Delta T_{90}(\lambda) = T_{90} \left[\frac{T_{90}}{T_{90}(X)} - 1 \right] \frac{\Delta\lambda}{\lambda} \qquad (6.2)$$

It is very important that wavelengths outside the passband in regions where the detector is still sensitive be blocked to a level less than a part in 10^4, of those in the passband. For a filter half width of 10 nm blocking to a part in 10^5 is required, and for a half width near 1 nm blocking must be to about a part in 10^6. The effects of any secondary peaks from the filter must also be eliminated. If the interference filter itself does not adequately attenuate these undesired wavelengths, an auxiliary blocking filter can be added for this purpose. In most cases, residual transmission at longer wavelengths is the more troublesome because of the exponential character of $L_\lambda(T_{90})$. Because the spectral transmittance of an interference filter can vary with the filter temperature (up to 0,02 – 0,03 nm/°C between 660 and 900 nm) and with angle of incidence of the incoming radiation (about 4 parts in 10^4 per angular degree), the filter temperature should be controlled (room

6.1 This includes the spectral transmittance of the filter and all other optical components and the spectral responsivity of the detector.

temperature control is usually sufficient) and the transmittance measured *in situ* or, if not, with a similar radiation beam impinging at the same angle. This angle should be carefully chosen to eliminate unwanted reflections. Note also that the wavelength λ appearing in Equation (6.1) is specified as the wavelength in vacuum ; if λ for the filter is measured in air, then the quantity λ in Equation (6.1) should be replaced by $n\lambda$, where n is the refractive index of air (with the value 1,000 27 for air at 20 °C and atmospheric pressure and at a wavelength of 650 nm ; the influence of variations in humidity and CO_2 content are negligible for this purpose).

When using a radiation thermometer to establish temperatures above about 2000 K it is necessary to use absorption filters or some other means of reducing the intensity of the radiation reaching the detector. Any filters that may be placed in the beam must be so oriented as to avoid reflections between them that can subsequently reach the detector, and to avoid transmission through the bandpass filter at an angle to the axis. Either of these faults is likely to modify the effective wavelength (*see* Section 6.2.3).

6.1.3 Detectors

The majority of radiation thermometers used for the realization of the ITS-90 use either a photomultiplier or a silicon photodetector as the detector. Typically a photomultiplier is used for wavelengths near 660 nm while a silicon photodetector is used for those near 900 nm. However, a photomultiplier with long-wavelength sensitivity can also be used in the near infrared and, conversely, a silicon photodetector can be used in the red region of the spectrum.

The spectral response of a photomultiplier depends on the photocathode employed. The photocathodes most commonly used in pyrometry are the S-20 types which give useful signals up to about 800 nm, but S-1 (to 1050 nm) and GaInAs (to 1100 nm) can also be employed, these being normally operated at temperatures of about −25 °C or below. If photocurrent ratios are to be the measure of radiance ratios then account must be taken of any non-linearity of the individual photomultiplier under the particular conditions of use. If the actual output voltage or current is used, then fatigue and the temperature coefficient of sensitivity must also be considered [Coates and Andrews

(1981)]. Any problem arising from these requirements can be alleviated if the photomultiplier is used in the photon counting mode ; this, however, involves more difficult measuring techniques [Coates (1975a)].

Silicon photodetectors generally show better linearity and stability than photomultipliers. The linearity and stability of silicon detectors for spectral radiation thermometry have been studied extensively [*see* in particular Jung (1979), Coslovi and Righini (1980) and Schaefer *et al.* (1983)].

It has been found that the departures from linearity increase both with increasing wavelength and increasing photocurrent. Jung has shown that, provided that the photocurrent is kept within the range from 3×10^{-10} A to 1×10^{-7} A and the wavelength is in the range from 600 nm to 900 nm, any non-linearity can easily be corrected for to within 2 parts in 10^4 (*see* equation 6.11 for consequent errors in temperature). If the corrections for non-linearity are not made, errors some twenty times this amount can be encountered ; thus for an accurate realization of the scale, it is essential that the non-linearity be measured (*see* Section 6.2.4).

In order to obtain optimum short-term stability and resolution a silicon detector should be stabilized in temperature and operated in the photovoltaic (i.e. unbiased) mode. Jung (1979) has shown that drift, dark current and noise are all lower for a silicon detector operated in this mode than for one operated in the photoconductive or biased mode.

6.2 Establishment of the ITS-90 above the Silver Point

6.2.1 General Principles

Equation (6.1) is an idealized expression of the spectral radiance ratio defining T_{90}. In practice, because any, supposedly monochromatic, radiation thermometer has a finite bandwidth we must write:

$$r = \frac{\int L_\lambda (T_{90}) \tau_c(\lambda)\, \tau_i(\lambda)\, s(\lambda)\, d\lambda}{\int L_\lambda [\, T_{90}(\mathrm{Ag})\,]\, \tau_c(\lambda)\, \tau_i(\lambda)\, s(\lambda)\, d\lambda} = \frac{\int L_\lambda (T_{90})\, S(\lambda)\, d\lambda}{\int L_\lambda [\, T_{90}(\mathrm{Ag})\,]\, S(\lambda)\, d\lambda} \qquad (6.3)$$

where r is the experimentally measured ratio of detector signals, $L_\lambda(T_{90}) = \pi^{-1} c_1 \lambda^{-5}\ [\exp\ (c_2/\lambda T_{90})\ - 1]^{-1}$, and $\tau_i(\lambda)$ is the spectral transmittance of the interference filter, $\tau_c(\lambda)$ is the spectral transmittance of all other optical components of the radiation thermometer, $s(\lambda)$ is the spectral responsitivity of the detector, and $S(\lambda)$ is the spectral

responsivity of the thermometer as a whole. The integrands in Equation (6.3) are normally zero outside the passband defined by the interference filter.

The realization of the scale according to Equation (6.3) requires the calibration of the thermometer at the silver (or gold, or copper) freezing point, the determination of the spectral responsivity of the thermometer, and the realization of a scale of radiance ratios which, in turn, requires measurement of the non-linearity of the detector, *see* Section 6.2.4.

6.2.2 Practical Methods

The blackbody and furnace apparatus for the fixed-point calibration have been described in Sections 2.2.3.3 and 2.2.5.

The monochromatic radiation thermometers employed to realize the scale are, in most cases, just photoelectric comparators of radiant fluxes. They do not carry a calibration in terms of detector output versus temperature but are used to transfer the blackbody radiance at the reference temperature $T_{90}(X)$ to a series of higher (or in some cases lower) temperatures established and subsequently maintained on a stable and reproducible radiation source, generally a tungsten strip lamp (*see* Section 6.4). This practice originated in the past from the lack of stable detectors that could maintain the scale over long periods.

When the visual optical pyrometer was the instrument used to carry out primary realizations of the international temperature scale at high temperatures, tungsten strip lamps were almost always used with the optical pyrometer both to establish the scale and by themselves subsequently to maintain it. With the advent of photoelectric thermometers, using photomultiplier or vacuum photocells as detectors, a much higher accuracy was achieved. But because the sensitivity of the new detectors tended to vary with use and time, the principles of using a tungsten strip lamp for realizing and maintaining the scale remained largely unchanged. The development of highly sensitive, linear and stable silicon photodetectors, however, has allowed a much simpler and more direct method to be used. Using such a detector, whose departures (if any) from linearity have been measured (*see* Section 6.2.4), in conjunction with an optical system designed to have a very stable optical throughput (*see* Section 6.4), equation (6.3) can be used directly to establish a continuous calibration of the combined detector-optical system in terms

of the ratios of the photocurrents of the detector when viewing the high temperature source and the blackbody at the silver (or gold or copper) point. Such a system can provide a realization of, and maintain, the ITS-90 at high temperatures just as well as a system using external tungsten strip lamps [Bussolino *et al.* (1987)].

If tungsten strip lamps are used, because they are not blackbody sources, equation 6.3 becomes

$$r = \frac{\int \varepsilon(\lambda,T')\, L_\lambda(T')\, \tau_w(\lambda)\, S(\lambda)\, d\lambda}{\int L_\lambda[\, T_{90}(\mathrm{Ag})\,]\, S(\lambda)\, d\lambda} \tag{6.4}$$

where $\tau_w(\lambda)$ is the spectral transmittance of the lamp window, and $\varepsilon(\lambda,T')$ is the spectral emissivity of the lamp filament which is at a true temperature T', but has, by the equality given by Equations (6.3) and (6.4), a radiance temperature T_{90}. T_{90} can be calculated exactly as before, but is now valid only for the particular wavelength used. If radiation thermometers working at different wavelengths are to be used the ITS-90 must normally be realized separately for each wavelength, although *see* Section 6.3 for futher comment on this.

The use of both silicon detector radiation thermometers and tungsten strip lamps allows the scale to be established in two ways and thus permits cross checks to be made which can add to the confidence of the maintained scale. For practical details of the various methods *see* Quinn and Ford (1969), Coslovi and Righini (1980), Tischler (1981), Jones and Tapping (1982) and Coates (1985).

If only one method is to be used, the choice between a detector-based method and a tungsten-source based method depends upon the preferred method of disseminating the scale outside the standards laboratory.

6.2.3 Spectral Responsivity and Effective Wavelength

The wavelength at which monochromatic radiation thermometers operate when being used to establish the ITS-90 is usually within the range 600 nm to 1000 nm. Although no wavelength is specified in the ITS-90, the use of red-sensitive photomultipliers (S-20 response) and silicon detectors results in this wavelength range being the optimum one.

Continuity with past-practice that requires a wavelength near 660 nm and the peak near 900 nm in the sensitivity curve of silicon detectors have led increasingly to the practice of carrying out realizations of the ITS-90 at both of these wavelengths. This has the great advantage of allowing a considerable measure of self checking to be obtained.

The relative spectral responsivity of the thermometer can either be measured directly by aiming the thermometer at the exit slit of a monochromator or it can be calculated as the product of its components, i.e. the spectral transmittances of the interference filter and of the other optical components and the spectral responsivity of the detector. When the filter transmittance and the detector responsivity are measured separately, they should be measured *in situ* so as to avoid errors due to different positioning and orientation. Details of the measurement of spectral responsivity are given in various papers describing the realization of radiation scales [*see* in particular Jones and Tapping (1982)]. The accuracy requirements for this measurement have been discussed by Coates (1977) and by Bedford and Ma (1983).

The concept of effective wavelength was introduced to avoid the cumbersome calculations required by equation (6.3). Representing the spectral band of the thermometer with a single (although temperature-dependent) wavelength allows the much simpler equation (6.1) to be used. The derivation of the effective wavelength from the measured spectral responsivity $S(\lambda)$ has been described in several papers [*see* in particular Kostkowski and Lee (1962), and Quinn and Ford (1969)].

Although the concept of effective wavelength is still commonly used due to its many advantages (it facilitates, for example, the estimation of all wavelength-dependent errors), a direct use of the spectral responsivity according to equation (6.3) is now practical using modern computational techniques. Moreover, new methods have been described by Coates (1977, 1979, 1985), Ruffino (1980) and Coppa *et al.* (1988) that require much less numerical integration and which can be made as accurate as is desired by the evaluation of successive terms in a series.

6.2.4 Radiance Ratios and Non-Linearity

The experimentally measured ratio of detector signals at two temperatures represents the ratio of the blackbody radiances at the same

temperatures only insofar as the detector (and associated electronics) is linear. In practice, even the most linear detectors show non-linearities that must be accounted for in accurate scale realizations.

The commonest technique for measuring non-linearity consists of a flux doubling method employing two radiation sources (usually lamps) and a beam-splitting device according to a scheme suggested by Erminy (1963). Other techniques that have been successfully applied in precision photoelectric thermometry rely on the use of sectored discs [Quinn and Ford (1969)] and of attenuating filters [Coslovi and Righini (1980)] and luminance dividers [Bonhoure and Pello (1988)]. Useful information on the mathematical handling of non-linearities is given by Jung (1979).

6.3 Tungsten Strip Lamps

Equation (6.1) defines T_{90} in terms of the spectral radiance of a blackbody at that temperature. It is common practice to establish and maintain the ITS-90 in this temperature range in terms either of tungsten strip lamps or, increasingly, directly in terms of silicon photodiode radiation thermometers.

Despite their not being blackbodies, tungsten strip lamps provide a convenient source of thermal radiation. Some evacuated lamps (Figure 6.3) have proved to be acceptably stable and reproducible (in the best cases to within some tens of millikelvins for hundreds of hours) when operated on dc current regulated to a part in 10^5, provided that they are not operated at radiance temperatures much above 1800 K. Their reproducibility can approach the ten millikelvin level if their use is restricted to the range of radiance temperatures from 1200 K to 1500 K, and if appropriate resistance corrections (which must be obtained from measurements of lamp current *and* lamp voltage) and base temperature corrections are applied [Jones and Tapping (1979)]. Above about 1800 K evaporation of, and to some extent thermal etching of and grain growth in, the tungsten will result in calibration changes [Quinn (1965) ; Quinn and Lee (1972)], while below about 1100 K the lead temperature coefficient and the ambient temperature coefficient become large. Gas-filled lamps are used from 1600 K to about 2500 K, but are more than an order of magnitude less stable than the evacuated type because of convection currents within the envelope.

Lamps having tungsten filaments so formed as to approximate cylindrical blackbody cavities [Quinn and Barber (1967)] have been used to extend the calibration range to about 3000 K. These lamps, however, occasionally exhibit abrupt changes in filament resistance and are more difficult to use. The radiance of their cavity aperture is very direction-sensitive so that the angle and field of view for calibration with any particular radiation thermometer must be carefully specified. Nevertheless these blackbody lamps are useful sources at temperatures above those accessible to tungsten strip lamps.

With any of the above lamps, the filament radiance varies with the base temperature and, at low temperatures, with ambient temperature. These temperatures should therefore be controlled and monitored. Lamp resistances can be used as stability checks or for calibration corrections.

As pointed out in section 6.2.2, the scale carried by a lamp is wavelength dependent, so, if a lamp is used to calibrate a thermometer working at a wavelength other than the wavelength used to calibrate the lamp, corrections must be applied. Ricolfi and Lanza (1983) and Battuello and Ricolfi (1984) derived experimentally the corrections for converting a calibration curve for a lamp corresponding to a scale realization at a wavelength near 660 nm to one corresponding to a wavelength near 900 nm. These corrections thus allow a lamp originally calibrated for a wavelength near 660 nm to be used for the calibration of a silicon detector thermometer at a wavelength near 900 nm without the need for a new calibration of the lamps at 900 nm.

6.4 Transfer Standard Radiation Thermometers

The dissemination of the radiometric part of an international temperature scale outside the national standards laboratory is carried out by means of a practical transfer instrument. In the days of the disappearing-filament optical pyrometer this was generally the tungsten strip lamp, which in turn would be used to calibrate or check the working disappearing-filament pyrometers. Direct calibrations of disappearing-filament pyrometers at national standards laboratories were carried out on occasion, but this practice was expensive and inefficient : a single calibrated tungsten strip lamp could be used to calibrate any number of optical pyrometers, and tungsten strip lamps were considered to be more

stable than the miniature pyrometer lamps built into disappearing-filament optical pyrometers.

The situation is different now that the disappearing-filament pyrometer has been almost entirely replaced by the much more stable silicon detector thermometer. A high-precision silicon detector transfer thermometer is shown in Figure 6.4 [Rosso and Righini (1985)]. This thermometer, and others of similar design, have an accuracy of better than 0,1 K from 800 K up to 1400 K and at higher temperatures a somewhat lesser accuracy which reaches about 1 K at 2000 K. Its long term stability is that of the silicon detector itself: the detector is mounted in a temperature-controlled enclosure and its drift is significantly below the equivalent of 0,1 K per month and does not exceed a few tenths of a kelvin in a year. Various schemes have been proposed for empirical calibration of such instruments using a number of fixed points [Bussolino *et al.* (1987)].

6.5 Practical Notes and Sources of Error in Radiation Thermometry

6.5.1 Practical Notes

In applying the procedures outlined in Section 6.2, the following points should be noted:

(a) For an accuracy of 10 mK in T_{90}, the ratio, r, of radiances must be determined with an uncertainty of between 2 and 10 parts in 10^4, depending upon λ and T_{90}. This follows from the relation:

$$\Delta T_{90} \approx \frac{\lambda (T_{90})^2}{c_2} \cdot \frac{\Delta r}{r} \tag{6.11}$$

(b) Only relative values of $S(\lambda)$, $\tau_c(\lambda)$, $\tau_i(\lambda)$ and $s(\lambda)$ are required.

(c) The mean or peak wavelength of $\tau_i(\lambda)$ must be measured to within about 0,02 nm for 10 mK accuracy in T_{90} (*see* Equation (6.2)).

(d) Because $\tau_c(\lambda) \cdot s(\lambda)$ appears in both integrands and varies relatively slowly with λ, for an accuracy equivalent to 10 mK, it need be measured only to within about ± 10% when the passband is < 20 nm.

(e) Direct measurement of the radiance ratios by means of photo-detector current ratios demands that, for an accuracy equivalent to 10 mK, the detector be linear to ≈ 1 part in 10^4. This cannot be

assumed to be the case, and any departures from linearity must be measured and corrected for [Jung (1979), Coslovi and Righini (1980)].

(f) The device most commonly used to produce precisely known energy ratios to measure detector nonlinearity (or to establish the ITS-90) is a radiance multiplier (*see* Section 6.2.4), several of which have been described, e.g. [Jones and Tapping (1982)]. In these devices two or more radiant fluxes are first matched to the silver point radiance via an arrangement of mirrors and shutters, and then by combining these fluxes an integer multiple of the silver point flux can be presented to the radiation thermometer. By extending this procedure and by other means almost any multiples of the silver point flux can be obtained [Coslovi and Righini (1980)].

(g) For an accuracy of 10 mK in the silver point realization, the emissivity, ε_c, of the blackbody cavity, must be known to about 1 part in 10^4. Examples of suitable designs are shown in Figure 2.5. For methods of calculating the emissivities of various blackbody cavities suitable for radiation thermometry *see* Bedford (1988), and Quinn (1990). If ε_c is different from unity it should appear as a factor in the denominator of Equations (6.3) and (6.4).

(h) The error ΔT_{90} in T_{90} resulting from an error $\Delta T_{90}(\mathrm{Ag})$ in the silver point measurement is given (in the short wavelength or Wien approximation, *see* Section 1.3.1) by:

$$\Delta T_{90} = \Delta T_{90}(\mathrm{Ag}) \left[\frac{T_{90}}{T_{90}(\mathrm{Ag})} \right]^2 . \qquad (6.12)$$

(i) Direct calculation of T_{90} from Equation (6.3) is an iterative procedure. If a first approximation is obtained from Equation (6.1) using for λ the wavelength at the peak of $\tau_i(\lambda)$, an accuracy of 10 mK can be achieved in two or three iterations.

(j) Several methods for avoiding the iterative calculation of Equation (6.3) have been proposed (*see* Section 6.2.3).

(k) Diffraction and scattering together produce an effect known as the size-of-source effect. A certain amount of radiant flux reaching the detector originates outside the geometrical field of view of the optical system of the thermometer. This results in a small source's having a lower apparent temperature than does a larger one actually at the same temperature. This is known as the size-of-source effect. The effect is approximately inversely proportional to the diameter of the

source. For a 1 mm diameter source, and assuming well-designed optics, this effect may be of the order of 0,2 K ; it is important that the magnitude of this effect for a particular radiation thermometer be measured. Two methods of measuring the size-of-source effect are illustrated in Figure 6.5 [Coates and Andrews (1978), Jones and Tapping (1982) and Ohtsuka and Bedford (1989)]. Battuello *et al.* (1990) obtained an effective reduction of the size-of-source effect by placing in front of the blackbody aperture a disc-shaped auxiliary heater that provided a uniform temperature distribution around the target of the thermometer.

6.5.2 Additional Sources of Error

(a) Any radiation thermometer will indicate too low a temperature if its entrance aperture is not properly filled, which may occur if stops, mirrors, prisms, etc. are used in an improper manner along the external optical path.

(b) Absorbing materials (dust, vapours) along the optical path or on radiation thermometer components will cause too low a temperature indication.

(c) Radiation from sources near to and hotter than the target can, if reflected along the optical path, cause the temperature indication to be much too high.

(d) Tungsten strip lamp calibrations change several degrees upon current reversal. The user must be sure that the polarity is correct.

(e) If windows are used between the target and radiation thermometer, the measured temperature must be corrected for the effect of window transmittance.

Figure 6.1 A radiation thermometer using a refracting optical system [after Jones and Tapping (1982)]
Section 6.1.

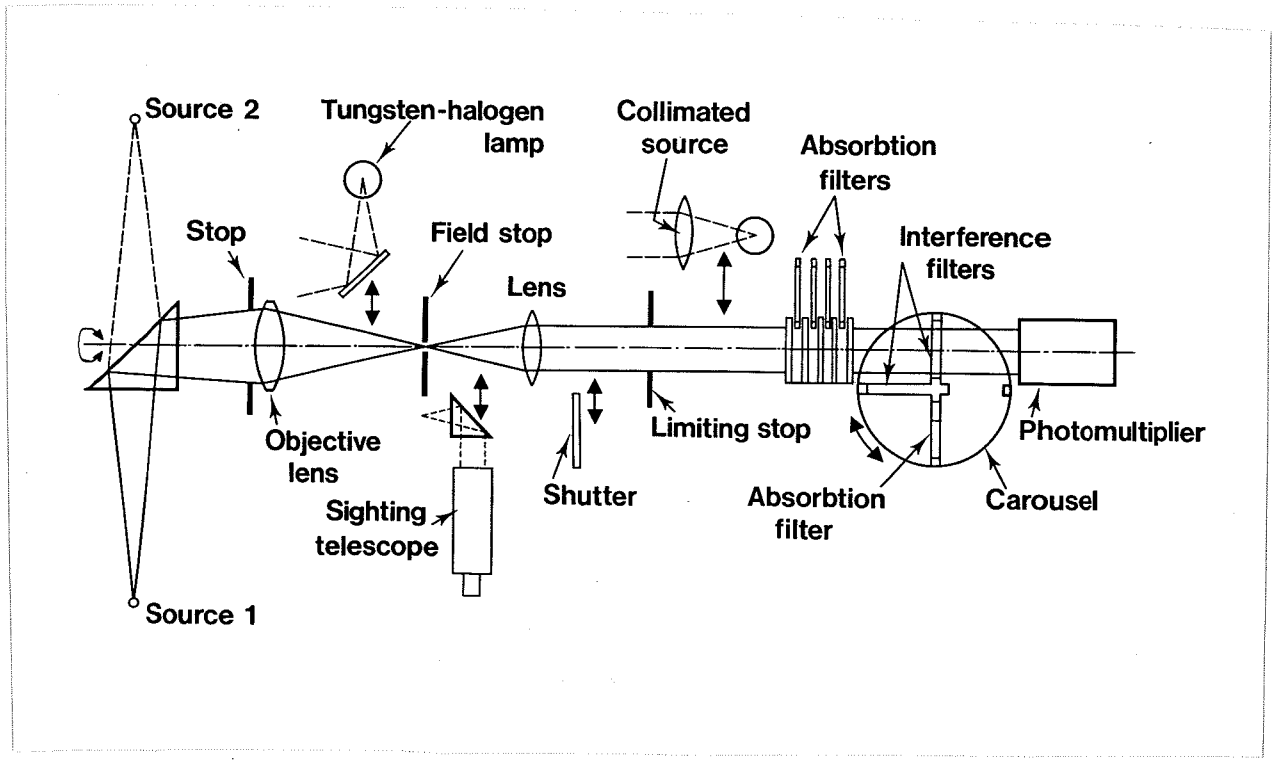

Figure 6.2 A radiation thermometer using a reflecting optical system [after Quinn and Chandler (1972)]. In later versions of this instrument a silicon photodetector has replaced the photomultiplier and the sectored disk no longer used.
Section 6.1.

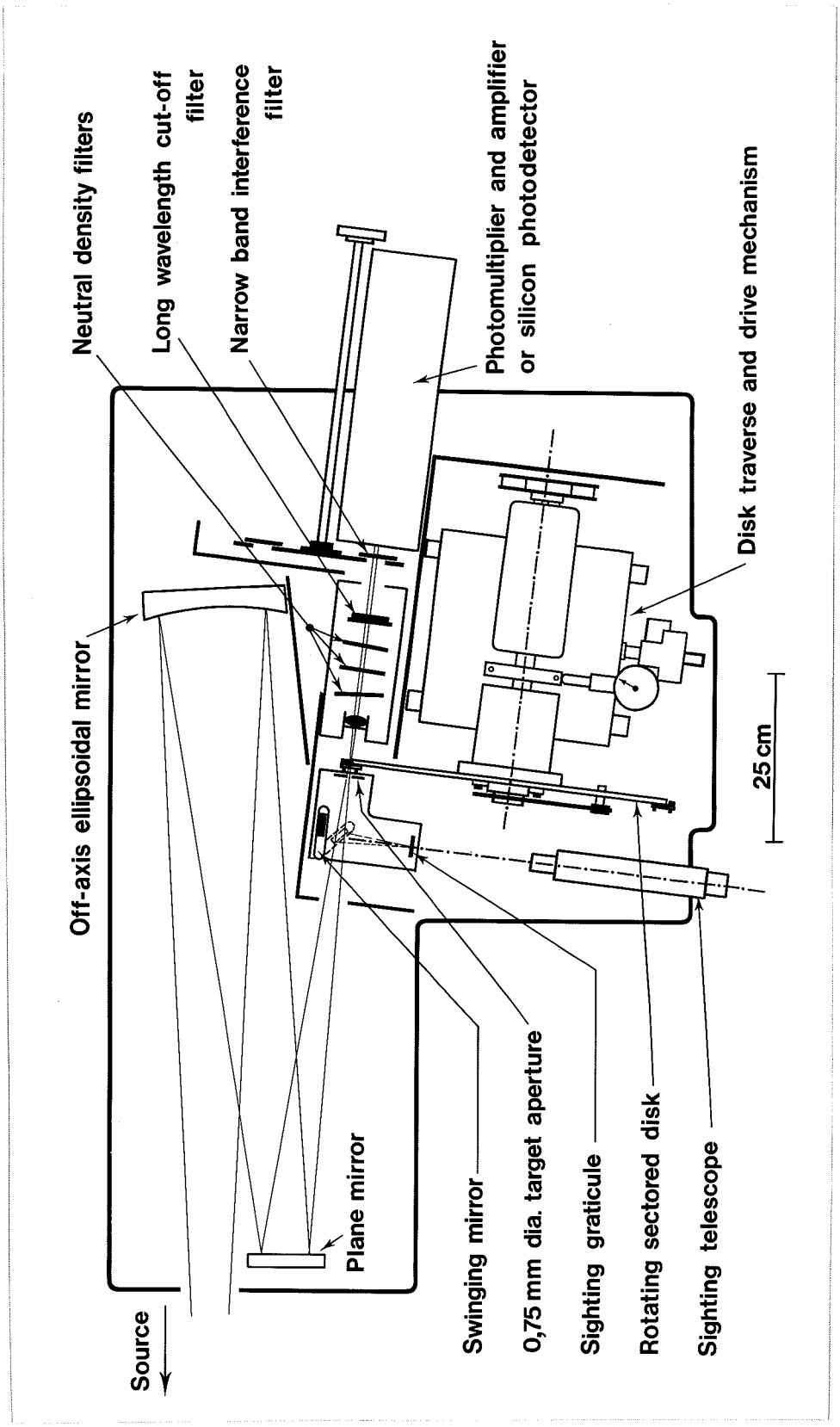

Figure 6.3 A high-stability vacuum-type tungsten strip lamp for use up to about 1700 °C.
Section 6.3.

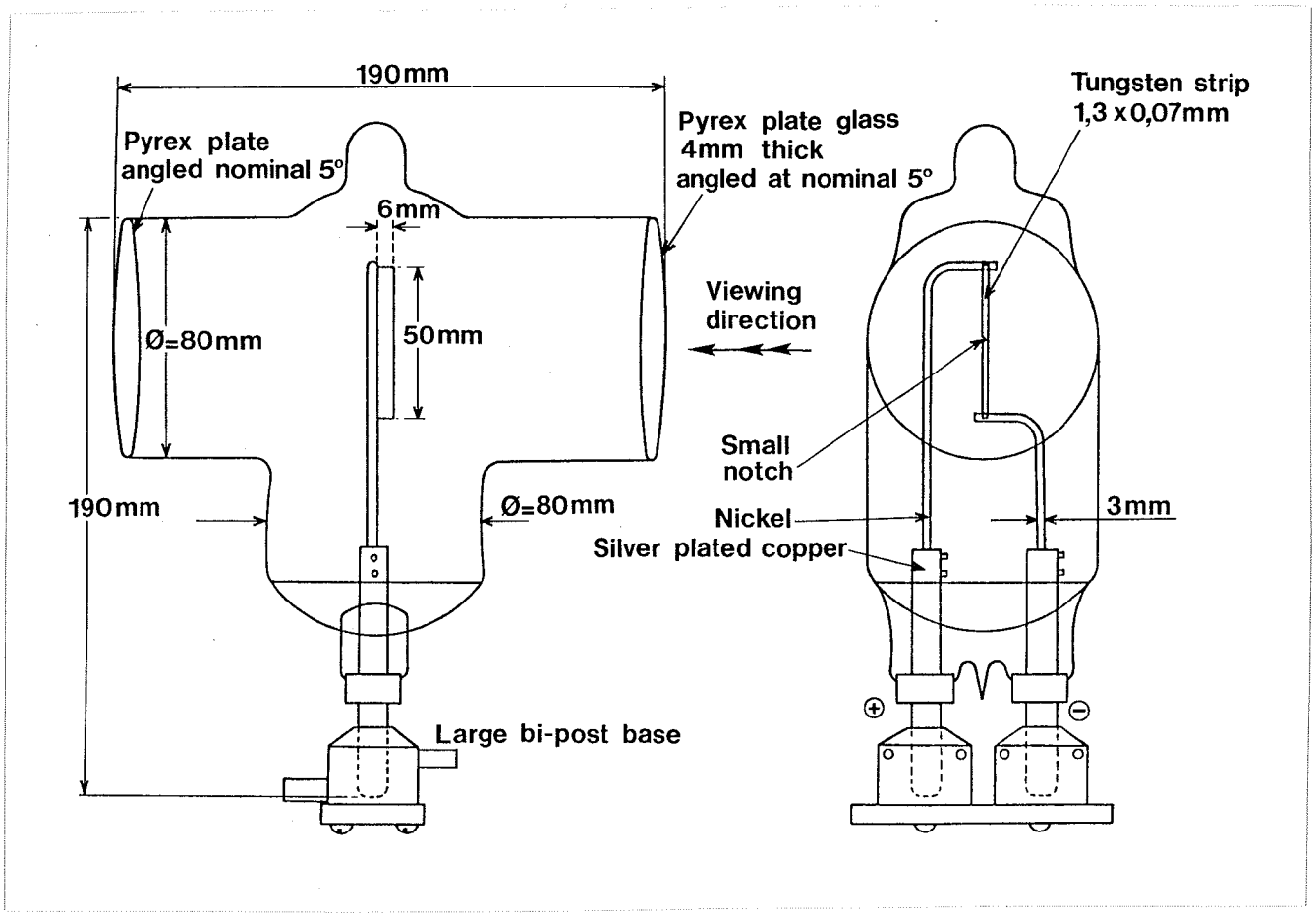

Figure 6.4 Schematic of the optical system of a transfer-standard radiation thermometer; T, target; L_1, moveable objective lens; L_2, objective lens; L_3, field lens; MD, mirror diaphragm; AS, aperture stop; FS, field stop; S, shutter; I, interference mirror; E, eyepiece [after Rosso and Righini (1985)].
Section 6.4.

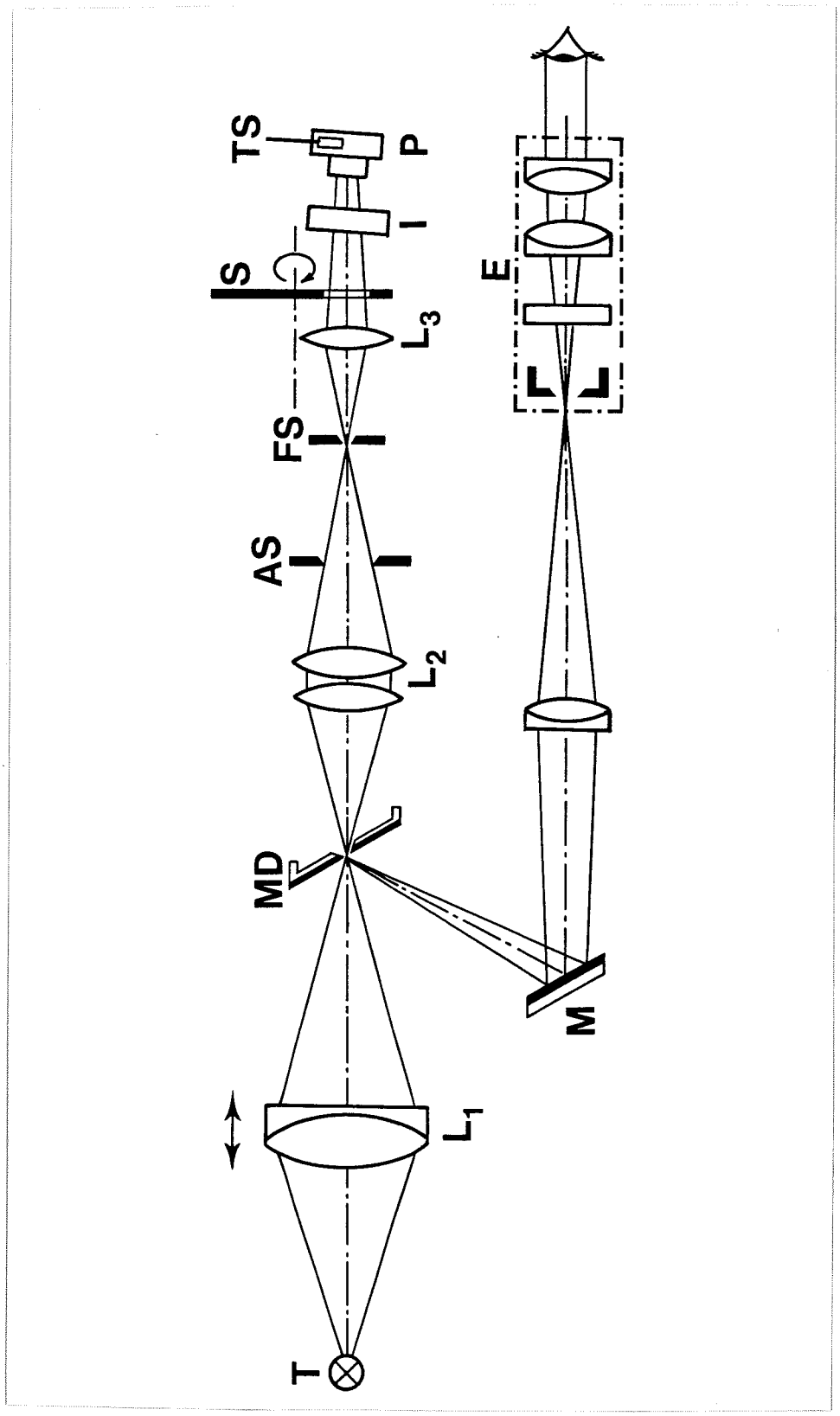

Figure 6.5 Methods for measuring the size-of-source effect. (a) using a source of variable diameter illuminated by a supplementary lamp; (b) using a range of apertures placed in the centre of a furnace. Section 6.5.1.

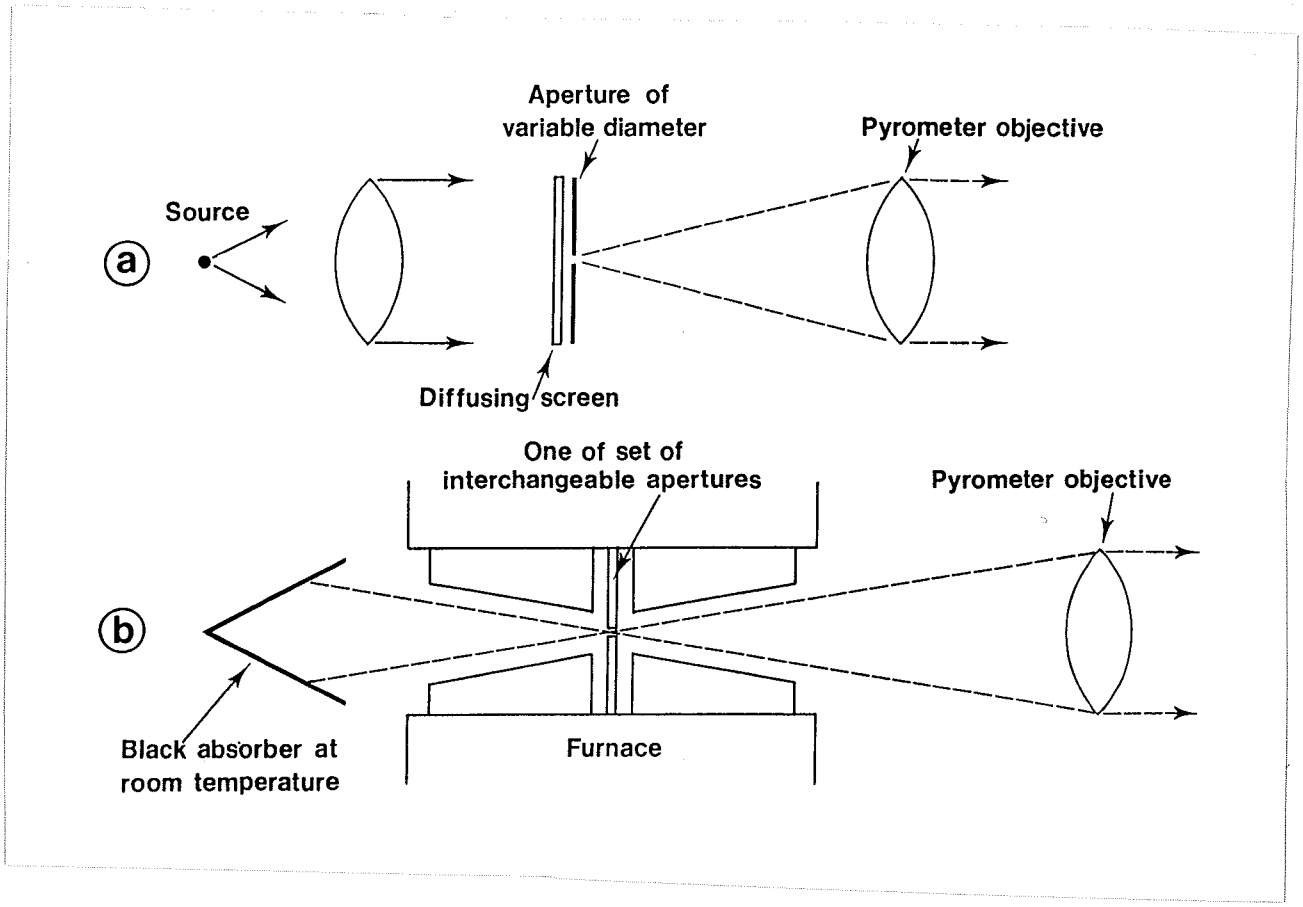

REFERENCES

Battuello, M., Lanza, F. and Ricolfi, T. (1990): Fixed-Point Technique for Approximating the ITS-90 between 420 °C and 1085 °C with an Infrared Thermometer ; Metrologia **27**, 75-82

Battuello, M. and Ricolfi, T. (1984): A Procedure for Calibrating Silicon Detector Pyrometers with Pyrometric Lamps ; Proc. 2nd Symposium on Temperature Measurements in Industry and Science, IMEKO TC-12, Suhl, 161-168

Bedford, R.E. (1988): Calculation of effective emissivity of cavity sources of thermal radiation. In Theory and Practice of Radiation Thermometry (de Witt, Nutter ed., Wiley Interscience), 653-772

See also :

Bedford, R.E. and Ma, C.K. (1974): Emissivities of Diffuse Cavities: Isothermal and Non-isothermal Cones and Cylinders ; J. Opt. Soc. Am. **64**, 339-349

Bedford, R.E. and Ma, C.K. (1975): Emissivities of Diffuse Cavities II: Isothermal and Non-isothermal Cylindro-Cones ; J. Opt. Soc. Am. **65**, 565-572

Bedford, R.E. and Ma, C.K. (1976): Emissivities of Diffuse Cavities III: Isothermal and Non-isothermal Double Cones ; J. Opt. Soc. Am. **66**, 724-730

Bedford, R.E., Ma, C.K., Chu, Z., Sun, Y. and Chen, S. (1988): Emissivities of Diffuse Cavities 4: Isothermal and Non-isothermal Cylindro-inner-cones ; Appl. Opt. **24**, 2971-2980

Bedford, R.E. and Ma, C.K. (1983): Effects of uncertainties in detector responsivity in thermodynamic temperature measured with an optical pyrometer ; High Temp. -High Pressures **15**, 119-130

Bonhoure, J. and Pello, R. (1988): Determination of the Departure of the International Practical Temperature Scale of 1968 from Thermodynamic Temperature in the Region between 693 K and 904 K ; Metrologia **25**, 99-105

Bussolino, G.C., Righini, F. and Rosso, A. (1987): Comparison of a Transfer Standard Pyrometer and of High Stability Lamps ; Proc. TEMP/MEKO 87 Thermal and Temperature Measurement in Science and Industry (IMEKO and Institute of Measurement Control, Sheffield), 77-86

Coates, P.B. (1975a): Fatigue and its Correction in Photon Counting Experiments ; J. Phys. E. **8**, 189-193

Coates, P.B. (1975b): The NPL Photon Counting Pyrometer ; Temperature **75**, 238-243

Coates, P.B. (1977): Wavelength specification in optical and photoelectric pyrometry ; Metrologia **13**, 1-5

Coates, P.B. and Andrews, J.W. (1978): A Precise Determination of the Freezing Point of Copper ; J. Phys. F. **8**, 277-285

Coates, P.B. (1979): The Direct Calculation of Radiance Temperatures in Photoelectric Pyrometry ; High Temp. - High Pressures **11**, 289-300

Coates, P.B. and Andrews, J.W. (1981): Measurement of Gain Changes in Photomultipliers ; J. Phys. E. **14**, 1164-1166

Coates, P.B. (1985): Analytic estimation of systematic errors in photoelectric pyrometry ; High Temp. - High Pressures **17**, 507-518

Coppa, P., Ruffino, G. and Spena, A. (1988): Pyrometer wavelength function: its determination and error analysis ; High Temp. - High Pressures **20**, 479-490

Coslovi, L. and Righini, F. (1980): Fast Determination of Non-Linearity of Photodetectors, Appl. Opt. **19**, 3200-3203

Erminy, D.E. (1963): Scheme for Obtaining Integral and Fractional Multiples of a Given Radiance ; J. Opt. Soc. Am. **53**, 1448-1449

Fischer, J. and Jung, H.J. (1989): Determination of the Thermodynamic Temperatures of the Freezing Points of Silver and Gold by Near-Infrared Pyrometry ; Metrologia **26**, 245-252

Jones, T.P. and Tapping, J. (1979): The Suitability of Tungsten Strip Lamps as Secondary Standard Sources Below 1064 °C ; Metrologia **15**, 135-141

Jones, T.P. and Tapping, J. (1982): A Precision Photoelectric Pyrometer for the Realization of the IPTS-68 above 1064.53 °C ; Metrologia **18**, 23-31

Jung, H.J. (1979): Spectral Nonlinearity Characteristics of Low-Noise Silicon Detectors and Their Application to Accurate Measurement of Radiant Flux Ratios ; Metrologia **15**, 173-181

Kostkowski, H.J. and Lee, R.D. (1962): Theory and Methods of Optical Pyrometry ; Temperature, Its Measurement and Control in Science and Industry **3** (Reinhold, New York), 449-481

Ohtsuka, M. and Bedford, R.E. (1989): Measurement of size-source effects in an optical radiation thermometer ; Measurement **7**, 2-6

Quinn, T.J. (1965): The Effects of Thermal Etching on the Emissivity of Tungsten ; Br. J. of Appl. Phys. **16**, 973-980

Quinn, T.J. and Barber, C.R. (1967): A Lamp as a Reproducible Source of Near Blackbody Radiation for Precise Pyrometry up to 2700 °C ; Metrologia **3**, 19-23

Quinn, T.J. and Chandler, T.R. (1972): The freezing point of platinum determined by the NPL photoelectric pyrometer ; Temperature, Its Measurement and Control in Science and Industry **4** (Instrument Society of America, Pittsburgh), 295-309

Quinn, T.J. and Ford, M.C. (1969): On the Use of the NPL Photoelectric Pyrometer to Establish the Temperature Scale Above the Gold Point (1063 °C) ; Proc. Roy. Soc. A **312**, 31-50

Quinn, T.J. and Lee, R. (1972): Vacuum Tungsten Strip Lamps with Improved Stability as Radiance Temperature Standards. Temperature, Its Measurement and Control in Science and Industry (Instrument Society of America, Pittsburgh) **4**, 395-411

Quinn, T.J. (1990): Temperature, 2nd edition ; Academic Press (London), 495 p.

Ricolfi, T. and Lanza, F. (1983): Relationships Between Radiance Temperature and Wavelength for Tungsten Strip Lamps ; High Temp. - High Pressures **15**, 13-20

Rosso, A. and Righini, F. (1985): A new transfer-standard pyrometer ; Measurement **3**, 131-136

Ruffino, G. (1980): Primary Temperature Measurement Above the Gold Point ; High Temp. - High Pressures **12**, 241-246

Schaefer, A.R., Zalewski, E.F. and Geist, J. (1983): Silicon detector nonlinearity and related effects ; Appl. Opt. **22**, 1232-1236

Tischler, M. (1981): High Accuracy Temperature and Uncertainty Calculation in Radiation Pyrometry ; Metrologia **17**, 49-58

APPENDIX 1

The International Temperature Scale of 1990 (ITS-90)

The following text is taken from *Metrologia*, 1990, **27**, 3-10. The official French text of the International Temperature Scale of 1990 (ITS-90) is published in the *BIPM Proc.-Verb. Com. Int. Poids et Mesures*, 1989, **57**, T1-21.

Metrologia 27, 3–10 (1990)

metrologia

The International Temperature Scale of 1990 (ITS-90)

H. Preston-Thomas

President of the Comité Consultatif de Thermométrie and Vice-President of the Comité International des Poids et Mesures
Division of Physics, National Research Council of Canada, Ottawa, K1A 0S1 Canada

Received: October 24, 1989

Introductory Note

The official French text of the ITS-90 is published by the BIPM as part of the Procès-verbaux of the Comité International des Poids et Mesures (CIPM). However, the English version of the text reproduced here has been authorized by the Comité Consultatif de Thermométrie (CCT) and approved by the CIPM.

The International Temperature Scale of 1990

The International Temperature Scale of 1990 was adopted by the International Committee of Weights and Measures at its meeting in 1989, in accordance with the request embodied in Resolution 7 of the 18th General Conference of Weights and Measures of 1987. This scale supersedes the International Practical Temperature Scale of 1968 (amended edition of 1975) and the 1976 Provisional 0,5 K to 30 K Temperature Scale.

1. Units of Temperature

The unit of the fundamental physical quantity known as thermodynamic temperature, symbol T, is the kelvin, symbol K, defined as the fraction 1/273,16 of the thermodynamic temperature of the triple point of water [1].

Because of the way earlier temperature scales were defined, it remains common practice to express a temperature in terms of its difference from 273,15 K, the ice point. A thermodynamic temperature, T, expressed in this way is known as a Celsius temperature, symbol t, defined by:

$$t/°\mathrm{C} = T/\mathrm{K} - 273{,}15\,. \tag{1}$$

The unit of Celsius temperature is the degree Celsius, symbol °C, which is by definition equal in magnitude to the kelvin. A difference of temperature may be expressed in kelvins or degrees Celsius.

The International Temperature Scale of 1990 (ITS-90) defines both International Kelvin Temperatures, symbol T_{90}, and International Celsius Temperatures, symbol t_{90}. The relation between T_{90} and t_{90} is the same as that between T and t, i.e.:

$$t_{90}/°\mathrm{C} = T_{90}/\mathrm{K} - 273{,}15\,. \tag{2}$$

The unit of the physical quantity T_{90} is the kelvin, symbol K, and the unit of the physical quantity t_{90} is the degree Celsius, symbol °C, as is the case for the thermodynamic temperature T and the Celsius temperature t.

2. Principles of the International Temperature Scale of 1990 (ITS-90)

The ITS-90 extends upwards from 0,65 K to the highest temperature practicably measurable in terms of the Planck radiation law using monochromatic radiation. The ITS-90 comprises a number of ranges and sub-ranges throughout each of which temperatures T_{90} are defined. Several of these ranges or sub-ranges overlap, and where such overlapping occurs, differing definitions of T_{90} exist: these differing definitions have equal status. For measurements of the very highest precision there may be detectable numerical differences between measurements made at the same temperature but in accordance with differing definitions. Similarly, even using one definition, at a temperature between defining fixed points two acceptable interpolating instruments (e.g. resistance thermometers) may give detectably differing numerical values of T_{90}. In virtually all cases these differences are of negligible practical importance and are at the minimum level consistent with a scale of no more than reasonable complexity: for further information on this point, see "Supplementary Information for the ITS-90" (BIPM-1990).

[1] Comptes Rendus des Séances de la Treizième Conférence Générale des Poids es Mesures (1967–1968), Resolutions 3 and 4, p. 104

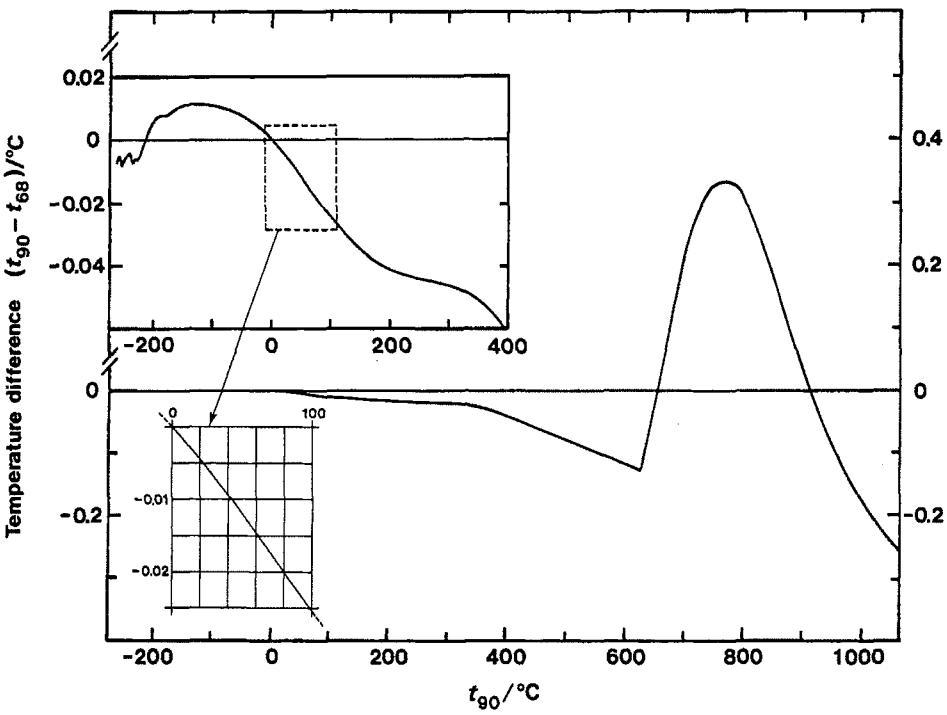

Fig. 1. The differences $(t_{90}-t_{68})$ as a function of Celsius temperature

The ITS-90 has been constructed in such a way that, throughout its range, for any given temperature the numerical value of T_{90} is a close approximation to the numerical value of T according to best estimates at the time the scale was adopted. By comparison with direct measurements of thermodynamic temperatures, measurements of T_{90} are more easily made, are more precise and are highly reproducible.

There are significant numerical differences between the values of T_{90} and the corresponding values of T_{68} measured on the International Practical Temperature Scale of 1968 (IPTS-68), see Fig. 1 and Table 6. Similarly there were differences between the IPTS-68 and the International Practical Temperature Scale of 1948 (IPTS-48), and between the International Temperature Scale of 1948 (ITS-48) and the International Temperature Scale of 1927 (ITS-27). See the Appendix and, for more detailed information, "Supplementary Information for the ITS-90".

3. Definition of the International Temperature Scale of 1990

Between 0,65 K and 5,0 K T_{90} is defined in terms of the vapour-pressure temperature relations of ^{3}He and ^{4}He.

Between 3,0 K and the triple point of neon (24,5561 K) T_{90} is defined by means of a helium gas thermometer calibrated at three experimentally realizable temperatures having assigned numerical values (defining fixed points) and using specified interpolation procedures.

Between the triple point of equilibrium hydrogen (13,8033 K) and the freezing point of silver (961,78 °C) T_{90} is defined by means of platinum resistance thermometers calibrated at specified sets of defining fixed points and using specified interpolation procedures.

Above the freezing point of silver (961,78 °C) T_{90} is defined in terms of a defining fixed point and the Planck radiation law.

The defining fixed points of the ITS-90 are listed in Table 1. The effects of pressure, arising from significant depths of immersion of the sensor or from other causes, on the temperature of most of these points are given in Table 2.

3.1. From 0,65 K to 5,0 K: Helium Vapour-Pressure Temperature Equations

In this range T_{90} is defined in terms of the vapour pressure p of ^{3}He and ^{4}He using equations of the form:

$$T_{90}/\mathrm{K} = A_0 + \sum_{i=1}^{9} A_i\,[(\ln(p/\mathrm{Pa}) - B)/C]^i\,. \qquad (3)$$

The values of the constants A_0, A_i, B and C are given in Table 3 for ^{3}He in the range of 0,65 K to 3,2 K, and for ^{4}He in the ranges 1,25 K to 2,1768 K (the λ point) and 2,1768 K to 5,0 K.

3.2. From 3,0 K to the Triple Point of Neon (24,5561 K): Gas Thermometer

In this range T_{90} is defined in terms of a ^{3}He or a ^{4}He gas thermometer of the constant-volume type that has been calibrated at three temperatures. These are the triple point of neon (24,5561 K), the triple point of equilibrium hydrogen (13,8033 K), and a temperature between 3,0 K and 5,0 K. This last temperature is determined using a ^{3}He or a ^{4}He vapour pressure thermometer as specified in Sect. 3,1.

Table 1. Defining fixed points of the ITS-90

Number	Temperature T_{90}/K	Temperature t_{90}/°C	Substance[a]	State[b]	$W_r(T_{90})$
1	3 to 5	−270,15 to −268,15	He	V	
2	13,8033	−259,3467	e-H_2	T	0,001 190 07
3	≈17	≈−256,15	e-H_2 (or He)	V (or G)	
4	≈20,3	≈−252,85	e-H_2 (or He)	V (or G)	
5	24,5561	−248,5939	Ne	T	0,008 449 74
6	54,3584	−218,7916	O_2	T	0,091 718 04
7	83,8058	−189,3442	Ar	T	0,215 859 75
8	234,3156	−38,8344	Hg	T	0,844 142 11
9	273,16	0,01	H_2O	T	1,000 000 00
10	302,9146	29,7646	Ga	M	1,118 138 89
11	429,7485	156,5985	In	F	1,609 801 85
12	505,078	231,928	Sn	F	1,892 797 68
13	692,677	419,527	Zn	F	2,568 917 30
14	933,473	660,323	Al	F	3,376 008 60
15	1234,93	961,78	Ag	F	4,286 420 53
16	1337,33	1064,18	Au	F	
17	1357,77	1084,62	Cu	F	

[a] All substances except ^{3}He are of natural isotopic composition, e-H_2 is hydrogen at the equilibrium concentration of the ortho- and para-molecular forms

[b] For complete definitions and advice on the realization of these various states, see "Supplementary Information for the ITS-90". The symbols have the following meanings: V: vapour pressure point; T: triple point (temperature at which the solid, liquid and vapour phases are in equilibrium); G: gas thermometer point; M, F: melting point, freezing point (temperature, at a pressure of 101 325 Pa, at which the solid and liquid phases are in equilibrium)

Table 2. Effect of pressure on the temperatures of some defining fixed points [#]

Substance	Assigned value of equilibrium temperature T_{90}/K	Temperature with pressure, p (dT/dp)/ $(10^8\,K\cdot Pa^{-1})$*	Variation with depth, l (dT/dl)/ $(10^{-3}\,K\cdot m^{-1})$**
e-Hydrogen (T)	13,8033	34	0,25
Neon (T)	24,5561	16	1,9
Oxygen (T)	54,3584	12	1,5
Argon (T)	83,8058	25	3,3
Mercury (T)	234,3156	5,4	7,1
Water (T)	273,16	−7,5	−0,73
Gallium	302,9146	−2,0	−1,2
Indium	429,7485	4,9	3,3
Tin	505,078	3,3	2,2
Zinc	692,677	4,3	2,7
Aluminium	933,473	7,0	1,6
Silver	1234,93	6,0	5,4
Gold	1337,33	6,1	10
Copper	1357,77	3,3	2,6

* Equivalent to millikelvins per standard atmosphere

** Equivalent to millikelvins per metre of liquid

[#] The Reference pressure for melting and freezing points is the standard atmosphere (p_0=101 325 Pa). For triple points (T) the pressure effect is a consequence only of the hydrostatic head of liquid in the cell

Table 3. Values of the constants for the helium vapour pressure Eqs. (3), and the temperature range for which each equation, identified by its set of constants, is valid

	^{3}He 0,65 K to 3,2 K	^{4}He 1,25 K to 2,1768 K	^{4}He 2,1768 K to 5,0 K
A_0	1,053 447	1,392 408	3,146 631
A_1	0,980 106	0,527 153	1,357 655
A_2	0,676 380	0,166 756	0,413 923
A_3	0,372 692	0,050 988	0,091 159
A_4	0,151 656	0,026 514	0,016 349
A_5	−0,002 263	0,001 975	0,001 826
A_6	0,006 596	−0,017 976	−0,00 4325
A_7	0,088 966	0,005 409	−0,00 4973
A_8	−0,004 770	0,013 259	0
A_9	−0,054 943	0	0
B	7,3	5,6	10,3
C	4,3	2,9	1,9

3.2.1. From 4,2 K to the Triple Point of Neon (24,5561 K) with ^{4}He as the Thermometric Gas. In this range T_{90} is defined by the relation:

$$T_{90} = a + bp + cp^2\,, \tag{4}$$

where p is the pressure in the gas thermometer and a, b and c are coefficients the numerical values of which are obtained from measurements made at the three defining fixed points given in Sect. 3.2, but with the further restriction that the lowest one of these points lies between 4,2 K and 5,0 K.

3.2.2. From 3,0 K to the Triple Point of Neon (24,5561 K) with ^{3}He or ^{4}He as the Thermometric Gas. For a ^{3}He gas thermometer, and for a ^{4}He gas thermometer used below 4,2 K, the non-ideality of the gas must be accounted for explicitly, using the appropriate second virial coefficient $B_3\,(T_{90})$ or $B_4\,(T_{90})$. In this range T_{90} is defined by the relation:

$$T_{90} = \frac{a + bp + cp^2}{1 + B_x(T_{90})\,N/V}\,, \tag{5}$$

where p is the pressure in the gas thermometer, a, b and c are coefficients the numerical values of which are obtained from measurements at three defining temperatures as given in Sect. 3.2, N/V is the gas density with N being the quantity of gas and V the volume of the bulb, x is 3 or 4 according to the isotope used, and the values of the second virial coefficients are given by the relations:

For ^{3}He,

$$B\,(T_{90})/\mathrm{m^3\,mol^{-1}} = \{16{,}69 - 336{,}98\,(T_{90}/\mathrm{K})^{-1} + 91{,}04\,(T_{90}/\mathrm{K})^{-2} - 13{,}82\,(T_{90}/\mathrm{K})^{-3}\}\,10^{-6}\,. \tag{6a}$$

For ^{4}He,

$$B_4\,(T_{90})/\mathrm{m^3\,mol^{-1}} = \{16{,}708 - 374{,}05\,(T_{90}/\mathrm{K})^{-1} - 383{,}53\,(T_{90}/\mathrm{K})^{-2} + 1799{,}2\,(T_{90}/\mathrm{K})^{-3} - 4033{,}2\,(T_{90}/\mathrm{K})^{-4} + 3252{,}8\,(T_{90}/\mathrm{K})^{-5}\}\,10^{-6}\,. \tag{6b}$$

Table 4. The constants A_0, A_i; B_0, B_i; C_0, C_i; D_0 and D_i in the reference functions of equations (9a); (9b); (10a); and (10b) respectively

A_0	−2,135 347 29	B_0	−0,183 324 722	B_{13}	−0,091 173 542
A_1	3,183 247 20	B_1	0,240 975 303	B_{14}	0,001 317 696
A_2	−1,801 435 97	B_2	0,209 108 771	B_{15}	0,026 025 526
A_3	0,717 272 04	B_3	0,190 439 972		
A_4	0,503 440 27	B_4	0,142 648 498		
A_5	−0,618 993 95	B_5	0,077 993 465		
A_6	−0,053 323 22	B_6	0,012 475 611		
A_7	0,280 213 62	B_7	−0,032 267 127		
A_8	0,107 152 24	B_8	−0,075 291 522		
A_9	−0,293 028 65	B_9	−0,056 470 670		
A_{10}	0,044 598 72	B_{10}	0,076 201 285		
A_{11}	0,118 686 32	B_{11}	0,123 893 204		
A_{12}	−0,052 481 34	B_{12}	−0,029 201 193		
C_0	2,781 572 54	D_0	439,932 854		
C_1	1,646 509 16	D_1	472,418 020		
C_2	−0,137 143 90	D_2	37,684 494		
C_3	−0,006 497 67	D_3	7,472 018		
C_4	−0,002 344 44	D_4	2,920 828		
C_5	0,005 118 68	D_5	0,005 184		
C_6	0,001 879 82	D_6	−0,963 864		
C_7	−0,002 044 72	D_7	−0,188 732		
C_8	−0,000 461 22	D_8	0,191 203		
C_9	0,000 457 24	D_9	0,049 025		

The accuracy with which T_{90} can be realized using Eqs. (4) and (5) depends on the design of the gas thermometer and the gas density used. Design criteria and current good practice required to achieve a selected accuracy are given in "Supplementary Information for the ITS-90".

3.3. The Triple Point of Equilibrium Hydrogen (13,8033 K) to the Freezing Point of Silver (961,78 °C): Platinum Resistance Thermometer

In this range T_{90} is defined by means of a platinum resistance thermometer calibrated at specified sets of defining fixed points, and using specified reference and deviation functions for interpolation at intervening temperatures.

No single platinum resistance thermometer can provide high accuracy, or is even likely to be usable, over all of the temperature range 13,8033 K to 961,78 °C. The choice of temperature range, or ranges, from among those listed below for which a particular thermometer can be used is normally limited by its construction.

For practical details and current good practice, in particular concerning types of thermometer available, their acceptable operating ranges, probably accuracies, permissible leakage resistance, resistance values, and thermal treatment, see "Supplementary Information for the ITS-90". It is particularly important to take account of the appropriate heat treatments that should be followed each time a platinum resistance thermometer is subjected to a temperature above about 420 °C.

Temperatures are determined in terms of the ratio of the resistance $R(T_{90})$ at a temperature T_{90} and the resistance R (273,16 K) at the triple point of water. This ratio, $W(T_{90})$, is[2]:

$$W(T_{90}) = R(T_{90})/R(273{,}16\ \mathrm{K})\,. \tag{7}$$

An acceptable platinum resistance thermometer must be made from pure, strain-free platinum, and it must satisfy at least one of the following two relations:

$$W(29{,}7646\ ^\circ\mathrm{C}) \geq 1{,}118\ 07\,, \tag{8a}$$

$$W(-38{,}8344\ ^\circ\mathrm{C}) \leq 0{,}844\ 235\,. \tag{8b}$$

An acceptable platinum resistance thermometer that is to be used up to the freezing point of silver must also satisfy the relation:

$$W(961{,}78\ ^\circ\mathrm{C}) \geq 4{,}2844\,. \tag{8c}$$

In each of the resistance thermometer ranges, T_{90} is obtained from $W_r(T_{90})$ as given by the appropriate reference function {Eqs. (9b) or (10b)}, and the deviation $W(T_{90}) - W_r(T_{90})$. At the defining fixed points this deviation is obtained directly from the calibration of the thermometer: at intermediate temperatures it is obtained by means of the appropriate deviation function {Eqs. (12), (13) and (14)}.

(i) – For the range 13,8033 K 273,16 K the following reference function is defined:

$$\ln[W_r(T_{90})] = A_0 + \sum_{i=1}^{12} A_i \left[\frac{\ln(T_{90}/273{,}16\ \mathrm{K}) + 1{,}5}{1{,}5}\right]^i . \tag{9a}$$

An inverse function, equivalent to Eq. (9a) to within 0.1 mK, is:

$$T_{90}/273{,}16\ \mathrm{K} = B_0 + \sum_{i=1}^{15} B_i \left[\frac{W_r(T_{90})^{1/6} - 0{,}65}{0{,}35}\right]^i . \tag{9b}$$

The values of the constants A_0, A_i, B_0 and B_i are given in Table 4.

A thermometer may be calibrated for use throughout this range or, using progressively fewer calibration points, for ranges with low temperature limits of 24,5561 K, 54,3584 K and 83,8058 K, all having an upper limit of 273,16 K.

(ii) – For the range 0 °C to 961,78 °C the following reference function is defined:

$$W_r(T_{90}) = C_0 + \sum_{i=1}^{9} C_i \left[\frac{T_{90}/\mathrm{K} - 754{,}15}{481}\right]^i . \tag{10a}$$

An inverse function, equivalent to equation (10a) to within 0.13 mK is:

$$T_{90}/\mathrm{K} - 273{,}15 = D_0 + \sum_{i=1}^{9} D_i \left[\frac{W_r(T_{90}) - 2{,}64}{1{,}64}\right]^i . \tag{10b}$$

The values of the constants C_0, C_i, D_0 and D_i are given in Table 4.

[2] Note that this definition of $W(T_{90})$ differs from the corresponding definition used in the ITS-27, ITS-48, IPTS-48, and IPTS-68: for all of these earlier scales $W(T)$ was defined in terms of a reference temperature of 0 °C, which since 1954 has itself been defined as 273,15 K

A thermometer may be calibrated for use throughout this range or, using fewer calibration points, for ranges with upper limits of 660,323 °C, 419,527 °C, 231,928 °C, 156,5985 °C or 29,7646 °C, all having a lower limit of 0 °C.

(iii) – A thermometer may be calibrated for use in the range 234,3156 K (−38,8344 °C) to 29,7646 °C, the calibration being made at these temperatures and at the triple point of water. Both reference functions {Eqs. (9) and (10)} are required to cover this range.

The defining fixed points and deviation functions for the various ranges are given below, and in summary form in Table 5.

3.3.1. The Triple Point of Equilibrium Hydrogen (13,8033 K) to the Triple Point of Water (273,16 K). The thermometer is calibrated at the triple points of equilibrium hydrogen (13,8033 K), neon (24,5561 K), oxygen (54,3584 K), argon (83,8058 K), mercury (234,3156 K), and water (273,16 K), and at two additional temperatures close to 17,0 K and 20,3 K. These last two may be determined either: by using a gas thermometer as described in Sect. 3.2, in which case the two temperatures must lie within the ranges 16,9 K to 17,1 K and 20,2 K to 20,4 K respectively; or by using the vapour pressure-temperature relation of equilibrium hydrogen, in which case the two temperatures must lie within the ranges 17,025 K to 17,045 K and 20,26 K to 20,28 K respectively, with the precise values being determined from Eqs. (11 a) and (11 b) respectively:

$$T_{90}/\mathrm{K} - 17{,}035 = (p/\mathrm{kPa} - 33{,}3213)/13{,}32 \qquad (11\,\mathrm{a})$$

$$T_{90}/\mathrm{K} - 20{,}27 = (p/\mathrm{kPa} - 101{,}292)/30\,. \qquad (11\,\mathrm{b})$$

The deviation function is[3]:

$$W(T_{90}) - W_r(T_{90}) = a[W(T_{90})-1] + b[W(T_{90})-1]^2 + \sum_{i=1}^{5} c_i\,[\ln W(T_{90})]^{i+n} \qquad (12)$$

with values for the coefficients a, b and c_i being obtained from measurements at the defining fixed points and with $n=2$.

For this range and for the sub-ranges 3.3.1.1 to 3.3.1.3 the required values of $W_r(T_{90})$ are obtained from Eq. (9 b) or from Table 1.

3.3.1.1. The Triple Point of Neon (24,5561 K) to the Triple Point of Water (273,16 K). The thermometer is calibrated at the triple points of equilibrium hydrogen (13,8033 K), neon (24,5561 K), oxygen (54,3584 K), argon (83,8058 K), mercury (234,3156 K) and water (273,16 K).

The deviation function is given by Eq. (12) with values for the coefficients a, b, c_1, c_2 and c_3 being obtained from measurements at the defining fixed points and with $c_4 = c_5 = n = 0$.

3.3.1.2. The Triple Point of Oxygen (54,3584 K) to the Triple Point of Water (273,16 K). The thermometer is calibrated at the triple points of oxygen (54,3584 K), argon (83,8058 K), mercury (234,3156 K) and water (273,16 K).

The deviation function is given by Eq. (12) with values for the coefficients a, b and c_1 being obtained from measurements at the defining fixed points, with $c_2 = c_3 = c_4 = c_5 = 0$ and with $n=1$.

3.3.1.3. The Triple Point of Argon (83,8058 K) to the Triple Point of Water (273,16 K). The thermometer is calibrated at the triple points of argon (83,8058 K), mercury (234,3156 K) and water (273,16 K).

The deviation function is:

$$W(T_{90}) - W_r(T_{90}) = a[W(T_{90})-1] + b[W(T_{90})-1]\ln W(T_{90}) \qquad (13)$$

with the values of a and b being obtained from measurements at the defining fixed points.

3.3.2. From 0 °C to the Freezing Point of Silver (961,78 °C). The thermometer is calibrated at the triple

Table 5. Deviation functions and calibration points for platinum resistance thermometers in the various ranges in which they define T_{90}

a Ranges with an upper limit of 273,16 K

Section	Lower temperature limit T/K	Deviation functions	Calibration points (see Table 1)
3.3.1	13,8033	$a[W(T_{90})-1]+b[W(T_{90})-1]^2 + \sum_{i=1}^{5} c_i[\ln W(T_{90})]^{i+n}$, $n=2$	2–9
3.3.1.1	24,5561	As for 3.3.1 with $c_4=c_5=n=0$	2, 5–9
3.3.1.2	54,3584	As for 3.3.1 with $c_2=c_3=c_4=c_5=0$, $n=1$	6–9
3.3.1.3	83,8058	$a[W(T_{90})-1] + b[W(T_{90})-1]\ln W(T_{90})$	7–9

b Ranges with a lower limit of 0 °C

Section	Upper temperature limit t/°C	Deviation functions	Calibration points (see Table 1)
3.3.2*	961,78	$a[W(T_{90})-1]+b[W(T_{90})-1]^2 + c[W(T_{90})-1]^3 + d[W(T_{90}) - W(660{,}323\,°\mathrm{C})]^2$	9, 12–15
3.3.2.1	660,323	As for 3.3.2 with $d=0$	9, 12–14
3.3.2.2	419,527	As for 3.3.2 with $c=d=0$	9, 12, 13
3.3.2.3	231,928	As for 3.3.2 with $c=d=0$	9, 11, 12
3.3.2.4	156,5985	As for 3.3.2 with $b=c=d=0$	9, 11
3.3.2.5	29,7646	As for 3.3.2 with $b=c=d=0$	9, 10

c Range from 234,3156 K (−38,8344 °C) to 29,7646 °C

3.3.3		As for 3.3.2 with $c=d=0$	8–10

* Calibration points 9, 12–14 are used with $d=0$ for $t_{90} \leq 660{,}323$ °C; the values of a, b and c thus obtained are retained for $t_{90} > 660{,}323$ °C, with d being determined from calibration point 15

[3] This deviation function {and also those of Eqs. (13) and (14)} may be expressed in terms of W_r rather than W; for this procedure see "Supplementary Information for ITS-90"

point of water (0,01 °C), and at the freezing points of tin (231,928 °C), zinc (419,527 °C), aluminium (660,323 °C) and silver (961,78 °C).

The deviation function is:

$$W(T_{90}) - W_r(T_{90}) = a[W(T_{90})-1] + b[W(T_{90})-1]^2 + c[W(T_{90})-1]^3 + d[W(T_{90}) - W(660{,}323\,°\mathrm{C})]^2 . \quad (14)$$

For temperatures below the freezing point of aluminium $d=0$, with the values of a, b and c being determined from the measured deviations from $W_r(T_{90})$ at the freezing points of tin, zinc and aluminium. From the freezing point of aluminium to the freezing point of silver the above values of a, b and c are retained and the value of d is determined from the measured deviation from $W_r(T_{90})$ at the freezing point of silver.

For this range and for the sub-ranges 3.3.2.1 to 3.3.2.5 the required values for $W_r(T_{90})$ are obtained from Eq. (10b) or from Table 1.

3.3.2.1. From 0 °C to the Freezing Point of Aluminium (660,323 °C). The thermometer is calibrated at the triple point of water (0,01 °C), and at the freezing points of tin (231,928 °C), zinc (419,527 °C) and aluminium (660,323 °C).

The deviation function is given by Eq. (14), with the values of a, b and c being determined from measurements at the defining fixed points and with $d=0$.

3.3.2.2. From 0 °C to the Freezing Point of Zinc (419,527 °C). The thermometer is calibrated at the triple point of water (0,01 °C), and at the freezing points of tin (231,928 °C) and zinc (419,527 °C).

The deviation function is given by Eq. (14) with the values of a and b being obtained from measurements at the defining fixed points and with $c=d=0$.

3.3.2.3. From 0 °C to the Freezing Point of Tin (231,928 °C). The thermometer is calibrated at the triple point of water (0,01 °C), and at the freezing points of indium (156,5985 °C) and tin (231,928 °C).

The deviation function is given by Eq. (14) with the values of a and b being obtained from measurements at the defining fixed points and with $c=d=0$.

3.3.2.4. From 0 °C to the Freezing Point of Indium (156,5985 °C). The thermometer is calibrated at the triple point of water (0,01 °C), and at the freezing point of indium (156,5985 °C).

The deviation function is given by Eq. (14) with the value of a being obtained from measurements at the defining fixed points and with $b=c=d=0$.

3.3.2.5. From 0 °C to the Melting Point of Gallium (29,7646 °C). The thermometer is calibrated at the triple point of water (0,01 °C), and at the melting point of gallium (29,7646 °C).

The deviation function is given by Eq. (14) with the value of a being obtained from measurements at the defining fixed points and with $b=c=d=0$.

3.3.3. The Triple Point of Mercury (−38,8344 °C) to the Melting Point of Gallium (29,7646 °C). The thermometer is calibrated at the triple points of mercury (−38,8344 °C), and water (0,01 °C), and at the melting point of gallium (29,7646 °C).

The deviation function is given by Eq. (14) with the values of a and b being obtained from measurements at the defining fixed points and with $c=d=0$.

The required values of $W_r(T_{90})$ are obtained from Eqs. (9b) and (10b) for measurements below and above 273,16 K respectively, or from Table 1.

3.4. The Range Above the Freezing Point of Silver (961,78 °C): Planck Radiation Law

Above the freezing point of silver the temperature T_{90} is defined by the equation:

$$\frac{L_\lambda(T_{90})}{L_\lambda\ [T_{90}(\mathrm{X})]} = \frac{\exp(c_2[\lambda\, T_{90}(\mathrm{X})]^{-1}) - 1}{\exp(c_2[\lambda\, T_{90}]^{-1}) - 1} . \quad (15)$$

where $T_{90}(\mathrm{X})$ refers to any one of the silver $\{T_{90}(\mathrm{Ag}) = 1234{,}93\ \mathrm{K}\}$, the gold $\{T_{90}(\mathrm{Au}) = 1337{,}33\ \mathrm{K}\}$ or the copper $\{T_{90}(\mathrm{Cu}) = 1357{,}77\ \mathrm{K}\}$ freezing points[4] and in which $L_\lambda(T_{90})$ and $L_\lambda(T_{90})(\mathrm{X})]$ are the spectral concentrations of the radiance of a blackbody at the wavelength (in vacuo) λ at T_{90} and at $T_{90}(\mathrm{X})$ respectively, and $c_2 = 0{,}014388\ \mathrm{m \cdot K}$.

For practical details and current good practice for optical pyrometry, see "Supplementary Information for the ITS-90" (BIPM-1990).

4. Supplementary Information and Differences from Earlier Scales

The apparatus, methods and procedures that will serve to realize the ITS-90 are given in "Supplementary Information for the ITS-90". This document also gives an account of the earlier International Temperature Scales and the numerical differences between successive scales that include, where practicable, mathematical functions for the differences $T_{90} - T_{68}$. A number of useful approximations to the ITS-90 are given in "Techniques for Approximating the ITS-90".

These two documents have been prepared by the Comité Consultatif de Thermométrie and are published by the BIPM; they are revised and updated periodically.

The differences $T_{90} - T_{68}$ are shown in Fig. 1 and Table 6. The number of significant figures given in Table 6 allows smooth interpolations to be made. However, the reproducibility of the IPTS-68 is, in many areas, substantially worse than is implied by this number.

[4] The T_{90} values of the freezing points of silver, gold and copper are believed to be self consistent to such a degree that the substitution of any one of them in place of one of the other two as the reference temperature $T_{90}(\mathrm{X})$ will not result in significant differences in the measured values of T_{90}.

Table 6. Differences between ITS-90 and EPT-76, and between ITS-90 and IPTS-68 for specified values of T_{90} and t_{90}

					$(T_{90}-T_{76})$/mK					
T_{90}/K	0	1	2	3	4	5	6	7	8	9
0						−0,1	−0,2	−0,3	−0,4	−0,5
10	−0,6	−0,7	−0,8	−1,0	−1,1	−1,3	−1,4	−1,6	−1,8	−2,0
20	−2,2	−2,5	−2,7	−3,0	−3,2	−3,5	−3,8	−4,1		

					$(T_{90}-T_{68})$/K					
T_{90}/K	0	1	2	3	4	5	6	7	8	9
10					−0,006	−0,003	−0,004	−0,006	−0,008	−0,009
20	−0,009	−0,008	−0,007	−0,007	−0,006	−0,005	−0,004	−0,004	−0,005	−0,006
30	−0,006	−0,007	−0,008	−0,008	−0,008	−0,007	−0,007	−0,007	−0,006	−0,006
40	−0,006	−0,006	−0,006	−0,006	−0,006	−0,007	−0,007	−0,007	−0,006	−0,006
50	−0,006	−0,005	−0,005	−0,004	−0,003	−0,002	−0,001	0,000	0,001	0,002
60	0,003	0,003	0,004	0,004	0,005	0,005	0,006	0,006	0,007	0,007
70	0,007	0,007	0,007	0,007	0,007	0,008	0,008	0,008	0,008	0,008
80	0,008	0,008	0,008	0,008	0,008	0,008	0,008	0,008	0,008	0,008
90	0,008	0,008	0,008	0,008	0,008	0,008	0,008	0,009	0,009	0,009
T_{90}/K	0	10	20	30	40	50	60	70	80	90
100	0,009	0,011	0,013	0,014	0,014	0,014	0,014	0,013	0,012	0,012
200	0,011	0,010	0,009	0,008	0,007	0,005	0,003	0,001		

					$(t_{90}-t_{68})$/°C					
t_{90}/°C	0	−10	−20	−30	−40	−50	−60	−70	−80	−90
−100	0,013	0,013	0,014	0,014	0,014	0,013	0,012	0,010	0,008	0,008
0	0,000	0,002	0,004	0,006	0,008	0,009	0,010	0,011	0,012	0,012
t_{90}/°C	0	10	20	30	40	50	60	70	80	90
0	0,000	−0,002	−0,005	−0,007	−0,010	−0,013	−0,016	−0,018	−0,021	−0,024
100	−0,026	−0,028	−0,030	−0,032	−0,034	−0,036	−0,037	−0,038	−0,039	−0,039
200	−0,040	−0,040	−0,040	−0,040	−0,040	−0,040	−0,040	−0,039	−0,039	−0,039
300	−0,039	−0,039	−0,039	−0,040	−0,040	−0,041	−0,042	−0,043	−0,045	−0,046
400	−0,048	−0,051	−0,053	−0,056	−0,059	−0,062	−0,065	−0,068	−0,072	−0,075
500	−0,079	−0,083	−0,087	−0,090	−0,094	−0,098	−0,101	−0,105	−0,108	−0,112
600	−0,115	−0,118	−0,122	−0,125*	−0,08	−0,03	0,02	0,06	0,11	0,16
700	0.20	0,24	0,28	0,31	0,33	0,35	0,36	0,36	0,36	0,35
800	0,34	0,32	0,29	0,25	0,22	0,18	0,14	0,10	0,06	0,03
900	−0,01	−0,03	−0,06	−0,08	−0,10	−0,12	−0,14	−0,16	−0,17	−0,18
1000	−0,19	−0,20	−0,21	−0,22	−0,23	−0,24	−0,25	−0,25	−0,26	−0,26
t_{90}/°C	0	100	200	300	400	500	600	700	800	900
1000		−0,26	−0,30	−0,035	−0,039	−0,044	−0,49	−0,54	−0,60	−0,66
2000	−0,72	−0,79	−0,85	−0,93	−1,00	−1,07	−1,15	−1,24	−1,32	−1,41
3000	−1,50	−1,59	−1,69	−1,78	−1,89	−1,99	−2,10	−2,21	−2,32	−2,43

* A discontinuity in the first derivative of $(t_{90}-t_{68})$ occurs at a temperature of $t_{90}=630{,}6$ °C, at which $(t_{90}-t_{68})=-0{,}125$ °C

Appendix

The International Temperature Scale of 1927 (ITS-27)

The International Temperature Scale of 1927 was adopted by the seventh General Conference of Weights and Measures to overcome the practical difficulties of the direct realization of thermodynamic temperatures by gas thermometry, and as a universally acceptable replacement for the differing existing national temperature scales. The ITS-27 was formulated so as to allow measurements of temperature to be made precisely and reproducibly, with as close an approximation to thermodynamic temperatures as could be determined at that time. Between the oxygen boiling point and the gold freezing point it was based upon a number of reproducible temperatures, or fixed points, to which numerical values were assigned, and two standard interpolating instruments. Each of these interpolating instruments was calibrated at several of the fixed points, this giving the constants for the interpolating formula in the appropriate temperature range. A platinum resistance thermometer was used for the lower part and a platinum rhodium/platinum thermocouple for temperatures above 660 °C. For the region above the gold freezing point, temperatures were defined in terms of the Wien radiation law: in practice, this invariably resulted in the selection of an optical pyrometer as the realizing instrument.

The International Temperature Scale of 1948 (ITS-48)

The International Temperature Scale of 1948 was adopted by the ninth General Conference. Changes from the ITS-27 were: the lower limit of the platinum resistance thermometer range was changed from −190 °C to the defined oxygen boiling point of −182,97 °C, and the junction of the platinum resistance thermometer range and the thermocouple range became the measured antimony freezing point (about 630 °C) in place of 660 °C; the silver freezing point was defined as being 960,8 °C instead of 960,5 °C; the gold freezing point replaced the gold melting point (1063 °C); the Planck radiation law replaced the Wien law; the value assigned to the second radiation constant became $1{,}438\times10^{-2}$ m · K in place of $1{,}432\times10^{-2}$ m · K; the permitted ranges for the constants of the interpola-

tion formulae for the standard resistance thermometer and thermocouple were modified; the limitation on λT for optical pyrometry ($\lambda T < 3 \times 10^{-3}$ m · K) was changed to the requirement that "visible" radiation be used.

The International Practical Temperature Scale of 1948 (Amended Edition of 1960) (IPTS-48)

The International Practical Temperature Scale of 1948, amended edition of 1960, was adopted by the eleventh General Conference: the tenth General Conference had already adopted the triple point of water as the sole point defining the kelvin, the unit of thermodynamic temperature. In addition to the introduction of the word "Practical", the modifications to the ITS-48 were: the triple point of water, defined as being 0,01 °C, replaced the melting point of ice as the calibration point in this region; the freezing point of zinc, defined as being 419,505 °C, became a preferred alternative to the sulphur boiling point (444,6 °C) as a calibration point; the permitted ranges for the constants of the interpolation formulae for the standard resistance thermometer and the thermocouple were further modified; the restriction to "visible" radiation for optical pyrometry was removed.

Inasmuch as the numerical values of temperature on the IPTS-48 were the same as on the ITS-48, the former was not a revision of the scale of 1948 but merely an amended form of it.

The International Practical Temperature Scale of 1968 (IPTS-68)

In 1968 the International Committee of Weights and Measures promulgated the International Practical Temperature Scale of 1968, having been empowered to do so by the thirteenth General Conference of 1967–1968. The IPTS-68 incoporated very extensive changes from the IPTS-48. These included numerical changes, designed to bring it more nearly in accord with thermodynamic temperatures, that were sufficiently large to be apparent to many users. Other changes were as follows: the lower limit of the scale was extended down to 13,81 K; at even lower temperatures (0,5 K to 5,2 K), the use of two helium vapour pressure scales was recommended; six new defining fixed points were introduced – the triple point of equilibrium hydrogen (13,81 K), an intermediate equilibrium hydrogen point (17,042 K), the normal boiling point of equilibrium hydrogen (20,28 K), the boiling point of neon (27,102 K), the triple point of oxygen (54,361 K), and the freezing point of tin (231,9681 °C) which became a permitted alternative to the boiling point of water; the boiling point of sulphur was deleted; the values assigned to four fixed points were changed – the boiling point of oxygen (90,188 K), the freezing point of zinc (419,58 °C), the freezing point of silver (961,93 °C), and the freezing point of gold (1064,43 °C); the interpolating formulae for the resistance thermometer range became much more complex; the value assigned to the second radiation constant c_2 became $1{,}4388 \times 10^{-2}$ m · K; the permitted ranges of the constants for the interpolation formulae for the resistance thermometer and thermocouple were again modified.

The International Practical Temperature Scale of 1968 (Amended Edition of 1975) (IPTS-68)

The International Practical Temperature Scale of 1968, amended edition of 1975, was adopted by the fifteenth General Conference in 1975. As was the case for the IPTS-48 with respect to the ITS-48, the IPTS-68(75) introduced no numerical changes. Most of the extensive textural changes were intended only to clarify and simplify its use. More substantive changes were: the oxygen point was defined as the condensation point rather than the boiling point; the triple point of argon (83,798 K) was introduced as a permitted alternative to the condensation point of oxygen; new values of the isotopic composition of naturally occurring neon were adopted; the recommendation to use values of T given by the 1958 ^{4}He and 1962 ^{3}He vapour-pressure scales was rescinded.

The 1976 Provisional 0,5 K to 30 K Temperature Scale (EPT-76)

The 1976 Provisional 0,5 K to 30 K Temperature Scale was introduced to meet two important requirements: these were to provide means of substantially reducing the errors (with respect to corresponding thermodynamic values) below 27 K that were then known to exist in the IPTS-68 and throughout the temperature ranges of the ^{4}He and ^{3}He vapour pressure scales of 1958 and 1962 respectively, and to bridge the gap between 5,2 K and 13,81 K in which there had not previously been an international scale. Other objectives in devising the ETP-76 were "that it should be thermodynamically smooth, that it should be continuous with the IPTS-68 at 27,1 K, and that is should agree with thermodynamic temperature T as closely as these two conditions allow". In contrast with the IPTS-68, and to ensure its rapid adoption, several methods of realizing the ETP-76 were approved. These included: using a thermodynamic interpolation instrument and one or more of eleven assigned reference points; taking differences from the IPTS-68 above 13,81 K; taking differences from helium vapour pressure scales below 5 K; and taking differences from certain well-established laboratory scales. Because there was a certain "lack of internal consistency" it was admitted that "slight ambiguities between realizations" might be introduced. However the advantages gained by adopting the EPT-76 as a working scale until such time as the IPTS-68 should be revised and extended were considered to outweigh the disadvantages.

APPENDIX 2

Revised Values for $(t_{90} - t_{68})$ from 630 °C to 1064 °C

The following text is taken from *Metrologia*, 1994, **31**, 149-153.

International Report

Revised Values for $(t_{90} - t_{68})$ from 630 °C to 1 064 °C

R. L. Rusby, R. P. Hudson and M. Durieux
(Members of Working Group 4
of the Comité Consultatif de Thermométrie)

Abstract. A revised table of differences $(t_{90} - t_{68})$ between values of temperature on the International Temperature Scale of 1990, ITS-90, and the corresponding values on the International Practical Temperature Scale of 1968, IPTS-68, is published at the request of the Comité Consultatif de Thermométrie (CCT). The revision affects only the range 630 °C to 1 064 °C, where the IPTS-68 specified the use of platinum-10 % rhodium versus platinum thermocouples. It follows from new intercomparisons of thermocouples carrying IPTS-68 calibrations with platinum resistance thermometers and radiation thermometers calibrated in accordance with the ITS-90. The largest change occurs at 760 °C, where the difference formerly tabulated as 0,36 °C is now 0,04 °C. The revision concerns only the assessment of the differences between the ITS-90 and the IPTS-68, and does not affect the ITS-90 in any way.

1. Introduction

This note has been prepared in response to a request from the Comité Consultatif de Thermométrie (CCT), at its 18th Meeting in September 1993, to publish a revised version of the table of differences $(t_{90} - t_{68})$ between values of temperature on the International Temperature Scale of 1990, ITS-90 [1], and the International Practical Temperature Scale of 1968, IPTS-68 [2]. The original version was published as Table 6 and Figure 1 of [1].

The particular problem arose in the temperature range 630,74 °C < t_{68} < 1 064,43 °C, in which range the IPTS-68 was defined using the platinum-10 % rhodium/platinum thermocouple. As a result, the precision and reproducibility of the scale were limited, generally at the level of about ±0,1 °C to 0,2 °C. This limitation affected all measurements and scale comparisons involving the IPTS-68.

When the text of the ITS-90 was published, it included a table of the scale differences $(t_{90} - t_{68})$. At that time there were no direct experimental data in this range on which the values could be based, and they were therefore deduced by indirect means (see Section 3). Several new experiments now suggest that the actual differences are up to 0,3 °C smaller than those tabulated and, although these too are subject to the uncertainties asociated with the use of thermocouples, it was concluded by the CCT that the table should be revised.

In other ranges, where the instruments specified in the ITS-90 are the same as they were in the IPTS-68, the differences $(T_{90} - T_{68})$/K and $(t_{90} - t_{68})$/°C were obtainable directly from equivalent calibrations on the two scales, and they are unchanged. The differences $(T_{90} - T_{76})$ between the ITS-90 and the Échelle Provisoire de Température de 1976 entre 0,5 K et 30 K, EPT-76, are also unaffected.

The revision of the table of differences does not affect the ITS-90 itself. The original Table 6 and Figure 1 were included in the text of the ITS-90 for information only, in order to document, as well as they were known, the changes in temperature values that followed from the introduction of the new scale. The number of significant figures given in the table was such as to allow smooth interpolation, but the text of the ITS-90 pointed out that "the reproducibility of the IPTS-68 is, in many areas, substantially worse than is implied by this number".

The revised differences are given in Table 1 in this note, and they are plotted in Figure 1, which is a new version of Figure 1 of [1].

2. The Revised Differences

The differences $(t_{90} - t_{68})$ do not define the ITS-90 and, indeed, the final preparation of Table 6 of the ITS-90

R. L. Rusby: Division of Quantum Metrology, National Physical Laboratory, Teddington, Middlesex TW11 0LW, UK.
R. P. Hudson: formerly of the Bureau International des Poids et Mesures, Pavillon de Breteuil, F-92312 Sèvres Cedex, France.
M. Durieux: University of Leiden, Kamerlingh Onnes Laboratorium, Nieuwsteeg 18, 2311 SB Leiden, the Netherlands.

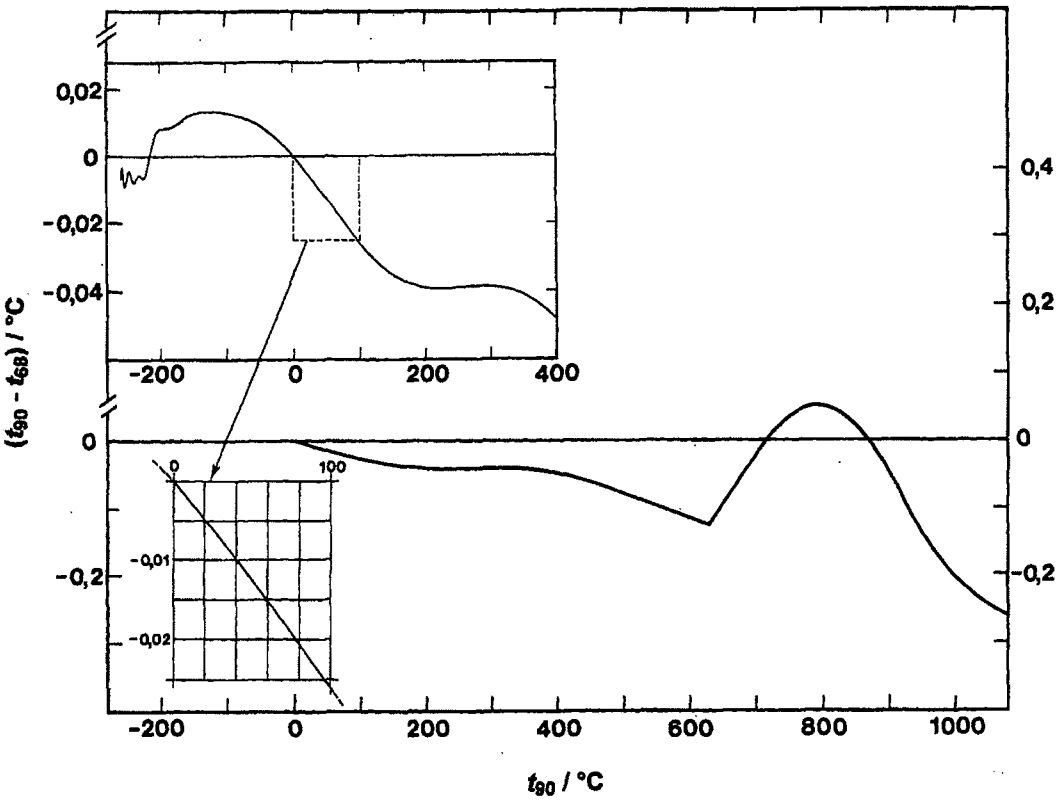

Figure 1. The revised differences $(t_{90} - t_{68})/°C$ as a function of Celsius temperature.

followed the adoption of the scale by the CCT. The procedure used for deriving the differences is discussed in Section 3.

At temperatures above 630 °C, the ITS-90 was derived from new thermodynamic determinations of the freezing temperatures of aluminium, silver, gold and copper, and from direct thermodynamic calibrations of platinum resistance thermometers, using spectral radiation pyrometry [3]. Thus it was derived *ab initio*, without reference to the type S (platinum-10 % rhodium/platinum) thermocouple. An account of the thermodynamic basis of the ITS-90 has been published [4].

Since type S thermocouples are not specified in the ITS-90, the direct determination of the differences $(t_{90} - t_{68})$ in the range $630{,}74\,°C < t_{68} < 1\,064{,}43\,°C$ requires experimental comparisons between the two scales: that is, type S thermocouples calibrated as specified in the IPTS-68 must be compared with platinum resistance thermometers and radiation thermometers which have been calibrated in accordance with the ITS-90. Several such experiments have now been carried out as part of an international collaborative effort leading to the derivation of new reference tables for type S and other thermocouples.

The results of experiments with twenty-four type S thermocouples in seven laboratories have been collated and reported by Burns et al. [5, 6], whose superposition of the $(t_{90} - t_{68})$ data for all twenty-four thermocouples is reproduced in Figure 2. A fifth-degree polynomial in t_{90} was fitted to the data by iteratively-reweighted least-squares regression, subject to the constraint that it should pass through the specified differences of $-0{,}125\,°C$ at $t_{90} = 630{,}615\,°C$, $-0{,}15\,°C$ at $961{,}78\,°C$, and $-0{,}25\,°C$ at $1\,064{,}18\,°C$. The final fit is indicated by the bold line in Figure 2, and its equation is [5-7]

$$\begin{aligned}(t_{90} - t_{68})/°C = {} & 7{,}868\,720\,9 \times 10^{1} \\ & - 4{,}713\,599\,1 \times 10^{-1}\,(t_{90}/°C) \\ & + 1{,}095\,471\,5 \times 10^{-3}\,(t_{90}/°C)^2 \\ & - 1{,}235\,788\,4 \times 10^{-6}\,(t_{90}/°C)^3 \\ & + 6{,}773\,658\,3 \times 10^{-10}\,(t_{90}/°C)^4 \\ & - 1{,}445\,808\,1 \times 10^{-13}\,(t_{90}/°C)^5.\end{aligned}$$

By a decision of the CCT, the scale differences given by this equation supersede the original differences in the range $630{,}615\,°C < t_{90} < 1\,064{,}18\,°C$. Table 1 of this note replaces Table 6 of [1], which was also published as Table 1.5 of the *Supplementary Information for the ITS-90* [8], and in Appendix A of the *Techniques for Approximating the ITS-90* [9]. The equation replaces (1.4) of the *Supplementary Information.*

Now that the differences are based on direct measurements, with an uncertainty comparable with the imprecision of the IPTS-68 in this region, it is not

Table 1. Revised differences between the ITS-90 and the IPTS-68, and the differences between the ITS-90 and the EPT-76.

					$(T_{90} - T_{76})$/mK					
T_{90}/K	0	1	2	3	4	5	6	7	8	9
0						-0,1	-0,2	-0,3	-0,4	-0,5
10	-0,6	-0,7	-0,8	-1,0	-1,1	-1,3	-1,4	-1,6	-1,8	-2,0
20	-2,2	-2,5	-2,7	-3,0	-3,2	-3,5	-3,8	-4,1		
					$(T_{90} - T_{68})$/K					
T_{90}/K	0	1	2	3	4	5	6	7	8	9
10					-0,006	-0,003	-0,004	-0,006	-0,008	-0,009
20	-0,009	-0,008	-0,007	-0,007	-0,006	-0,005	-0,004	-0,004	-0,005	-0,006
30	-0,006	-0,007	-0,008	-0,008	-0,008	-0,007	-0,007	-0,007	-0,006	-0,006
40	-0,006	-0,006	-0,006	-0,006	-0,006	-0,007	-0,007	-0,007	-0,006	-0,006
50	-0,006	-0,005	-0,005	-0,004	-0,003	-0,002	-0,001	0,000	0,001	0,002
60	0,003	0,003	0,004	0,004	0,005	0,005	0,006	0,006	0,007	0,007
70	0,007	0,007	0,007	0,007	0,007	0,008	0,008	0,008	0,008	0,008
80	0,008	0,008	0,008	0,008	0,008	0,008	0,008	0,008	0,008	0,008
90	0,008	0,008	0,008	0,008	0,008	0,008	0,008	0,009	0,009	0,009
T_{90}/K	0	10	20	30	40	50	60	70	80	90
100	0,009	0,011	0,013	0,014	0,014	0,014	0,014	0,013	0,012	0,012
200	0,011	0,010	0,009	0,008	0,007	0,005	0,003	0,001		
					$(t_{90} - t_{68})$/°C					
t_{90}/°C	0	-10	-20	-30	-40	-50	-60	-70	-80	-90
-100	0,013	0,013	0,014	0,014	0,014	0,013	0,012	0,010	0,008	0,008
0	0,000	0,002	0,004	0,006	0,008	0,009	0,010	0,011	0,012	0,012
t_{90}/°C	0	10	20	30	40	50	60	70	80	90
0	0,000	-0,002	-0,005	-0,007	-0,0010	-0,013	-0,016	-0,018	-0,021	-0,024
100	-0,026	-0,028	-0,030	-0,032	-0,034	-0,036	-0,037	-0,038	-0,039	-0,039
200	-0,040	-0,040	-0,040	-0,040	-0,040	-0,040	-0,040	-0,039	-0,039	-0,039
300	-0,039	-0,039	-0,039	-0,040	-0,040	-0,041	-0,042	-0,043	-0,045	-0,046
400	-0,048	-0,051	-0,053	-0,056	-0,059	-0,062	-0,065	-0,068	-0,072	-0,075
500	-0,079	-0,083	-0,087	-0,090	-0,094	-0,098	-0,101	-0,105	-0,108	-0,112
600	-0,115	-0,118	-0,122	-0,125	-0,11	-0,10	-0,09	-0,07	-0,05	-0,04
700	-0,02	-0,01	0,00	0,02	0,03	0,03	0,04	0,05	0,05	0,05
800	0,05	0,05	0,04	0,04	0,03	0,02	0,01	0,00	-0,02	-0,03
900	-0,05	-0,06	-0,08	-0,10	-0,11	-0,13	-0,15	-0,16	-0,18	-0,19
1 000	-0,20	-0,22	-0,23	-0,23	-0,24	-0,25	-0,25	-0,25	-0,26	-0,26
t_{90}/°C	0	100	200	300	400	500	600	700	800	900
1 000		-0,026	-0,30	-0,35	-0,39	-0,44	-0,49	-0,54	-0,60	-0,66
2 000	-0,72	-0,79	-0,85	-0,93	-1,00	-1,07	-1,15	-1,24	-1,32	-1,41
3 000	-1,50	-1,59	-1,69	-1,78	-1,89	-1,99	-2,10	-2,21	-2,32	-2,43

envisaged that any further changes to the table will be necessary. It should be noted that differences deduced by inspection of reference tables for thermocouples or, at lower temperatures, for industrial platinum resistance thermometers, will inevitably not reproduce these differences exactly, as a result of the experimental and fitting procedures used in their derivation. In deriving the reference function for the type S thermocouple, as described in [5], the above equation was applied to the IPTS-68 calibration of a particular thermocouple. The annealing treatment and experimental history of this thermocouple, which will have had a significant bearing on the result, are also described.

3. Additional Information

Where platinum resistance thermometers were the specified interpolating instruments in both the ITS-90 and the IPTS-68, the generation of the scale differences was largely a mathematical exercise: coefficients for a chosen thermometer were calculated according to the requirements of each scale, pairs of equivalent temperature values were derived at the desired intervals, and the differences were calculated. The calculations were unambiguous, although the results would be affected by calibration errors and slightly different results would follow from using different thermometers

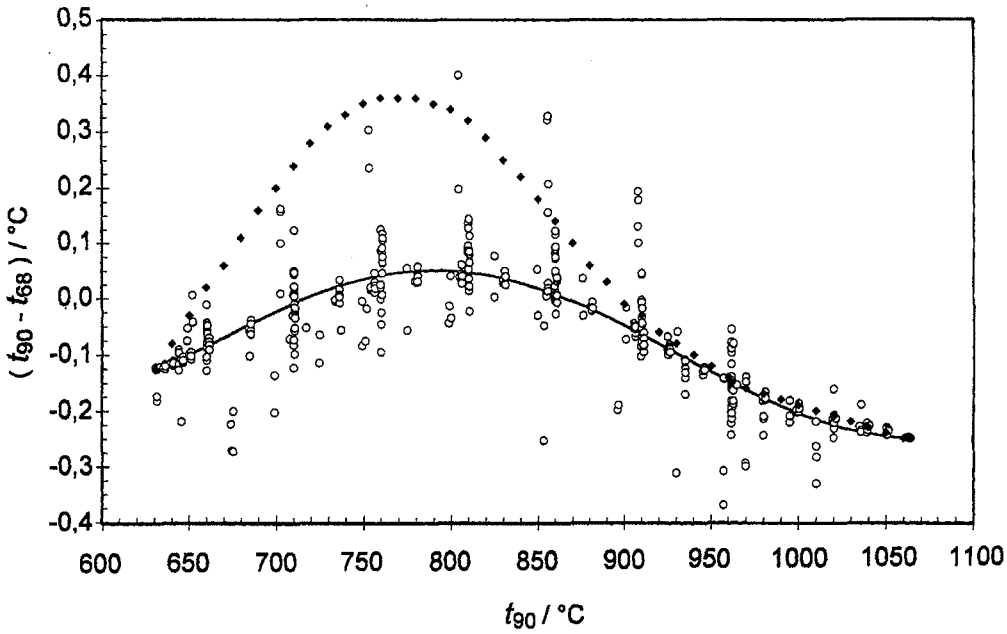

Figure 2. Values of $(t_{90} - t_{68})/°C$ as measured in comparisons between type S thermocouples and platinum resistance thermometers at seven national laboratories (from [5], reproduced by kind permission of G. W. Burns). The line represents the fifth-degree polynomial fitted to the data, and the diamonds are the values as published in the ITS-90 document [1].

because of the so-called non-uniqueness of both scales. In view of the uncertainties and non-uniqueness, the values of the scale differences in Table 6 of [1] were rounded to the nearest 0,001 K.

At temperatures above the freezing point of gold, the scale differences follow from the change in the value assigned to this fixed point. The calculations were exact in so far as wavelength-dependent effects are small, i.e. to the extent that the Wien approximation applies.

For the range in which the thermocouple was specified in the IPTS-68, no ITS-90 calibrations of thermocouples were available when Table 6 of [1] was drawn up. It was necessary to generate the differences on the assumption that they were represented by the best estimate of the thermodynamic errors which had been found to exist in the IPTS-68. In effect the following identity was used:

$$(t_{90} - t_{68}) \equiv (t - t_{68}) - (t - t_{90}),$$

where t is the thermodynamic temperature. The term $(t - t_{90})$ was taken to be zero, since the ITS-90 had been derived so as to represent the state-of-the-art thermodynamic calibrations of platinum resistance thermometers and determinations of the fixed-point temperatures. The scale differences were therefore assumed to be given by $(t - t_{68})$.

The state of knowledge of $(t - t_{68})$ in this region was far from satisfactory, however, as the difficulties of thermodynamic thermometry were compounded by difficulties in the use of thermocouples. The measurements of t in this range were predominantly based on spectral radiation pyrometry. That is, the spectral radiance of a black body at the required temperature was compared with that of a reference black body whose thermodynamic temperature is inferred from other work. In the experiments considered (see [4] for details), the reference black body was either maintained at the freezing point of gold or at a temperature below 630 °C measured using a platinum resistance thermometer. The temperature of the comparison black body was thus obtained and compared with the value of t_{68} measured using a thermocouple. Three experiments gave results which were consistent within reasonable limits, and were also broadly consistent with independent results from noise thermometry.

Further information was available from two experiments [10, 11] in which resistance thermometers were compared with thermocouples. Although these could not yield thermodynamic data, they did lead to estimates for the discontinuity in the derivative $\mathrm{d}(t - t_{68})/\mathrm{d}t_{68}$ at $t_{68} = 630{,}74$ °C, the temperature of the junction between the resistance thermometer and the thermocouple ranges in the IPTS-68. The experiments of Bedford et al. [10] suggest that the discontinuity in the derivative was about 0,005, in contrast with the earlier result of Evans and Wood [11], who found a value of about 0,001. In preparing Table 6 of the ITS-90, the discontinuity in $\mathrm{d}(t_{90} - t_{68})/\mathrm{d}t_{68}$ was chosen to be consistent with Bedford's value, which fitted well with the radiation thermometry results referred to above.

However, Figure 2 clearly shows that the differences originally derived are not consistent with the new directly-measured values. The peak value of $(t_{90} - t_{68})$ is reduced by about 0,3 °C, and the discontinuity in the derivative at $t_{68} = 630{,}74$ °C implied by the new results

is approximately 0,001 4, closely similar to the result of Evans and Wood.

It therefore appears that the thermodynamic calibrations of a comparatively small number of thermocouples which led to the values of $(t - t_{68})$ were not fully consistent with the later thermodynamic calibrations of platinum resistance thermometers on which the ITS-90 was based [3]. Assessments of the differences $(t - t_{68})$ are now more accurately given by the measured differences $(t_{90} - t_{68})$, rather than vice versa. However, both are subject to the uncertainties which are inherent in the IPTS-68.

Since the recent comparisons of resistance thermometers with thermocouples did not reproduce the expected scale differences, it is of interest to look again at the earlier intercomparisons of Evans and Wood [11]. Table 5 of their paper details the calibration data (W_{68}, t_{68}) for nine platinum resistance thermometers at the freezing points of tin, zinc, antimony, silver and gold. These data may be accurately converted to (W_{90}, t_{90}) and coefficients may be calculated following the procedure specified in the ITS-90, except that the antimony point (near 630 °C) must be used in place of the aluminium point. This is unlikely to affect the interpolation properties of the ITS-90 deviation equation by a large amount, and it can be assumed that the resulting approximation to the ITS-90 will be accurate enough for the present purpose.

Three of Evans and Wood's calibrations have been examined – the first calibrations of thermometers A1, B1 and N1, the latter being a thermometer whose IPTS-68 alpha coefficient was marginally below the minimum permitted value. The "pseudo" ITS-90 calibrations were compared with the θ values of the quadratic interpolations above 630 °C, which Evans and Wood derived from the measurements at the freezing points of antimony, silver and gold. Adding the differences $(t_{90} - \theta)$ to Evans and Wood's $F(\theta) \boxminus (\theta - t_{68})$ leads to $(t_{90} - t_{68})$. The results for the three thermometers are very similar, and they agree within about 0,02 °C with the values published here in Table 1.

This is a remarkable result, indicating an extraordinary consistency in thermocouple and resistance thermometry at the NBS/NIST spanning more than twenty years. That the consensus represented in Figure 2 is less good is likely to be due to two causes. One is that greater random and systematic variations are only to be expected in pooling results from seven laboratories. The other is that the results obtained inevitably depend on the source and treatment of the thermometers and thermocouples. References [5] and [6] detail these variations and identify the laboratories from which the data in Figure 2 originate. Thermocouple variability may also have been partly responsible for other apparent discrepancies, such as those concerning the discontinuity in the derivative at 630 °C referred to above.

In conclusion, it must be clear that by virtue of using platinum resistance thermometers in place of thermocouples, the reproducibility of the ITS-90 in this range is considerably better than that of the IPTS-68. The underlying irreproducibility of the IPTS-68 needs to be borne in mind when considering the conversion of thermal data from the IPTS-68 to the ITS-90.

References

1. *The International Temperature Scale of 1990 (ITS-90)*, Sèvres, BIPM, 1990; *Metrologia*, 1990, **27**, 3-10 and 107.
2. *The International Practical Temperature Scale of 1968 (IPTS-68)*, Amended edition 1975, Sèvres, BIPM, 1976; *Metrologia*, 1976, **12**, 7-17.
3. Jung H. J., *PTB Mitteilungen*, 1989, **99**, 351-356.
4. Rusby R. L., Hudson R. P., Durieux M., Schooley J. F., Steur P. P. M., Swenson C. A., *Metrologia*, 1991, **28**, 9-18.
5. Burns G. W., Strouse G. F., Mangum B. W., Croarkin M. C., Guthrie W. F., Marcarino P., Battuello M., Lee H. K., Kim J. C., Gam K. S., Rhee C., Chattle M. V., Arai M., Sakurai H., Pokhodun A. I., Moiseeva N. P., Perevalova S. A., de Groot M. J., Jipei Zhang, Kai Fan, Shuyuan Wu, In *Temperature: Its Measurement and Control in Science and Industry*, Vol. 6 (Edited by J. F. Schooley), New York, American Institute of Physics, 1992, 537-540, 541-546.
6. Guthrie W. F., Croarkin M. C., Burns G. W., Strouse G. F., Marcarino P., Battuello M., Lee H. K., Kim J. C., Gam K. S., Rhee C., Chattle M. V., Arai M., Sakurai H., Pokhodun A. I., Moiseeva N. P., Perevalova S. A.. de Groot M. J., Jipei Zhang, Kai Fan, Shuyuan Wu, In *Temperature: Its Measurement and Control in Science and Industry*, Vol. 6 (Edited by J. F. Schooley), New York, American Institute of Physics, 1992, 547-552.
7. Burns G. W., Scroger M. G., Strouse G. F., Croarkin M. C., Guthrie W. F., *Temperature-Electromotive Force Reference Functions and Tables for the Letter-designated Thermocouple Types Based on the ITS-90*, NIST Monograph 175, 1993.
8. *Supplementary Information for the International Temperature Scale of 1990*, Sèvres, BIPM, 1990.
9. *Techniques for Approximating the International Temperature Scale of 1990*, Sèvres, BIPM, 1990.
10. Bedford R. E., Ma C. K., Macready W., Steski D., *Metrologia*, 1986/87, **23**, 197-205.
11. Evans J. P., Wood S. D., *Metrologia*, 1971, **7**, 108-130.

Received on 25 April 1994.

APPENDIX 3

List of Acronyms

LIST OF ACRONYMS USED IN THE PRESENT VOLUME

Laboratories, committees

ASMW	Amt für Standardisierung, Messwesen und Warenprüfung (now PTB (Berlin Institute))
BIPM	Bureau International des Poids et Mesures
BNM	Bureau National de Métrologie, Paris (France)
CCT	Comité Consultatif de Thermométrie
CGPM	Conférence Générale des Poids et Mesures
CIPM	Comité International des Poids et Mesures
EPT-76	Echelle Provisoire de Température de 1976
IGSN	International Gravity Standardization Network
IMGC	Istituto di Metrologia G. Colonnetti, Turin (Italy)
INM	Institut National de Métrologie, Paris (France)
IPTS-68	International Practical Temperature Scale of 1968
ITS-27	International Temperature Scale of 1927
ITS-48	International Temperature Scale of 1948
ITS-90	International Temperature Scale of 1990
NBS	National Bureau of Standards (USA) (now NIST)
NIM	National Institute of Metrology, Beijing (People's Rep. of China)
NIST	National Institute of Standards and Technology, Gaithersburg (USA) (formerly NBS)
NPL	National Physical Laboratory, Teddington (United Kingdom)
NRC	National Research Council of Canada, Ottawa (Canada)
NRLM	National Research Laboratory of Metrology, Tsukuba (Japan)
PTB	Physikalisch Technische Bundesanstalt, Braunschweig (Fed. Rep. of Germany)
VNIIM	D.I. Mendeleyev Institute for Metrology, St. Petersburg (Russian Fed.)
VNIIFTRI	Physicotechnical and Radiotechnical Measurements Institute, Gosstandart, Moscow (Russian Fed.)
VSL	Van Swinden Laboratorium, Delft (Netherlands)

Scientific terms

CMN	Cerium magnesium nitrate
OFHC	Oxygen-Free High Conductivity Copper
PTFE	Polytetrafluorethylene